NASA
CR
3303
c.1

NASA Contractor Report 3303

LOAN COPY: RE
AFWL TECHNIC
KIRTLAND AFB
TECH LIBRARY KAFB, NM
0062075

Atmospheric Lidar Multi-User Instrument System Definition Study

CONTRACT NAS1-15476
AUGUST 1980

NASA

TECH LIBRARY KAFB, NM

0062075

NASA Contractor Report 3303

Atmospheric Lidar Multi-User Instrument System Definition Study

R. V. Greco, *Editor*
General Electric Company
Valley Forge, Pennsylvania

Prepared for
Langley Research Center
under Contract NAS1-15476

National Aeronautics
and Space Administration

Scientific and Technical
Information Office

1980

PREFACE

This Final Report is submitted by General Electric Company to the National Aeronautics and Space Administration, Langley Research Center, Hampton, Virginia, as required by Contract NAS1-15476, Atmospheric Lidar Multi-User Instrument System Definition Study.

This document presents a brief description of the science requirements, covers the space transportation system accommodation capabilities and the Lidar Multi-User Instrument System requirements. Discussions are given on each of the major subsystems. The significant results of the Study are given in the section on System Definition. The document closes with a summary of the programmatics involved in the continuation of the Program.

Technical support in the performance of this study was furnished under subcontract by Hughes Aircraft Corporation, Laser Systems Division, Culver City, California, and ITEK, Optical Systems Division, Lexington, Massachusetts.

The following individuals contributed significantly to the results of this study.

G. Frippel	General Electric
H. W. Halsey	General Electric
D. A. Hetzel	General Electric
U. Pollvogt	General Electric
L. Hill	Hughes Aircraft (Section 6)
N. Hazen	ITEK (Section 5)

Requests for further information concerning this report will be welcomed by:

R. V. Greco, Program Manager
General Electric Space Division
P.O. Box 8555
Philadelphia, Pennsylvania 19101
(215) 962-5629

FOREWORD

An important goal of the research program undertaken with the Shuttle/Spacelab system in the 1980's will be to contribute to and advance the understanding of the processes governing the earth's atmosphere and evaluating its susceptibility to manmade and natural perturbations. The powerful diagnostic potential of a lidar system for probing the composition, structure, and dynamics of the atmosphere makes lidar a key element of that program, both for its own unique capabilities and for its role as part of a broader atmospheric instrument system. A lidar system will also take advantage of such Shuttle features as large payload capability and sequential flight opportunities to develop the potential of laser instrument systems in space in an evolutionary manner.

The need for, and potential of, a spaceborne lidar system for atmospheric studies have been widely recognized. In September 1975, the Atmosphere, Magnetosphere, and Plasmas-in-Space (AMPS) Science Definition Working Group identified a number of scientific problems whose solution would be advanced through the use of a spaceborne lidar. Among these were the understanding of the mechanisms controlling the ozone distribution in the stratosphere and mesosphere, determination of the distribution of tropospheric and stratospheric aerosols and an understanding of their radiative effects, and an investigation of the distribution of metallic atoms in the lower ionosphere and their role in the ion distribution. A detailed study of air pollution measurement requirements, conducted for NASA by Stanford Research Institute (June 1975), identified a number of important air pollution problems that could be addressed by a lidar system.

In addition, recent results from scientific groups around the world have demonstrated the utility of lidar systems for remote measurement of a diversity of atmospheric parameters such as aerosol and cloud distributions, minor species concentrations

including H_2O, O_3, and SO_2, and wind fields.

In October 1976, NASA convened a blue ribbon international panel of lidar experts to review both the potential applications of spaceborne lidar techniques to atmospheric measurements and the state of instrumentation currently available for such applications. The group concluded that: (1) lidar has promising applications to aeronomy, tropospheric, and stratospheric research, with the tropospheric potential being particularly important due to the deficiency of other spaceborne techniques, and (2) lidar has unique characteristics in its very high spatial resolution and its high sensitivity to trace gases and aerosols.

In view of the above history and widespread agreement from the scientific community that an atmospheric lidar system could be an important part of the Shuttle/Spacelab atmospheric research program, NASA initiated in September 1977 an in-depth scientific and technological review in preparation for a system definition and design study for a Shuttle/Spacelab multi-user Lidar System. This activity is managed by an Atmospheric Lidar Study Office at the Langley Research Center and utilizes the expertise of an international Atmospheric Lidar Working Group.

In July 1978 NASA Langley Research Center awarded a study contract (NAS1-15476) to the General Electric Space Division. The study purpose was to establish both the feasibility and system definition for an evolutionary multi-user Lidar Instrument to be flown aboard the Shuttle, as a Spacelab Payload, and accommodate a wide range of experiments identified by the scientific community.

This report contains the results of the study. In summary, the study concluded that significant science can be accomplished with a basic Lidar Instrument, and that it can evolve to accomplish additional experimentation by the incorporation of appropriate lasers and detectors. It was further established that the basic Lidar

Instrument was technologically ready and minimal technology development was required for growth equipment. It is the recommendation of the study that Lidar Program implementation be initiated.

TABLE OF CONTENTS

		PAGE
	SUMMARY	xvii
SECTION 1	INTRODUCTION	1
	STUDY GOAL AND OBJECTIVES	1
	STUDY TECHNICAL GROUND RULES	3
	STUDY SCHEDULE	4
	STUDY RATIONALE	6
SECTION 2	EXPERIMENT ANALYSIS	9
	INTRODUCTION	9
	SEED ANALYSIS	11
	EXPERIMENT QUANTIFICATION	12
	PARAMETRIC ANALYSIS	17
	RESULTS	30
SECTION 3	STS ACCOMMODATION	33
	INTRODUCTION	33
	LIDAR PHYSICAL AND FUNCTIONAL ACCOMMODATION ON SHUTTLE/SPACELAB	36
	LIDAR OPERATIONS	52
	STS SAFETY	67
	STS DEFICIENCIES	68
SECTION 4	SYSTEM REQUIREMENTS	69
	MISSION REQUIREMENTS	69
	PERFORMANCE REQUIREMENTS	72
	SYSTEM DESIGN REQUIREMENTS	74
	SYSTEM DESIGN APPROACH	74
	SUBSYSTEM REQUIREMENTS ALLOCATION	80
SECTION 5	RECEIVER SUBSYSTEM	89
	INTRODUCTION	89
	SUBSYSTEM REQUIREMENTS	90
	PARAMETRIC TRADES	92
	DESIGN	117
	GROWTH OPTIONS	128
	RISK ASSESSMENT	129
SECTION 6	SOURCES SUBSYSTEM	131
	INTRODUCTION	131
	LASER SOURCE SELECTION	132
	VISIBLE AND NEAR VISIBLE SOURCE DEFINITION	149
	NEODYMIUM LASER SUBSYSTEM, MODULE 1: NEODYMIUM LASER	155
	NEODYMIUM LASER SUBSYSTEM, MODULE 2: TWENTY WATT DOUBLER	174
	NEODYMIUM LASER SUBSYSTEM, MODULE 3: TWENTY WATT MIXER	179
	DYE LASER SUBSYSTEM, MODULE 4: DYE LASER	180
	DYE LASER SUBSYSTEM, MODULE 5: TUNABLE DOUBLER	196
	ANCILLARY OPTICS: MODULES 6 AND 7	196
	EXPERIMENT ACCOMMODATION WITH MODULAR VISIBLE AND NEAR VISIBLE SOURCES SYSTEM	199
	CW CO_2 SOURCE	209

TABLE OF CONTENTS (CONTINUED)

		PAGE
SECTION 6	PULSED CO_2 LASER SOURCE	223
	SPECIAL SOURCES	234
	SUMMARY	238
	REFERENCES	242
SECTION 7	DETECTOR SUBSYSTEM	245
	INTRODUCTION	245
	DETECTOR REQUIREMENTS AND TYPES	245
	DETECTOR SUBSYSTEM AND COMPONENTS	251
	DETECTOR PROCESSOR	256
	DETECTOR SUBSYSTEM PHYSICAL SUMMARY	259
	RISK ASSESSMENT	260
SECTION 8	COMMAND AND DATA HANDLING SUBSYSTEM	261
	INTRODUCTION	261
	REQUIREMENTS	262
	DESIGN	265
SECTION 9	SYSTEM DEFINITION	283
	GENERAL	283
	SYSTEM CONFIGURATION	283
	SYSTEM ARRANGEMENT AND TEST	293
	SYSTEM DESIGN & CAPABILITIES SUMMARY	293
SECTION 10	PROGRAMMATICS	303
	PROGRAMMATIC PLANNING RATIONALE	303
	LIDAR PROGRAM DEFINITION	304
	LIDAR PROGRAM SCHEDULE	306
	WORK BREAKDOWN STRUCTURE	309
	LIDAR PROGRAM COST	312
	SUPPORTING RESEARCH AND TECHNOLOGY IDENTIFICATION AND LONG LEAD ITEMS	319
SECTION 11	CONCLUSIONS AND RECOMMENDATIONS	321

LIST OF FIGURES

		PAGE
SECTION 1		
1-1	Study Goal and Objectives	1
1-2	Study Technical Ground Rules	3
1-3	Atmospheric Lidar Definition Study Schedule	5
1-4	Allocation of System Requirements	6
1-5	Formulation of Lidar Program	7
SECTION 2		
2-1	Experiment Analysis Topics	10
2-2	Experiment Subsets	14
2-3	Background	18
2-4	Rayleigh Scattering vs. Wavelength	18
2-5	Initial Candidate Laser Types Developed From Science Fundamentals	19
2-6	Eye Safety Nomograph	25
2-7	Signal to Noise Ratio	28
2-8	Signal To Noise Ratio vs. Receiver Diameter	29
2-9	Single Shot Return Signal vs. Altitude	30
2-10	Expected Error H_2O Dial	30
SECTION3		
3-1	Shuttle Orbiter/Spacelab	34
3-2	Spacelab Flight Configurations and Services	36
3-3	Spacelab Pallet	38
3-4	Lidar Electrical Power	40
3-5	Lidar Thermal Control	42
3-6	Aft Flight Deck	46
3-7	Orbiter Pointing Capabilities	50
3-8	Lidar Operations	53
3-9	Lidar Cycle - Three Flights Per Year	58
3-10	Lidar Mission Cycles	59
3-11	Sample Potential Target Areas	61
3-12	Passes Over U.S.A. in 1 Day	64
3-13	Lidar Experiment Opportunities Timeline	65
SECTION 4		
4-1	Conceptual Lidar Growth Scenario	71
4-2	System Definition By Subsystem	76
4-3	System Design Approach	77
4-4	System Block Diagram	84

LIST OF FIGURES (CONTINUED)

		PAGE
SECTION 5		
5-1	Image Quality Requirements	92
5-2	Receiver Sizing Characteristics Parameter Trades	94
5-3	Optical Layouts Considered	97
5-4	Design Type Comparison	99
5-5	Design Type Comparison Image Quality	101
5-6	Focal Plane Optics - Basic Options	103
5-7	Limitation on Field of View	104
5-8	Collimating Focal Plane Optics	105
5-9	Transmittance/Coatings Component Data	108
5-10	Transmittance/Coatings	109
5-11	Polarization Effects for one 45° Surface	111
5-12	Stray Light Control	112
5-13	Mirror Trades	114
5-14	Error Budget	117
5-15	Primary-Secondary Metering Concepts	118
5-16	Receiver Thermal Design	120
5-17	Thermal Sensitivity Analyses (Representative)	121
5-18	Lidar Receiver Telescope Baseline Design Layout	124
5-19	Lidar Receiver Telescope Baseline Design Parameters	124
5-20	Active Electromechanical Devices	125
5-21	Receiver Electrical Block Diagram	126
5-22	Interface Definition	127
5-23	Growth Options	128
SECTION 6		
6-1	Identification of Functional Requirements for Visible and Near Visible Sources From SEED.	132
6-2	Methods of Obtaining the 215 nm Wavelength for Experiment 25.	148
6-3	Visible and Near Visible Sources System	152
6-4	Visible and Near Visible Sources System - Flight Engineering Status	156
6-5a	Transverse Pumping of Dye Laser	166
6-5b	Longitudinal Pumping of Dye Laser	166
6-6	Neodymium Laser: Representative Existing Design Examples	168
6-7	Two Joule Breadboard Laser	170
6-8	2J Nd:YAG Oscillator/amplifier layout	171
6-9	Two Kilowatt Power Supply	173
6-10	One Kilowatt Power Supply	173
6-11	High Average Power Frequency Doubling Module	178
6-12	Generic Dye Laser Block Diagram	180
6-13	Dye Laser Configurations	182
6-14	Examples of Spectral Control Loops	186
6-15	Typical Commercial Systems Capabilities	190
6-16	Optical Schematic of Dye Laser	195
6-17	Performance Provided By Seven Module System	200

LIST OF FIGURES (CONTINUED)

		PAGE
SECTION 6		
6-18a	System Configuration for Experiments 1-6	205
6-18b	System Configuration for Experiments 7, 11a.	205
6-18c	System Configuration for Experiments 8, 12a, 21	206
6-18d	System Configuration for Experiments 11b, 11c	206
6-18e	System Configuration for Experiment 12b	207
6-18f	System Configuration for Experiment 25	207
6-19	Physical/Optical Conceptualization for Seven Module System	208
6-20	Requirements Specification for Seven Module System	208
6-21	Basic Control Circuit For Stabilized Laser	217
6-22	Dither Method of Obtaining Frequency Discriminant for Stabilizing Laser Frequency	218
6-23	Stark Cell Frequency Stabilization	221
6-24	Conceptualization of CW CO_2 Laser	222
6-25	Intracavity Low Pressure CW Model Selection Scheme	228
6-26	Etalon Method of SLM Selection With Length Control	230
6-27	Possible System Block Diagram for CO_2 DIAL Experiments	232
6-28	Conceptualization of Pulsed CO_2 Laser	233
6-29	Source Development Timeline	241
SECTION 7		
7-1	Experiment Hardware Requirements	246
7-2	Detector Types	249
7-3	Detector Type Descriptions	250
7-4	Detector Type Requirements	250
7-5	Detector Subsystem Block Diagram	251
7-6	Detector Package Detail Block Diagram	252
7-7	Initial Narrow Band Interference Filter Bandwidth Assessment	253
7-8	Requirements for Photomultiplier Tubes	254
7-9	Processor Unit Requirements	256
7-10	Detector Processor Channel Block Diagram	257
7-11	Detector Processor Block Diagram	258
7-12	Detector Subsystem Physical Characteristics Summary	259
SECTION 8		
8-1	The End To End STS Data System	261
8-2	Science Requirements	263
8-3	Experiment Grouping By Requirements	264
8-4	Lidar Data Processes	265
8-5	Spacelab CDMS and Orbiter Avionics	267
8-6	STS Data System Links and Ground Facilities - Block Diagram	267
8-7	Rationale For Selected Approach	274
8-8	Lidar C&DH Subsystem	276
8-9	Lidar C&DM Functions	278
8-10	Lidar C&DM Capability	279
8-11	Lidar Software	280
8-12	Characteristics of Lidar C&DM	282

LIST OF FIGURES (CONTINUED)

		PAGE
SECTION 9		
9-1	System Functions	284
9-2	System Configuration	286
9-3	Lidar Basic Thermal Control Options	288
9-4	Thermal Control Subsystem Block Diagram	289
9-5	Alternate Configurations	291
9-6	System Assembly & Test Flow Plan	294
9-7	Lidar Assembly	295
9-8	System Arrangement	296
SECTION 10		
10-1	Programmatics	303
10-2	Study Technical Ground Rules	305
10-3	Lidar Summary Program Schedule	307
10-4	Lidar Basic Program Schedule	307
10-5	Lidar Schedule Risk Assessment	309
10-6	Work Breakdown Structure	310
10-7	Work Breakdown Structure (continued)	310
10-8	Lidar Cost Ground Rules	313
10-9	Lidar MUIS Cost	315
10-10	Lidar Program Funding Profile	316
10-11	Lidar Basic Program Cost Risk Assessment	317
10-12	Lidar Operations and Evolutionary Options	318
SECTION 11		
11-1	Conclusions	321

LIST OF TABLES

		PAGE
SECTION 2		
2-1	Experiment Class Descriptions	13
2-2	Experiment Quantification	16
2-3	Eye Safety Damage Mechanisms	23
2-4	Apertures and Effective Areas	26
SECTION 3		
3-1	Pointing Requirements	48
3-2	Real-Time Pointing Requirements	51
3-3	Lidar Preflight Ground Operations-Activity Descriptions	56
3-4	Experiment Operating Criteria	62
SECTION 4		
4-1	System Requirements Summary	75
4-2	System Performance Trade Summary	81
4-3	Subsystems Requirements	82
SECTION 6		
6-1	Visible and Near-Visible Candidates	140
6-2	Mixing: Applicable Experiments	145
6-3	Examples of Wavelength Flexibility with Modular System	150
6-4	2J Nd:YAG Laser Characteristics	172
6-5	Commercial Systems Comparison Data	193
6-6	Laboratory Systems Comparison Data	194
6-7	$CWCO_2$ Laser Source Requirement	209
6-8	CW CO_2 Laser Comparison	211
6-9	Pulsed CO_2 Device Comparison	225
SECTION 9		
9-1	System Performance Trade Summary	285
9-2	GSE Definition	297
9-3	System Test Requirements Matrix	298
9-4	Phase 1-System Design Characteristics Summary	298
9-5	Maximum Accommodation-System Design Characteristics Summary	299
9-6	System Power & Mass Margin Summary	299
9-7	System Evolutionary Capability	300
9-8	Preliminary System Interface Requirements For Principal Investigators	301

LIST OF ACRONYMS AND ABBREVIATIONS

ACRONYMS

AC	Alternating Current
ADP	Ammonium Di-Hydrogen Phosphate
AFD	Aft Flight Deck
C&DH	Command and Data Handling Subsystem (Lidar)
CDMS	Command and Data Management Subsystem (Shuttle)
CERVIT	Trade Name for A Low Expansion Glass
CO_2	Carbon Dioxide
CW	Continuous Wave
DC	Direct Current
DCC	DC Excited Conventional CO_2 Laser
DCWG	DC Excited Waveguide CO_2 Laser
DOMSAT	Domestic Communication Satellite
DSDS	Data Systems Dynamic Simulation
EC	Experiment Computer
ECAS	Experiment Computer Application Software
ECOS	Experiment Computer Operating System
EGSE	Electrical Ground Support Equipment
EPDB	Electric Power Distribution Box
ETR	Eastern Test Range
EU	Engineering Units
F	Fundamental
FD	Frequency Doubled
FQ	Frequency Quadrupled
FSR	Full Scale Response
FT	Frequency Tripled
FWHM	Full Width Half Maximum
GSFC	Goddard Space Flight Center
HRDM	High Rate De-Multiplexer
HRM	High Rate Multiplexer
IPS	Instrument Pointing System
IR	Infrared
JSC	Johnson Space Center
KBPS	Kilobits Per Second
KDP	Potasium Dihydrogen Phosphate
KD*P	Potasium Dideuterium Phosphate
KSC	Kennedy Space Center
LIDAR	Light Detection and Ranging
LO	Local Oscillator
MBPS	Megabits Per Second
MCC	Mission Control Center
MGSE	Mechanical Ground Support Equipment
MMU	Mass Memory Unit
MTU	Master Timing Unit
MUIS	Multi-User Instrument System
NASA	National Aeronautics and Space Administration
Nd:YAG	Neodymium: Yttrium-Aluminum-Garnet
OPA	Optical Parametric Amplifier
OPF	Orbiter Processing Facility
OPO	Optical Parametric Oscillator
PI	Principal Investigator

PK	Photocathode
POCC	Payload Operation Control Center
PS	Payload Specialist
PZT	Piezoelectric Tuner
RAU	Remote Acquisition Unit
RF	Radio Frequency
RFWG	Radio Frequency Waveguide CO_2 Laser
RMS	Root-Mean-Square
SDPF	Spacelab Data Processing Facility
SEED	Science Objectives Experiment Descriptions Evolutionary Flow Document
SH	Second Harmonic
SL	Spacelab
SLM	Single Longitudinal Mode
SRS	Stimulated Raman scattering
STS	Space Transportation System
TEA	Transverses Electrical Atmosphere
TDRSS	Tracking and Data Relay Satellite System
TH	Third Harmonic
ULE	Trade Name for Ultra Low Expansion Glass
UV	Ultra Violet
WBS	Work Breakdown Structure
WIP	Wire Ion Plasma
YAG	Yttrium-Aluminum-Garnet

ABBREVIATIONS

β	laser beam divergence
B	peak spectral brightness
b	absorption coefficient
c	velocity of light
^{o}C	degrees Celcius
cm	centimeters
D	aperture of beam diameter
dc	direct current
e	electronic charge
ϵ_o	permittivity of free space
f	frequency
f	focal length
g	gain
h	height of shaped laser beam
I	intensity
J	Joules
K	thermal conductivity
k	wave vector magnitude
$\mathcal{K}$	Gladstone-Dale constant
kg	kilograms
km	kilometers
kw	kilowatts
m	electronic mass
m	meters
mm	millimeters
um	micrometers

ABBREVIATIONS (CONTINUED)

mr	milliradians
n	refractive index
Ne	electron number density
nm	nanometers
P	peak power
P	average power
pm	picometers
Re	earth radii
ρ	density
ν	frequency
$\Delta\nu$	frequency bandwidth
τ	laser pulse length
T	temperature
θ	polar coordinate
ϕ	azimuth coordinate
w	width of shaped laser beam
w	frequency
wp	plasma frequency
Δf	laser bandwidth
δf	laser frequency dither
δP	modulation depth of laser power

SUMMARY

The Atmospheric Lidar Multi-User Instrument System Study (NAS1-15476) was performed for NASA Langley Research Center to quantify and definitize a spaceborne Lidar system for atmospheric studies. The primary inputs to this effort were the Science Objectives Experiment Description and Evolutionary Flow Document, called the SEED, generated by the Atmospheric Lidar Working Group and the Space Shuttle Payload Accommodation Handbook. These documents, along with the RFP defined study goal, study objectives, and technical ground rules formed the framework of the study consisting of four major tasks.

The first task was to perform an experiment evolutionary analysis. This task involved the analysis of the experiments contained in the SEED, in order to extract, and resolve performance requirements, establish priorities and generate protocols which allowed the definition of the baseline instrument system. The experiments were grouped into subsets and prioritized to match the instrument system evolutionary growth sequence. Technical deficiencies were identified in this task.

The second task was the system definition effort. This involved the identification of the evolutionary instrument system, the definition and description of the basic instrument system, and the definition of its operation and support requirements.

The third task was the generation of a program plan for the hardware phase of the program. This plan contained program operating guidelines, cost estimates, schedules, research and development requirements, and a risk assessment.

The fourth task was the supporting studies which included a Shuttle deficiency analysis, a preliminary safety hazard analysis, the identification of long lead items, and development studies required.

As a result of the study an evolutionary Lidar Multi-User Instrument System (MUIS) was defined. The MUIS occupies a full Spacelab pallet and was defined as utilizing its "fair share" of Spacelab resources. The base Lidar has a weight of 1300 kg, occupies a volume of 25,000 liters and uses a power of 250 watts (standby mode) to 3000 watts (maximum demand experiment).

The "base" Lidar MUIS will provide a 2 joule frequency doubled Nd:YAG laser that can also pump a tuneable dye laser with wide frequency range and bandwidth. A modular laser design provides for multiple wavelength capability. Special design provisions, including beam divergence angle control, were defined to assure eye safe laser operation. In addition, accomodation of up to a total of four lasers is provided including other Nd:YAG lasers, CW CO_2 lasers, an "on axis" pulsed CO_2 laser and special lasers (Principal Investigator provided). The MUIS includes a 1.25 meter diameter aperture Cassegrain receiver, with a moveable secondary mirror to provide precise alignment with the laser. The receiver can transmit the return signal to up three single and multiple PMT detectors by use of a rotating fold mirror. Provisions to provide a flip-out mechanism for the fold mirror allows the MUIS to accommodate "on-axis" heterodyne or special detectors.

The MUIS has an autonomous data subsystem for system control and display,and payload specialist "quick look" data evaluation. The structural, thermal and power subsystems were defined to provide flexible system operation and accommodation of growth equipment to accomplish envisioned experiments.

Throughout the system definition the envisioned Spacelab usage requirements were incorporated. The Lidar MUIS will use only its fair share of Spacelab resources, has modularity that permits its operation on up to three flight missions per year (with refurbishment and reconfiguration), and is capable of both day/night operation.

The Lidar MUIS Program can be implemented to permit initial launch in 1984-1985 time period and incorporates features that provide a 10-year operational life (at up to 3 flights per year). Its design can accommodate both envisioned evolutionary growth and Principal Investigator equipment.

In this report the experiment analysis is followed by the Space Transportation System capabilities description and the system requirements. Following this are descriptions of the major subsystems; the laser source, the receiver, the detector, and the command and data handling subsystems. The remainder of the report contains the system description, the programmatics and the conclusions and recommendations.

1.0 INTRODUCTION

1.1 STUDY GOAL AND OBJECTIVES

This report documents the results of the National Aeronautics and Space Administration (NASA) Langley Research Center contract NAS1-15476,"Atmospheric Lidar Multi-User Instrument System Definition Study". The study results are fully responsive to the defined goal and objectives which are shown in (Figure 1-1).

GOAL

- IDENTIFY AND DEFINE AN EVOLUTIONARY MULTI-USER LIDAR SYSTEM

OBJECTIVES

- ANALYZE SCIENCE OBJECTIVES, EXPERIMENT, DESCRIPTION AND EVOLUTIONARY FLOW DOCUMENT (SEED)
- IDENTIFY AND DEFINE SYSTEM, SUBSYSTEMS AND ASSEMBLIES OF A MODULAR LIDAR
- PREPARE PROGRAM PLAN
- IDENTIFY TECHNOLOGY DEVELOPMENT, LONG LEAD ITEMS, SAFETY AND SHUTTLE DEFICIENCY STUDIES

Figure 1-1. Study Goal and Objectives.

The study goal, identification and definition of an evolutionary multi-user Lidar system, was accomplished. The Lidar system defined is capable of performing a wide range of atmospheric measurements from the Shuttle Orbiter, as a Spacelab pallet mounted system. Furthermore, the defined system is technologically ready for implementation on a schedule that will permit operational missions in the mid 1980's.

To achieve this goal, the specific major objectives of the study were analyzed and assessed. These key objectives shown in Figure 1-1, were completed and provide a firm basis for implementation of a high confidence, low risk Lidar Program.

The analysis of the SEED quantified the atmospheric measurements required by the specific experiment classes and the laser, receiver, and detector characteristics required to provide the experiment accuracy. These instrument system requirements were then assessed for commonality and combined into logical "groups" that would form a modular Lidar Instrument. Trade-off analyses were then conducted to identify the system, subsystem and assembly definitions. Additional criteria such as instrument flexibility, technological readiness and relative cost were considered in the conduct of this effort. The resulting modular Lidar Instrument was then analyzed to provide a specific design definition for each subsystem and assembly, to establish confidence that the design concept was viable and to provide the definition depth necessary for the Lidar Program Plan. The major efforts in the formulation of this Program Plan were the determination of schedule and cost, and their associated variability with risk. The establishment of the schedule and cost by a "bottoms up" approach from the assembly level resulted in definition of a low-risk program schedule and establishment of a high-confidence program cost. Finally the Lidar Instrument definition and Program Plan were used to identify the technology development equipment, the long lead items, and the safety aspects of the program.

1.2 STUDY TECHNICAL GROUND RULES

The study was conducted using technical ground rules defined in Figure 1-2. These ground rules identified the "first level" criteria for the assessments, analyses and trade studies conducted within the study. It was recognized that a realistic programmatic rationale had to be in concert with the Shuttle era philosophy for multi-user, multi-flight experiment payloads. Cost criteria requires the accommodation of the largest number of experiments, to assure maximum use in orbit, and hence a high scientific return on payload investment. A modular design was mandated since this approach can provide cost effective accommodation for the desired three flights per year with potential reconfiguration between flights.

- INSTRUMENT DEFINITION FOR MAXIMUM LIFE AT LOWEST OVERALL COST
  - ACCOMMODATE THE LARGEST NUMBER OF EXPERIMENTS
  - COST EFFECTIVE ACCOMMODATION
- MODULAR DESIGN
  - LOWEST EXPERIMENT INTEGRATION TIME
  - PERMIT RECONFIGURATIONS BETWEEN FLIGHT
  - CAPABILITY TO PERFORM 3 MISSIONS/YEAR
- FLEXIBILITY
  - SEVERAL TYPES OF MEASUREMENTS DURING ANY ONE MISSION
  - ACCOMMODATE PRINCIPAL INVESTIGATOR LASERS AND DETECTORS
  - CAPABILITY FOR "TARGET OF OPPORTUNITY"
  - PROVIDE PAYLOAD SPECIALIST "QUICK LOOK" DATA
- GROWTH
  - MAXIMUM ACCOMMODATION OF LASERS AND DETECTORS
  - TIME PHASED IMPLEMENTATION
- FIRST MISSION SUCCESS POTENTIAL
  - HIGH

Figure 1-2. Study Technical Ground Rules.

The ground-rule to produce a flexible instrument design was imposed for diverse considerations. For a single flight configuration/mission, a flexible instrument can

accommodate several types of experiment measurements, preventing any single failure from causing total mission failure. Accommodation of principal investigator lasers and detectors is achieved by simple, clean interfaces. A flexible control and data handling subsystem, using prestored experiment sequences commanded by the payload specialist, is required to accommodate "targets of opportunity". Lidar instrument system growth calls for sophisticated configuration management to provide for maximum simultaneous accommodation of lasers and detectors, with time phased implementation based upon scientific priority and/or technology status of the equipment.

First mission success potential is established to provide high confidence in acquiring experimental data and relates directly to the instrument flexibility. Achievement of this technical ground rule is provided by multiple experiment measurement capability, and reliability of components and subsystems.

1.3 STUDY SCHEDULE

The Atmospheric Lidar Definition Study was performed in accordance with the schematic shown in Figure 1-3. The effort consisted of four major task areas, logically phased to provide for systematic progression from the science requirements, through the system design to the programmatic planning and supporting studies. Figure 1-3 defines the primary subtasks within each task area to show the primary thrust of the effort.

Three major reviews were conducted during the course of the study. The analysis task review was the first major contractual milestone. This review assessed progress, and expanded and clarified the science requirements. The mid-term review was a formal presentation to Langley Research Center's Study Office and the Science Working Group. This resulted in guidance for the final phase of the study. The final oral review, was a comprehensive presentation of study results, assessments, trade-offs, and options, that led to the Lidar instrument definition and programmatic planning. This

was an open meeting presented to the Langley Research Center Study Office, the Science Working Group, and interested industry technical personnel.

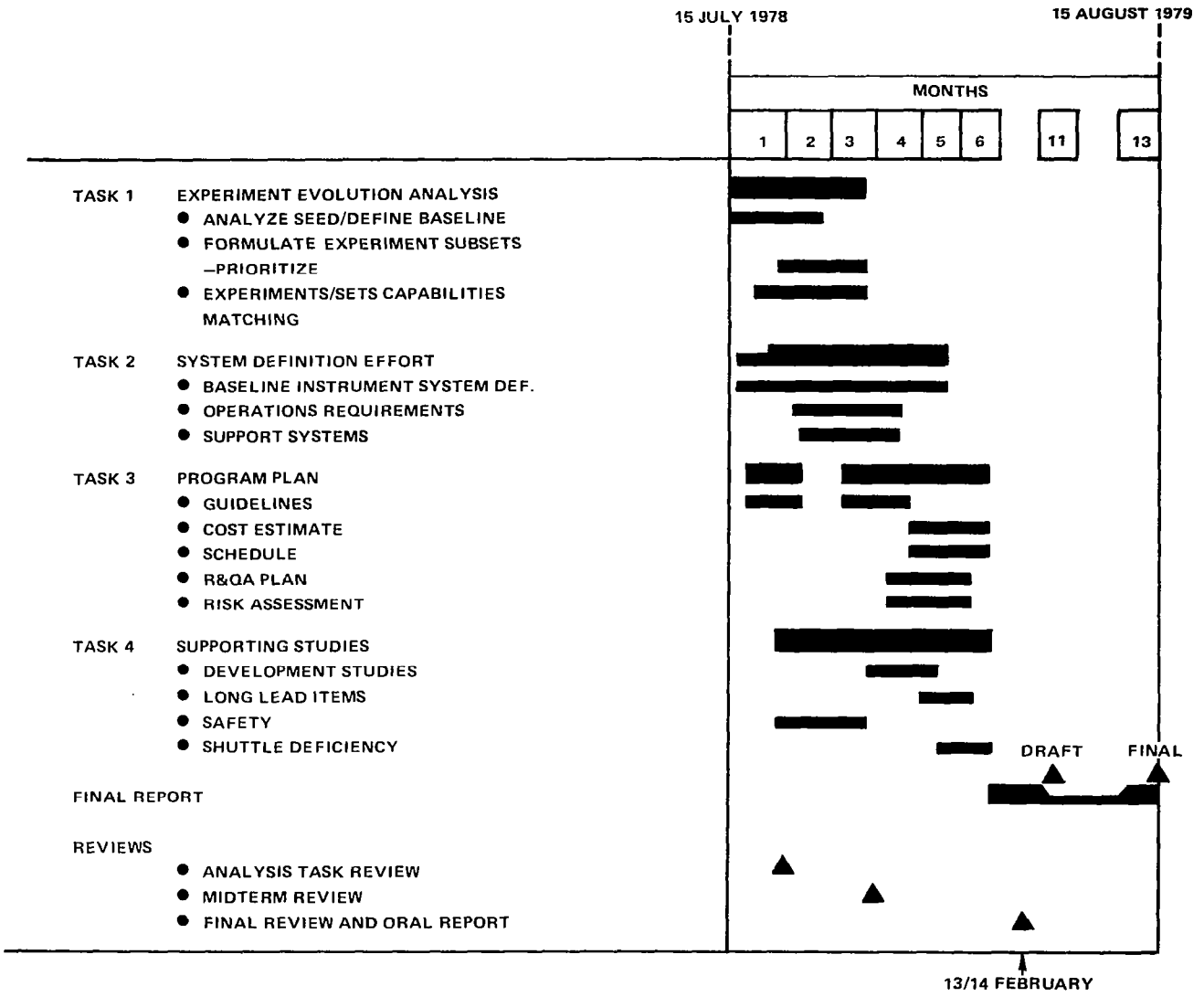

Figure 1-3. Atmospheric Lidar Definition Study Schedule.

1.4 STUDY RATIONALE

The study was conducted within the framework defined by the goal, objectives and technical groundrules. The science requirements were used as the driver for the Lidar system and subsystem requirements, as shown in Figure 1-4. Constraints influencing requirements determination included the technology status of primary instrument equipment, the resources, and operational features of the Shuttle. Technology status provided basic inputs for Lidar instrument evolutionary growth. Equipment requiring technology development was deferred in time compared to state-of-the-art equipment. STS constraints of weight, power, volume, payload specialist capability and time, became the boundary conditions for the Lidar instrument definition. Additionally, ground operational factors were considered to permit the required three flight missions per year with possible reconfiguration between missions.

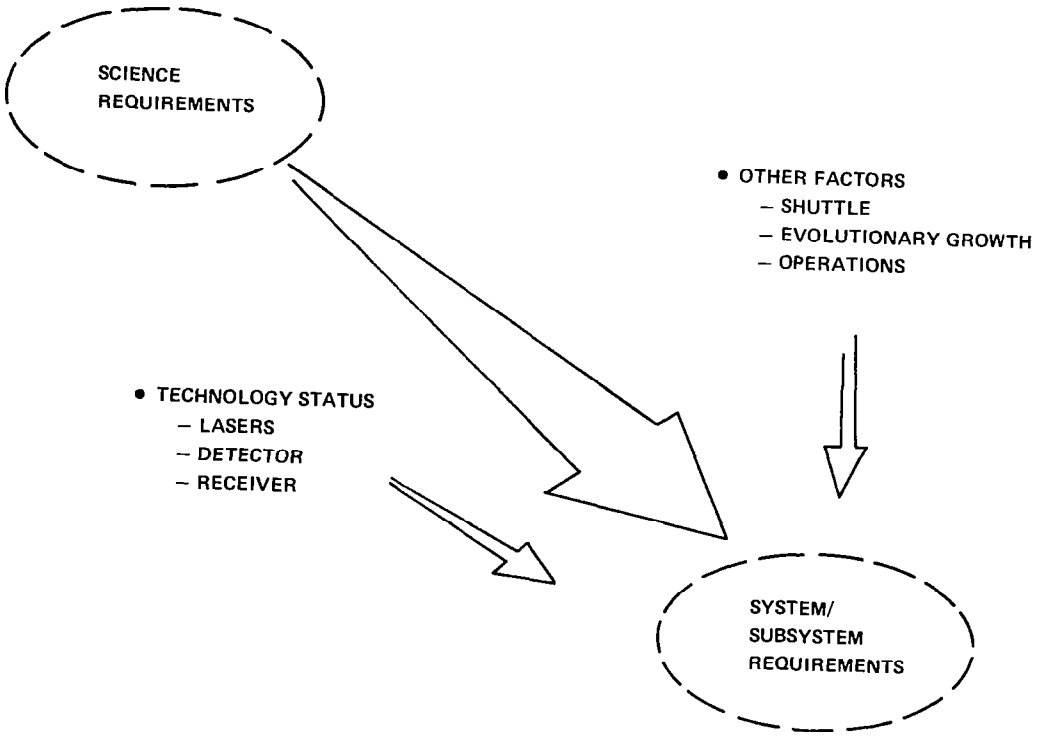

Figure 1-4. Allocation of System Requirements.

This allocation of system requirements was used as the foundation for the formulation of the program as shown in Figure 1-5. Technical trade-offs, design/definition options, and cost assessments were conducted to achieve the system/subsystem definition which was then evaluated against programmatic factors, such as cost, schedule and risk in arriving at the total Lidar program formulation.

The breadth and complexity of the study required the iterative and interactive approach of the described rationale to arrive at the final study results. These iterations were performed to provide assurance that the Lidar design and programmatics conformed to the program goal and objectives in a technologically ready and cost effective manner.

Identification of commercial products in this report is to adequately describe the materials and does not constitute official endorsement, expressed or implied, of such products or manufacturers by the National Aeronautics and Space Administration.

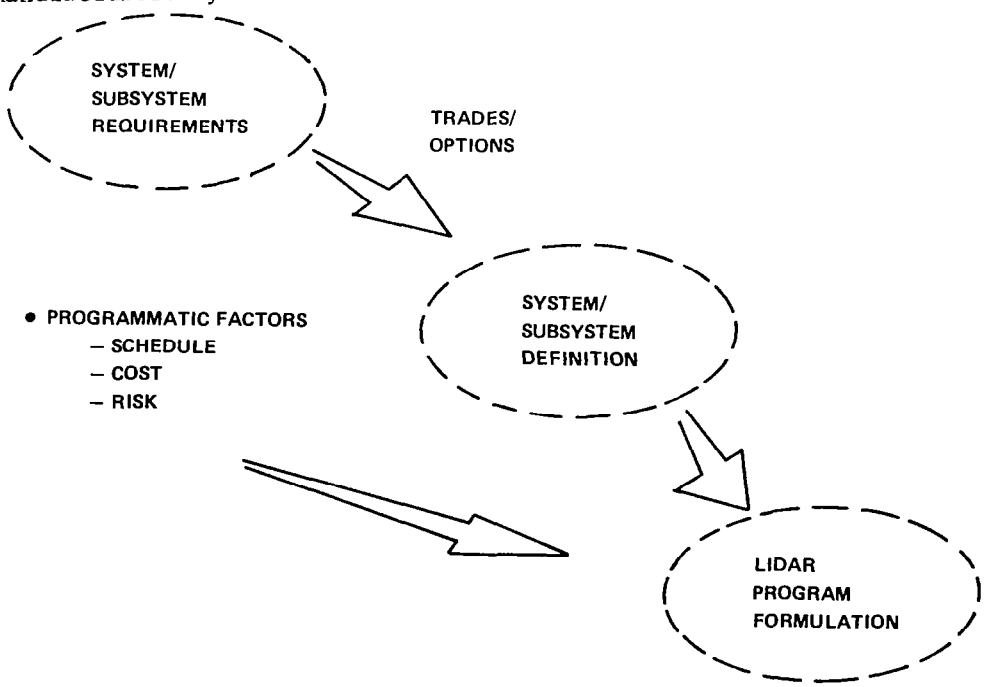

Figure 1-5. Formulation of Lidar Program.

2.0 EXPERIMENT ANALYSIS

2.1 INTRODUCTION

Task 1 of the study, the experiment evolutionary analysis, began with an analysis of the Science Objectives Experiment Descriptions Evolutionary Flow Document, which is hereafter referred to as the SEED. The forgoing has been incorporated in a NASA document titled "Shuttle Atmosphere Research Program" (NASA Document No. SP-433). This analysis, as shown in Figure 2-1, along with additional inputs from published material, NASA, the Science Working Group members and General Electric led to the quantification of selected experiments which were then used throughout the remainder of the analysis. This was an iterative process during which updates of the SEED were generated by the Science Working Group.

The quantification of the experiments was a process which allowed the experiments to be described in terms of a common set of normalized parameters called a unit Lidar. This allowed the optical signal received at the Lidar to be described in terms of the unit Lidar for both background and species scattering.

Parametric analyses were then performed using the quantified experiment science requirements as a basis for generating technology trades from the hardware state of the art. Constraints, such as eye safety and the Space Transportation System capabilities were factored into the iterative process by which the baseline Lidar parameters were developed. The analysis was tempered throughout by the low risk requirement for the first blocks of experiment hardware.

During the latter part of the parametric analysis it became possible to separate the

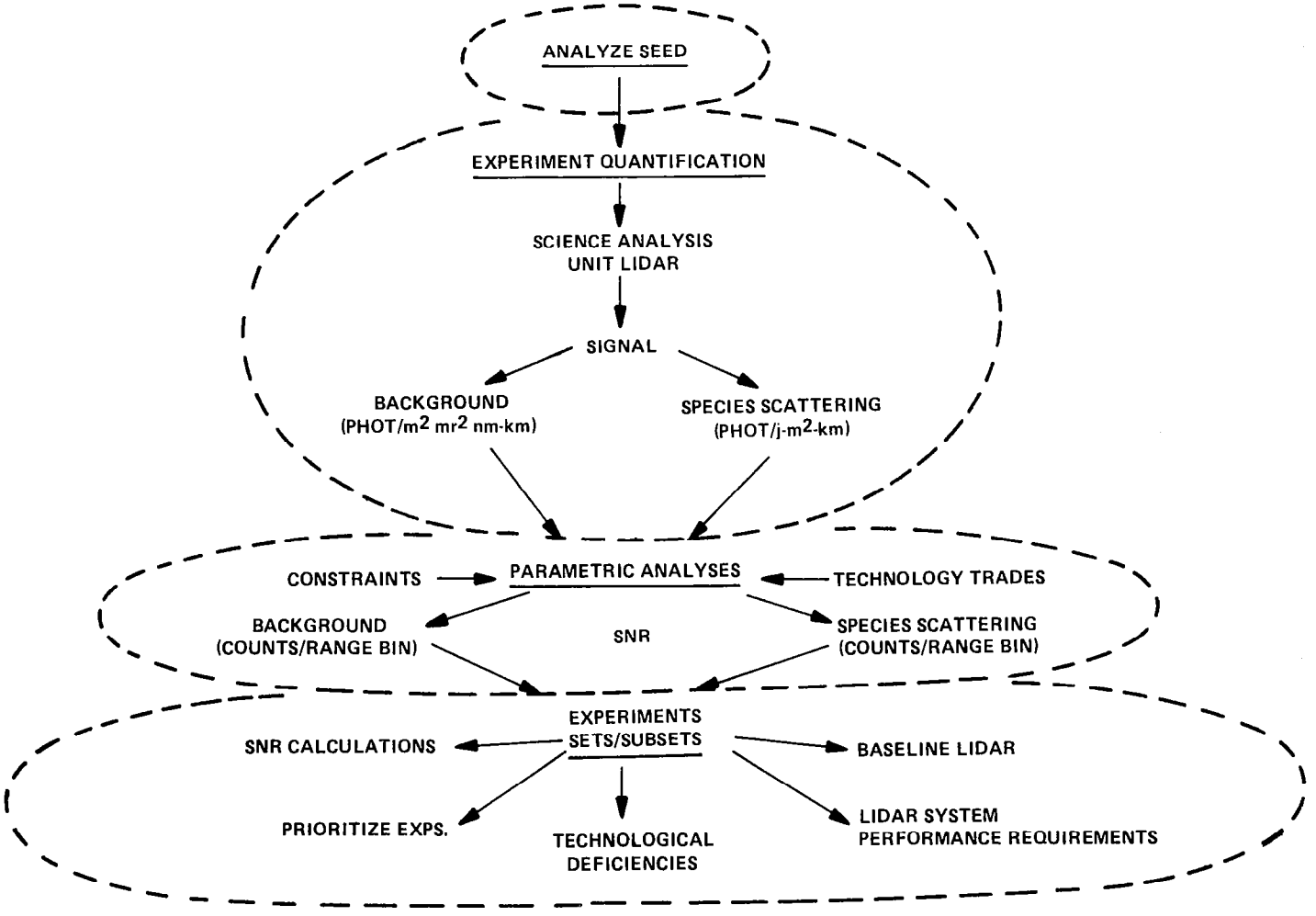

Figure 2-1. Experiment Analysis Topics.

experiments into meaningful sets and subsets which could be performed in a logical progression of hardware growth steps without compromising the low risk requirement for the initial flight sequences. Prioritization of the experiments was then done on the basis of technical risk, with the early subsets presenting the least risk.

Lidar performance parameters were then finalized and technological deficiencies and long lead items were identified for further use in the system definition effort.

2.2 SEED ANALYSIS

The SEED was analyzed in order to determine the experiment science requirements. The information which was extracted included the primary wavelength of interest, the bandwidth, the specie to be detected and the measurement method or technique to be used. In some cases there was considerable latitude in the choice of parameters, for example experiment classes one through six could be done at most wavelengths, while in other cases almost no latitude was available, such as the experiment classes which utilize resonant fluorescence.

Other requirements were obtained from the SEED such as the required accuracy, from which the signal to noise ratio required per range bin could be calculated. In addition the SEED contained some information on correlative sensors and hardware configurations. Information on data requirements was also extracted which gave information on resolution, both spatial and temporal, pointing, geographic coverage desired and on numerous other aspects of each experiment.

Where complete information was not available from the experiment simulation contained in the SEED other sources were tapped to provide a clear picture of what was required for each experiment class. The literature was searched for information on how the experiments had been performed on the ground or from aircraft, specific questions were asked of NASA and members of the Science Working Group and discussions were held

with investigators elsewhere in the science community.

This body of information was sifted, culled and assembled into a set of working matrices in which experiment classes were portrayed against the known parameters. For those areas where no information was available assumptions were made, based upon General Electrics' background in Lidar applications, to complete the matrix to a point where quantification of the experiments could be done.

For referrence, the experiment class descriptions are shown in Table 2-1 along with the wavelength of interest as found in the SEED. Figure 2-2 indicates one of the types of matrices which were used to present the information gathered, this figure also shows the information on experiment sets and subsets which was actually generated further along in the iterative study process. The initial figures of this type simply presented wavelength vs. experiment classes. It was only after many iterations and the development of a philosophy of hardware procurement timelines that the final distribution shown here was obtained. This figure will be discussed in more detail later in this report.

2.3 EXPERIMENT QUANTIFICATION

A science analysis was performed on the parameters in terms of a hypothetical normalized Lidar instrument. This unit Lidar was defined as:

Energy output - 1 Joule at any wavelength
Receiver area - 1 square meter
Receive FOV - 1 milliradian
Filter bandwidth - 1 nm
Range Bin length - 1 km

This particular set of parameters was chosen for two major reasons. First, when evaluated at the primary mid-visible wavelength discussed in the SEED (530 nm), the unit Lidar provided a good "first cut" at defining the system from an engineering

Table 2-1. Experiment Class Descriptions

EXP. CLASS	TITLE	WAVELENGTH OF INTEREST
1.	MEASURE CLOUD TOP HEIGHT	530/1060 nm
2.	PROFILING OF TROPOSOPHERIC CLOUDS AND AEROSOLS	530/1060 nm
3.	CIRRUS ICE/WATER DISCRIMINATION	530 nm
4.	PROFILES OF NOCTILUCENT CLOUDS AND CIRCUMPOLAR PARTICULATE LAYERS	530/1060 nm
5.*	EARTH SURFACE ALBEDO MEASUREMENT	530/1060 nm
6.	STRATOSPHERIC AEROSOL BACKSCATTER PROFILES	530/1060 nm
7.	ALKALI ATOM DENSITY PROFILES	589/671/770 nm
8.	IONOSPHERIC METAL ION DISTRIBUTIONS	280 nm & OTHER RESONANCE LINES
9.	WATER VAPOR PROFILES	TWO NEAR 720 AND 940 nm
10.	ATMOSPHERIC SPECIES MEASUREMENTS – IR LASER GROUND AND CLOUD RETURNS	TWO IN 9–11 μm RANGE
11.	CHEMICAL RELEASE DIAGNOSTICS	SEVERAL IN 400-600 nm RANGE
12.	STRATOSPHERIC OZONE CONCENTRATION PROFILES	265 nm to 300 nm
13.	UPPER ATMOSPHERIC TRACE SPECIES MEASUREMENT USING TWO SATELLITE EARTH OCCULTATION	TWO IN 9 – 11 μm REGION OR SCANNING LASER
14.	SODIUM TEMPERATURE AND WINDS	589 nm
15.	SURFACE PRESSURE AND CLOUD TOP PRESSURE AND HEIGHT MEASUREMENT	TWO NEAR 760 nm
16.	VERTICAL PROFILES OF ATMOSPHERIC PRESSURE	TWO NEAR 760 nm
17.	TROPOSPHERE/TROPOPAUSE TEMPERATURE PROFILES	TWO NEAR 760 nm
18.	ALTITUDE DISTRIBUTION OF ATMOSPHERIC CONSTITUENTS IR DIAL	TWO IN 9 – 11 μm RANGE
19.	MEASURE CLOUD TOP WINDS TO ± 5 m/SEC	350 nm - 1100 nm + 9-11 μm
20.	AEROSOL WINDS BETWEEN GROUND AND 30 km ALTITUDE	0.35 TO 11 μm
21.	OH DENSITY PROFILES 35-100 km	~ 300 nm
22.	SIMULTANEOUS MEASUREMENT OF METALIC ATOM, ION AND OXIDE PROFILES	280, 285, 500 nm (THREE SIMULTANEOUS)
23.	TROPOSPHERIC NO_2 CONCENTRATION PROFILE – TOTAL BURDEN OF NO_2	442 + 448 nm (TWO SIMULTANEOUS)
24.	STRATOSPHERIC AEROSOL COMPOSITION	9 - 11 μm
25.	NO DENSITY PROFILES BETWEEN 70 AND 150 km ALT.	215 TO 227 nm
26.	ABUNDANCE AND VERTICAL PROFILES OF ATOMIC OXYGEN	225 nm TRANSMIT 844.9 RECEIVE

*#5 IS PART OF #2

EXPERIMENTS	LASERS	Nd X 2 VERY NARROW LONG PULSE (3μs)	TWO EACH OF IIA AND ONE OF IIB	Nd X 2 POL 1000: 1	TUNABLE PULSED CO_2 HET DET	TUNABLE CW CO_2 HET DET	TWO EACH OF IIB	TWO EACH OF II	Nd X 2 X 3 · D N	Nd X 2 · D N X 2	Nd X 2 · D N	Nd X 4	Nd X 2	1 P M T	2 P M T (INCLUDES 1060 COOLED)	9 11 nm CRYO HET	2 PMT + POL	3 PMT	FAB-PER.	DETECTORS	EXPERIMENTS
26		225.6								225.6					844.9							26
25										215					215							25
24						9 11 nm											9-11 nm					24
23								*442 2 448 6								442.2 448.6						23
22				279.6 285.2 500															279.6 285.2 500			22
21										300					300							21
20			530			9-11 nm											9 11 nm			530		20
19			530			9-11 nm											9 11 nm			530		19
18						*9-11 nm											9-11 nm					18
17									*TWO NEAR 760						760							17
16															760							16
15															760							15
14											589									589		14
13						*9 11 nm	*9-11 nm										9 11 nm					13
12											280 300		265		265-300							12
11										455 4 493 4		589			455 4 493.4 589							11
10						*8-11 nm	*9-11 nm										9-11 nm					10
9									*TWO NEAR 720 OR 940						940 720							9
8											279 6				279.6							8
7												589 770 671			589 770 671							7
6													530 + 1060			530 + 1060						6
4																						4
3					630 1000:1 POLARIZED													530				3
2													530 + 1060			530 + 1060						2
1													530 + 1060			530 + 1060						1
EXPERIMENT SUBSET NO.		VIII	VII	VI	VA	V	IV	IIIA	III	IIB	IIA	II	IA	I	IA II IIA IIB III IIIA VIII	I	IV V	VA	VI	VII	EXPERIMENT SUBSET NO.	

*TWO SIMULTANEOUS OR NEAR SIMULTANEOUS WAVELENGTHS
:MULTIPLE WAVELENGTHS
EXPERIMENT NO 5 IS INCLUDED AS PART OF EXPERIMENT NO 2
WAVELENGTHS ARE IN NANOMETERS EXCEPT AS INDICATED

Figure 2-2. Experiment Subsets.

viewpoint, thus allowing the preliminary engineering assessments of size, weight, power, etc., to proceed without waiting for the completion of the science analysis. Second, the unit Lidar parameters are all in the range of parameters to be considered for the final system and provide an excellent basis for starting the parametric analysis. In addition, the unit Lidar allows the experiment science requirements to be defined in terms of a common set of equipment parameters which provides an effective method of comparing the experiment requirements over a broad range of experiment classes. The unit Lidar was used to determine background and signal in terms of photons/m^2-$mrad^2$-nm-km for background and photons/m^2-j-km for signal.

The initial science analysis was done using a worst case analysis in which the background was assumed to be a zenith sunlit 100% reflective Lambertian reflector and the specie signal return was Rayleigh scattering. This technique provided both a limiting case for the Lidar parametric analysis and a conservative basis for the system design definition.

The experiment quantification was done in a series of study elements. The element titles are listed in Table 2-2. Examples of the type of information provided are shown on Figure 2-3 which is a plot of background for both zenith sunlight and zenith full moonlight on a 100% Lambertian reflector, and on Figure 2-4 which is a plot of Rayleigh scattering as a function of wavelength for various signal return heights for the median Shuttle altitude of 300 km.

Table 2-2. Experiment Quantification

QUANTIFIED ELEMENTS
BRIGHTNESS OF MOONLIT EARTH
EARTH BACKGROUND – ZENITH SUN – 100% LAMBERTIAN
EARTH REFLECTIVITY – BACKGROUND & EARTH RETURN
WAVELENGTH RANGE OF INTEREST
CANDIDATE LASERS FOR SHUTTLE ATMOSPHERIC LIDAR
RAYLEIGH BACKSCATTER SIGNALS FOR Nd LASERS
RAYLEIGH BACKSCATTER SIGNALS FOR EXPERIMENT CLASS 9
RAYLEIGH BACKSCATTER SIGNALS FOR EXPERIMENT CLASS 12
PROGRAM SLID (SATELLITE LIDAR)
RAYLEIGH SCATTERING VS λ FOR VARIOUS ALTITUDES
ESTIMATES OF RECEIVED PHOTONS DUE TO SODIUM FLUORESCENCE
ESTIMATES OF RECEIVED PHOTONS DUE TO MAGNESIUM ION FLOURESCENCE
EXPECTED PHOTON LEVELS FROM CLOUD BACKSCATTER
CHEMICAL RELEASE DIAGNOSTICS
POLARIZED COMPONENTS WORST CASE RETURN
EYE SAFETY REQUIREMENTS
TRADE OFF CONSIDERATIONS FOR LIDAR SCALING
DAY BACKGROUND REDUCTION IN FRAUNHOFER LINES
WATER VAPOR DIAL SIGNAL RETURN ESTIMATES
WORST CASE S/N ANALYSIS FOR ICE/WATER POLARIZATION EXPERIMENT

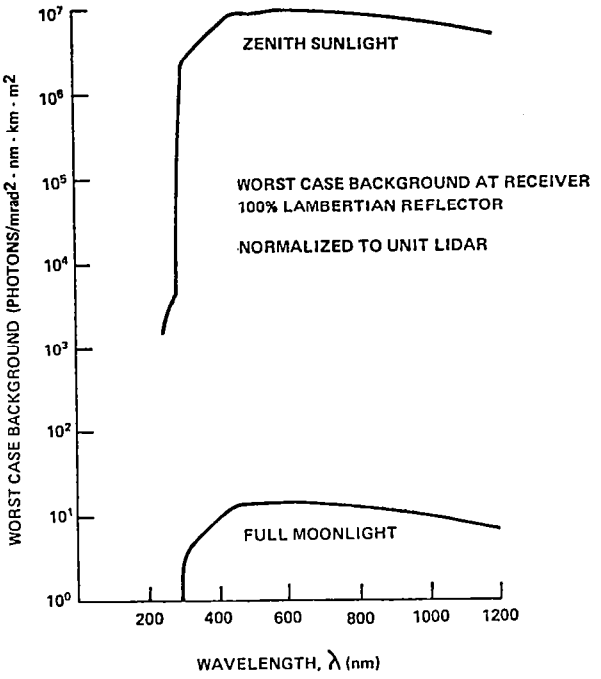

Figure 2-3 Background.

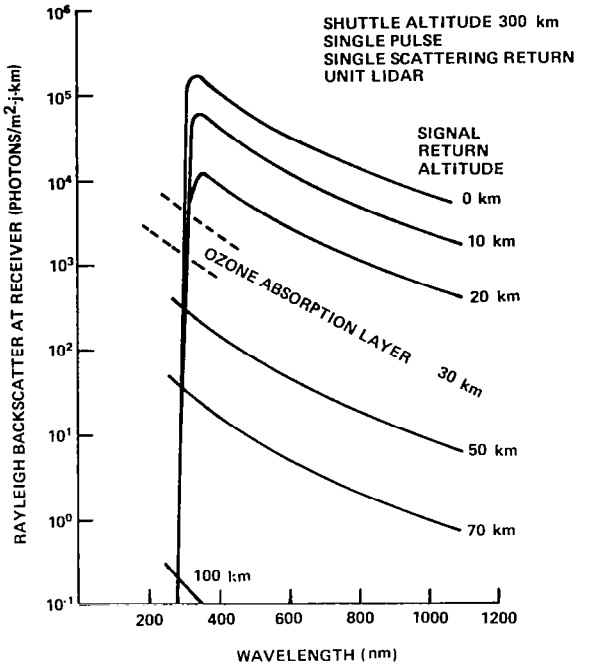

Figure 2-4. Rayleigh Scattering vs. Wavelength.

2.4 PARAMETRIC ANALYSIS

2.4.1 TECHNOLOGY TRADES

Analyses were conducted which utilized the quantified experiment results as a basis for performing technology trades in order to develop the hardware blocks which were best suited to meet the needs of the system. The major items considered in this area were lasers, detectors, receivers and the possible need for an active coalignment method between the laser transmitter and the receiver. The technology trades were first done from a science requirement standpoint and later, as the basic system began to evolve, identified system constraints were added, such as technology limitations of the hardware, eye safety, and the constraints imposed by the Space Transportation System (power, energy, cooling limitations, and crew time).

2.4.2 MAJOR LASER TRADES

The initial consideration given to the lasers covered the wavelengths of interest and availability, the average power consumed to obtain approximate energies per pulse and repetition rates, and to a lesser extent the beam quality, shape, divergence, and pulse length capabilities of various lasers. The initial candidate laser types are shown in condensed form in Figure 2-5. Other lasers were considered, of course, but the requirement for low technical risk in the early flights and the technology status of other laser types limited their usefulness in this matrix. Many trades were conducted on the various hardware options. The major trades for each option are discussed in the following paragraphs.

The areas for which major trades were conducted are described below;

- Average Power-

  The maximum average power available is limited by Shuttle capabilities and the requirements of the other experiments which may be onboard at the time in question. The results of systems analyses indicate that the laser subsystem can be allotted about one half the total power available to the Lidar system. The results of this analysis indicate that the laser subsystem will have about 1500 watts available to it.

- Energy Per Pulse/Repetition Rate

  A primary driver on laser energy is that laser pumped dye lasers require maximum pump energy per pulse in order to achieve reasonable output energies. A limitation on laser energy is the energy density limitations on the ground required to meet eye safety, requirements, particularly in the wavelength region between 400 and 700 nanometers. Neodymium-YAG lasers, for example, were evaluated in the 0.5 joule to 4 joules per pulse range. The analysis indicated

	EXPERIMENT NUMBER	1	2	3	4	* 5	6	7	8	9	10	11	12	13	14	15	16	17	18	19	20	21	22	23	24	25	26
LASER TYPE	Nd	X	X	X	X	X	X	P	P	P		P	X	X	P	P	P	P	X	X	X	X	P	P		P	P
	RUBY	X	X	X	X	X	X	P	P	P		P	P		P	P	P	P	X			X				P	
	LASER PUMPED DYE	X	X	X		X		X	X	X		X	X		X	X	X	X				X	X	X		X	X
	FLASH PUMPED DYE							X	X	X		X	X		X	X	X	X									X
	CO_2 PULSE	X																	X	X	X				X		
	CO_2 CW										X			X													
	EXCIMER	X										X	X									X			X	X	

* #5 IS PART OF #2
X - POTENTIAL SOURCE
P - PUMP FOR DYE

Figure 2-5. Initial Candidate Laser Types Developed From Science Fundamentals.

that the available power could support a laser operating range from 0.5 joule per pulse at a 40 Hz rate up to 4 joules per pulse at a 5 Hz rate. The 0.5j/40Hz laser has insufficient energy to pump the dye laser module to give the required energy output levels. With low energy levels out of the dye laser then a large receiver area would be required to achieve useable signal to noise ratios. The 4 joule/5 Hz laser on the other hand represents the near term technology limit in lasers to meet the flight requirement. The associated receiver size required fits easily into the available space, but the beam divergences required to meet eye safety limitations are large. The results of this trade indicated that a 2 joule neodymium-YAG laser operating at 10 Hz was the optimum choice for the baseline laser.

- Beam Quality/Shape/Divergence

This analysis evaluated a multimode versus a single mode baseline laser. Using the stipulations that the receive beam divergence shall never be less than the transmit beam divergence, that eye safety criteria on the ground must be met at all times and day beam divergence must be small enough so that a reasonable signal to noise ratio is obtained with available filters, then the daytime beam divergence for the laser can be calculated. The analysis indicated that a multimode laser required a collimating telescope of about 350 millimeters in diameter to achieve that beam divergence, while a single mode laser could be collimated with less than a 100 millimeter aperture. In addition, the multimode laser forces a penalty of approximately 1.5 times on the eye safety problem due to hot spots within the beam. The results of this trade slightly favored the single mode over the multimode laser for the baseline system.

2.4.3 Major Detector Trades

In the detector area consideration was given to the types of detectors, quantum efficiency, noise level, gain, bandwidth, and dynamic range. The major trades in the detector area involved the choice of photodiodes versus photomultiplier tubes. The quantification of the experiments shows that much of the data obtained with the Lidar instrument will be in the photon counting mode at night. While very good quantum efficiencies are available with photodiodes, particularly in the red and near infrared, the counting of single photon events is not practical because of low signal levels out of the devices. In addition, most solid state photodiodes do not have good quantum efficiencies at the shorter visible and ultra-violet wavelengths. For these reasons the result of this trade indicated that photomultiplier tubes should be used in the near IR to the UV spectral areas. Other detector types were considered for special experiment classes. For example, at the far infra-red wavelengths a cryogenic heterodyne detector is required. In addition, one detector must be capable of separating the two polarization components for the cirrus ice/water experiment and a high resolution dispersive element is required with appropriate detecting elements for other experiment classes.

2.4.4 Major Receiver Trades

In the receiver area the major driver from the science standpoint is the affect of aperture selection. Second order affects such as coatings and the number of surfaces in the telescope are discussed in the receiver section of this report. Apertures in the range of 0.5 meter diameter to 2.5 meter diameter were considered. During the evaluation it was apparent that the receiver selection is a compromise between cost/size; however, the technical guideline that the receiver accommodate all experiment classes drove the selection to the larger size range. Aperture was traded with signal to noise ratio for the various system parameters of laser energy,

field of view and filter bandwidth. The result of the system trade indicated that a receiver diameter of 1.25 meter could be used. This size for the receive mirror is adequate to provide the required signal to noise ratios with the laser size chosen, even though the science desires tend to drive the mirror to the largest possible size.

2.4.5 CONSTRAINTS

The constraints on the system involved the limitations in energy density at or near ground level due to eye safety constraints, the Space Transportation system constraints of power, total energy, cooling, volume, weight and crew availability time and the limitations of existing or forseable technology. In addition the requirement for low risk in the early flight blocks was considered.

2.4.5.1 Eye Safety

The basis for the eye safety considerations used in the study was the American National Standard for the Safe Use of Lasers (ANSI-Z136.1-1976). This document details the maximum permissible exposure (MPE) allowed for human exposure as a function of wavelength. In addition, a set of criteria for use in the eye safety analysis was assumed. These criteria include the following items:

- For Day - The day adapted eye with a pupil diameter of 2.5 mm
- For Night - A 10-inch diameter telescope over land and 50 mm binoculars over sea
- Atmospheric scintillation effects give hot spots which are 10 times the mean energy density
- Multimode laser beam inhomogeneities are 3 times the mean energy density
- Gaussian laser beam peak inhomogeneities are 3 times the mean energy density
- Atmospheric Transmission is 50%

These criteria were selected as conservative, reasonable values and are not intended as the final word on eye safety requirements. They are used in the analysis to show that published eye safe energy densities on the ground and in near ground air space can be met with a system of the size and type under consideration. The development of the operational eye safety criteria will require a stringent examination of parameters, such as scintillation, and a detailed analysis of the Lidar system parameters, operating procedures and safeguards in order to achieve a standard of safety which is acceptable.

The damage mechanisms encountered in humans and the wavelength regions involved are shown in Table 2-3. In addition the experiment class numbers are shown for the particular wavelength regions. The table also indicates that below 300 nm, the absorption in the ozone layer provides additional protection from radiation damage.

Table 2-3. Eye Safety Damage Mechanisms

DAMAGE MECHANISMS		
WAVELENGTH RANGE	MECHANISM	EXPERIMENT CLASS NO.
< 315 nm	CORNEAL & SKIN	8, 12, 21, 22, 25, 26
315 – 400 nm	CORNEAL & SKIN & SMALL RETINAL	19, 20
400 – 1500 nm	RETINAL TO VARYING DEGREES	1, 2, 3, 4, 6, 7, 9, 11, 14, 15, 16, 17, 23
10.6 nm	CORNEAL & SKIN	10, 13, 18, 19, 20, 24
BELOW 300 nm OZONE ABSORPTION PROTECTS VIEWER		

The calculated results of the eye safety status of various lasers is most easily presented as shown on the nomograph of Figure 2-6. The right hand side of the graph indicates the maximum permissible exposure (MPE) in joules per cm^2 for various apertures from the day adapted eye up to the 6-inch telescope (plotted as a function of wavelength). The apertures and effective areas used to generate the nomograph are shown in Table 2-4.

The left side of the nomograph (Figure 2-6) shows the energy density in J/cm^2 on the ground from a 200 km orbit plotted as a function of laser energy for laser beam divergence,s between 0.1 mr and 10 mr. To use the nomograph, the wavelength of interest is chosen on the right side of the ordinate, this value is moved vertically to intersect the curve for the particular aperture under consideration. The value of the maximum permissible exposure in joules per cm^2 can be read from the energy density axis on the left. The laser energy of interest is then chosen on the left side of the absissa and moved vertically until it intersects the MPE line. The intersection of the two lines indicates the minimum laser beam divergence, within the safety criteria previously established, which can be used without exceeding the eye safe energy density at ground level. The example shown on the nomograph uses the 530 nm wavelength of an Nd-YAG doubled laser at an energy of 0.73 joules for a 10-inch telescope on the ground. The nomograph indicates that a minimum beam divergence of about 5 mr would produce an eye safe situation. Note that this nomograph is conservative in that it includes a factor of three to account for multimode beam inhomogeneities which would be reduced to a two times factor for a single mode laser.

In evaluating several cases on the nomograph for different wavelengths, apertures, and laser energies it becomes apparent that inflight adjustable laser (and receiver) beam divergence is required to obtain the maximum eye safe energy density and the

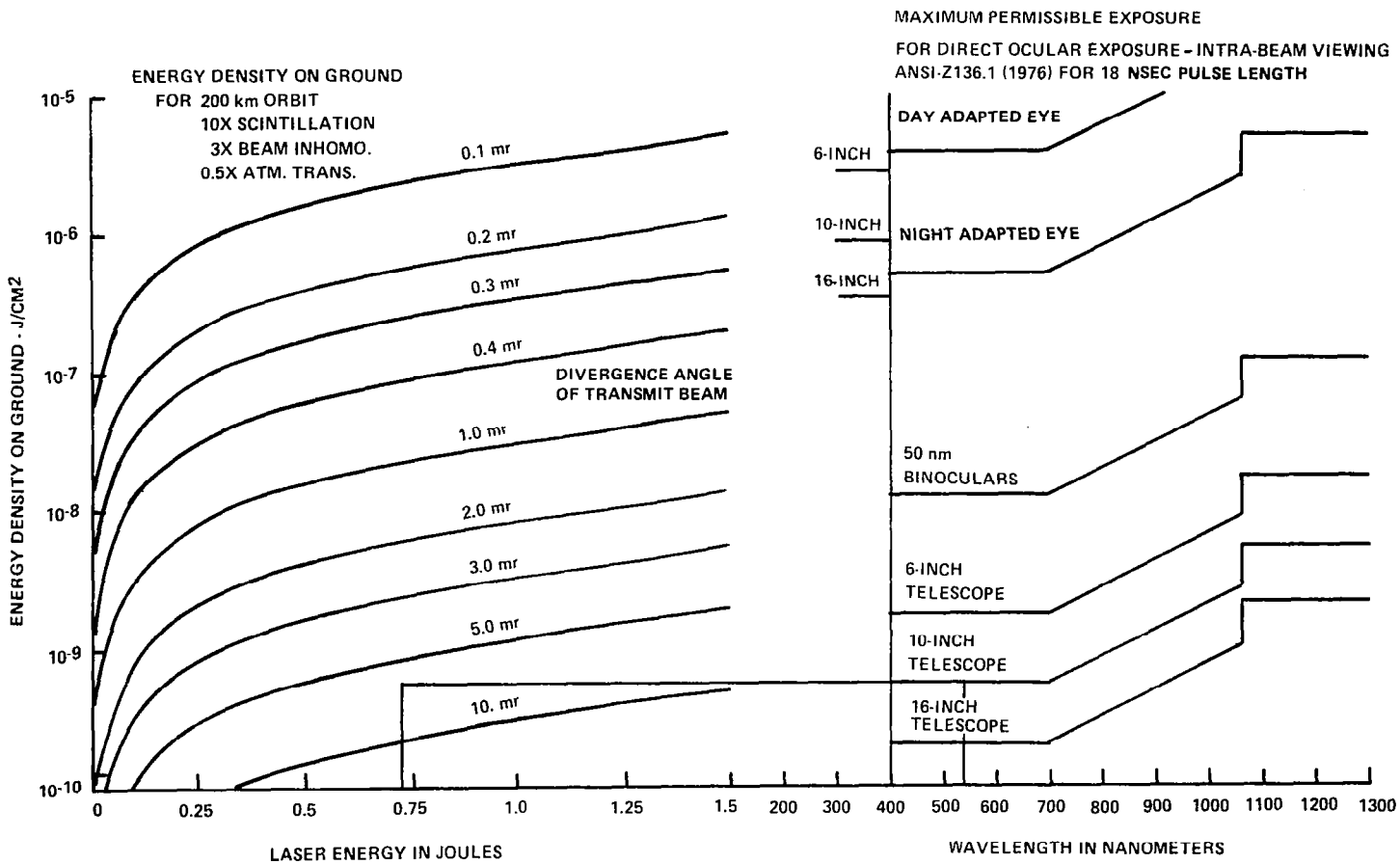

Figure 2-6. Eye Safety Nomograph.

Table 2-4. Apertures and Effective Areas

OCULAR	DIAMETER	OPTICAL TRANSMISSION	EFFECTIVE AREA
DAY ADAPTED EYE	2.5 MM	1	0.049 CM^2
NIGHT ADAPTED EYE	7.0 MM	1	0.38 CM^2
BINOCULARS	50 MM	0.82	16.1 CM^2
6-INCH TELESCOPE	152 MM	0.78	128 CM^2
10-INCH TELESCOPE	254 MM	0.78	356 CM^2
16-INCH TELESCOPE	406 MM	0.78	910 CM^2

narrowest beam divergence. This is necessary to obtain the maximum science return for each experiment and to meet different eye safety requirements for day/night and land/sea. A small receive field of view in the daytime is required in order to obtain reasonable signal to noise ratios. The transmit beam divergence must be large enough to provide eye safe energy density levels on the ground and at the same time should be small enough so that the entire transmitted beam can be seen by the receiver. More detailed discussions are given in the hardware descriptions for the receiver and transmitter on the methods which may be employed to adjust the received field of view and the transmitted beam divergence. The adjustment of the beam divergences to meet the different requirements for day and night operation is accomplished by the use of stored commands in the Command and Data Handling Subsystem which re-triggered either by correlative sensors which determine the light level on the earth's surface of by the payload specialist.

Another point which can be inferred from the nomograph is that it may be possible to perform many experiments at the neodymium tripled wavelength of 353 nm while filtering out the fundamental and doubled components. This would provide minimum physiological impact since there is a minimum eye hazard at this wavelength.

Additional factors must be considered in any eye safety scintillation discussion. These factors include some evidence which indicates that there is only a 15 cm maximum dimension to scintillation induced hot spots in the laser beam, with much larger distances between the spots. More work, however, should be done on the entire problem of scintillation before definitive criteria can be established.

The 10 watt CW CO_2 laser is eyesafe at ground level for all beam divergences. The 15 joule pulsed CO_2 laser is eyesafe at ground level for all beam divergences greater than 0.11 milliradian when a gaussian beam distribution and a factor of 4 times for atmospheric scintillation are assumed. The results of the eye safety study do indicate, however, that the Shuttle Lidar system can be designed to meet all known eye safety standards.

2.4.6 SIGNAL TO NOISE RATIO

Calculations of the signal to noise ratio required and signal to noise ratio to be expected with the baseline Lidar system were made for selected experiment classes. The methods used to calculate these values are shown in Figure 2-7, with the method used to determine the requirement shown at the top and the measured SNR at the bottom of the figure.

–METHOD USED TO DETERMINE SNR REQUIREMENTS

- LENGTH OF MEASUREMENT ALONG FLIGHT PATH (ΔX) IS FROM SEED GIVEN IN SCIENCE OBJECTIVES
- SHUTTLE VELOCITY OF $\approx$ 8 KM/SEC
- LASER REPETITION RATE IS 10 Hz
- NUMBER OF SHOTS PER MEASUREMENT IS:

$$\frac{\Delta X}{\text{SHUTTLE VELOCITY}} \times \text{REPETITION RATE} = \#\ \text{SHOTS/MEASUREMENT}$$

- REQUIRED ACCURACY IS GIVEN IN SCIENCE OBJECTIVES
- S/N REQUIRED PER MEASUREMENT OBTAINED FROM ACCURACY
- S/N REQUIRED PER SHOT IS:

$$\frac{\text{S/N PER MEASUREMENT}}{\sqrt{\text{NO. SHOTS/MEAS.}}} = \text{S/N PER SHOT}$$

– MEASURED S/N = $\dfrac{\text{RAYLEIGH COUNTS}}{\sqrt{\text{RAYLEIGH COUNTS + BACKGROUND COUNTS}}}$

Figure 2-7. Signal to Noise Ratio.

The measured SNR values were first prepared using a large nomograph which plotted the background in photons/m^2-mr^2-nm-km and the signal received in photons/j-m^2-km against the optical efficiency of the system, filter bandwidth, mirror diameter, receiver field of view, range bin length, and the transmitted energy. As the program progressed the signal to noise calculations were reduced to a number of computer programs, each for a different measurement technique.

Representative results of these calculations are shown for two different measurement methods, the first in Figure 2-8, is a plot of signal to noise ratio per range bin for Experiment Classes 1 and 2 which satisfy Science Objective number 3 from the SEED. SNR is plotted as a function of receiver diameter for signal return heights of 0 and 20 km at night with fixed receiver/transmitter co-alignment and for 20 km signal return height during day with both passive and active co-alignment. The required SNR is also shown on the graph. This chart shows how changing the receiver diameter affects SNR, and that in order to meet the accuracy requirements of the SEED

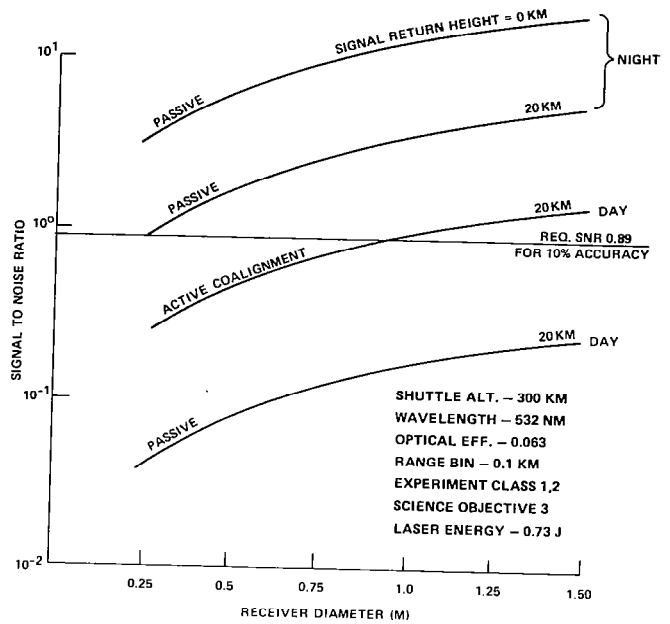

Figure 2-8. Signal To Noise Ratio vs. Receiver Diameter.

that active co-alignment is required for day operation. This is because active co-alignment allows the receiver beam divergence to be reduced to approximately the same value as is used for the transmitter while keeping the two exactly aligned. This calculation was done for Rayleigh scattering, which is equivalent to a zero db cloud, and provides a conservative approach to the signal to noise ratio problem. The second result is shown in the graphs of Figures 2-9 and 2-10, which considers experiment class 9, the water vapor Dial experiment. Figure 2-9 shows the counts per range bin plotted as a function of altitude at several concentration values for the system parameters shown. The graph of Figure 2-10 shows the percent error to be expected in the measurement of water vapor concentration plotted as a function of altitude. This calculation is representative of one of the most difficult experiments, in terms of obtaining an adequate signal to noise ratio. This calculation was done for the night

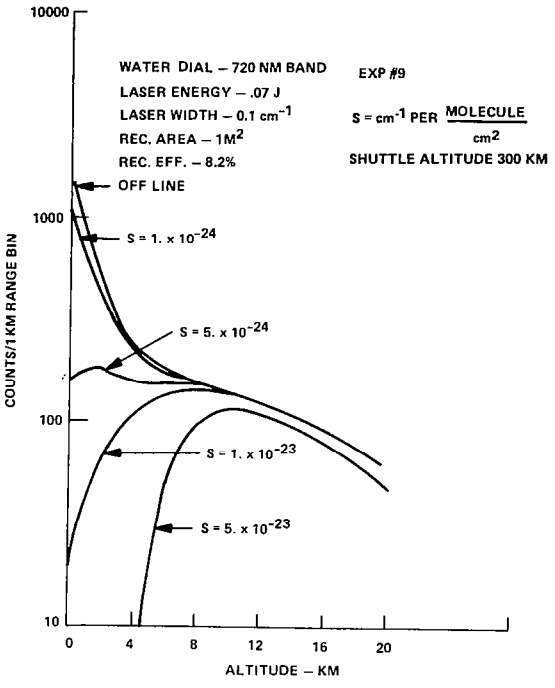

Figure 2-9. Single Shot Return Signal vs. Altitude.

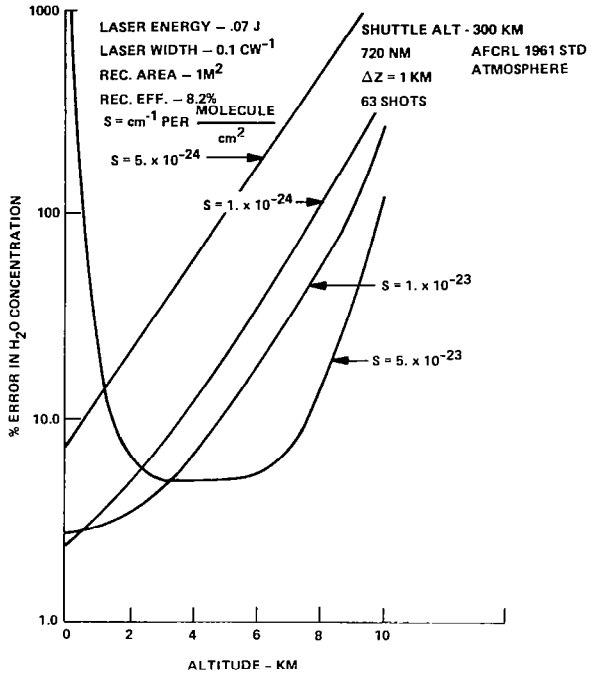

Figure 2-10. Expected Error H_2O Dial.

background case and a Shuttle altitude of 300 km. The number of shots was chosen at 63 which corresponds to the required horizontal resolution at a 10 Hz laser repetition rate.

2.5 RESULTS

The specific results obtained indicated that the receiver transcends all the experiments while the laser and the detector are experiment unique. The analysis also indicated that the system requires the largest receiver area useable in the space available and the largest laser energy consistent with meeting the eye safety constraints. In addition the analysis indicated that some on-orbit co-alignment between the transmitter and the receiver is required in order to meet the accuracy requirements in daytime operation for most experiment classes.

Direct quantified results of the work performed in these analysis and the iterative refining process which accompanied it are shown in Table 2-2. Experiment sets and subsets, as shown in Figure 2-2, were developed with a logical priority of experiments in the same order as the subset numbers. This prioritization of course is based simply on the order in which it is proposed to procure hardware. In practice a large number of other variables may influence the order of experiment classes and hardware acquisition.

The baseline Lidar parameters were developed and system performance requirements were generated as part of the iterative process which included inputs from all the Lidar subsystems. In addition, technological deficiencies were identified. These items will be discussed later in this report.

3.0 STS ACCOMMODATION

3.1 INTRODUCTION

NASA's Space Shuttle and its primary payload carrier, the European developed Spacelab, when operational in the 1980's, will introduce a new era in space experimentation.

The Space Shuttle Orbiter is the basic element of NASA's Space Transportation System (STS) replacing conventional boosters to lift up to 30,000 kg of cargo weight into near earth orbit and then return to earth. The Spacelab, which is mounted into the Orbiter cargo bay is a multipurpose payload carrier designed to provide a number of basic resources and services to experiments/payloads. Spacelab stays attached to the Orbiter during the entire length of orbital operation and returns with the Orbiter.

Another important element for the operation of the STS is NASA's Telemetry and Data Relay Satellite System (TDRSS) which establishes the primary communication link between the flight and ground segments of the STS.

The study to develop a Lidar system concept was based on STS usage and the following NASA developed ground rules:

- Lidar will fly on Spacelab missions, i.e. will be part of a dedicated Spacelab payload
- Lidar will be mounted on a Spacelab pallet
- Lidar will fly on multidiscipline Spacelab missions
- Lidar will fly up to three times a year

These groundrules are important since they determine:

- Lidar interfaces to the STS
- The on-orbit environmental conditions Lidar will be exposed to
- The integration and checkout constraints

Figure 3-1 shows a typical, conceptual Spacelab mission configuration that includes the Lidar facility. Shown is the Shuttle Orbiter in a pallet-only Spacelab configuration containing a Lidar with a cosmic ray experiment directly mounted into the Orbiter cargo-bay. Such a multidiscipline payload requires Orbiter attitudes that allow periods of deep space viewing,solar viewing if the telescope is a solar telescope, and earth viewing for Lidar.

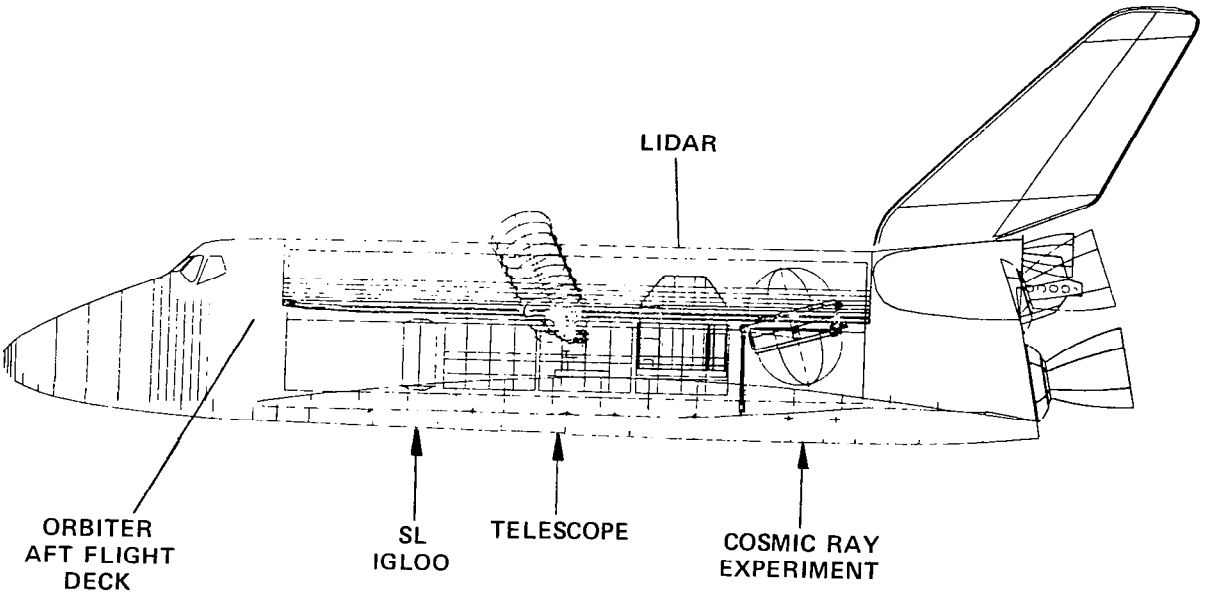

Figure 3-1. Shuttle Orbiter/Spacelab.

The capability of Shuttle/Spacelab to repeatedly fly large, complex payloads with large resource requirements (weight, power) permits development of such multi-user research facilities as Lidar, (an evolutionary system with a ten year lifetime).

While Shuttle/Spacelab presents exciting, new opportunities for space experimentation it is crucial to understand the constraints the STS places on the Lidar system design and configuration to obtain maximum science return.

Shuttle/Spacelab flights will be limited to 7 to 10 days initially. While 30 day flights are advertised, they will not be possible until availability of auxiliary electrical power and heat rejection sources to augment the basic Orbiter on orbit capability.

From an operational point of view, Lidar will enter a rather fixed and rigid ground operations schedule to be integrated with the Spacelab and the Shuttle Orbiter. The possibilities, for instance, for testing Lidar functions on the ground will diminish with each higher level of STS integration leading to the scheduled launch date.

Lidar system design requires consideration of STS orbit and attitude capabilities and limitations, and significant communication "black-out" times due to TDRSS occultations. Also important are potential constraints due to the fact that available resources have to be shared with companion payloads/instruments which will fly on the same mission.

A significant outcome of the STS accommodation analysis was the formulation of a number of Lidar system design guidelines which, in turn, led to a Lidar system concept that accommodates most of the experiment requirements within the STS capabilities and constraints.

The Lidar system developed during this study is capable of being flown as part of most forseeable Spacelab missions. It uses standard Spacelab interfaces, can be easily integrated into Spacelab, and uses only its "fair share" of available STS resources. In addition, the Lidar system approach realizes the unique role trained Shuttle crew members can play during on-orbit operations, but at the same time acknowledges that on-orbit operations and crew time are STS resources that need to be budgeted carefully and effectively to assure maximum scientific return on the overall Shuttle/ Spacelab mission.

3.2 LIDAR PHYSICAL AND FUNCTIONAL ACCOMMODATION ON SHUTTLE/SPACELAB

Lidar will be developed as a Spacelab payload and fly on Spacelab missions. Spacelab is a modular payload carrier. It consists of a pressurized module and pallets. Figure 3-2 shows the various possibilities of combining the modular Spacelab elements into Spacelab flight configurations. Three basic configurations exist: module-only configuration, module/ pallet configuration, and pallet-only configuration.

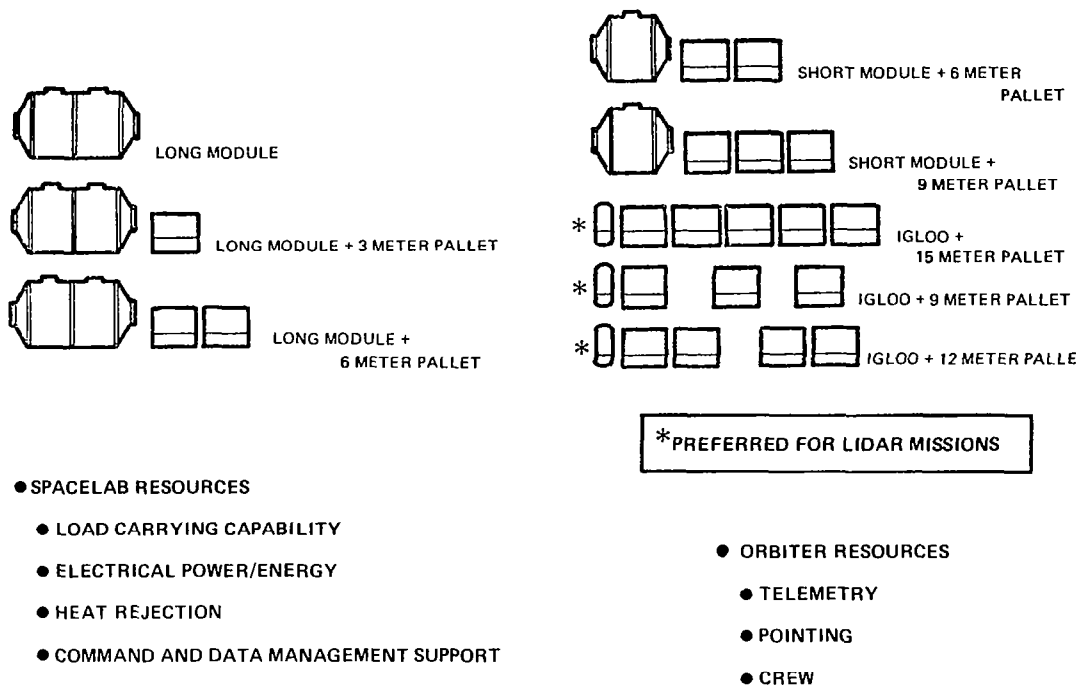

Figure 3-2. Spacelab Flight Configurations and Services.

The Lidar can fly in a long-module or in a short-module configuration. In module/pallet configurations the Spacelab crew (payload specialists) will enter the pressurized module and conduct experiment operations from there. In pallet-only configurations the Orbiter/Spacelab crew will remain inside the Orbiter and experiment operations will be conducted from the Orbiter aft flight deck (AFD). Since Lidar requires a significant amount of electrical power during experiment operations, it is anticipated that Lidar will fly primarily on pallet-only Spacelab missions. Pallet-only configurations supply significantly more electrical power to experiments

than configurations utilizing the Spacelab-module, since the module life support system uses a large amount of the overall power available from the Orbiter. This does not mean, however, that certain Lidar experiments requiring less than full electrical power could not be conducted on module/pallet missions. The Lidar system is designed to be accommodated and operated in either Spacelab configuration.

Spacelab and the Orbiter make a number of basic resources and services available to payloads.

Spacelab provides:

- Load carrying capability
- Electrical Power/Energy
- Heat Rejection
- Command and Data Management Support

The Orbiter, in addition, provides

- Telemetry and ground communication
- Limited pointing capability
- Trained crew members for experiment operation

Those parameters which have significant impact on the Lidar system design are:

- Electrical power available from Spacelab
- The thermal environment on the Spacelab pallet
- The interface to the pallet structure
- The interface to the pallet freon cooling loop
- The interface to the Spacelab command and data management system
- The resources available to Lidar monitoring and control equipment in the Orbiter aft flight deck.

The impact of each one of these parameters will be discussed in the following sections.

3.2.1 ACCOMMODATION ON THE SPACELAB PALLET

The Spacelab pallet is a U-shaped structure that mounts into the Orbiter cargo bay with a set of trunnion and keel fittings. Figure 3-3 shows a 2-pallet train with the "Igloo" which in pallet-only configurations houses Spacelab subsystem equipment normally accommodated in the Spacelab module. The "Igloo" is not available for experiment equipment. Payloads like Lidar are mounted to the pallet with pallet hardpoint available at standard locations. Light experiment equipment can be mounted directly to honeycomb panels covering the inside of the pallet.

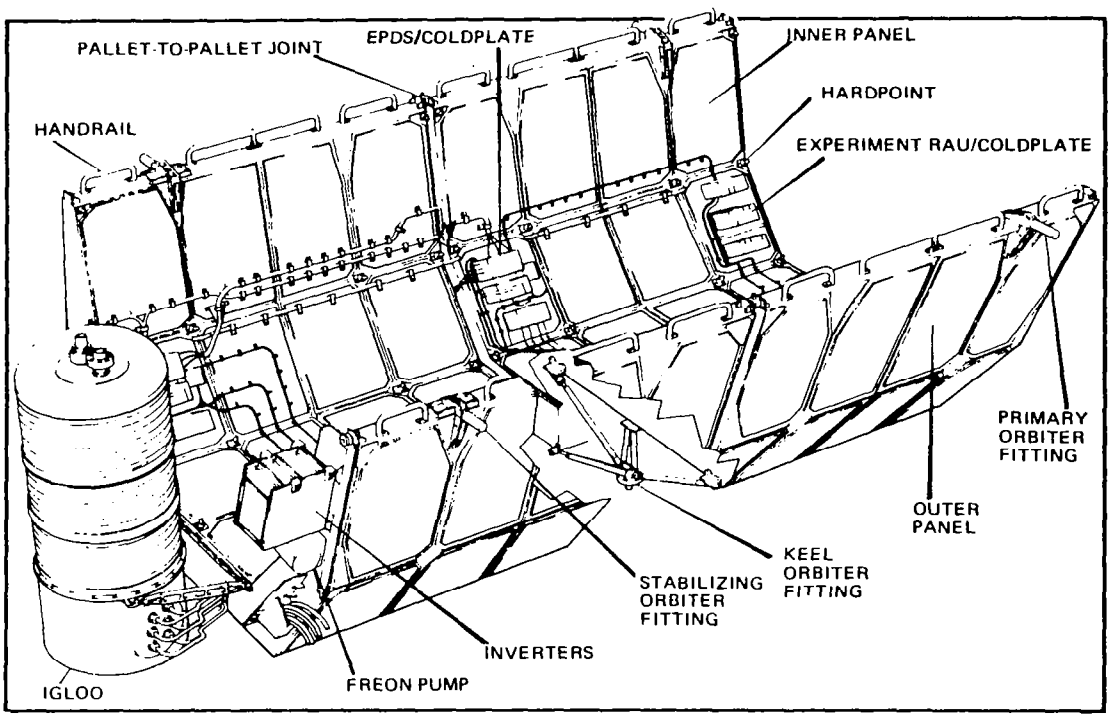

Figure 3-3. Spacelab Pallet.

Each pallet carries a standard set of Spacelab subsystem equipment mounted to a Spacelab coldplate in a standard location. Of importance to Lidar is the Spacelab electrical power distribution box (EPDB) and a Spacelab experiment remote acquisition unit (RAU). The EPDB makes standard 28 volt dc electrical power available to Lidar,

and the RAU allows Lidar to interface with the Spacelab command and data management system. Also available for Lidar is the pallet freon cooling loop for Lidar thermal control and heat rejection.

The spacelab pallet is designed to carry nominally about 3000 Kg of payload equipment. However, the average load carrying capability of a pallet is very much a function of the actual S/L flight configuration and can be significantly lower.

In order to fulfill the overall requirement of making Lidar a payload that can be easily integrated into Spacelab, and that can fly on many of NASA's planned Spacelab missions, the following set of guidelines were adopted:

LIDAR DESIGN GUIDELINES

- Keep Lidar mass below the average load carrying capabilities of flight configured Spacelab pallets
- Use available pallet hardpoints for Lidar mounting
- Use standard pallet flight configuration

3.2.2 ELECTRICAL POWER FOR LIDAR

Lidar electrical power is provided by Spacelab which, in turn, receives power from the Orbiter from a set of fuel cells dedicated to Spacelab. Figure 3-4 shows, in a very simplified form, the basic features of the power distribution system. Spacelab receives 7 kw maximum continuous power of 28 $\pm$ 4 volt dc (12 kw peak for 15 minutes every 3 hours). This power is distributed by the Spacelab electrical power distribution system to operate:

- Basic Spacelab subsystem equipment, which consumes a considerable amount of the 7 kw available, especially in the Spacelab module
- Mission dependent Spacelab subsystem equipment, which is equipment primarily designated to support experiment operations
- Experiment equipment

The power available to Lidar was derived by assuming that other payloads/experiments are in a standby mode during Lidar operations, with about 1 kw allocated standby power.

- SPACELAB ELECTRICAL POWER

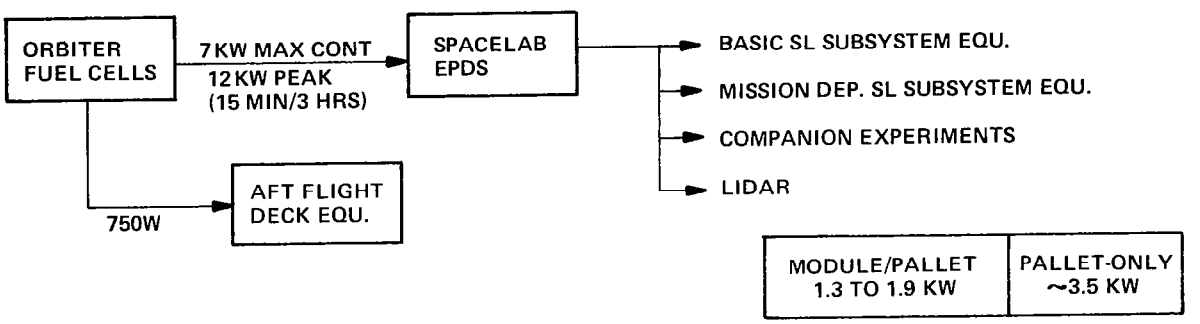

Figure 3-4. Lidar Electrical Power.

The power available in Spacelab module/pallet configurations is significantly less than in pallet-only configurations. This limits the use of Lidar on Spacelab flights that carry the module; however, it is still possible to carry out meaningful Lidar measurements also on such flights. To exploit the full potential of the Lidar facility developed during this study, Lidar will have to be flown on pallet-only missions and operated from the Orbiter AFD.

Spacelab and payload equipment mounted in the Orbiter AFD have 750 watts of additional power available. About 300 to 400 watts of this can be available to dedicated payload equipment, while the rest is being used by Spacelab controls and displays.

One important feature of the Orbiter/Spacelab power distribution system is the fact that power to experiments is not available during certain ground and flight operational phases. This is of concern to those Lidar configurations which need continuous power, e.g., to run thermoelectric coolers to keep the photocathodes of particular detectors at low temperatures at all times. Spacelab independent electrical power sources will then have to be provided, both on the ground and in flight.

In addition to electrical power, electrical energy is also a limited resource on every Shuttle/Spacelab mission. This is primarily important for Lidar stand-by and non-operating modes. It means specifically that standby and heater power for thermal control should be minimized.

Design guidelines developed for Lidar electrical power/energy usage are:

- Use standard 28 $\pm$ 4 volt dc Spacelab power
- Interface with the pallet mounted Spacelab electrical power distribution box
- Limit demand for Lidar standby and heater power
- Provide auxiliary power resources, if needed, for periods when Spacelab power is not available.

3.2.3 LIDAR THERMAL CONTROL

Two Lidar thermal control issues and their interrelationship with the Orbiter/Spacelab capabilities in this area had to be investigated:

- Lidar heat rejection
- Lidar temperature control

The primary mode for rejecting experiment generated heat loads is through Spacelab and Orbiter cooling loops.

Figure 3-5 shows a schematic of the Spacelab pallet freon loop as used in pallet-only configurations. Heat is transferred from the pallet freon loop to the Orbiter liquid cooling in the Orbiter payload heat exchanger. Heat is finally radiated into space via the Orbiter radiator panels mounted to the insides of the cargo bay doors. Depending on the total Orbiter heat load and on orbital attitudes, the radiator panels can be augmented with Orbiter flash evaporators to achieve maximum heat rejection capabilities.

- SPACELAB PALLET COOLING LOOP

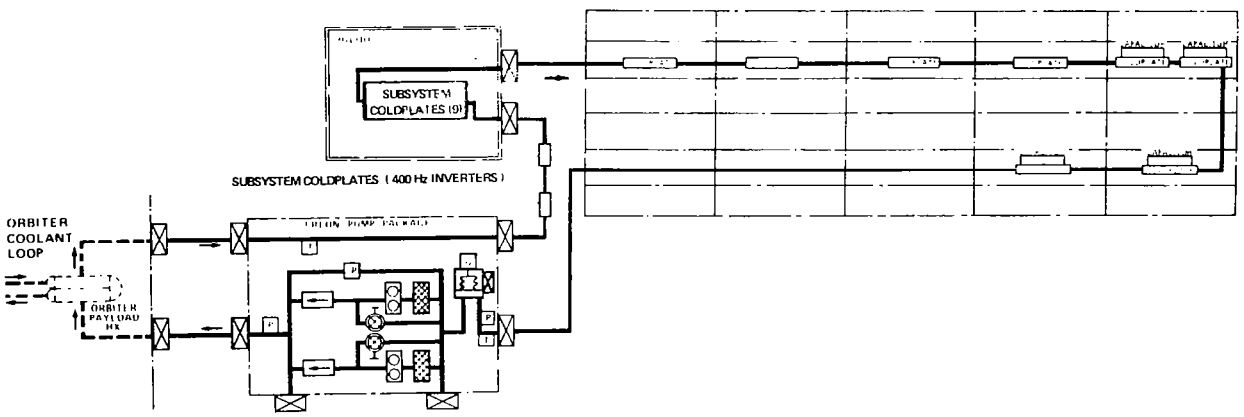

Figure 3-5. Lidar Thermal Control.

Payload equipment can interface with the pallet freon loop either through Spacelab provided coldplates on the pallet, or through a qualified, payload provided heat exchanger that ties directly into the freon loop.

The capacity of the Orbiter/Spacelab heat rejection system matches the available electrical power: The Orbiter can reject 8.5 kw of heat (maximum) continuously from Spacelab and its payload. The power available from the Orbiter is 7 kw maximum continuous. The slightly higher heat rejection capability allows the accommodation of metabolic heat loads from Spacelab crew members (in module configurations), and some

heat leaks into the system under hot environmental conditions in the Orbiter cargo bay.

Lidar temperature control, and in particular the temperature control of critical Lidar components such as the primary mirror and detectors, is of more significance and not as straight forward as Lidar heat rejection. Lidar temperatures and the design of the thermal control system are impacted by the temperature extremes on the Spacelab pallet and by the freon loop temperatures. Pallet steady state temperatures can reach + 120°C and -150°C under worst case hot and cold conditions, respectively. Actual temperatures, of course, are a function of the orbital parameters and timelines of a particular mission, as well as of the actual pallet/payload configuration.

The freon loop temperature is determined by the total heat load in the loop and the heat load distribution. In pallet-only configurations the freon loop temperatures available to experiments is usually lower than in module/pallet configurations. For design purposes it had to be assumed that the freon loop temperatures for Lidar can reach from 19°C to 35°C (which is too high for the control of various detectors foreseen for Lidar).

Based on the considerations discussed above, the following Lidar design guidelines were developed:

- Use the Spacelab pallet freon loop for Lidar heat rejection and temperature control of non-critical Lidar components
- Provide dedicated temperature control capabilities for temperature sensitive components

- Design the overall Lidar thermal control system to accommodate worst hot and cold case conditions (Lidar non-operational), to assure that Lidar can be flown on both astronomy/astrophysics and solar physics type missions.

3.2.4 LIDAR COMMAND AND DATA HANDLING

The Lidar command and data handling (C&DH) will be discussed separately in more detail in Section 8 limiting this section to a brief identification of major issues related to Shuttle/Spacelab accommodation capabilities and constraints with significant impact on the Lidar C&DH concept and design.

Spacelab provides a Command and Data Handling system (CDMS) in support of experiment operations. It consists of:

- the Spacelab experiment computer with peripherals for experiment monitoring and control, and data analysis.
- a mass memory unit to store experiment programs
- a high rate data assembly (multiplexer and recorder) that can handle many channels of high bit rate experiment data.

The Spacelab CDMS also provides the interface to the Orbiter avionics system which establishes telemetry and communication links to ground control centers, and also handles the command uplink from the ground.

The basic issue that confronts all Spacelab payloads is to what extent the Spacelab CDMS should be used for payload operations. The options range from a complete reliance on the Spacelab CDMS to being completely independent of it, and to use a dedicated Lidar processor with its own peripherals for Lidar control.

Of major concern for Lidar, if heavy reliance on the Spacelab CDMS is selected, is the impact on Lidar software development, integration and test, and on mission and experiment planning.

Using the Spacelab experiment computer means early commitment of Lidar software and experiment timelines and procedures. Using a dedicated Lidar processor means autonomy and flexibility in software development and experiment planning, and much easier integration into Spacelab. This is particularly important for a multiuser facility that is planned to be flown several times a year on a variety of different missions.

A significant constraint to be taken into account for the Lidar C&DH design and also for the on-orbit operational philosophy of Lidar, is the limited command uplink capability of the Orbiter/Spacelab system. This constraint, in addition to communication black-outs due to TDRSS occultations essentially eliminates the possibility of real-time Lidar control from the ground.

Finally, it is important to realize that the resources in terms of volume, panel area, power and cooling for experiment dedicated controls and displays in the Orbiter aft flight deck (AFD) are limited. Figure 3-6 shows a layout of the AFD. The mission station on the left will be manned by the mission specialist. It has Orbiter and Spacelab controls and monitoring equipment for the operation of Spacelab, i.e. the Spacelab subsystem equipment. The payload station will be manned by the payload specialist(s). Three panel areas (designated L10, L11, and L12) are available for experiment equipment. Any dedicated Lidar controls and displays will be located in this area.

The limiting factor on the AFD is the available heat rejection capability. This limits the power that can be used to 750 watts, which has to be shared between Spacelab equipment and experiment equipment. About 300 to 400 watts of electrical power (28 + 4 volt dc) can be expected to be available to experiments.

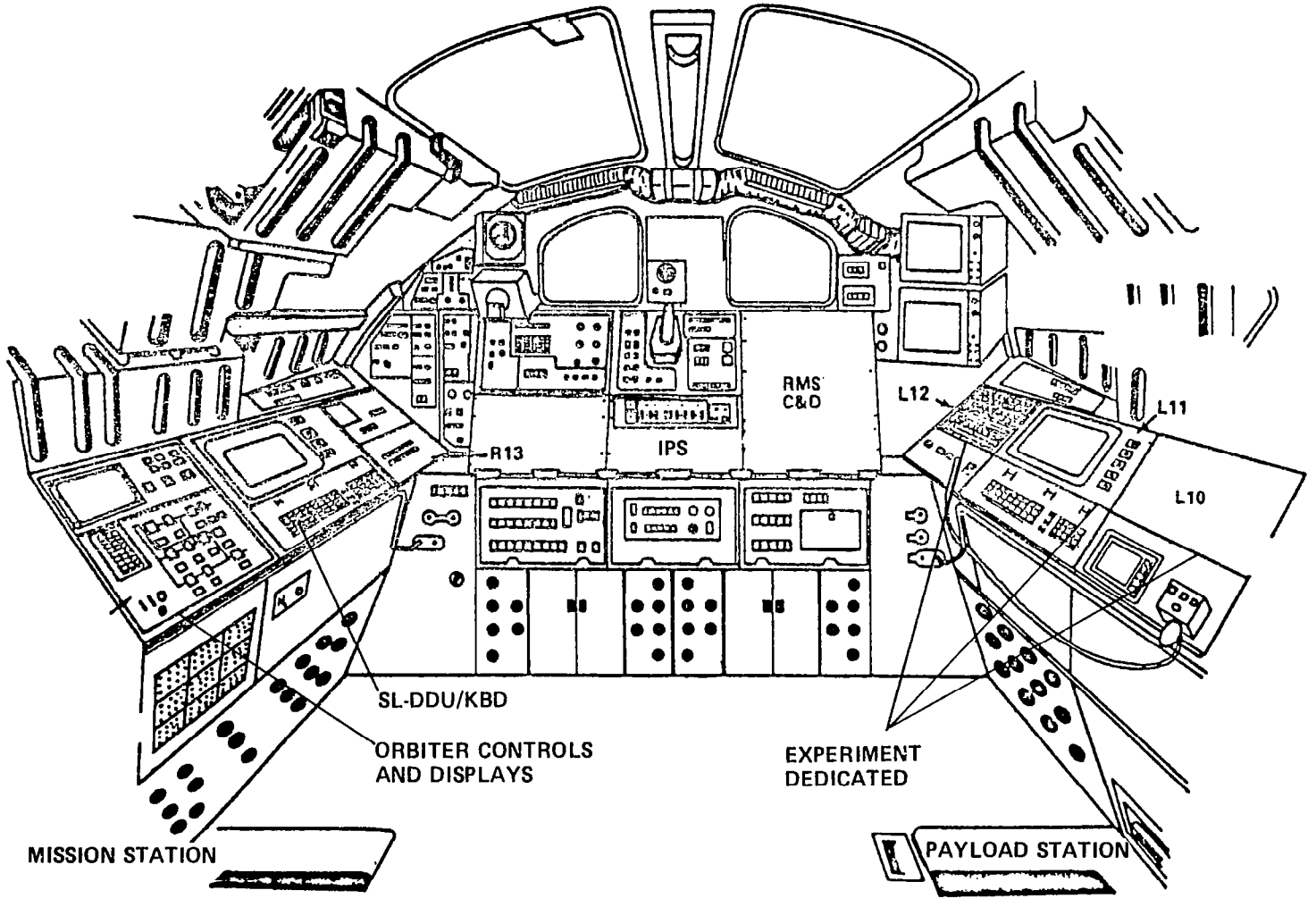

Figure 3-6. Aft Flight Deck

Design guidelines for the Lidar C&DH derived from the above considerations are rather general and were primarily intended to assure that adequate trade studies were conducted to arrive at the optimum Lidar C&DH concept:

- Configure Lidar C&DH for maximum flexibility and autonomy for ground and flight operations.
- Limit Lidar dedicated controls and displays to what can be accommodated in the Orbiter AFD.

3.2.5 LIDAR POINTING

Lidar pointing requirements received particular attention during this study. A first analysis of the SEED revealed that experiment pointing requirements were not defined quantitatively enough to serve as a basis for an analysis of pointing requirement accommodation by the Orbiter/Spacelab. The Lidar Science Working Group, therefore, generated pointing requirements in quantitative form as shown in Table 3-1. Pointing requirements are separated into real-time requirements and after the fact pointing knowledge requirements.

EXPLANATION FOR TABLE

1. The real-time pointing accuracy ($\Delta\theta$) required for each experiment was determined from the most stringent of:
   a. the need to keep the transmitted wavelength on a doppler or pressure-broadened line by the formula $\sin(\Delta\theta) = c\Delta\lambda/\lambda V$. In general $\Delta\lambda$ is one third of the line full width at half maximum (FWHM).
   b. the need to keep the return signal within the bandpass of the detector
   c. the need to point at an external object (retroreflecting subsatellite).

2. The post-flight pointing accuracy ($\Delta\theta'$) was determined from the most stringent of:
   a. the need to determine actual return-signal height to better than the range-resolution cell. In general ΔZ was taken as one third of the range cell size; except in the case of experiments 15, 16, 17 where ΔZ is the required accuracy. $\Delta\theta'$ and ΔZ are related by

$$\Delta Z = R\left[\sec(\Delta\theta') - 1\right]$$

$$\Delta\theta' \approx \sqrt{2\Delta Z/R}$$

Table 3-1. Pointing Requirements

Exp. No.	Wavelength Region (λ nm)	Bandwidth ($\Delta\lambda$ nm) atm (pm)	Bandwidth ($\Delta\lambda$ nm) det	Real Time Pointing Accuracy ($\Delta\theta$ millirad)	Vertical Resolution (ΔX m)	Wind Velocity Horizontal Component (ΔV m/s)	Post Flight Pointing Knowledge ($\Delta\theta'$ millirad)
1	530	NC		NC	50		17
2	530,1060	NC		NC	50		17
3	530	NC		NC	50		17
4	530, dye	NC		NC	100		24
6	530,1060	NC		NC	100		24
7	589	.3		20	100		24
8	280	.15		20	100		24
9a	720	2		100	300		40
9b	940	.3		12	500		50
10	Two in 9-11 μm region	1	20	NC (Note 1)	N/A		NC
11	493,589	.3		17 (Note 2)	200		17
12	265-300	NC		NC	100		24
13	9-11 μm	N/A	N/A	0.1 to 0.01	N/A		N/A
14	589	1	4	NC ($\sim 3^{o}$)	300	10	2
15	760	2		NC ($\sim 5^{o}$)	10		8
16	760	2		NC ($\sim 5^{o}$)	10		8
17	770	2		NC ($\sim 5^{o}$)	20		11
18	Two in 9-11 μm region	20-1000	20	NC (Note 1)	300		40
19a	530	NC	4	NC ($\sim 10^{o}$)	50	2	0.3 (Note 3)
19b	9-11 μm	NC	20	NC (Note 1)	50	2	0.3 (Note 3)
20a	530	NC	4	NC ($\sim 10^{o}$)	300	2	0.3 (Note 3)
20b	9-11 μm	NC	20	NC (Note 1)	300	2	0.3 (Note 3)
21	300	.15		20	1000		NC
22a	300	.15		20	100		24
22b	500	.3		20	100		24
23	448	$\sim$100		NC	100		24
24	9-11 μm	NC		NC	1000		NC
25	215	.15		20	1000		NC
26	225	$\sim$10		NC	1000		NC

Note 1 - real-time pointing control is not critical as long as the heterodyne detector can compensate for variable-frequency returns caused by shuttle tilting; i.e. by a tunable local oscillator, or by a broadband IF filter bank.

Note 2 - real-time pointing needs are much more stringent for analyzing large distance releases ($\approx$ 5 earth radii).

Note 3 - this level of absolute pointing accuracy is needed only when the ground return is not available.

b. the need to reduce the unknown component of shuttle velocity below the required wind-measurement accuracy. This is very scenario-dependent, and was evaluated here by assuming the Lidar would be pointing 5° fore and aft of the plane to the shuttle velocity vector, at an off-nadir angle of 45°. The equation used here was

$$\sin(\Delta\theta') = \frac{\Delta V}{\sin\phi_1 \, V \cos\phi_2}$$

where ϕ_1 and ϕ_2 are the off nadir angle in the plane to V, and the fore and aft angle, respectively.

3. Note that most linewidth-dependent real-time pointing requirements can be relaxed by broadening the transmitted laser linewidth at the expense of SNR.

Since the Lidar system will be hard-mounted to the Spacelab pallet, pointing will have to be accomplished with the Shuttle Orbiter. The Orbiter pointing capabilities are explained in Figure 3-7. The Orbiter can point any vector defined in the Orbiter Navigation Base with the accuracies defined in Figure 3-7. The alignment of Spacelab pallets, and hence of Lidar, in the Orbiter Navigation Base, however, is only known with an accuracy of at best 2° to 3°. In addition the position of the pallet in the Orbiter cargo bay can change due to the changing thermal environment on orbit.

Based on the pointing requirements in Table 3-1 and the Orbiter pointing capabilities it was determined for each of the 26 experiment classes of the SEED whether;

a) Orbiter pointing was adequate to fulfill the experiment requirements

b) Orbiter pointing had to be augmented with a Lidar provided attitude reference system to eliminate the alignment uncertainty in the Orbiter cargo bay

c) a highly accurate pointing mount was required

The results of the pointing accommodation analysis are shown in Table 3-2. It is shown how the real time pointing and post flight pointing knowledge requirements can be fulfilled for all 26 experiment classes. Most experiments can be conducted with the Orbiter pointing capabilities, i.e., including a 3° pallet/Lidar alignment

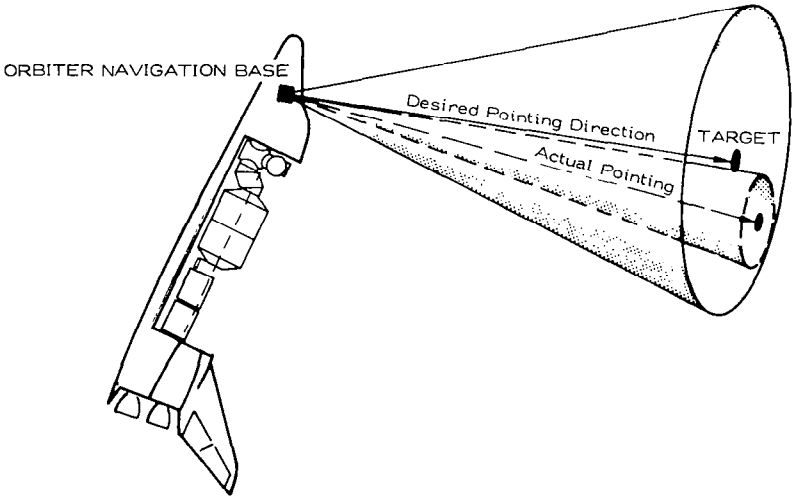

- **SPACELAB PALLET MISALIGNMENT IN ORBITER NAVIGATION BASE: $>2^{o}$ AND VARYING**

Pointing Accuracy (Half-Cone Angle) Utilizing Orbiter IMU

(Reference: Vol. XIV, Ref. D, Table 3.2)

Type of Pointing	Pointing Accuracy (3 Sigma) (Half-Cone Angle)	IMU-Drift Rate (3 Sigma)	Duration Between IMU Alignments
Inertial	± 0.5 deg	0.105 deg/hr/axis	1.0 hours
Augmented Inertial	± 0.44 deg	0	N/A
Earth-Surface-Fixed Target*	± 0.5 deg	0.105 deg/hr/axis	0.5 hours
Orbital Object	TBD	TBD	TBD
Local Vertical*	± 0.5 deg	0.105 deg/hr/axis	1 hour

*Tracking with TDRS, 100 n mi. (185 km) circular orbit.

Figure 3-7. Orbiter Pointing Capabilities.

Table 3-2. Real-Time Pointing Requirements

	REAL-TIME			POST-FLIGHT			
EXP. NO	ORBITER POINTING	O. P. LIDAR AUGMENTED	POINTING MOUNT	ORBITER POINTING	O. P. LIDAR AUGMENTED	POINTING MOUNT	REMARKS
1	X				X		
2	X				X		
3	X				X		
4	X				X		
6	X				X		
7		X			X		
8		X			X		
9a	X				X		
9b		X		X			
10	X			X			
11		X	X[1]		X		X[1] FOR DISTANT CLOUDS
12	X				X		
13			X	N.A.	N.A.	N.A.	SUB-SATELLITE WINDS
14	X					X	
15	X				X		
16	X				X		
17	X				X		
18	X				X		
19a	X			X			WINDS, ONE-DIMENSIONAL PROOF OF CONCEPT MEASUREMENTS, GROUND RETURN REQUIRED.
19b	X			X			
20a	X			X			
20b	X			X			
21		X		X			
22a		X			X		
22b		X			X		
23	X				X		
24	X			X			
25		X		X			
26	X			X			

uncertainty, if the actual pointing knowledge can be determined post-flight with an accuracy that basically eliminates the 3° misalignment error. Consequently a Lidar provided attitude reference system is required.

A Lidar provided attitude reference system could be implemented in a number of ways. It would allow an independent Lidar attitude determination with greater accuracy, if required, than available from Orbiter ephimeris data. This information could be used to generate after the fact pointing knowledge, or the Lidar attitude reference system could interface directly with the Orbiter attitude control system in real time and point the Orbiter and Lidar with Orbiter pointing capabilities, but with the misalignment error removed.

A highly accurate pointing mount, e.g., the Spacelab Instrument Pointing System, is required for experiment classes 11 and 13 in order to point Lidar at chemical release clouds released several earth radii (R_E) away from Earth, and to subsatellites.

Accurate windfield measurements, of course, also require highly accurate Lidar pointing to rapidly varying directions. However, one dimensional proof of concept type measurements can be carried out with the Orbiter pointing capabilities if a ground return signal is available, which allows elimination of unknown Orbiter velocity components.

A design requirement derived from the pointing analysis was:

- Design Lidar to accommodate its own attitude reference system.

3.3 LIDAR OPERATIONS

The operational environment for Lidar, both on the ground and in flight, has been assessed with the objective in mind to assure that operational requirements which could impact the Lidar system design are recognized from the beginning.

Figure 3-8 shows schematically one complete Lidar mission cycle: The Lidar system will originally be shipped from the Lidar manufacturer to KSC for pre-Level IV integration.

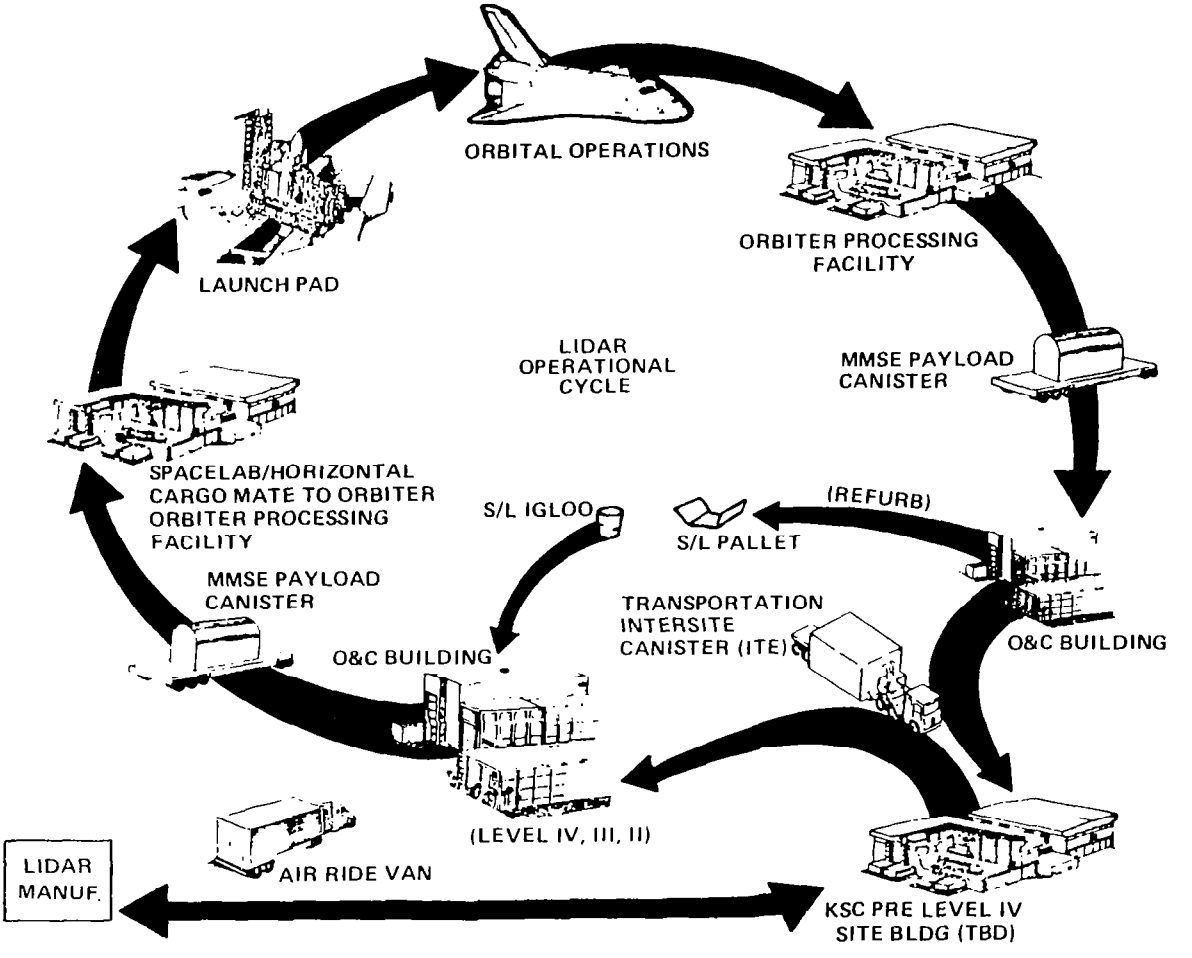

Figure 3-8. Lidar Operations.

Lidar will then be handed over to the NASA Spacelab integration team for Level IV, III and II integration in the O&C building. A totally integrated Spacelab will be moved from the O&C building to the Orbiter processing facility (OPF) for integration with the Orbiter (Level I integration). The Orbiter will then be erected into vertical position in the vertical assembly building (VAB, not shown), moved to the launch pad and launched.

After orbital operations are completed the Orbiter lands and is transferred to the OPF where Spacelab will be removed. The complete Spacelab and its payload will be moved back into the O&C building and de-integrated. Lidar will be turned over to the Lidar project team and moved back to the pre-level IV facility for maintenance, refurbishment, etc. and be readied for the next flight. For major refurbishment Lidar or some of its components might be returned to the Lidar manufacturer.

3.3.1 LIDAR GROUND OPERATIONS

3.3.1.1 Lidar Integration

The Lidar integration levels are defined in Table 3-3, which also shows the status of all Lidar to Shuttle/Spacelab interfaces (simulated vs. actual) as a function of integration level.

Design guidelines for Lidar derived from ground operations analysis are:

- Use standard Spacelab interfaces to facilitate Lidar/Spacelab integration
- Avoid non-standard, special checkout/support procedures during on-line integration activites as far as possible for early missions.

3.3.1.2 Lidar GSE Requirements

To support Lidar integration and test, the necessary mechanical and electrical ground support equipment has to be defined and developed along with the Lidar flight system. GSE required for Lidar integration and test includes:

- Shipping containers
- Ground handling equipment to support all pre-level IV integration activities (e.g., Lidar mechanical support stand)
- Ground cooling unit to operate Lidar liquid cooling loops
- Unit testers for lasers, detectors, etc.
- Ground power unit to simulate Spacelab power interface
- Ground command and data handling unit to allow end to end operation and testing of the complete Lidar system (incl. RAU simulator to simulate interface to Spacelab CDMS)
- Simulated pallet structure for environmental testing

The ground command and data handling unit shall be designed to handle and support the following tasks, in addition to supporting pre-level IV integration and tests:

- Level IV, III, II, I integration which might require interfacing with Shuttle/Spacelab EGSE
- Lidar experiment and facility software integration and verification
- Flight operations support at the payload operations control center (POCC)
- Post-flight engineering data reduction and analysis

Since this requires duplication of flight controls and displays in the ground unit, it could also be made available for crew training at various integration levels.

Table 3-3. Lidar Preflight Ground Operations-Activity Descriptions

ACTIVITY	DEFINITION	ACTIVITY SCOPE	LOCATION	FLIGHT VS SIMULATED INTERFACES
PRE-LEVEL IV INTEGRATION	LIDAR FLIGHT SET INTEGRATION • RECEIVER • LASER • DETECTORS • SUPPORTING SUBSYSTEMS	• LIDAR INSTRUMENT ASSEMBLY INTEGRATION, TEST AND CALIBRATION • LIDAR INSTRUMENT RECONFIRURATION, INTEGRATION, TEST AND CALIBRATION	• CONTRACTOR SITE FOR INITIAL DEVELOPMENT • KSC BLDG. TBD FOR LAUNCH TURN AROUND	• FLIGHT–LIDAR INSTRUMENT HARDWARE SIMULATED–SL PALLET & HW –SL CABLING & PLUMBING –SL/ORBITOR DATA SYSTEM –SL/ORBITER POWER –SL/ORBITER THERMAL
LEVEL IV INTEGRATION	INTEGRATION AND CHECKOUT OF EXPERIMENT EQUIPMENT WITH SPACELAB	LIDAR INSTRUMENT INTEGRATION TO THE S/L INTERFACING HARDWARE. INITIAL COMBINED PAYLOAD COMPATIBILITY TESTING WITH COMPANION PAYLOADS (E.G., EMI) INITIAL MISSION SIMULATION (TRAINING)	KSC O&C BUILDING LEVEL IV INTEGRATION AREA	• FLIGHT–LIDAR INSTRUMENT HARDWARE –SL PALLET & HW SIMULATED (LIDAR & SLGSE) –SL CABLING & PLUMBING –SL/ORBITER DATA SYSTEMS –SL/ORBITER THERMAL –SL/ORBITER POWER
LEVEL III INTEGRATION	COMBINATION, INTEGRATION AND CHECKOUT OF ALL S/L EXPERIMENT MOUNTING ELEMENTS (E.G., RACKS, RACK SETS AND PALLET SEGMENTS) WITH EXPERIMENT EQUIPMENT ALREADY INSTALLED	ASSEMBLY OF THE ALREADY INTEGRATED EXPERIMENT RACKS AND/OR PALLETS INTO RACK/FLOOR SETS AND PALLET TRAINS, FOLLOWED BY MECHANICAL INTEGRATION OF THESE WITH THE ALREADY CHECKED OUT BASIC S/L INTO A COMPLETE SL FLIGHT CONFIGURATION	KSC O&C BUILDING LEVEL III/II CHECKOUT AREA	MECHANICAL INTEGRATION OF SPACELAB PAYLOAD ELEMENTS
LEVEL II INTEGRATION	INTEGRATION & CHECKOUT OF THE COMBINED EXPERIMENT EQUIPMENT AND THE EXPERIMENT MOUNTING ELEMENTS (E.G., RACKS, RACK SETS AND PALLET SEGMENTS) WITH THE FLIGHT SUBSYSTEM SUPPORT ELEMENTS (I.E., CORE SEGMENT, IGLOO) AND EXPERIMENT SEGMENTS WHEN APPLICABLE	FUNCTIONAL VERIFICATION OF S/L PAYLOAD HARDWARE & SOFTWARE INTERFACES TO THE ON BOARD SUBSYSTEMS FOLLOWED BY AN OVERALL SYSTEMS' CHECK AND AN ABBREVIATED MISSION SIMULATION	KSC O&C BUILDING LEVEL III/II CHECKOUT AREA	FLIGHT–LIDAR INST. HARDWARE –SL PALLET & HW –SL CABLE & PLUMBING –SL POWER –SL THERMAL SIMULATED –ORBITER DATA SYSTEM –ORBITER POWER –ORBITER THERMAL
LEVEL I INTEGRATION	INTEGRATION AND CHECKOUT OF THE SPACELAB AND ITS PAYLOADS WITH THE SHUTTLE ORBITER, INCLUDING THE NECESSARY PRE-INSTALLATION TESTING WITH SIMULATED INTERFACES	FUNCTIONAL VERIFICATION OF THE SPACELAB/ORBITER HARDWARE & SOFTWARE INTERFACE, FOLLOWED BY A FINAL ORBITER INTEGRATED TEST TO ALLOW LIMITED END TO END TESTING TO ORBITER STACKING WITH OTHER SHUTTLE ELEMENTS.	KSC OFF AND LAUNCH PAD	FLIGHT–ALL INTERFACES SIMULATED–ONLY THOSE NECESSARY FOR PRE-INSTALLATION TESTING

3.3.1.3 Ground Operations Timeline

A ground operations timeline was developed based on the requirement of three Lidar flights per year and with the following assumptions:

a) Lidar will be maintained, refurbished, re-configured in an off-line facility at KSC between flights.

b) One major refurbishment cycle per year is planned, which allows Lidar or Lidar components to be returned to the Lidar manufacturer.

c) NASA on-line integration timelines were taken from currently available NASA documentation. These integration timelines will change and might shorten for later flights.

d) Seven day missions were selected as baseline.

e) Time between flights was equally spaced, except for the major refurbishment cycle.

Figure 3-9 shows a one year Lidar cycle with three flights. Based on the assumption stated above it can be concluded that three flights per year can be supported with one set of flight hardware.

3.3.1.4 Lidar Mission Cycles

A Lidar mission cycle was defined and generated to develop an understanding of Lidar operational cost, mission planning and analysis effort, and experiment development timelines. A mission cycle contains:

- Experiment analysis and requirements definition after experiments have been selected (from a response to a Lidar AO) for a particular mission.
- Experiment engineering which includes support to experiment development, experiment accommodation analysis and development of all mission selected documentation.

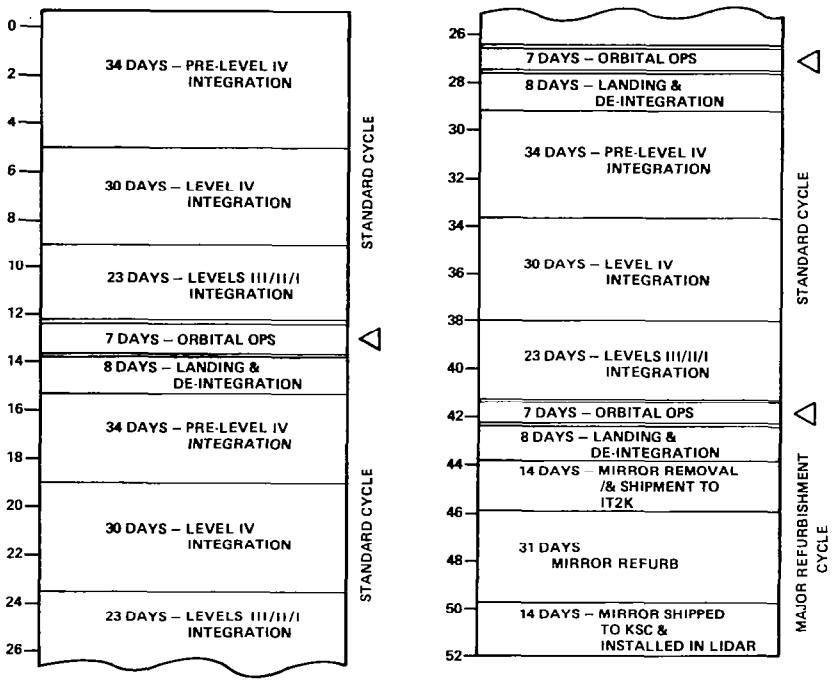

Figure 3-9. Lidar Cycle - Three Flights Per Year.

- Experiment implementation and test which includes checkout of experiment hardware, initial payload specialist training and experiment software verification
- Pre-level IV and level IV through I integration, flight and post-flight deintegration
- Post mission support which includes engineering data analysis

A complete mission cycle is expected to last about 30 months. It is interesting to note, with three flights per year, that up to seven separate Lidar flights can be at some stage of implementation simultaneously, as shown in Figure 3-10.

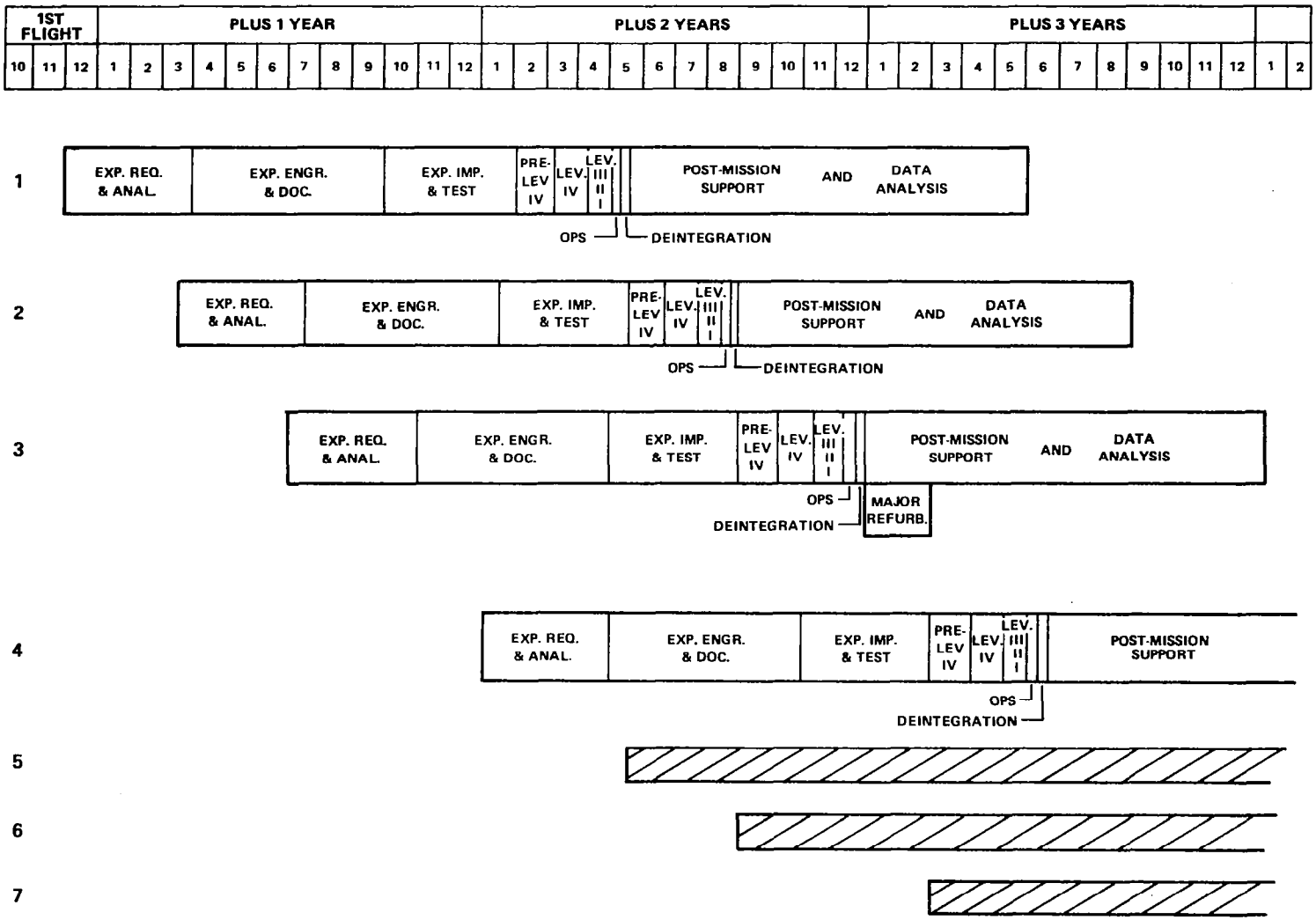

Figure 3-10. Lidar Mission Cycles.

3.3.2 LIDAR FLIGHT OPERATIONS

The Lidar flight operational analysis concerned itself primarily with:

- Lidar orbit and target area requirements and experiment timelines.
- Communication timelines
- Crew interfaces and constraints

The primary tool which was used for orbit, target area and timeline analysis was the Mission Model module of GE's Data System Dynamic Simulation (DSDS) program.

3.3.2.1 Orbits, Target Areas and Experiment/Communication Timelines

An analysis of the experiment requirements listed in the SEED led to the following conclusions:

- Most experiment requirements can be met with a 57° inclination, 300 km circular orbit
- Most experiment objectives do not require specific target areas but can be met by day/night measurements on a global coverage basis.

The 57° inclination constraint is dictated by the fact that Shuttle launches will only be possible from Cape Kennedy (ETR) during early years of Shuttle operations. Orbital inclination above 57° can only be achieved by Western Test Range launches. This means, of course, that any Lidar experiments in polar regions can only be planned for after WTR launches become available. Several experiments planned with Lidar will require WTR launches.

As far as specific target areas are concerned it was identified that some experiments would also like to access target areas which exhibit certain characteristics (e.g. dust storms, industrial plumes, etc.), in addition to making measurements on a global coverage basis. Sample potential target areas, therefore, were identified for the DSDS operations analysis (Figure 3-11), to evaluate the impact on on-orbit operations

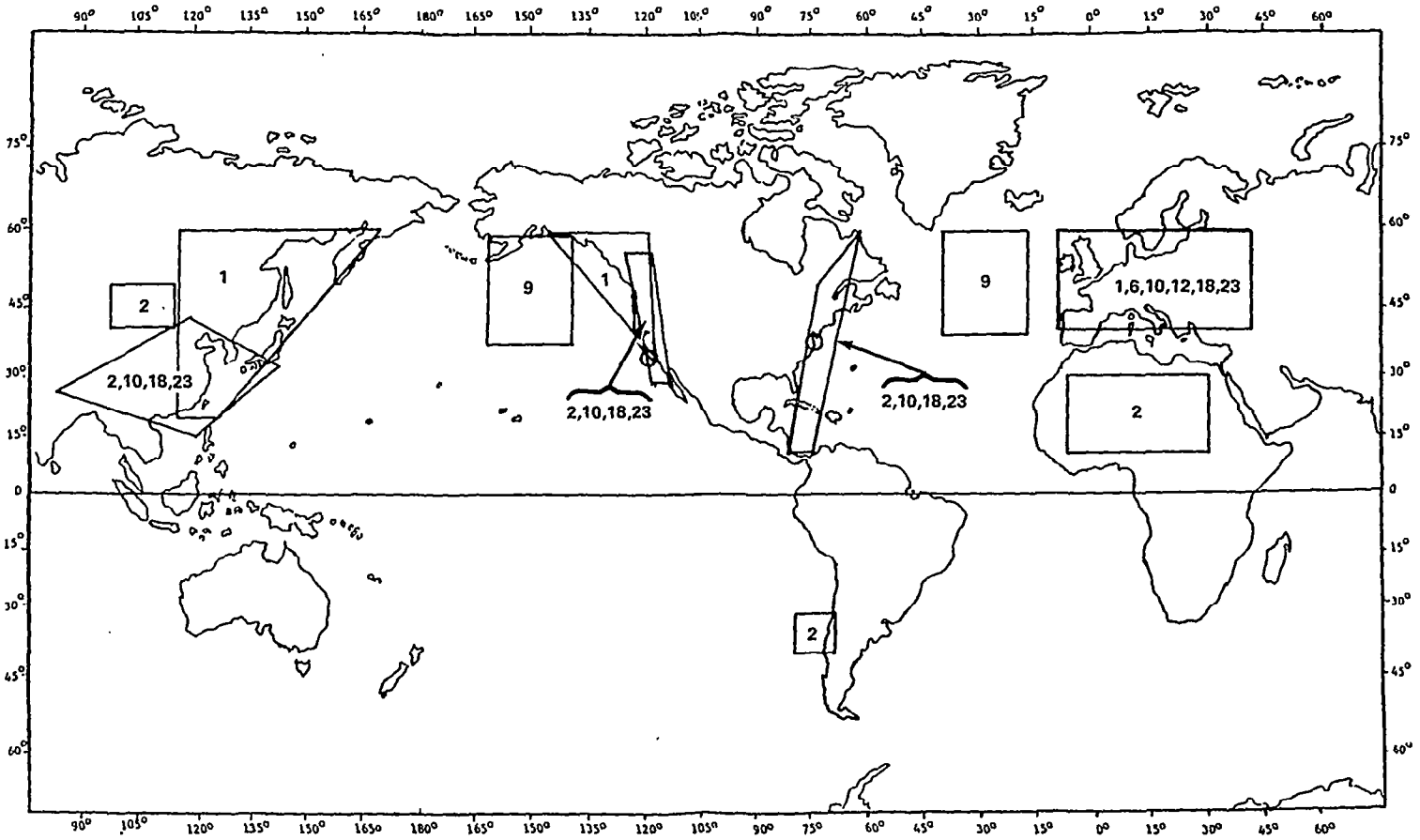

Figure 3-11. Sample Potential Target Areas.

and experiment timelines. The numbers in each target area indicate the experiment class with potential interest in that target area. Table 3-4 shows, for a few experiment classes, the desired observations and target areas selected for these

Table 3-4. Experiment Operating Criteria

EXP	DESIRED OBSERVATIONS	SELECTED AREAS FOR OBSERVATION
1	HIGH % CLOUD COVER	NORTH ATLANTIC & CITIES OF NW EUROPE JAPAN & NE CHINA & NE RUSSIA NW USA & W CANADA
2	DOWNWIND OF CITIES & DESERTS	SAHARA DESERT MONGOLIAN DESERT
6	AEROSOLS NEAR HIGH LATITUDE CITIES	NORTH ATLANTIC AND CITIES OF NW EUROPE
8,19,20	TROPICAL CLOUD TOPS & AEROSOLS	$\pm 20^{\circ}$ FROM EQUATOR
9	WATER VAPOR	1 LONG PASS (30 MIN) WITH 50% LAND/SEA

observations.

The parameters listed below were used for the DSDS analysis, in addition to target areas:

1) Inclination - 57°
2) Altitude - 300 km circular
3) Launch date - 7 a.m. local on a winter date in 1983
4) Number of Orbits - 112 (7 days)

Outputs of the DSDS analysis are:

- Ground trace data
- Target area acquisition and loss data
- Experiment opportunity timelines
- TDRSS acquisition/loss profile

Figure 3-12 shows a typical ground trace pattern over the U.S. in 1 day. This gives some appreciation for what is possible during a 7 day mission in terms of, for instance, acquiring targets of opportunities, e.g., a volcano eruption or other limited events of interest. Once certain target areas have been identified as necessary to achieve the experiment objectives, careful mission planning has to be conducted to assure maximum viewing time of the selected areas. Again, it needs to be pointed out that most experiment objectives will be met with day/night measurements on a global coverage basis, at least initially.

Figure 3-13 shows a typical Lidar experiment opportunity timeline for a 24 hour period. Shown are typical opportunities for 5 selected target areas. Target opportunities are limited to only a few minutes during each overpass. Depending on experiment requirements this can lead to complex on-orbit operational procedures, not only for Lidar itself but more so for the total payload/mission.

For global coverage measurements, of course, experiment opportunities are available continuously for the total 24-hour period which lends itself to much easier and much more efficient experiment and mission planning. Also shown in Figure 3-13 are the TDRSS occultations, based on one TDRS antenna on the Orbiter, which is Orbiter baseline. As can be seen, a significant portion of the mission (~45%) is without real time communication between the ground and the Orbiter.

Conclusions and Lidar design guidelines that were derived from the flight operations analysis can be summarized as follows:

- Conclusions:
  - Oppportunities to collect meaningful data occur over the entire 24-hour day
  - Viewing opportunities of specific target areas are restricted and of short duration

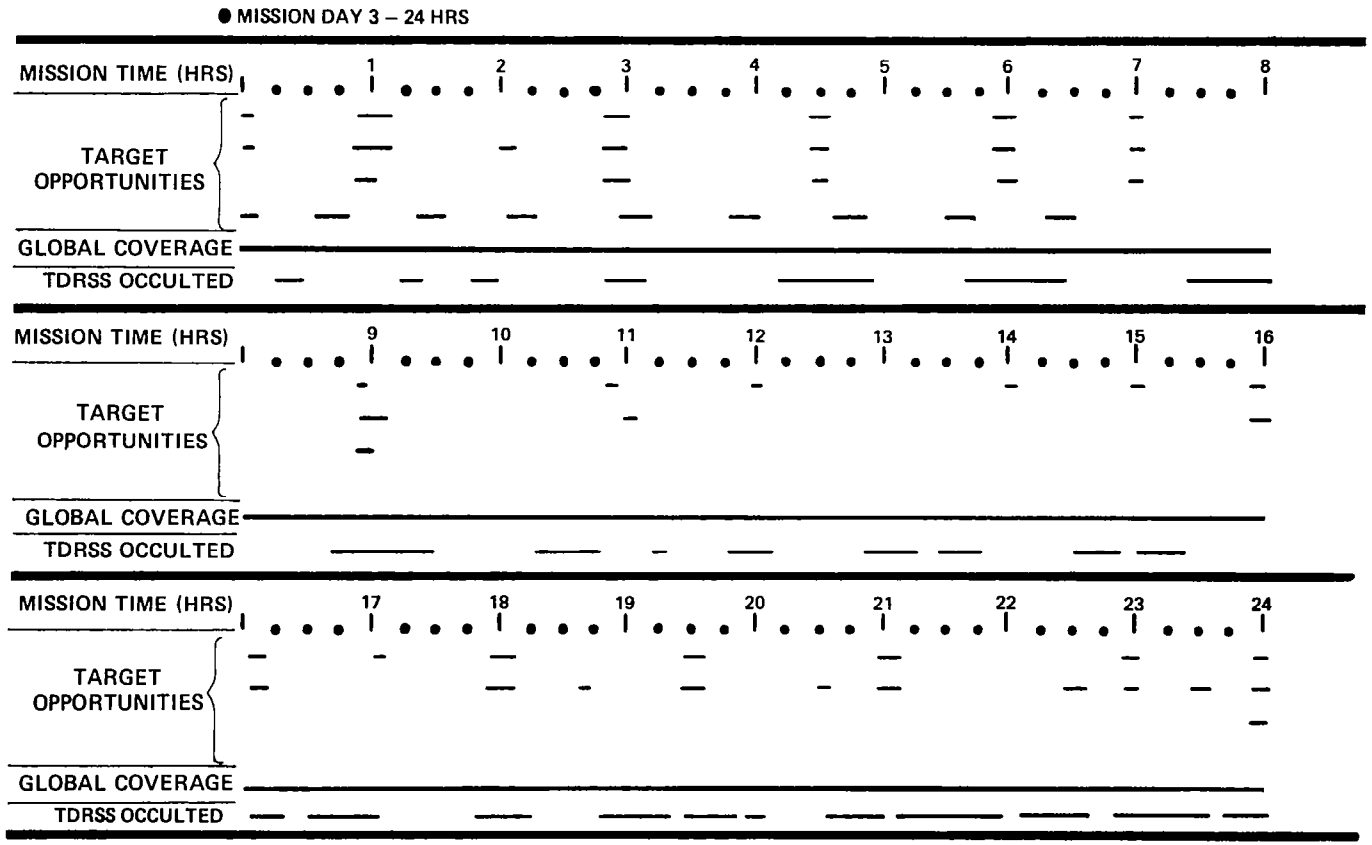

Figure 3-13. Lidar Experiment Opportunities Timeline.

- TDRSS occultation is significant ($\sim$45%) in the baseline configuration (one TDRS antenna)

- Guidelines:
  - Develop preprogrammed Lidar operatiions with little or no real-time deviation
  - Operate Lidar from the Orbiter AFD with little or no reliance on real-time ground communications.

If two TDRS antennas are flow the real-time communication coverage increases to better than 90%, allowing essentially continuous contact between onboard crew and the PI on the ground. However, real-time command and control possibilities from the ground will not be improved, since this is restricted by the command uplink capabilities of the Shuttle.

3.3.2.2 Crew Interfaces

Lidar will most likely fly on Spacelab pallet-only missions because of electrical power requirements, and thus will be operated from the Orbiter AFD. Lidar configurations/experiments which require less than full power might also fly on module/pallet missions in which case Lidar will be operated from the Spacelab module, but with the same set of controls and displays. Because of larger resources in the module, additional controls and displays could be accommodated in that case.

In the previous section it was shown that Lidar can continuously collect meaningful data over the entire mission period. Crew time, however, is a resource that needs to be scheduled and budgeted like any other resource on-orbit. This requires that Lidar can be operated not only by the payload specialist, but also by the Orbiter crew, i.e., the mission specialist(s) and pilot if necessary. The Lidar system, therefore, should be designed in such a way that all crew members can operate Lidar with only a minimal amount of training.

It was also concluded that on-orbit operations have to be pre-programmed to a large extent, and that real-time control from the ground is not realistic. This, in addition, points to a Lidar operational concept that lends itself to relatively simple crew interfaces and operations, and that does not require complex on-orbit operational steps that can only be carried out by a highly specialized and trained payload specialist.

3.4 STS SAFETY

In order to assure that no hidden safety hazards exists in the selected Lidar concept, a brief hazard analysis was carried out.

The overriding STS safety requirement is to assure the retention of the capability for the safe recovery of the Orbiter/Spacelab and the crew.

Experiments/payloads need to be designed for inherent safety and hazard elimination and or control. Of significant impact on overall payload complexity is the requirement to provide emergency ejection/retraction capability for experiments which extend outside the Orbiter cargo bay envelope during any phase of on-orbit operations. To avoid this increase in Lidar system complexity it was decided to constrain Lidar to stay within the Orbiter cargo bay envelope at all times during on-orbit operations.

The preliminary Lidar hazard analysis shows that no hazard exists which cannot be eliminated or controlled by appropriate design (e.g., dye-laser fluid containment).

Astronaut eye safety can be easily handled by covering the viewports from the aft flight deck into the Shuttle cargo bay during operation of the visible and near visible lasers, operation at the far infra-red wavelengths is eye safe since the ports are opaque at these wavelengths.

3.5 STS DEFICIENCIES

The Lidar system developed during this study is capable of meeting most experiment requirements identified in the SEED within the capabilities and constraints of the STS.

Experiment objectives cannot be fully met in two areas:

1. Wind measurements which require a scanning system with highly accurate pointing. This is not an STS deficiency since accurate pointing is an experiment responsibility.
2. Measurements in polar regions. This is due to an STS deficiency, but only during early missions, until WTR launches become possible.

There are three areas in which improved STS capabilities can improve Lidar performance capabilities and operational flexibility. These are:

- Increased availability of electrical energy
- Increased command uplink capabilities
- Baseline use of 2nd TDRS antenna on the Orbiter.

4.0 SYSTEM REQUIREMENTS

General - The Lidar system requirements are based upon the needs of science (Section 2), the constraints of the Space Transportation System (Section 3), and the study goals and system objectives (Section 1). The key system challenge is to develop requirements and a design approach which will effectively and efficiently support the evolutionary goal of the Lidar system. The accomplishment of the goal will be paced by current and anticipated technology status throughout the intended 10 year life of the program.

The following sections discuss the mission requirements, the system requirements and constraints, and a system design approach which supports the program objectives.

The system design approach is intended to yield a Lidar instrument system which satisfies all of the requirements and allows the allocation of system functional requirements to the various subsystems.

It should be noted that the system requirements interact strongly with the design of the system. It was not reasonable to establish quantitative requirements at the beginning of the effort because technology evaluations of laser, telescopes, detectors, etc., had not been performed. The system requirements were the result of design iterations based on the science needs and the constraints and limitations introduced by current and future technology, logical growth, physical limitations, operations, and reasonable cost considerations.

4.1 MISSION REQUIREMENTS

The basic Lidar mission requirements are defined as follows:

- Accomplish science contained in the SEED in a safe, evolutionary, cost effective manner
- Establish a logical growth plan to achieve the above consistent with

technology availability

- Utilize Space Transportation System (STS)
  - Launch, orbit, & return
  - Single Spacelab (SL) Pallet
- Support refurbishment and/or reconfiguration at launch site
  - 3 launches/year rate
- Provide a 10 year useful life
- Define modular assemblies

Safety of the flight crew is of paramount importance and creates significant system requirements which are discussed in Section 4.4. The SEED science requirements, coupled with the need for cost effectiveness, indicate the selection of a growth plan which will complement the science data return, as the state of the supporting technologies continue to develop. Figure 4-1 illustrates a growth scenario which allows major portions of the system (receive telescope, structure thermal control, command and data handling and electrical power subsystems) to remain virtually unchanged as the pacing laser technology develops. System growth is localized to the sources, detectors, and correlative sensors. This approach not only provides for system growth but, when carefully implemented, allows for significant configuration flexibility from flight to flight.

The utilization of the Spacelab Pallet and its associated subsystems (such as thermal control and command data system) during launch, orbit and return established constraints on the system for volume, mass, power, thermal, physical handling, integration, and operations. These constraints are defined in Section 3.0 and the resulting system level requirements are defined and discussed in more detail later in this section.

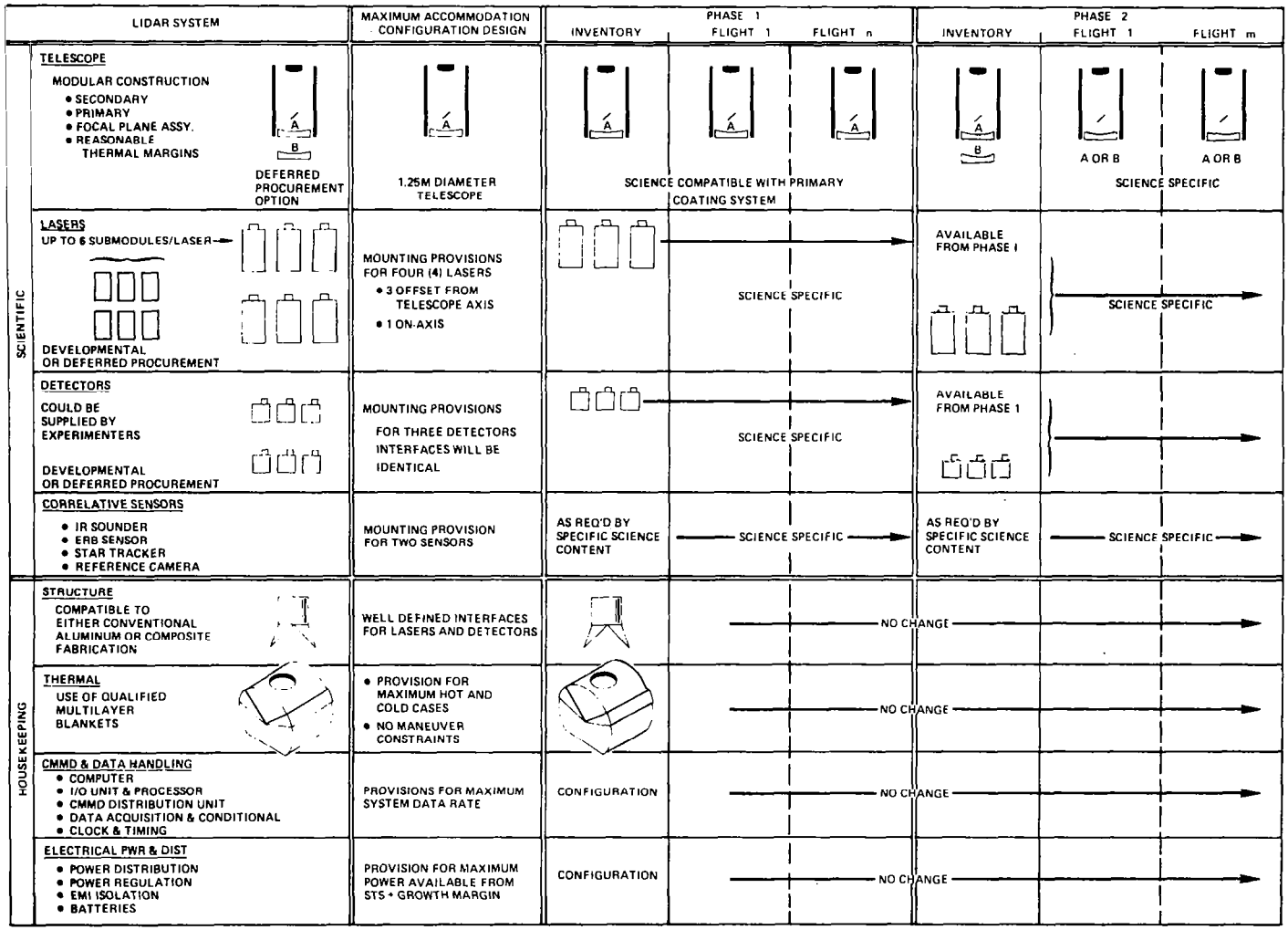

Figure 4-1. Conceptual Lidar Growth Scenario

The 10 year useful life requirement, at 3 flights per year, indicated that Lidar will spend the majority of its life on the ground. Thus it is similar to an airplane rather than a spacecraft. This creates requirements with respect to durability of the equipment in an environment that is less well defined and controlled than the normal orbital environment. Weight and cost permitting, it is a goal to create a system which is capable of reliable, repeatable assembly and disassembly. Modularity of the various Lidar assemblies, with straightforward and repeatable interfaces will contribute substantially to the reduction of human assembly and check-out error. This modular approach is required to the lowest practical level of system assembly to assure the consistent integrity of the system. Modularity also enhances, by minimizing the assembly and check-out, the timeline of the Lidar system.

4.2 PERFORMANCE REQUIREMENTS

4.2.1 SIGNAL AVAILABILITY

System performance requirements reflect directly the needs of the science defined by the twenty six experiment classes discussed in Section 2.0. The science evaluation has indicated that the laser signal return must be maximized to assure meaningful data. Hence the system requires the highest power laser and the largest diameter telescope that can be provided consistent with key limiting constraints.

The major limiting constraints are:

1. - Development status and associated availability of lasers with adequate efficiency to insure signal quality within the power limits available from the STS. The doubled Nd-YAG laser family appear to best meet this dual requirement for both availability and efficiency as indicated in Section 6.0

2. - STS provision for all necessary services, via the Spacelab interfaces, to the Lidar system. The Lidar system is required to live within the power limitations of the STS/SL and within the dimensional envelopes established by the payload bay and

the availability of control and display areas on the aft flight deck of the STS. In addition, thermal compatibility to both the Spacelab and STS thermal control systems must be assured by the Lidar thermal control system to maintain an acceptable thermal environment for its equipment.

3. - Size limitations induced by the use of a single Spacelab Pallet. This limit was customer-defined after a series of preliminary task studies indicated that a telescope of less than 1.5 meters in diameter would adequately meet the needs of the Lidar science.

4.2.2 SIGNAL DYNAMIC RANGE

The Lidar system must be capable of operation in both day and night time frames. To meet this overall performance requirement the laser, (for reasons of eye safety previously discussed) and the telescope (to maintain an acceptably low noise level) must be provided with beam dispersion and field of view adjustment capability. The precise range was developed during the study based upon the dynamic range of the detectors and the processing accuracy of the data management system.

4.2.3 RETURN SIGNAL LOCATION

For some of the experiments the geodetic location of the return signal is significant with respect to both the data itself and for purposes of correlation with other sensing systems. An analysis of the science requirements indicates that a 0.5 degree post-flight pointing knowledge, when coupled with ephemeris data, will be adequate for most experiments. As the STS pointing uncertainty, defined in Section 3.0, is in excess of this requirement, the Lidar system must provide a correlative attitude sensing system.

Active (real-time on-orbit) pointing, required to support the wind evaluation experiments, will require the determination of the Lidar line of sight with respect to the STS inertial reference system about three orthogonal axes. In addition, the

STS must be maneuvered to establish and maintain the correct pointing attitude based on the Lidar line of sight orientation. The Lidar system, being a fully integrated optical assembly, is capable of orderly growth to meet these requirements.

4.3 SYSTEM DESIGN REQUIREMENTS

The system design requirements for the Lidar system are derived from an analysis of the SEED, the mission requirements and operational capability, and the constraints of the STS/Spacelab. The system requirements are listed in Table 4-1 which notes the particular subsystems and operational areas that are affected.

These system design requirements, when coupled with the system design approach will create the initial allocation for the Lidar subsystems defined in Figure 4-2. The cross-hatched items of this figure are provide by Spacelab and support the Lidar interfaces to the STS and the ground.

4.4 SYSTEM DESIGN APPROACH

The design of the Lidar system was achieved by defining the priorities of the applicable system requirements and then performing trade studies relating system performance to system constraints until a cohesive, balanced design was achieved. Such a design must: provide adequate performance; be technologically achievable within the time period of the program; lend itself to orderly growth and be capable of being realistically costed. Figure 4-3 illustrates the above process and is discussed in further detail in the following paragraphs.

The prioritization of requirements established that safety, of both the crew and the population in the target areas, was of first order concern and not a tradeable item. This then created definite limits for ground level incident laser energy which, when coupled with direct solar illumination, became a forcing function with respect to telescope size. STS/SL accomodation, on the other hand, placed an upper limit on the

Table 4-1. System Requirements Summary

REQUIREMENT	SUBSYSTEM IMPACT
PERFORMANCE	
SEED ANALYSIS INDICATES THAT LIDAR REQUIRES:	
• GLOBAL COVERAGE - ETR & WTR LAUNCH	– THERMAL-COMMAND/DATA
• DAY & NIGHT OPERATION	– LASER-TELESCOPE-THERMAL
• 200 TO 400 KM ALTITUDES	– LASER
OPERATIONS	
MISSION REQUIREMENTS ANALYSIS INDICATES THAT LIDAR REQUIRES:	
1) COMPATIBILITY TO ORBITER AND SPACELAB STANDARD INTERFACES	
• MAXIMUM ACCOMODATION OF SUN ANGLES WITH RESPECT TO THE RECEIVER TELESCOPE AXIS	– CONFIGURATION
• ACCOMMODATE ANY PRIOR STS MANEUVER HISTORY WITHOUT PRE-CONDITIONING TIME INTERVAL	– THERMAL
2) MAXIMIZE COMPATIBILITY TO OTHER SPACELAB PAYLOADS	
• POWER – 3500 WATTS OPERATIONS 200 WATTS STANDBY	–LASER-THERMAL
• WEIGHT – $\lesssim$ 2300 Kg (5000 LBS.) PALLET CAPABILITY	– DESIGN MARGINS
• THERMAL – MEET SPACELAB COOLANT LOOP TEMPERATURE INTERFACE RANGE - 0° TO 40° C	– THERMAL-DETECTOR
• LOCATION – ANYWHERE IN CARGO BAY	– STS-MISSION MANAGER
3) OPTIMIZE PRE-FLIGHT INTEGRATION INTERFACES	
• INSURE RAPID RECONFIGURATION	– CONFIGURATION
• ESTABLISH SYSTEM CONFIDANCE VIA A WELL INTEGRATED TEST PLAN	– USE PROVEN DESIGN APPROACHES
• SIMPLIFY HARDWARE/SOFTWARE AND SOFTWARE/SOFTWARE INTERFACES	– COMMAND AND DATA
4) ASSURE OPERATIONAL CONTROL BY ANY CREW MEMBER	
• PRE-SET EXPERIEMNT SEQUENCES ON ORBIT - ABILITY TO SELECT AND COMMAND	– COMMAND
• ON-ORBIT TARGETS OF OPPORTUNITY TO BE DEFINED TBD HOURS PRIOR TO EXECUTION-STS MISSION MANAGER et el 0.5 HOURS PRIOR TO EXECUTION-LIDAR	– MISSION PLANNING
• REAL-TIME TELEMETRY & COMMAND IS NOT REQUIRED AT ALL TIMES	– COMMAND & DATA HANDLING
• AUTOMATED SYSTEM – HOUSEKEEPING DATA – ALARMS FOR CRITICAL HOUSEKEEPING FUNCTION – SUCH AS TEMPERATURE DIFFERENTIAL ON PRIMARY MIRROR	– DISPLAYS – COMMAND & DATA ELEMENTS
• SEMI-AUTOMATED ALIGNMENT TECHNIQUES	– COMMAND & DATA HANDLING

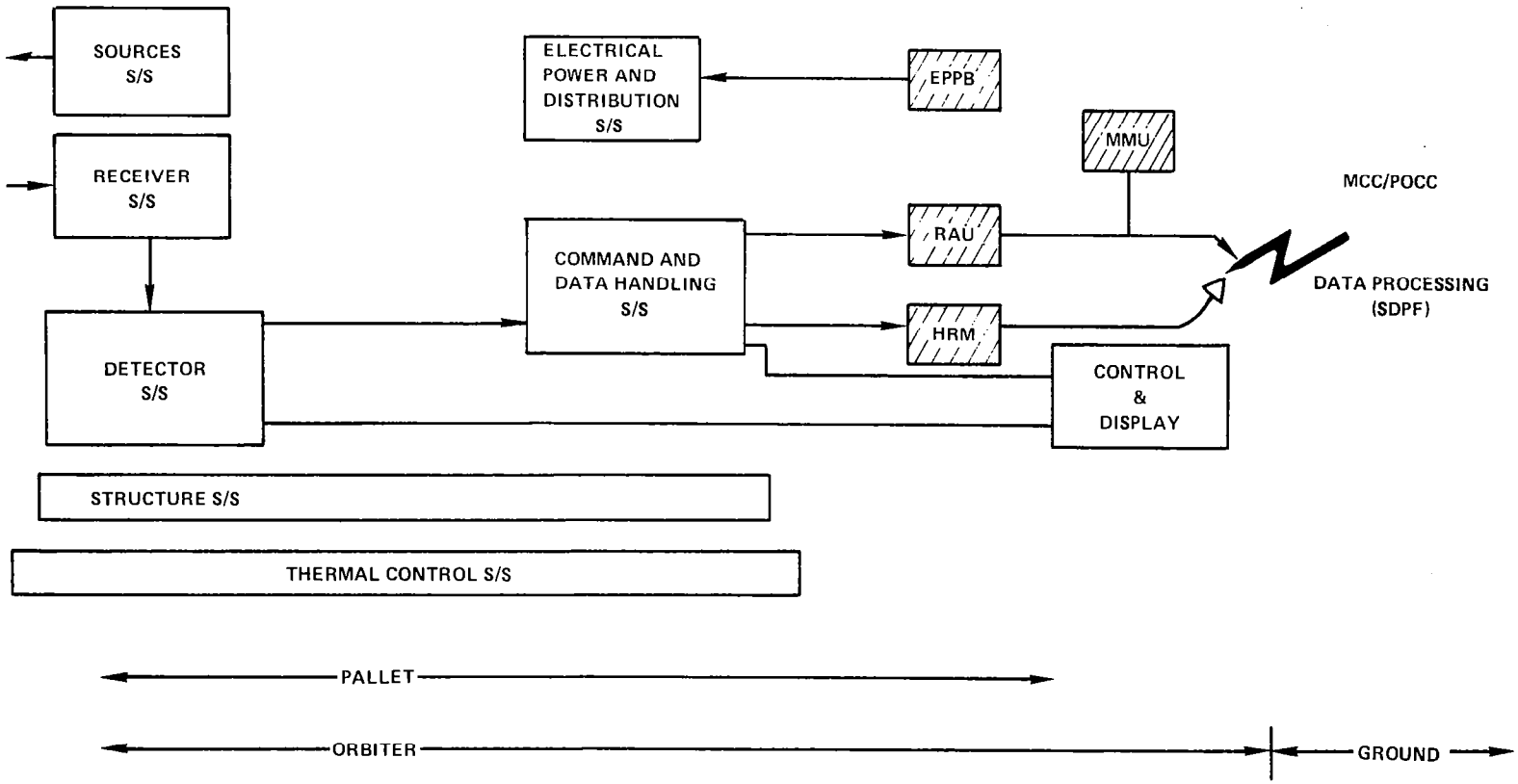

Figure 4-2. System Definition by Subsystem.

SAFETY

- CREW SAFETY
- EYE SAFETY

CONSTRAINTS

TECHNOLOGY

- STS/SPACELAB ACCOMMODATION
  - TELESCOPE SIZE
  - LASER POWER
  - THERMAL CONTROL
  - STRENGTH & STIFFNESS
  - CMMD & DATA HANDLING
  - POWER & ENERGY MANAGEMENT
  - DETECTOR ARRANGEMENT
- DEVELOPMENT STATUS

PERFORMANCE TRADES

GROWTH

- ORDERLY GROWTH OF SCIENCE EQUIPMENT INVENTORY
- MINIMIZE IMPACT OF SCIENCE GROWTH ON SUPPORTING SUBSYSTEMS

MODULARITY

COST

- ESTABLISH ACCEPTABLE COST PATH TO ACHIEVE SEED REQUIREMENTS

TIME DEPENDENT

Figure 4-3. System Design Approach.

size of the telescope which could be accomodated. Diameters ranging from 2.5M to 1.0M were evaluated. The 2.5M telescope required on-orbit deployment through the STS door envelope severely impacting the safety of the crew in the event of a malfunctioning stowage sequence. A 1.25M telescope was the largest telescope of reasonable focal length (cost consideration) which could be installed without violating the STS door envelope. Signal return analysis, as discussed in Section 2.0, indicated that the 1.25M telescope would satisfy the science requirements when used in conjunction with the lasers defined in Section 6.0.

Co-alignment sensitivity of the lasers and telescope was also considered in the signal return analysis and its impact on performance was recognized as a key consideration in the design. Performance, cost, and weight trades to evaluate the consequences of both passive and active co-alignment approaches were performed, resulting in the choice of an active system. An adjustable secondary mirror in the telescope was selected via additional trade studies as the most appropriate point for incorporation of this capability. Impact of the system thermal control requirements (absolute temperature control of the detector, thermal gradient control of the telescope and mass heat removal from the lasers and supporting electronics) was evaluated via a series of trade studies. Separate thermal control of each item versus collective control of the entire Lidar system was assessed for the probable operating modes of the STS. The latter approach was selected due to its collectively greater thermal capacitance and its inherent ability to de-couple the Lidar system from the broad (~300°C) payload bay temperature changes which can take place within an orbit. The selection of a thermal approach was closely related to the co-alignment trades and some of the detailed configuration trades for the telescope.

The Command and Data Handling area was the subject of a key system level trade study - the use of the SL experiment control computer or the inclusion of a dedicated Lidar

computer. Some of the major considerations in this trade were: compatability to ground test and pre-flight integration; integration impact of experiment modification; i.e., minimal time prior to launch; on-orbit operations including both housekeeping and quick-look science evaluation; and the growth capability of the system throughout its intended 10 year life. These, and other considerations were evaluated with respect to weight, power requirements, cost, and overall system compatibility. The results of these trades, a dedicated Lidar computer, are described in Section 8.0.

Structural considerations were inherent to the major configurational trades used to define the acceptable telescope size as well as the laser and detector arrangement and the thermal control techniques. Co-alignment requires that deformations, either thermally or mechanically induced, be minimized. Hence, all load paths should be as short and direct as possible. Section 9.0 summarizes the key trades in the structural area which resulted in the use of a torus type support structure for the telescope, lasers, and detectors.

Electrical power and distribution requirements did not have major impacts upon either the system or its configuration. The basic trade between a regulated and unregulated power bus is discussed in Section 9.0 as part of the Electrical Subsystem discussion.

The system requirements for growth of the science content under the ten year operational life and a flight frequency of every 120 days were the major drivers for modularity of the system. A modular design of the laser assembly which allows for growth and flight-to-flight-modification of the laser was defined. The structural assembly of the lasers, detectors and correlative sensors, which is alignment critical, was also modularized at the major interface attach points. The detector assemblies are designed to accept different photomultiplier assemblies with little if any modification. The telescope can accept modification of its optic elements within

its structural assembly.

Table 4-2 summarizes the major system trades discussed above, which were performed to determine both the allocation of subsystem requirements and the final design for the Lidar system. Other associated trade studies at the subsystem level were also performed to characterize the final design relationships and are presented in Sections 5, 6, 7, 8 & 9.

The trade studies described above resulted in the allocation of subsystem requirements addressed in the next section. It should be noted that some of the key subsystem requirements could not be quantified at this point in the study because they are defined based on the best compromise between the requirements of the science and the availability of flight hardware and were developed as part of the subsystem definition trade studies to be addressed later in this report.

4.5 SUBSYSTEM REQUIREMENTS ALLOCATION

The subsystem requirements allocation are based upon the system performance requirements and the near and far term capability of industry to supply the necessary equipment in response to those requirements. The subsystem requirements summarized in Table 4-3 are those which will satisfy the near and far term requirements of the science. The direct science subsystems - Sources, Detectors, and Receiver Telescope have been allocated sufficient growth margin to assure accomplishment of the entire science challenge by means of an orderly growth sequence. The supporting subsystems - Command and Data Handling, Thermal Control, Electrical Power, and Structure are specified to accommodate the entire science requirement with little or no modification throughout the entire 10-yr. life of the Lidar.

Significant system parameters such as weight, power, commands, and engineering data,

Table 4-2. System Performance Trade Summary

TRADES	VARIABLES EVALUATED
TELESCOPE – TYPE – APERTURE – f NO.	– FOV-RANGE – FILTER DIAMETER – ALIGNMENT – ARRANGEMENT – ERROR APPORTIONMENTS – GROWTH
LASER Nd YAG EXCIMER RUBY FLASH PUMPED DYE	– AVAILABILITY – EFFICIENCY – GROWTH – POWER
DETECTOR OPTICAL ACCESS	– TYPES – ARRANGEMENT – GROWTH
COMMAND & DATA AUTONOMOUS/DEPENDENT DIGITAL/ANALOG ONBOARD/GRD.PROCESSING STORED/REAL TIME CMMDS	– TRAINING – DATA RATES – COMPLEXITY – REPEATABILITY – GROWTH – INTEGRATION TIME CYCLES – INTERFACES
THERMAL CONTROL ACTIVE/PASSIVE COLLECTIVE/DISBURSED	– ABSOLUTE TEMP. – FLUXES: INTERNAL & EXTERNAL – GRADIENTS – POWER
ALIGNMENT PASSIVE/ACTIVE RECEIVER/SOURCE	– TOLERANCES/COST – SIGNAL/NOISE – COMPLEXITY/RELIABILITY – THERMAL

Table 4-3. Subsystems Requirements

		REQUIREMENTS TRACEABILITY
SOURCES	POWER: TRADE STUDY RESULTS PULSE RATE. MAX – 10 Hz PULSE CHARACTERISTICS – ADJUSTABLE: SINGLE SHOT TO 10 HZ OVERALL EFF. – TRADE STUDY RESULTS	– SCIENCE – AVAILABILITY – SYSTEM TRADES
RECEIVER	SPECTRAL RANGE: 0.2 – 12.0 MICROMETERS FILTER BANDPASS RANGE: 0.01 TO 5.0 NANOMETERS IMAGE QUALITY: DIFFRACTION LIMITED @ 10.6 UM STRAY LIGHT REJECTION RATIO: 10^{-3} MAXIMUM CLEAR FILTER APERTURE: 45 mm DIAMETER: TRADE STUDY RESULTS ALIGNMENT ADJUSTMENT 2 mr	– SCIENCE – SYSTEM TRADES
DETECTOR	DYNAMIC RANGE: 10^5 DETECTION CAPABILITY: – PHOTON COUNTING – HETERODYNE DETECTION – POLARIZATION SEPARATION – HIGH DISPERSION ELEMENT FILTERS: 24 WAVELENGTHS	– SCIENCE – AVAILABILITY
COMMAND & DATA HANDLING	100 DISCRETE, 10 SERIAL COMMANDS @ 10 CMMDS/SEC 10 NS SYSTEM CLOCK – 10 MS GMT SL/STS COMPATIBLE SEMI-AUTOMATED	– SCIENCE
POWER	DISTRIBUTE 3500 WATTS – UNREGULATED 28 VOLTS/ REGULATED 5V TLM INTERNAL REGULATION PROVIDED BY EACH COMPONENT CRYO COOLING PROTECTION VIA BATTERIES	– STS – SYSTEM TRADES
THERMAL	3500 WATTS INTERNAL DISSIPATION WORST CASE HOT/COLD CONDITIONS – STS 0° TO 40°C COOLANT INTERFACE TO SPACELAB HEAT 25°C MAXIMUM DETECTOR TEMPERATURE 10°C MAXIMUM TELESCOPE GRADIENT CLOSED LOOP CONTROL VIA COMPUTER	– STS – SYSTEM TRADES
STRUCTURE	SUPPORT AND PROTECT ALL COMPONENTS CONVENTIONAL MATERIALS & ASSEMBLY 10 YEAR LIFE – AIRFRAME NOT SPACECRAFT PHILOSOPHY	– STS – SYSTEM TRADES

thermal control, etc. have been explored in sufficient detail to assure the adequacy of the allocations in support of both the total science requirements and the 10 year operating life.

The simplified system block diagram showing some of the salient subsystem functional allocations is shown in Figure 4.4.

The following sections discuss in some detail the subsystem requirements listed in summary form in Table 4-3.

4.5.1 SOURCE SUBSYSTEM

The source subsystem consists of the lasers and associated power supplies, heat exchangers, etc. required to meet the needs of the science. It must have sufficient output power to provide an adequate signal return at the various wavelengths defined, within the electrical power limitations placed by the STS/SL. Its divergence angle must be adjustable to insure adequate eye safety margins for both sunlit and night operation. It must be capable of performing between 200 to 400 KM altitude. It shall have minimal warm-up time and not require stand-by power during periods of non-use. The pulse rate shall be adjustable up to a maximum of 10 HZ. The laser line of sight shall maintain its relationship to the mounting plane of the laser as determined by trade studies. Weight and volume are not critical parameters with respect to the laser but do interact strongly with the system configuration and are defined by trade studies. It shall be a modular assembly which is capable of being reconfigured and tested within a thirty day period.

4.5.2 RECEIVER SUBSYSTEM

The receiver subsystem consists of the receive telescope and its associated control electronics. Experiment requirements dictate that it should be a diffraction limited system at the 10.6 micron wavelength. The telescope shall be contained in a

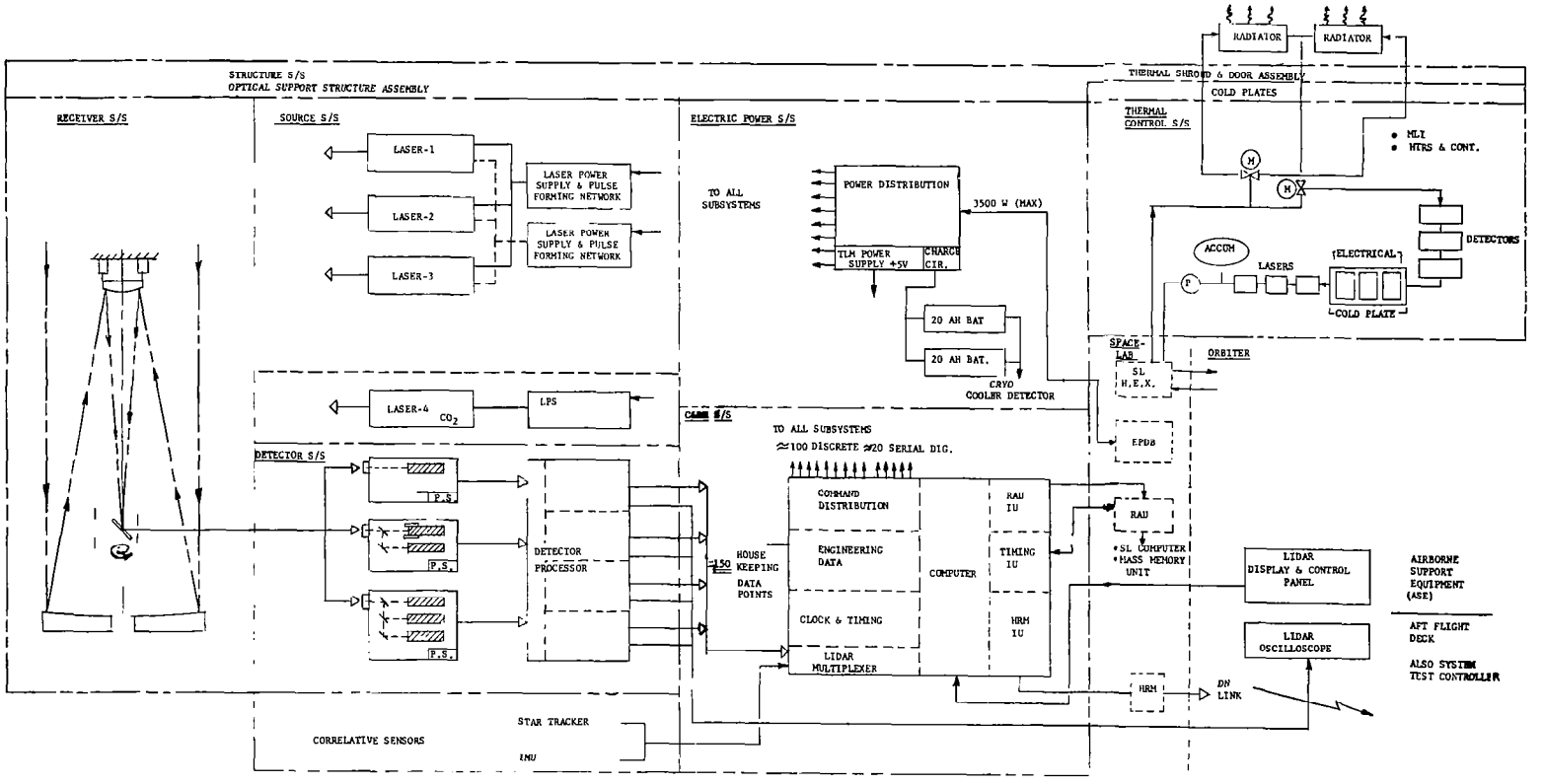

Figure 4-4. System Block Diagram.

controlled thermal environment. It shall be capable of maintaining adequate image quality during periods of extended ($\sim$ 1.5 hours) earth viewing. The use of interchangeable refractive elements to satisfy a spectral range of 0.2 to 12 micrometers is permitted as long as the interchangeability does not degrade the internal alignment of the telescope. The type, aperture, focal length, exit pupil diameter, and alignment requirements are derived from system level trade studies. There is a strong interaction between the aperture and focal length of the telescope with respect to packaging the instrument on one Spacelab pallet within the STS cargo bay. The system trades, based on science needs, were directed at defining the largest practical aperture consistent with the above constraints. The telescope is not technology limited and does not pace the development of the system. It is, however, required to be capable of achieving modest functional growth to assure satisfying all of the science requirements. Hence, a modular design is a requirement.

4.5.3 DETECTOR SUBSYSTEM

The detector subsystem consists of a number of detector assemblies each of which contains one or more filters and photomultipliers, and a detector processor. The photomultiplier/filter assemblies are defined by the particular wavelength of interest as noted in the science requirements. The detector processor provides the functional capability required to identify the signal with respect to discrete ranges. The detectors subsystem must provide a dynamic range capability of 10^5 to accommodate the anticipated return signal variations under all conditions of operation. The detector assemblies shall be capable of accommodating all the wave lengths required to perform a particular experiment. This is based on a configurational analysis, which indicates that it is not desirable to split the returned signal prior to exiting the telescope. The detector assemblies must be capable of providing adequate internal thermal control of filters, cryo-cooler, etc. when their mounting plate temperature is maintained at $25^{o}C$ or less. The detector

assemblies and the detector processor shall provide internal power regulation to suit their needs when supplied with 28 $\pm$ 4 Volts DC. Modularity within the detector assembly to allow for photomultiplier/filter substitution shall be provided.

4.5.4 COMMAND AND DATA HANDLING SUBSYSTEM

The science need for global coverage coupled with the frequent unavailability of a command link via the TDRSS system creates a requirement for onboard automony for the command sequences. The capability to acquire science at any time an orbit requires that the command techniques be comparatively simple and straightforward; i.e., those which can be implemented by any watch-standing crewman, not just the payload specialist. The system must provide pre-programmed experiment sequences which need only to be initiated by the duty crewman. These commands sequences will be stored on orbit and utilized as directed by the mission manager's and flight director's time line.

Real-time commands from the ground are severely limited due to the low effective up-link bit rate available and hence are not suitable for experiment control. They can, however, be utilized to direct the substitution of experiment sequences if required. The system should be capable of responding to such commands within 0.5 hrs.

Spacelab/STS compatibility is required. It can be achieved via integration with the Spacelab experiment control computer or by means of a dedicated Lidar computer. The latter approach, based on preliminary analysis, appears to be the best with respect to minimizing extensive, costly software integration with Spacelab/STS. The subsystem design discussion in Section 8 treats this in more detail and presents trades that led to these conclusions.

The subsystem shall provide approximately 100 commands at a rate of 10/sec. Commands shall be both discrete and serial digital. It shall provide a 10 nanosecond system

clock and establish a 10 msec correlation to GMT as defined by the STS/SL interface. It shall provide processing of system status information - temperature, voltages, etc. and display the output with associated limit values to the operator so that corrective commands can be initiated. It shall provide an on-orbit alignment capability that will aid the operator in aligning the receive telescope to the laser.

4.5.5 ELECTRICAL POWER DISTRIBUTION SUBSYSTEM.

The electrical power distribution subsystem shall accept power, 4500 watts maximum, from the STS/SL interface and provide relay distribution to the elements of the Lidar system upon command. The main power bus shall be unregulated and will provide 28 ± 4 volts DC. 5 - volt regulated power shall be provided for LIDAR telemetry, sensing, and control requirements. A charge circuit to maintain the charged status of an auxillary power source, required to assure adequate cooling of detector elements during brief periods of STS/SL bus power denial, shall be provided. The auxiliary power source shall utilize flight proven batteries for energy storage. Harness/connector assemblies shall be separated into power, command, data, etc., segments. The system shall meet all EMI requirements of STS/SL.

4.5.6 THERMAL CONTROL SUBSYSTEM

The thermal critical subsystem shall provide suitable protection and conditioning for all Lidar equipment when installed on a Spacelab pallet. It shall have auxiliary ground interfaces to assure the same degree of protection during appropriate ground operation periods. It shall maintain control within Lidar operational limits without regard to prior STS maneuver history. It shall meet all of the STS/SL thermal interface requirements. It shall utilize 200 watts maximum of power during periods of non-Lidar operation.

4.5.7 STRUCTURE SUBSYSTEM

The structure subsystem shall provide adequate alignment, protection, and support to all elements of the Lidar system, in all of the defined environments, throughout its 10 year useful life. It shall assure the modularity of the Lidar system by providing repeatable field interfaces for critical equipment. It shall be designed to enhance ready access to all items of equipment so that sequential disassembly is not required. It shall be capable of being repaired and/or refurbished in the event of accidental damage without replacement of the entire assembly.

4.5.8 SYSTEM DESIGN APPROACH SUMMARY

Analysis of Lidar requirements at all levels coupled with an understanding of the system constraints introduced by the STS, SL, safety, technology, operations and growth created the design envelope for the Lidar system. System design trade studies were then utilized to quantitatively assess the impact of alternate preliminary system designs upon the performance of the system. The results of these trade studies established subsystem performance and design requirements which insure the performance integrity of the system and allow procurement of achievable hardware within the time content of the program.

5.0 RECEIVER SUBSYSTEM

5.1 INTRODUCTION

In the following presentation, the receiver will be considered to consist of two subsets; the telescope optics - those elements which collect incoming radiation and contribute to the formation of an image at the focal plane; the focal plane optics - those elements necessary to relay the light from the image to the detector package and to provide the optical characteristics appropriate for the narrowband filter.

The early phase of the receiver effort was devoted to an examination of the experiment descriptions in the revised SEED document in order to extract those requirements which bore on the definition of the receiver system. In addition, parametric size and cost relationships were derived to assist in scaling the receiver as part of the total payload.

In the receiver subsystem definition phase, each of the design aspects of the reciever was examined and in each case criteria were established, trade-offs evaluated, and conclusions drawn. In the optical design area these included the optical layout and type, image quality derivation, nature of the focal plane optics, implications of various coating options on the system transmittance, expected polarization effects, and the control of scattered light in the system. In the packaging design, a system level error budget was established, and structural concepts and thermal designs were developed to achieve a coordinated balance with respect to the budget. The specification of the nature of the primary mirror was also considered in the same light. Drawing on the design characteristics above, a baseline receiver design was modelled and its essential elements and interface properties detailed.

In the programmatic area, the cost and schedule requirements for the baseline receiver design were examined in detail by customary ITEK methods and these data

incorporated into the system level resource estimates to be reported elsewhere. An assessment of risk areas and identification of options for later phase growth were also undertaken and will be discussed herein.

5.2 SUBSYSTEM REQUIREMENTS

Analysis of the SEED has established a number of specific quantitative characteristics which must be satisfied by the receiver telescope. First, the experiments are in many cases signal limited and benefit from having a maximum practical collecting area and throughput. This argues for sizing the receiver to be the largest that can be easily accommodated in the Shuttle bay. The fields of view required by the experiments range from 0.1 to 6.0 milliradians with a number of intermediate sizes to be available. There does not, however, seem to be a requirement for a continuously variable field stop. The spectral range encompassed by the experimental techniques is very broad, extending from 200 nanometers to 12 micrometers, with a number of individual experiments operating at two or more wavelengths. The filter bandwidths required are similarly broad, extending from 0.04 nanometers to 5.0 nanometers.

Image quality requirements for most experiments seem best defined in relation to the expected field of views for the particular experimental techniques. Larger fields of view demand lesser quality than smaller ones. The experiments involving heterodyne detection, however, will require diffraction limited performance at the operating wavelengths.

Signal-to-noise analysis by GE has been used to establish the stray light requirement. A stray light rejection ratio of better than 10^{-3} has been used as the basis for design evaluation.

Another significant constraint on the receiver optical design is the aperture diameter of the narrow bandwidth filter. Vendor inquiries by GE have indicated that 45 mm is a practical maximum; this number has been used in the receiver design.

Finally, a qualitative but essential requirement constraining the design is that it be totally compatible with the other elements of the Lidar system and the Shuttle/Spacelab vehicle.

Before examining the various optical design types for the receiver telescope, the image quality requirements must first be established. The only experiments for which image quality specifications are stated in the SEED document are those involving heterodyne detection, which require "diffraction-limited" performance. Although the term diffraction-limited is somewhat loose, it is taken to mean 0.075 wavelength rms. This quantity matches Rayleigh's quarter wave criterion, which was originally defined for one quarter wavelength peak-to-peak of spherical aberration. In defining an image quality criterion for other experiments a geometrical blur circle of 1/4th of the field of view diameter, (the "geometrical" blur circle being defined by tracing geometrical rays through the lens system and ignoring diffraction effects) has been chosen as the controlling criterion.

For later error budgets analyses, it is useful to state image quality uniformly in terms of wavelengths rms. Figure 5-1 translates the 1/4th field of view blur cicle diameter into waves rms for different fields of view, with the values corresponding to the first 12 SEED experiments being identified. (Experiment 5 has been included as part of experiment no. 2 in the revised SEED). The waves rms wavefront error refers to the amount of defocus required in a perfect lens of the appropriate focal ratio and focal length to produce the 1/4th field of view geometrical blur circle. The reference wavelength is that for the heterodyne experiments; 10.6 micrometers.

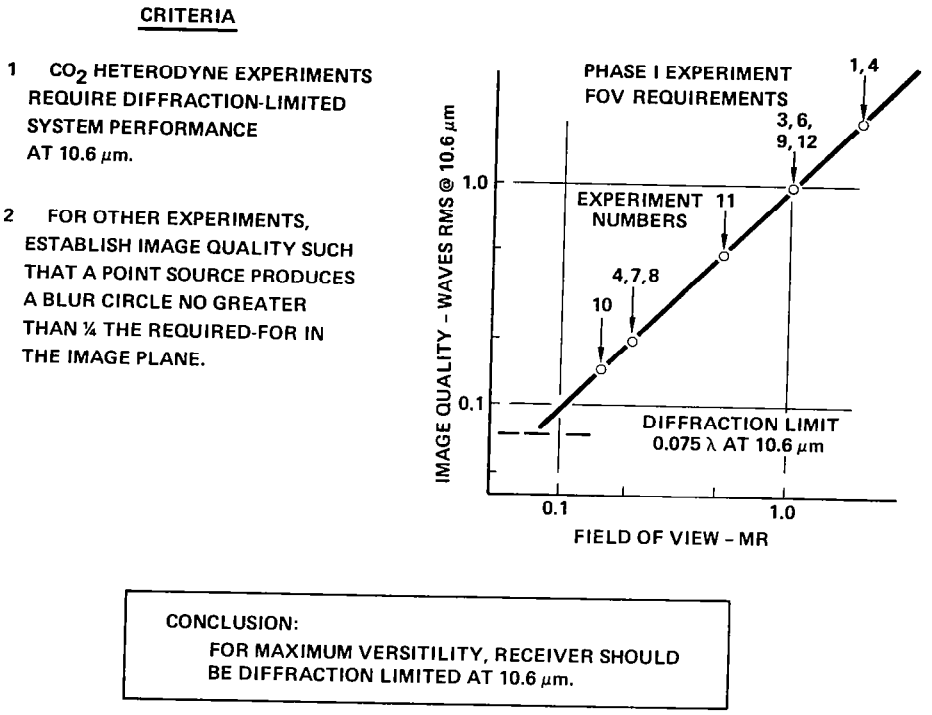

Figure 5-1. Image Quality Requirements.

For most of the experiments shown, image quality which is substantially less than diffraction limited is acceptable. The best image quality required for any experiment is the controlling value, however, and the telescope should be designed to be diffraction limited at 10.6 micrometers. The image quality can be allowed to degrade in regions away from the center of the field of view, however, since the heterodyne experiments operate with very small field of views.

5.3 PARAMETRIC TRADES

Along with the specific requirements derived from the SEED, a number of broader design considerations must be borne in mind. Some relate to the general mission characteristics, others are implied by the science requirements or fabrication aspects.

First, the receive telescope must fit within the volume available in the Lidar system/Shuttle envelope while at the same time achieving the largest practical collecting area. The length to diameter ratio must also be consistent with the envelope specification, although ease of fabrication argues for a slow focal ratio for the primary mirror.

The broad spectral range virtually requires that only reflective elements be used for those optics common to all experiment paths; likewise coatings must be chosen carefully to optimize transmittance over the range with attention to experiment priorities. The optical layout should also be chosen with regard to its polarization properties so as to not unduely compromise measurements of polarized signals (e.g., experiment 3).

As a general goal, the receiver should be operationally capable in a passive state, i.e., it should be capable of accomplishing its function immediately upon opening the Lidar system door without regard to preceding mission timelines or requiring "warm-up". The design should also be conservative and incur low risk both in its development and its operational use. Finally, the receiver should be as versatile as possible in its early forms while incorporating points of departure for logical growth options to be exercised during the projected 10-year lifetime.

5.3.1 RECEIVER

It was necessary early in the study to establish the general size of the receiver telescope in coordination with the broader system level considerations. Toward this end the size and weight characteristics associated with a variety of primary mirror diameters and focal ratios were evaluated over the range of interest for a Shuttle-constrained payload, as shown in Figure 5-2.

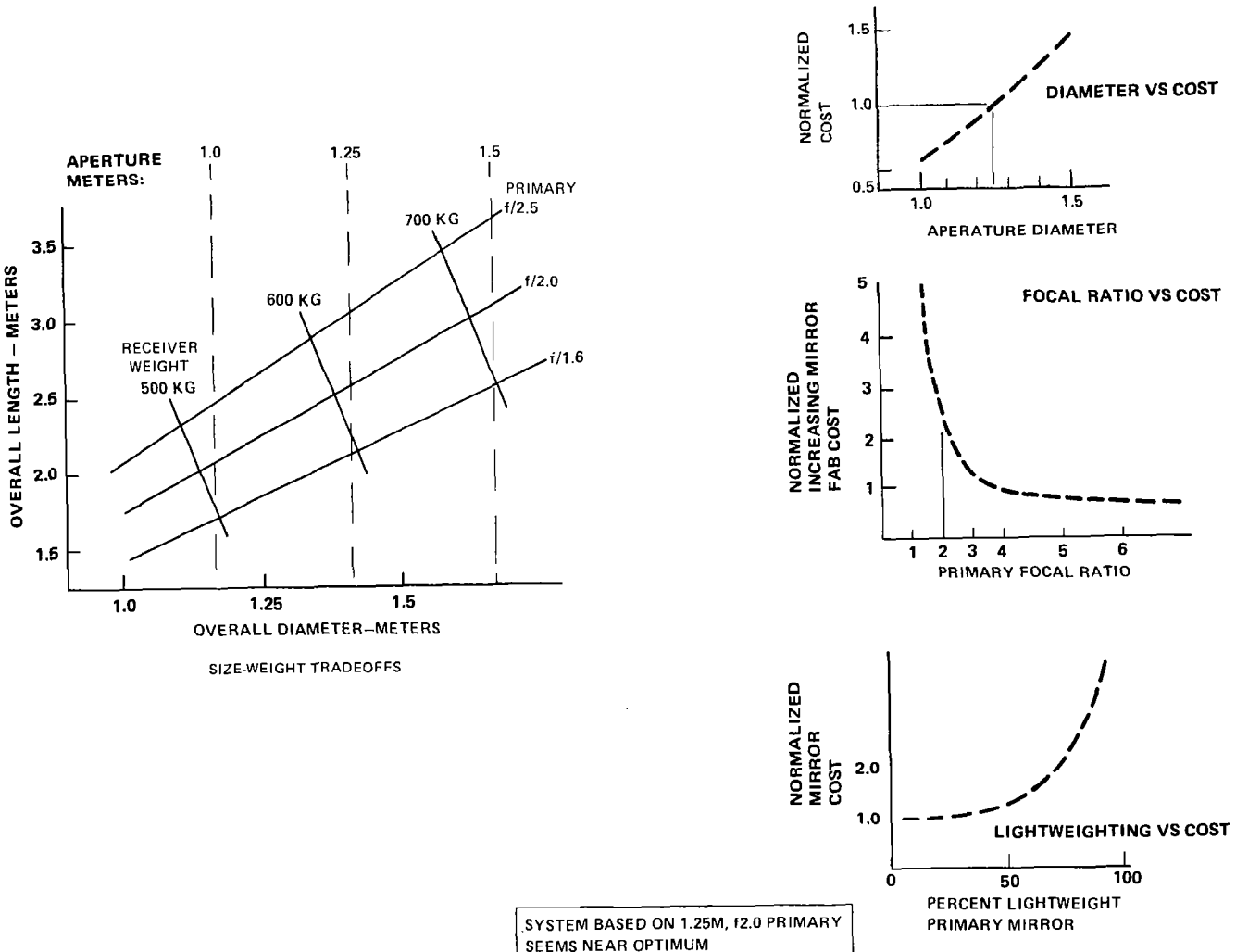

Figure 5-2. Receiver Sizing Characteristics Parameter Trades.

As shown in the left figure, the receiver diameter is proportional to the mirror diameter over the ranges evaluated and the overall length is also dependent on the primary focal ratio. Likewise, the receiver weight is principally dependent on mirror diameter but there is an additional effect from the primary focal ratio due to the telescope tube length. The parametric relationships shown are approximations, of course, and do not include effects of such second order factors as secondary mirror magnification, primary mirror support method, and field of view vs. tube diameter.

Receiver system cost is another aspect of the sizing trade studies. Although not as subject to explicit quantitative consideration, it is known that system costs scale up as size increases. This is because of increased material costs, fabrication time, larger fabrication and alignment tooling, more difficult handling, and many other factors. At the right is shown this power curve where the cost is related to the diameter squared; an empirical relationship generally in conformance with experience.

Focal ratio also contributes to cost; the faster the system, the more difficult it is to make. The center right figure shows the effect on fabrication cost of the primary mirror focal ratio. Note that the cost increments are relatively small above f/4, but are rising very steeply below f/2. These are a result of increased fabrication shop hours, more difficult testing and tighter alignment sensitivities and tolerances. Although the increased costs associated with producing a faster primary optical surface will be diluted at the system level, it seems reasonable to use a focal ratio of 2.5 or perhaps 2.0 unless forced by compelling packaging factors to a faster system.

The lower right figure depicts the cost effectiveness of lightweighting the primary mirror blank. Weight reductions of up to 50% can be achieved economically, thereby reducing total system weight. This level of lightweighting has been assumed in the overall weight estimates discussed above.

As a result of these parametric studies and other system level considerations, a receiver based on a 1.25 meter diameter f/2.0 primary seems near optimum for the Lidar system; such a model has been used as the reference for other aspects of this definition study.

A number of optical layouts were considered for the Lidar receiver; these are shown in the chart of Figure 5-3, along with the factors used in deriving the relative merit of each. On the left are more conventional layouts; all are drawn to the same scale, with each having an f/2.0 primary, so as to best represent the trade between length-to-diameter ratio and primary mirror focal ratio. The detailed ranking of these layouts will be discussed later. On the right are shown two unconventional layouts which were considered. Shown at the top right is a Cassegrain telescope with a parabolic collimator that provides a collimated output beam without requiring any refracting components. It will therefore operate over any wavelength range for which suitable mirror coatings are available. However, the entrance aperture is centered on the optical axis, the collimated beam returns on the image formed by the Cassegrain telescope, and the hole in the diagonal fold mirror needed to pass the image forms an "obstruction" in the output collimated beam. Thus a large image is not compatible with the small beam diameter required to pass through existing interference filters. This could be remedied with added optics for each sensor, but only at the cost of further reducing transmittance. A logical alternative is the eccentric pupil confocal parabola design. The central obstruction is eliminated, and only two mirrors are required to obtain a collimated output. Such a design, however, requires either a very large fast primary mirror from which the off axis element is cut, or the fabrication and test of a non-axisymmetric element, also very costly. For the reasons cited above, the unconventional designs were not considered in the final merit rankings.

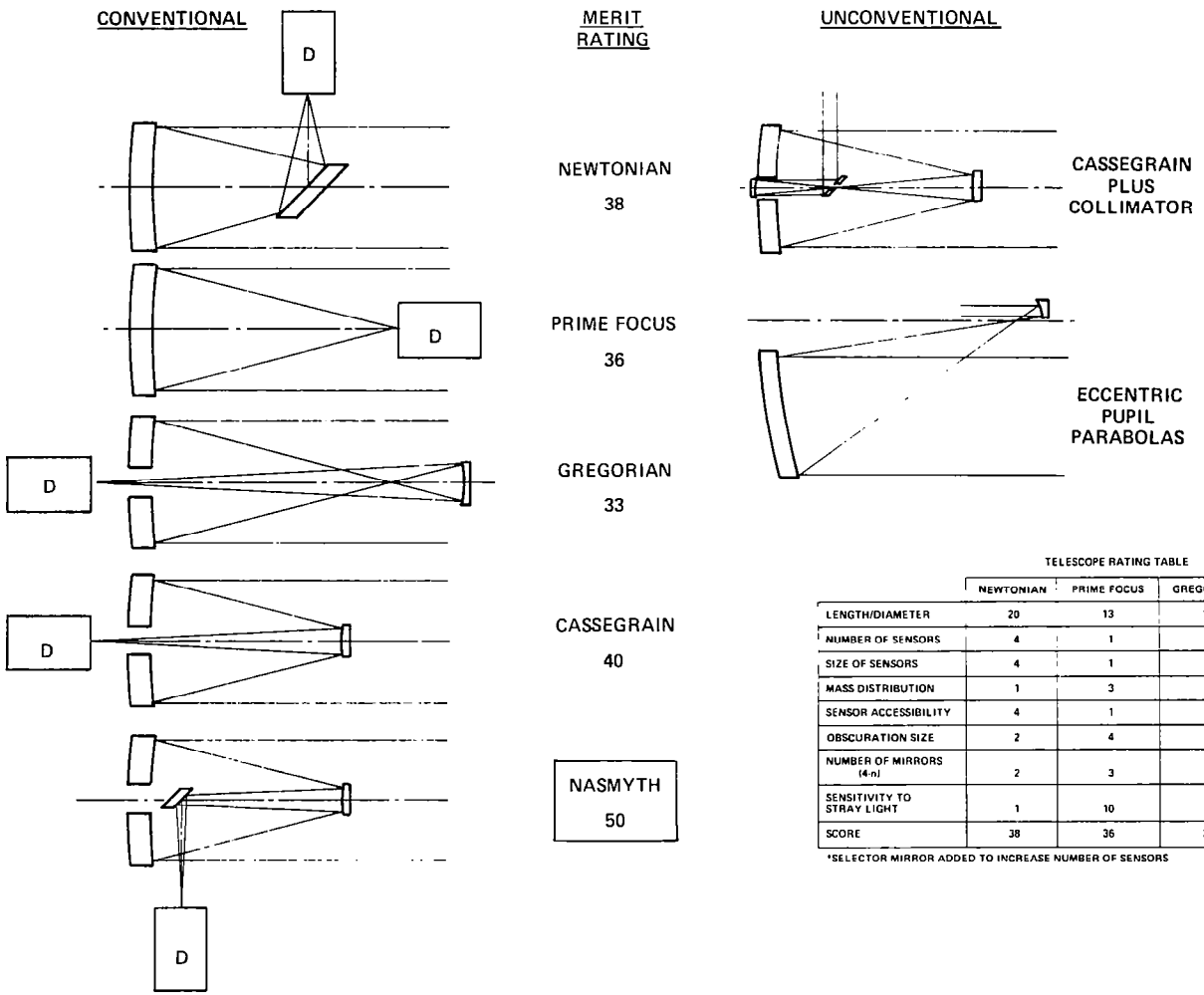

TELESCOPE RATING TABLE

	NEWTONIAN	PRIME FOCUS	GREGORIAN	CASSEGRAIN	NASMYTH
LENGTH/DIAMETER	20	13	10	14	20
NUMBER OF SENSORS	4	1	3*	3*	4
SIZE OF SENSORS	4	1	2	2	4
MASS DISTRIBUTION	1	3	2	4	5
SENSOR ACCESSIBILITY	4	1	2	2	3
OBSCURATION SIZE	2	4	3	4	4
NUMBER OF MIRRORS (4-n)	2	3	1*	1*	1
SENSITIVITY TO STRAY LIGHT	1	10	10	10	9
SCORE	38	36	33	40	50

*SELECTOR MIRROR ADDED TO INCREASE NUMBER OF SENSORS

Figure 5-3. Optical Layouts Considered

A detailed merit ranking matrix was constructed including each of the conventional layouts and the merit factors shown; the summary scores are listed beside each design. Length-to diameter considerations were heavily weighted and indicate a preference for the Newtonian and Nasmyth designs.

The number and size of sensor packages relate to the versatility of the Lidar system. The Gregorian focus and Cassegrain focus configurations received moderate downrating in this respect reflecting limitations on available volume behind the primary due to the Shuttle pallet configuration. This also relates to sensor accessibility for prelaunch maintenance, etc. Mass distribution considered the moments about the center of gravity, a structural mounting factor. The Nasmyth focus, in which the mass is most nearly concentrated at the center of gravity, was ranked best. Ratings for obstruction size and number of mirrors ranked the telescopes according to transmittance. In this respect, the prime focus design is the most desirable approach. In susceptibility to stray light, only the Newtonian design was downrated due to its detector being located too near the front plane of the telescope, thus increasing the potential of detecting scattered light.

As the summary merit rating shows, the Nasmyth focus design appears to be the most desirable of the five configurations for the Lidar mission.

Three design types have been considered for the Lidar receiver: Ritchey-Chretien, Classical Cassegrain and Dall-Kirkham. Each has conic section mirrors. Figure 5-4 summarizes the important differences between these types.

The aspheric departure from the nearest sphere is largest for the hyperboloidal primary and the smallest for the elliptical primary, but the difference in cost impact is not significant. The convex spherical secondary of the Dall-Kirkham is easier to test and less costly to fabricate than the hyperboloidal secondaries of the

other two designs. The cost differential is a relatively small fraction of the overall Lidar program costs, but it is of sufficient magnitude to be considered along with other factors in the trade-off analysis.

	PRIMARY	SECONDARY	DIFFRACTION-LIMITED FIELD OF VIEW (2)	VARY (3) MAGNIFICATION	INTERNAL FINE GUIDANCE(4)	RELATIVE DECENTER (5) SENSITIVITY
RITCHEY – CHRETIEN (RC)	CONCAVE HYPERBOLOID	CONVEX HYPERBOLOID	>6	NO	POSSIBLE	2X
CLASSICAL CASSERAIN (CC)	CONCAVE PARABOLOID	CONVEX HYPERBOLOID	≥6	YES	POSSIBLE	2X
DALL KIRKHAM (DK)	CONCAVE ELLIPSOID	CONVEX SPHERE (1)	2.6	NO	POOR	1X

(1) CONVEX SPHERE EASIER TO TEST AND FABRICATE THAN CONVEX HYPERBOLOID
(2) DESIGN ABERRATIONS ONLY, MILLIRADIANS, BEST FOCUS
(3) INTERCHANGEABLE FOCAL LENGTH SECONDARIES WITH SAME PRIMARY
(4) BY ROTATING SECONDARY MIRROR ABOUT PRIME FOCUS
(5) RELATIVE AMOUNT OF COMA INTRODUCED BY SECONDARY DECENTER

CONCLUSION: CLASSICAL CASSEGRAIN HAS MAXIMUM VERSATILITY

Figure 5-4. Design Type Comparison.

Representative relative fields of view are tabulated for each of the designs. Although both the RC and CC offer larger fields, the image quality and fields of view for all three are adequate for Lidar. The field characteristics are further quantified in the next figure.

The Classical Cassegrain has one advantage which offers some growth potential. Its parabolic primary may be used with a variety of secondary mirrors to provide a change in magnification while maintaining the position of the output image. Thus changing the secondary mirror alone would allow (for example) changes in filter size and field of view without any other change in the optical system. With the Dall-Kirkham and Ritchey-Chretien designs, the figure of the primary mirror is specific to a particular combination of secondary mirror magnification and output image position. Thus a change in either magnification or output image position would require a new

primary mirror. With respect to Lidar system coalignment considerations, both the Ritchey-Chretien and the Classical Cassegrain offer an advantage by permitting modest variations in line of sight direction through lateral motion of the secondary mirror. The relative merits will be shown quantitatively in the next figure; they are a significant factor in the design choice.

In sensitivity to decenter errors, the Dall-Kirkham design enjoys a factor of two advantage over the other two designs. In no case, however, do the tolerances present a design or fabrication problem. Axial alignment data are not presented in the comparative analysis, since they are the same for both Classical Cassegrain and Ritchey-Chretien. It presents another argument for using the slowest primary mirror than can fit in the available space.

In weighing these three design types, the Ritchey-Chretien design offers no advantage over the Cassegrain and suffers through reduced growth options. It has not been considered further. The choice between Classical Cassegrain and Dall-Kirkham is not as clear cut. The former offers growth potential in terms of internal fine pointing by moving the secondary mirror and magnification change without replacing the primary mirror, while the latter offers modest cost reduction and lower sensitivity to secondary mirror displacement. The misalignment sensitivity of a Classical Cassegrain with an f/2.0 primary is tolerable, however, and its added cost is a small fraction of the total project cost. It has therefore been chosen for its versitility and growth potential.

5.3.2 IMAGE QUALITY

Two of the factors previously introduced are considered quantitatively in Figure 5-5. On the left, the image qualities of the three design types are tabulated as a function of field radius. Comparison to figure 5-1 will show that all the designs are

well within tolerance, with substantial margins to account for fabrication and alignment errors and environmental effects; the Cassegrain and Ritchey designs enjoy a marginal advantage, however.

RMS WAVEFRONT ERROR (10.6 μm) AT EDGE OF FIELD, COLLIMATED TELESCOPE, OPTIMUM FOCUS

	ON AXIS	1.0	2.0	3.0
D-K	.002	.057	.114	.172
C-C	0	.003	.009	.019
R-C	0	.002	.008	.019

D-K: DALL-KIRKHAM
C-C: CLASSICAL CASSEGRAIN
R-C: RITCHEY-CHRETIEN

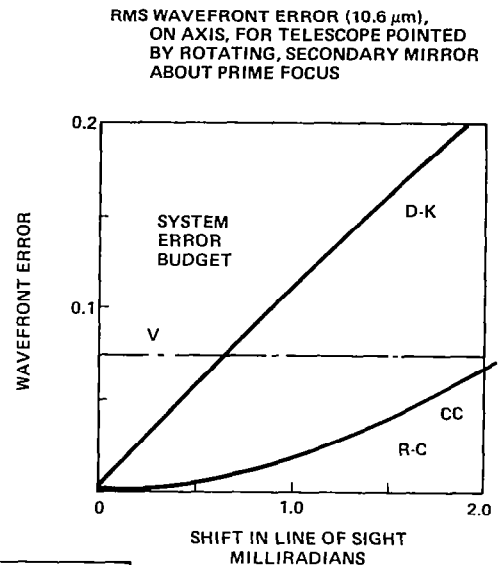

CONCLUSION:
CLASSICAL CASSEGRAIN BEST SUITED TO EVOLUTIONARY LIDAR

Figure 5-5. Design Type Comparison Image Quality.

On the right is shown the results of an analysis of pointing capability. Displacement of the axis of the secondary mirror from coincidence with the axis of the primary mirror can introduce both image displacement and coma in the output image. The amount of image displacement or coma introduced is a function of the distance separating the two axes at specific points. Image displacement is a function of the distance from the center of the curvature of the secondary mirror to the axis of the primary mirror for all three design types. Any combinations of tilt and decenter of the secondary mirror which produce the same separation will produce the same image displacement. The corresponding point for determining coma is called the "neutral point", and its

position on the axis of the secondary mirror varies with the design type. For Dall-Kirkham, it is coincident with the center of curvature of the secondary. For the Classical Cassegrain, it is coincident with prime focus.

As shown in the figure, the Dall-Kirkham design has considerably more sensitivity than the other two designs, monopolizing the total system error budget with less than 1 milliradian offset without regard to other factors. On the other hand, both the Classical Cassegrain and the Ritchey-Chretien can be used to achieve line-of-sight motions in excess of +1 milliradian while incurring errors which are a small fraction of the error budget.

The data presented here simply reinforce the conclusion reached previously, that the Classical Cassegrain design is best suited to the evolutionary Lidar system.

5.3.3 FOCAL PLANE OPTICS

In considering the design options for the focal plane optics, two possibilities exist for the placement of the narrow band filter. These are shown in Figure 5-6 along with their characteristic advantages and disadvantages.

Narrow bandwidth Fabry-Perot etalon-type filters have the property that the wavelength of maximum transmittance shifts toward shorter wavelengths as the angle of incidence increases. The bandwidth of the filter does not change significantly for small tilt angles (a few degrees), so that the entire spectral transmittance curve is displaced toward shorter wavelengths as the angle increases. The quantity of broad-band background radiation transmitted by the filter is not reduced by this effect, but the transmittance for monochromatic laser radiation will change with angle of incidence. The result is a reduction in the signal-to-background ratio at non-normal angles of incidence for the filter.

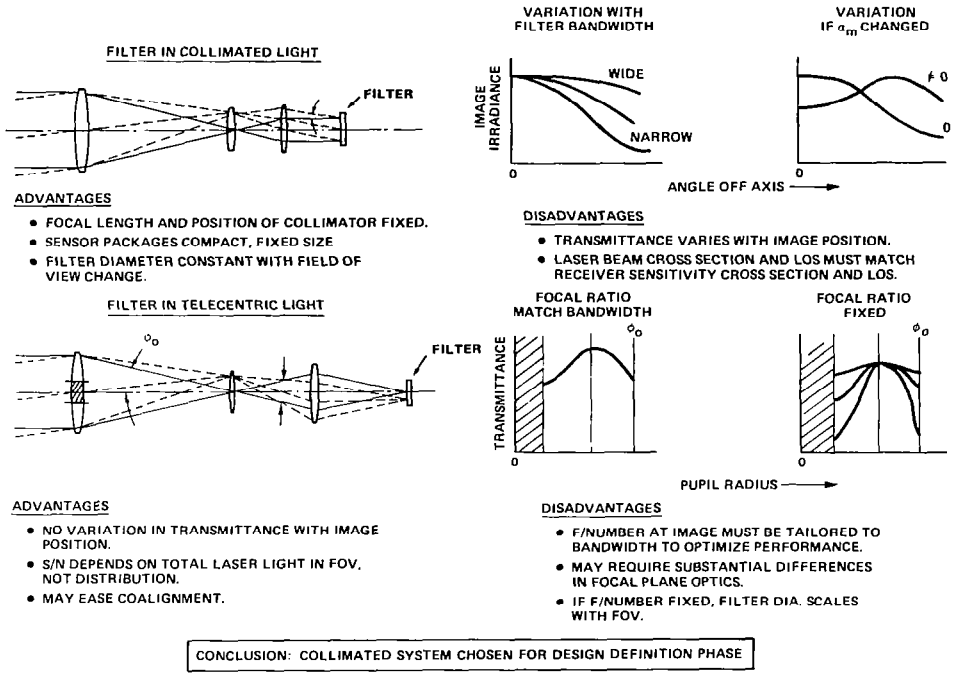

Figure 5-6. Focal Plane Optics - Basic Options.

With the filter placed in collimated light at the exit pupil of the system, the angle of incidence on the filter is a function of the field angle (β) of the telescope. For a given telescope diameter and filter diameter, larger field angles necessarily require greater filter bandwidths. Designing the filter for maximum transmittance at an angle other than normal incidence will improve the situation somewhat, if the transmitter radiation pattern is suitable.

In the alternative telecentric arrangement where the filter is placed in an image plane, the angle of incidence becomes a function of pupil radius. Here, for a fixed focal ratio system, the required filter diameter (at constant bandwidth) scales with the field of view, or alternatively, the focal ratio at the image must be tailored to the desired bandwidth.

In considering the relative merits of these two options, the telecentric arrangement has significant disadvantages with respect to its universal application across a range of experimental requirements while offering no compelling compensatory advantage. The collimated arrangement, on the other hand, offers the advantages of fixed filter diameter and focal plane optical design across the experimental spectrum. After examining the correlation of individual experiment bandwidth and field of view requirements with the properties of the collimated arrangement and specified filter and telescope diameters, shown in Figure 5-7, the collimated arrangement has been chosen as best suited for the design definition phase. This trade should be re-examined later, however, as more specific science requirements become available.

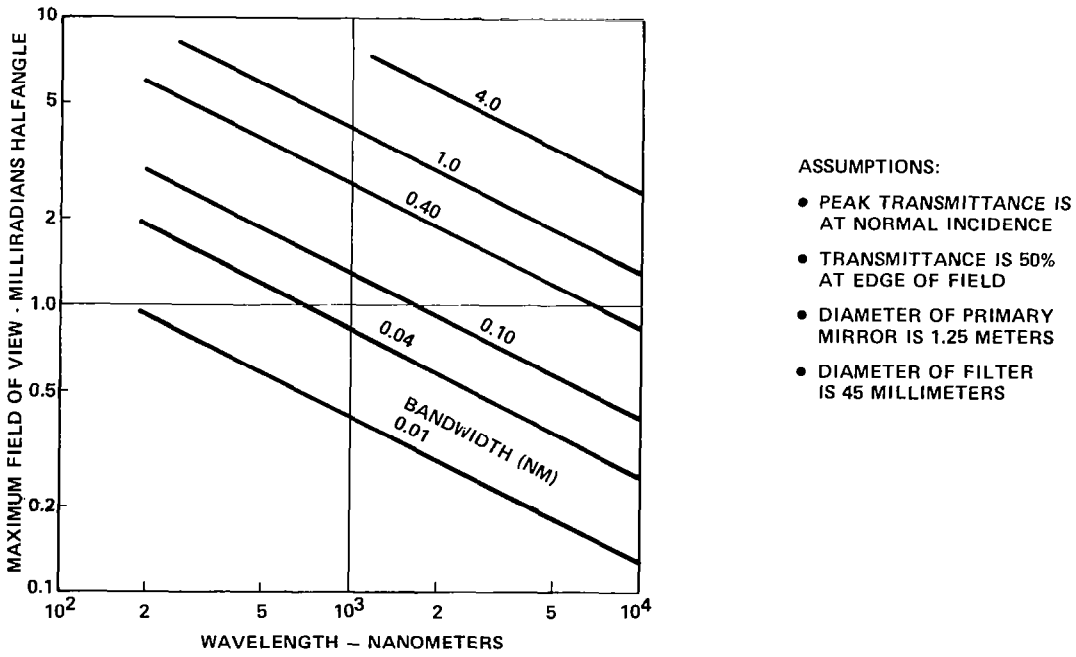

Figure 5-7. Limitation on Field of View.

Figure 5-7 shows the relation of maximum field of view and wavelength to different FWHM filter bandwidths for the filter in collimated light with a primary diameter of 1.25 meters and a filter diameter of 45 millimeters. The field of view limitations with a 45 mm filter diameter are adequate to match those called out in the revised SEED experiment matrix except for experiment 16, where the specified full beamwidth requirement of 0.6 milliradian field is marginally too large. Figure 5-7 assumes that the filter is designed for maximum transmittance at normal incidence. If the filter is designed for maximum transmittance at an angle of incidence off normal, it is possible to expand the field of view somewhat. This approach would be adequate to meet the field of view requirement for experiment 16.

The focal plane optics will be refractors, with separate lenses being provided for different wavelength regions. The telescope is required to provide three output channels, selectable through rotation of the fold mirror in the Nasmyth telescope. Figure 5-8 shows the basic optical configuration options, based on an f/14 output image and a 1.25 meter telescope aperture diameter.

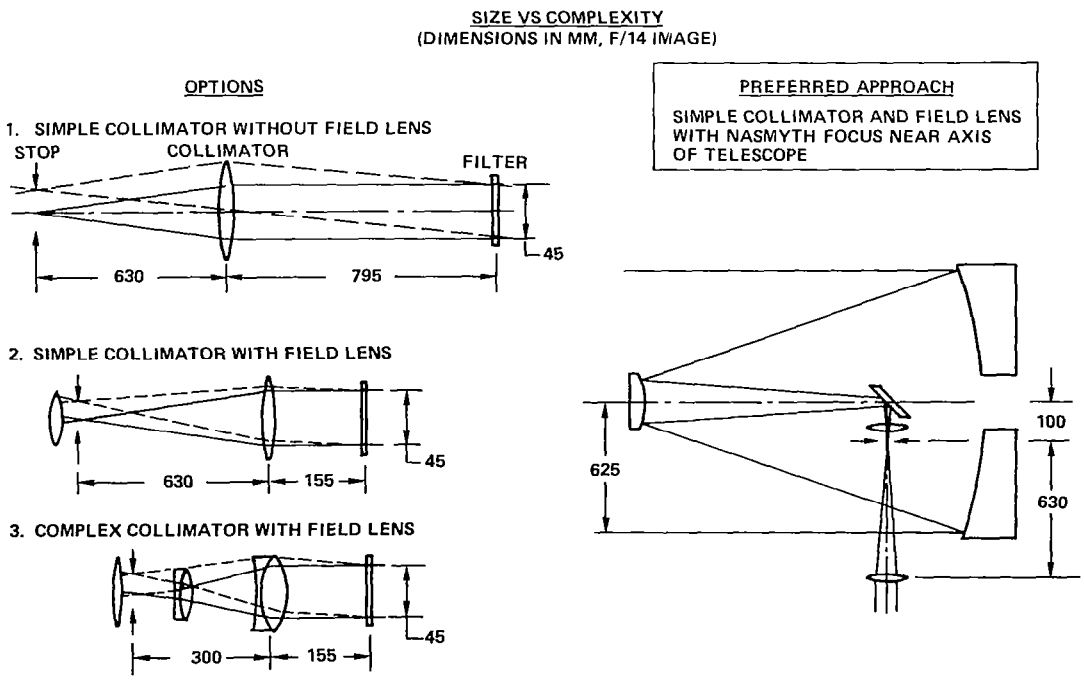

Figure 5-8. Collimating Focal Plane Optics.

The simplest option is a single collimator lens without field lens (1). The length of this can be substantially reduced by adding a field lens (2). Any further reduction in length requires use of a more complex telephoto design for the collimator (3). The latter will impact transmittance, particularly for ultra-violet experiments.

If the total length of the focal plane optics must be included in each sensor package, the latter will be very large, occupying a significant fraction of the available Shuttle bay volume, if the simpler configurations (numbers 1 or 2) are used. Conversely, use of fold mirrors and more complex optics to reduce the size of the sensor package will reduce transmittance, and thus reduce performance. For this reason, it is preferable to incorporate the focal plane optics in the Nasmyth telescope as shown in the right side of Figure 5-8. This approach is compatible with the second form of focal plane optics shown on the left, and three separate channels can still be selected by rotating the fold mirror. At f/14, this design is compatible with both a 1.25 meter aperture diameter and a 45 millimeter filter diameter; furthermore, if the focal plane is chosen to be close to the axis as shown, the focal distance to the collimator lens can be accommodated in the traverse of the primary beam, allowing the filter and sensor to be placed immediately adjacent, outside the receive telescope housing.

5.3.4 COATINGS AND POLARIZATION

The photon-limited nature of the Lidar experiments requires the receiver to have the highest possible transmittance at the receive wavelength used in each experiment. The extremely large spectral range (200-12,000 nanometers) makes it difficult to find mirror coatings and impossible to find single refracting materials which are optimum for all experiments, however, the refracting elements can be confined to the light paths of specific experiments. This allows different refracting materials to be used for different experiments. The primary, secondary and fold mirrors must perform for

all experiments flown on a specific mission, and therefore must have suitably broad-band reflecting coatings.

Figure 5-9 (left) shows the magnitude of the problem, using the best commercially available coating technology. The upper scale shows the wavelengths of the individual experiments listed in the SEED document. The lower portion shows the effective transmittance of the three mirror cascade, using three aluminum (1), three silver (2), or one aluminum plus two silver (3) mirrors. The aluminum mirrors are overcoated with a single layer of magnesium flouride to protect against oxidation. The silver mirrors have a proprietary three-layer protective overcoating.

It is clear that three aluminum mirrors are required for experiments at wavelengths shorter than 400 nanometers. It is also clear that three silvered mirrors would be preferable at wavelengths between 400 and 2000 nanometers. The applicability of these coating options to individual experiments described in the SEED are depicted in Figure 5-10.

In addition to the reflecting surfaces, there will be a minimum of two refracting elements for each focal plane optics set, with a minimum of four air-glass surfaces. In the visible and ultraviolet, typical uncoated air-glass surfaces will have a dielectric reflectivity of about 5 percent. Thus the maximum transmittance of uncoated visible or ultraviolet lens systems will be 85 percent or less, depending on the internal absorption. The situation is worse in the infrared, where the higher index of refraction increases the reflectivity of each surface.

Dielectric surface reflectivity can be reduced by adding antireflecting coatings to each surface. Such coatings are generally ineffective over spectral regions greater than one octave. If separate refractive lens sets are used for separate spectral bands, such coatings can be used. Figure 5-9 (right) shows 3 typical examples. Each

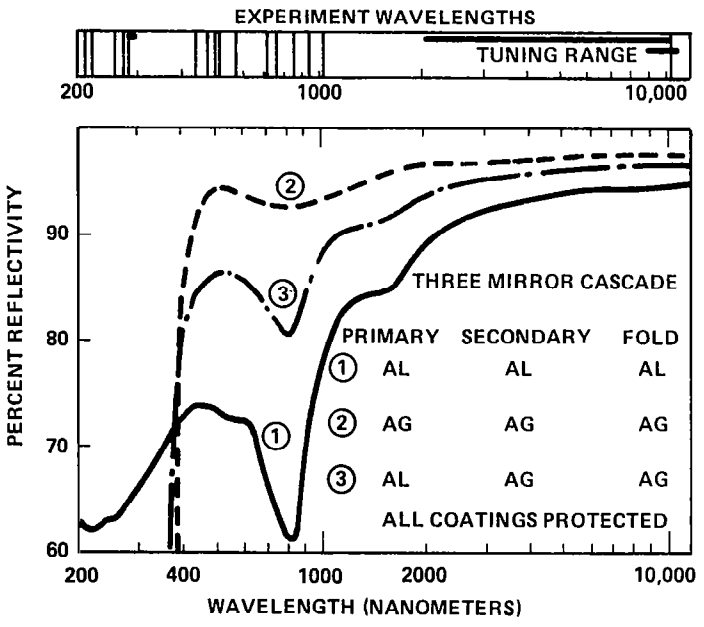

CONVENTIONAL MIRROR COATING OPTIONS

TWO ELEMENTS, ANTI-REFLECTION COATED CHOSEN FOR SPECIFIC SPECTRAL REGION*

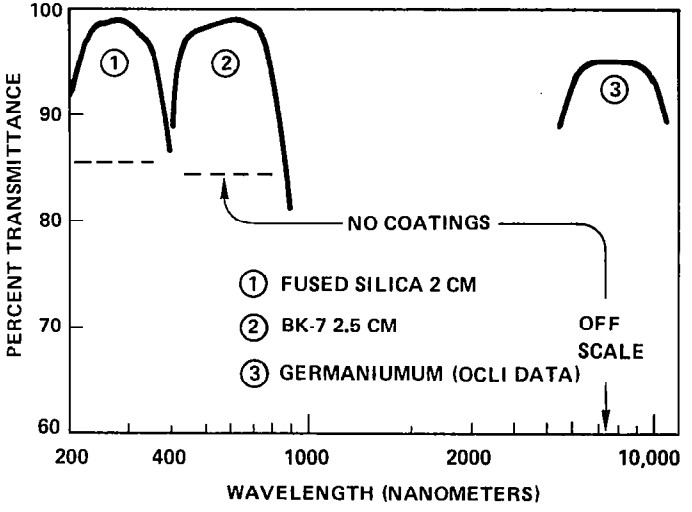

TYPICAL REFRACTOR TRANSMITTANCE CURVES

*SIMULTANEOUS USE AT 530 AND 1060 NM REQUIRES HIGH INDEX FOCAL PLANE OPTICS WITH SPECIAL AR COATINGS.

Figure 5-9. Transmittance/Coatings Component Data.

curve represents two elements, and includes the effects of internal absorption of light. The fused silica curve (1) has been tailored for ultraviolet experiments, the Schott BK-7 glass curve (2) for visible light, and the Germanium curve (3) for the far infrared. Note that each curve is plotted only over its own spectral band. Also shown are representative levels without anti-reflecting coatings; such levels, of course, are associated with considerably broader spectral ranges in each case.

RELATION OF COATINGS TO EXPERIMENTS

EXPERIMENT	1	2	3	4	6	7	8	9	10	11	12A	12B
ALUM.	OK	OK	OK	OK	OK	OK	REQ	OK	OK	OK	REQ	REQ
SILVER	PREF	PREF (530)	PREF	PREF	PREF (530)	PREF	X	PREF	OK	PREF	X	X

PREF: OFFERS 20% GAIN IN TRANSMITTANCE IN EACH INDICATED EXPERIMENT CLASS

EXP.	13	14	15	16	17	18	19A	19B	20A	20B	21	22	23	24	25	26
ALUM.	OK	OK	OK	OK	OK	OK	OK	OK	OK	OK	REQ	REQ	OK	OK	REQ	OK
SILVER	OK	PREF	PREF	PREF	PREF	OK	PREF	OK	PREF	OK	X	X	PREF	OK	X	PREF

CONCLUSION: SILVER VERY DESIREABLE FOR EARLY EXPERIMENTS, ALUMINUM NECESSARY FOR UNIVERSAL USE

REPRESENTATIVE TRANSMITTANCES
NET; INCLUDING TELESCOPE, FOCAL PLANE OPTICS, OBSCURATION

TELESCOPE COATINGS	UV	MID-VISIBLE	NEAR IR	FAR IR
ALUMINUM	55%	65%	75%	80%
SILVER	–	85%	85%	< 85%

Figure 5-10. Transmittance/Coatings.

There are several experiments in which two wavelengths exactly one octave apart are involved (530 and 1060 nanometers). We have examined the problem of providing special coatings for that case, and have found that a suitable coating can be designed. A high-index substrate is required (n=1.8), but the reflectivities can be reduced to about 0.5 percent at both wavelengths simultaneously.

The applicability of the aluminum and silver coating system to the wavelength requirements of the individual experiments described in the SEED is shown in Figure

5-10 (top). As can be seen, although silver is preferable (offering 20% gain) for many experiments, aluminum is absolutely necessary for some (8, 12A, 12B, 21, 22, 25). It is recommended that the final choice be made at a later time when a better definition of the science requirements for the actual mission exists. For now, aluminum would appear necessary for universal use. The production costs for either coating system are comparable.

Shown below in Figure 5-10 are representative transmittances for the receiver system. Three factors sum to give the net transmittance forward of the narrow bandpass filter; the mirror reflectivities, refracting element transmittances and central obscuration due to the secondary mirror and baffling. Light loss from the latter will be on the order of 8 to 10 percent in the baseline configuration. The figures shown are guides for the two alternative coating options and for four general spectral areas. Data for specific wavelengths, particularly between 700-900 nanometers, will vary.

The effect of the polarizing properties of the chosen optical layout on the conduct of polarization-sensitive experiments (e.g. 3) has been examined. The primary and secondary mirrors, being at near-normal incidence, will introduce no polarizing effects; however, the 45° fold mirror will. Figure 5-11 shows the results of a calculation of the reflectivity ratio for the two planes of polarization of a single 45° surface with each of the two coating options, and depicts an estimate of the combined errors that might be expected due to temporal stability and calibration.

A review of the literature on the conduct of such scientific experiments indicates that for a linearly polarized outgoing beam, substantial (30%) depolarization can be expected in the return signal. Thus, with appropriate choice of equipment, alignment and calibration of the receive telescope polarization properties, one can reasonably

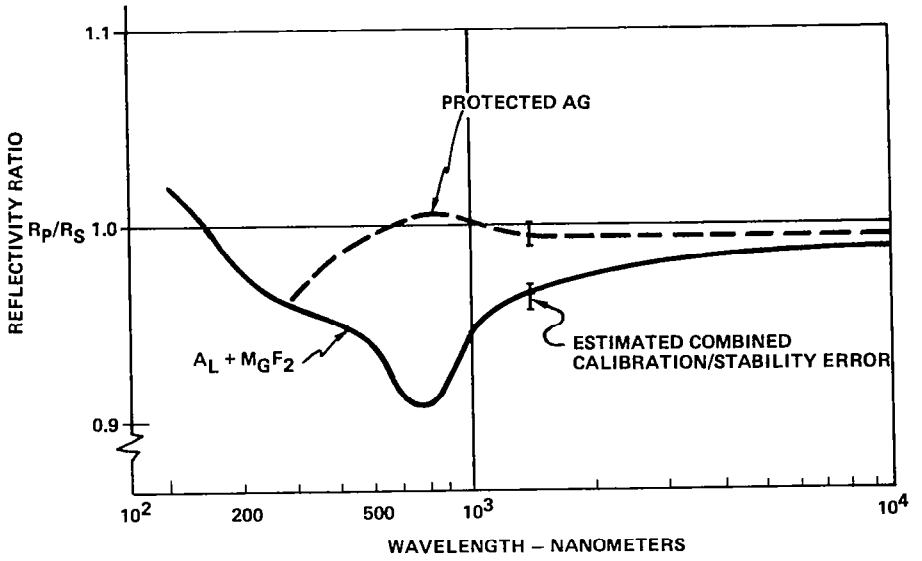

• PHASE I OPTICAL CONFIGURATION DOES NOT PRECLUDE CONDUCTING POLARIZATION EXPERIMENTS WITH POSSIBLE REDUCED ACCURACY.

Figure 5-11. Polarization Effects for one 45° surface.

expect to carry out such experiments, although with possible reduced accuracy. For maximum effectiveness, however, an obvious growth option to be considered later is to retract the fold mirror and permit the telescope output beam to continue through the focal plane optics and detector arranged along the axis of the telescope.

The requirement for stray light suppression has been cited earlier. The stray light suppression ratio is taken to mean that the total stray light from all sources should be less than 10^{-3} of that reaching the detector from within the field-of-view by direct imagery. Four sources of stray light are identified by their characteristics in Figure 5-12.

The first of these, direct stray light, can be eliminated completely from the baseline design because the sensor package is located far below the telescope's front aperture and can be adequately baffled. Regarding the next, primary reflection there

must be a mechanical structure in front of the primary mirror to support the fold mirror, field lenses and baffling. Any light striking this structure can be reflected to the secondary mirror, and thence directly to the detector via the image forming optics, since it appears to arise within the field of view. This primary stray light cannot be eliminated completely, and is reduced only by painting the structure black and configuring it to minimize the amount of light directed toward the secondary mirror. In addition, light reflected from the structure in front of the mirror may enter the detector from outside the field of view through the hole at the side of the telescope for Nasmyth focus. This secondary stray light is controlled by minimizing the solid angle subtended at the detector by areas of the telescope structure directly illuminated by outside light sources. To the degree that this requires baffling within the incoming beam, it may provide additional sources of primary stray light, hence a trade off between these two may be made.

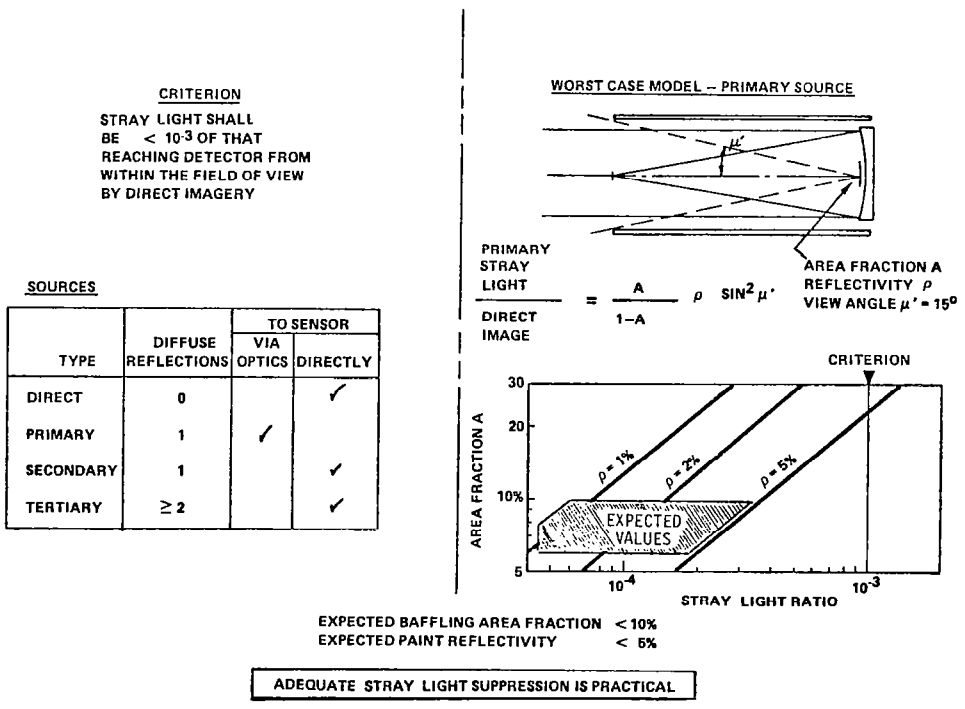

Figure 5-12. Stray Light Control.

Tertiary stray light, which reflects two or more times off diffuse black paint within the telescope structure before it reaches the detector, will under normal circumstances, be well below 10^{-3} of that arriving from within the field of view.

We have performed a worst case analysis of the primary stray light source problem, for normal Lidar viewing conditions, as illustrated in Figure 5-12. The main assumption in this analysis is that the source of stray light is the terrestrial scene, which is everywhere of the same brightness as that falling within the field of view. The structure and baffles in front of the primary mirror are represented by a flat black disk of reflectivity, ρ, having an area, A, and measured as a fraction of the primary mirror area. Under these conditions, the ratio of primary stray light to direct image irradiance is given by the equation shown. The graph shows that even with a 5 percent reflectivity and a closed light path structure producing a 20 percent area obstruction, the design specfication can be met.

The reflectivity range of 1 to 5 percent represents typical diffuse black paints: Martin Marietta black, which is the lowest reflectivity diffuse coating presently available, has a diffuse reflectivity of less than 0.5 percent across the visible spectrum. Furthermore, baffling area ratios well under 10% should be possible. It is therefore reasonable to keep the stray light rejection ratio to less than 10^{-4} from primary, secondary and tertiary sources.

5.3.6 MIRROR CONSIDERATIONS

The most critical optical component in the receiver system is the primary mirror; this is because of its size, fabrication cost, thermal exposure to the outside world, and secondary effects (e.g., weight) on the rest of the system. In defining the mirror, both the form and material must be considered and compared against the various trade factors. (Figure 5-13).

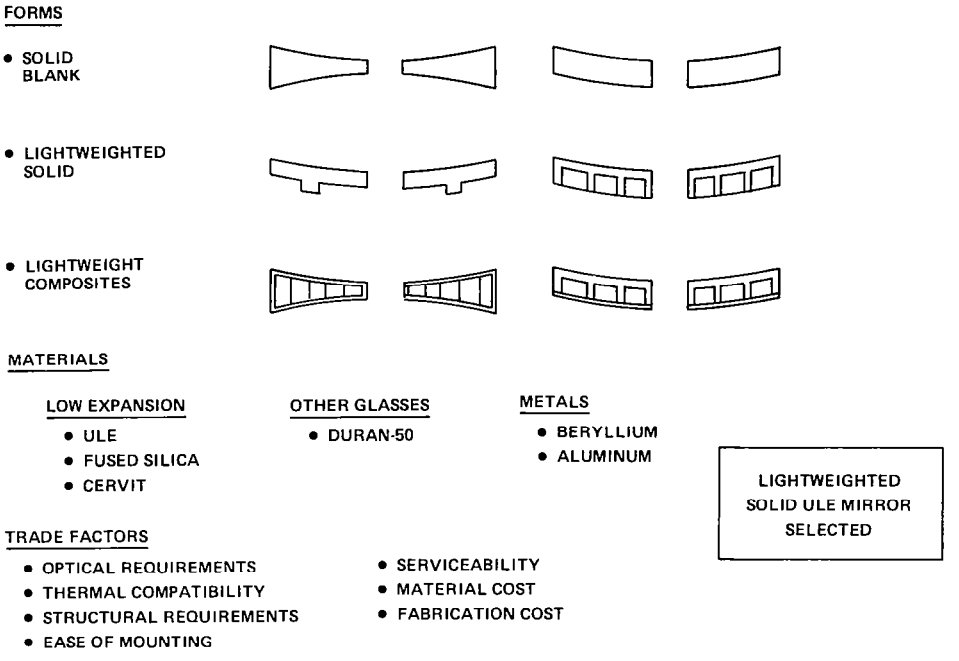

Figure 5-13. Mirror Trades.

Three general mirror forms have been used in telescopes of this sort and each has variations. The solid blanks are typified by low cost and high weight. With modest additional cost material can be removed by diamond machining techniques yielding a lightweighted solid. Experience has shown that significant weight reduction can be achieved before the cost starts rising steeply due to tight tolerances and thin walls. A third form is the light-weight composite where several elements are joined

to form the mirror. These can be all the same material, such as a silica honeycomb spacer laser with silica face sheet fused together, on different materials such as a galssy face sheet joined to a graphite epoxy honeycomb substrate. All lightweight composites are high cost, because of both the blank fabrication and the additional care and time necessary to figure the relatively thin face sheets.

After considering all the value factors described and their interrelationships with other aspects of the receiver system definition, we conclude that the lightweighted solid form is the most satisfactory for the Lidar telescope. Further, lightweighting from the back to approximately 50 percent weight reduction (from a classically-sized solid) appears to offer the best return with regard to reduced structural weight while not incurring the fabrication difficulties, high cost and more complex mounts associated with extremely light weight mirrors.

Mirror materials examined in this study include the metals such as aluminum and beryllium, the common glasses, and the low expansion glasses, particularly fused silica and Corning's ULE titanium silicate.

The metals, although offering advantages in certain specific areas (e.g., thermal conductivity, high stiffness for beryllium, low cost for aluminum), do not offer general utilitarian value across the board. Furthermore, beryllium involves exceptionally high blank costs and aluminum has a high sensitivity to thermal transients and gradients. Both metals require alternate plated layers into which are worked the actual optical surfaces. Neither metal seems to have compelling advantage for the Lidar mirror.

The choice between the various glasses can be made primarily on the basis of thermal properties as discussed in Section 5.4.2. ULE fused silica (or the similarly low expansion CERVIT) is the most practical choice on the basis of its insensitivity to thermal gradients.

5.3.7 ERROR BUDGET

In any optical system an error budget must be established to apportion the total allowable system error into all its constituent parts. This should be done in a way that recognizes all possible contributors to error and balances relaxed tolerances in some areas with tighter ones in others. In this way the error budget is one tool in the design process: on the one hand determining the requirements on each subsystem while on the other being responsive to change as it develops that a different balance of tolerances may be more desirable. The error budget which has been developed for the Lidar receiver system is summarized in Figure 5-14. This budget has already been iterated several times and recognizes some design trade-offs which have already been made, namely to budget the permissible errors heavily toward thermal and structural areas so as to address the goal of a structurally reliable receiver capable of operating over a reasonable temperature range with passive thermal design only, while at the same time not making the basic fabrication tolerances unnecessarily tight. These trades were conducted at a level of detail beyond that illustrated. The total system wavefront error has been set at the diffraction limit at 10.6 micrometers.

As presently budgeted, the individual fabrication tolerances for the primary and secondary mirrors are $.012\lambda$ rms at 10.6 um which are equivalent to surface figure qualities of about 1/2 wave peak-valley in the visible. This quality can be achieved quite cost effectively and permits much larger parts of the budget to be allocated to gravity release structural factors in the primary mirror and metering structure and to a broad thermal soak range for the metering structure. The other areas are allocated error budgets proportionately based on experience with similar systems, although it should be noted that the alignment errors have been made more generous than usual to allow for routine maintenance and alignment in the field.

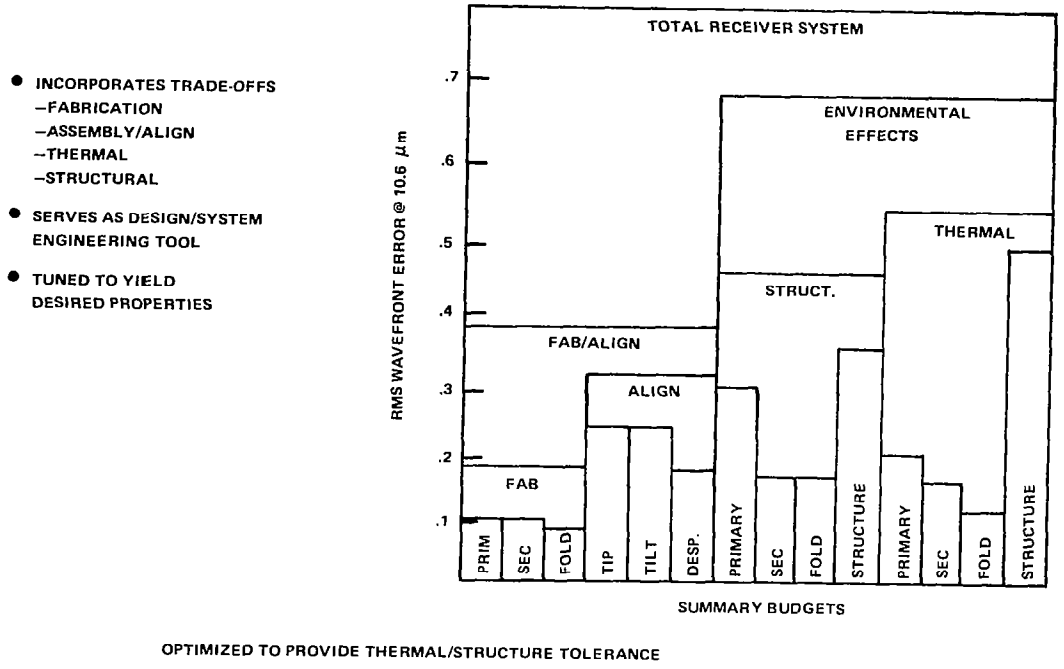

Figure 5-14. Error Budget.

5.4 DESIGN

5.4.1 RECEIVER STRUCTURE DESIGN

The Lidar structural and metering design must fulfill a number of different requirements while maintaining the optical performance dictated by the optical tolerances. It must have the strength to withstand the Shuttle launch environment (random vibration and steady state acceleration) with the launch thrust vector most likely perpendicular to the optical axis. Furthermore, the stiffness must be high enough to place any natural frequency resonances well above those expected during the mission. More general requirements include a high design margin of safety, reasonable weight control, and due attention to modularization, serviceability and maintainability so as to be compatible with repeated flights with short turn around requirements.

The principal contributors to system error relating to the structure are anticipated to be orbital gravity release (in both the structure and the mirrors) and the Orbiter thermal environment. As described earlier, these areas have been assigned a generous proportion of the total allowable system error so as to alleviate the design complexity. Nonetheless they do lead to some exclusions in material choice which will be described later.

A number of different concepts are candidates for the telescope metering structure on Lidar. The more common possibilities are illustrated in Figure 5-15 which also lists some of their strengths and weaknesses. At first appearances all can be made to meet or exceed the optical design criteria.

METERING CONCEPT	COST	LAUNCH DESIGN SAFETY MARGIN	STIFFNESS/ WEIGHT	OPTICAL PERFORMANCE	THERMAL/BAFFLING COMPATIBILITY	ACCESSIBILITY TO INTERIOR	REMARKS
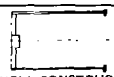 SHELL CONSTRUCTION	LOW	EXCELLENT	EXCELLENT	EXCEEDS OPTICAL DESIGN CRITERIA	EXCELLENT, SHROUDED AND BAFFLES EASY GOOD THERMAL PATHS	DIFFICULT -REQUIRES ACCESS HATCHES	BEST APPROACH FOR LOW COST, HIGH DESIGN MARGIN, STIFFNESS CHARACTERISTICS
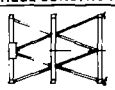 TRUSS CONSTRUCTION	HIGHEST	GOOD	FAIR	EXCEEDS OPTICAL DESIGN CRITERIA	FAIR-CAN BE SHROUDED WITH ADDITIONAL WEIGHT	FAIR	FAIR-GOOD DESIGN AND STIFFNESS CHARACTER CAN BE ATHERMAL BUT BUDGET DOES NOT REQUIRE;
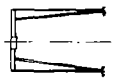 RODS & SHELL	LOW	GOOD	GOOD	EXCEEDS OPTICAL DESIGN CRITERIA	FAIR – CAN BE SHROUDED WITH ADDITIONAL WEIGHT	GOOD	RODS FOR METERING SHELL FOR STRENGTH/STIFFNESS OPTICAL BUDGET DOES NOT REQUIRE RODS; USE ① ABOVE
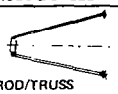 ROD/TRUSS	LOWEST	POOR	FAIR	MEETS OPTICAL DESIGN CRITERIA	POOR–NO MOUNTING FOR SHROUDS OR BAFFLES	EXCELLENT	POOR CHOICE FOR STIFFNESS/ STRENGTH, OPTICAL CONSIDERATIONS

- SHELL (MONOCOQUE) CONSTRUCTION OFFERS BEST COMBINATION FOR SIMPLICITY, RUGGEDNESS AND COST

Figure 5-15. Primary-Secondary Metering Concepts.

The rod/truss or tripod structure is the simpliest and lowest cost but is the least stiff or, alternatively, incurrs the largest obscuration of the aperture. Although providing excellent accessibility, it is poor from the point of view of stray light or thermal isolation.

The more complex truss construction can be used to achieve greater stiffness and more elaborate thermal design but at the expense of higher cost and fabrication complexity.

The monocoque shell structure is relatively low cost and provides excellent strength, stiffness, and general ruggedness. It tends to be heavier than other designs and the accessibility to the interior is difficult, but this latter property is actually desirable for Lidar because of the need to isolate the telescope from the potentially contaminating environment of the Shuttle and the integration and launch operations. Thermal properties of the monocoque shell structure are good since the design provides not only paths for thermal equilization but also limits the radiation viewing factors.

The rod and shell structure offers an elaboration on the basic shell approach by the incorporation of additional rods to perform the metering function while retaining the shell exterior for structural integrity. This design offers the advantages of the basic shell construction plus more precise metering at the expense of more complexity and cost.

For the Lidar application, the monocoque shell approach seems the best by virtue of its simplicity, excellent structural and thermal properties, and relatively low cost. The additional complexity of metering rods does not seem justified by the optical design criteria and error budget, subject to an appropriate choice of shell material discussed later.

5.4.2 RECEIVER THERMAL DESIGN

The thermal design of the receiver has been guided by a number of considerations as shown in Figure 5-16. First is that the design be compatible with the total system approach; this considers the Lidar system as an integrated thermal design with the components largely isolated from the outside world. The receiver will achieve much of its thermal conditioning through interaction with other components within the package. Further, it is desirable that thermal conditions be achieved by passive means so as to minimize the operational and system constraints. This is in support of the design goal that the receiver be capable of continuous, earth-looking operation without regard to mission operational history. An additional feature of the design is to establish tolerances that allow fabrication, alignment and testing of the receiver telescope at room temperature (say 20°C) while permitting performance within specification at operational temperatures below 0°C. A final consideration in the design is that direct solar radiation will not impinge on the secondary mirror support spider or the interior of the telescope tube. The implications of this are discussed later in this report.

DESIGN CRITERIA

- COMPATIBLE WITH G.E. LIDAR SYSTEM THERMAL DESIGN
- DESIGN SHOULD BE PASSIVE IF POSSIBLE
- VIEWING TIME: CONTINUOUS, EARTH – LOOKING
- NO DIRECT SOLAR LOAD ON SECONDARY MIRROR/SPIDER

DESIGN BUDGETS

(FROM DETAILED ERROR BUDGET)

STRUCTURE (INVAR)	
SOAK	30°C
DIAM. GRADIENT	10°
MIRROR (ULE)	
SOAK	>30°
AXIAL GRADIENT	3°
RADIAL GRADIENT	5°

Figure 5-16. Receiver Thermal Design.

Thermal analyses have been performed to establish the losses through the front aperture and other paths for worst case temperatures, the gradients that might be expected in the critical elements of the receiver, and the effects of those gradients on optical performance. These data have been used to guide the error apportionments within the error budget and the choice of materials for the mirror and the metering structure as are presented in Figure 5-17.

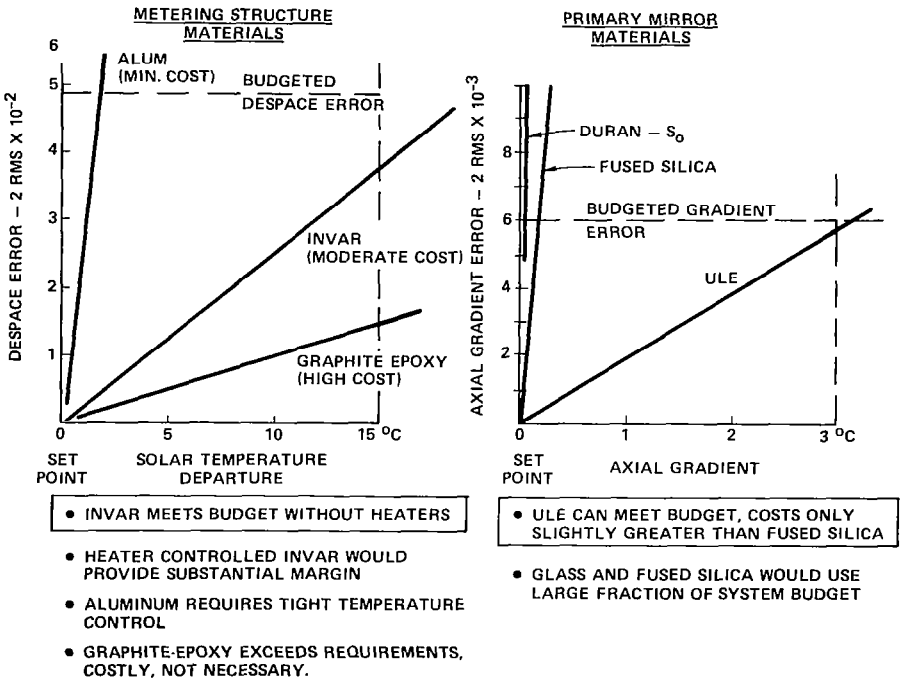

Figure 5-17. Thermal Sensitivity Analyses (Representative).

The resulting budget has been arranged to permit soak temperature variation of 30°C for both the structure and the mirror substrate while maintaining acceptable performance. Structural diametral gradients are tolerable up to 10°C, well above those that might be encountered. By the same token, permissable mirror axial and radial gradients of 3°C and 5°C respectively are in excess of those expected during operation.

More detailed design work in later program phases may produce a somewhat altered error budget to reflect differently weighted trade-offs, but it has been demonstrated that it is feasible to achieve the goal of steady state earth-looking operation by passive thermal means given the boundary conditions described earlier. Thermal soaks and gradients are expected to be well within budgeted values for the designated unheated Invar metering shell, the ULE primary mirror, and all other elements.

Figure 5-17 shows two representative thermal sensitivity analyses conducted under the thermal design. As mentioned earlier, the goal is for broad tolerance to the thermal environment; the error budget has already been weighted to reflect this intent. For the metering structure, it is a goal to retain adequate metering over a temperature range which includes room temperature (for fabrication, alignment and integration convenience) while allowing operation in orbit at temperatures of $0^{o}C$ and below without active thermal control. This forms the principal criterion for the choice of structural material. The metering properties of three candidate materials have been examined and compared with the temperature range and the mechanical despace budget; the results are shown in Figure 5-17 (left). It can be seen that aluminum, although low in cost, would require tight active temperature control (within $2^{o}C$) to remain within tolerance, whereas Invar can adequately meet the budget without heaters. Graphite-epoxy is also more than adequate but considerably more expensive and not necessary for this application. The disadvantage of Invar is its weight and this must be traded off against the expense and operational invonvenience of an active thermal control system for an aluminum structure or the fabrication costs associated with a graphite-epoxy structure. Our evaluation is that, for the Lidar system, this trade favors Invar.

In the figure to the right, similar considerations are examined with respect to materials for the primary mirror. It can be shown that the critical thermal parameter

is the axial temperature gradient imposed by the periodic orbital day-night cycle. Corning's ULE fused silica, readily available, can meet performance requirements for the expected axial gradients of less than 3° C (indeed, it was used to set the budget). Conventional fused silica, only slightly less expensive, and low expansion glasses such as Duran-50 would require a revised budget with an unnecessarily large apportionment for axial gradient. ULE, therefore, is the material of choice.

5.4.3 RECEIVER TELESCOPE BASELINE DESIGN

The design definition phase has been concentrated on establishing the key elements which are necessary parts of the Lidar receiver, determining their criticality, identifying options and performing trade-offs, and assembling a baseline configuration which appears to be most desirable and has been shown to be feasible in all essential aspects.

All the conclusions reached earlier have been incorporated into a detailed design layout. Figure 5-18 depicts this layout, somewhat simplified for clarity. This design layout has been the model for which the cost and schedule estimates have been prepared. Details of the design configuration are presented in the following four figures.

The essential features of the baseline Lidar receiver design are shown in figure 5-19; these have resulted from the analyses and trade-offs described earlier.

Three active devices have been identified for the Lidar receiver. The requirements for each are shown in Figure 5-20 along with the design concepts which have been evolved. These concepts have been incorporated in the baseline design and are reflected in the electronics requirements, interface definition, and resource estimation.

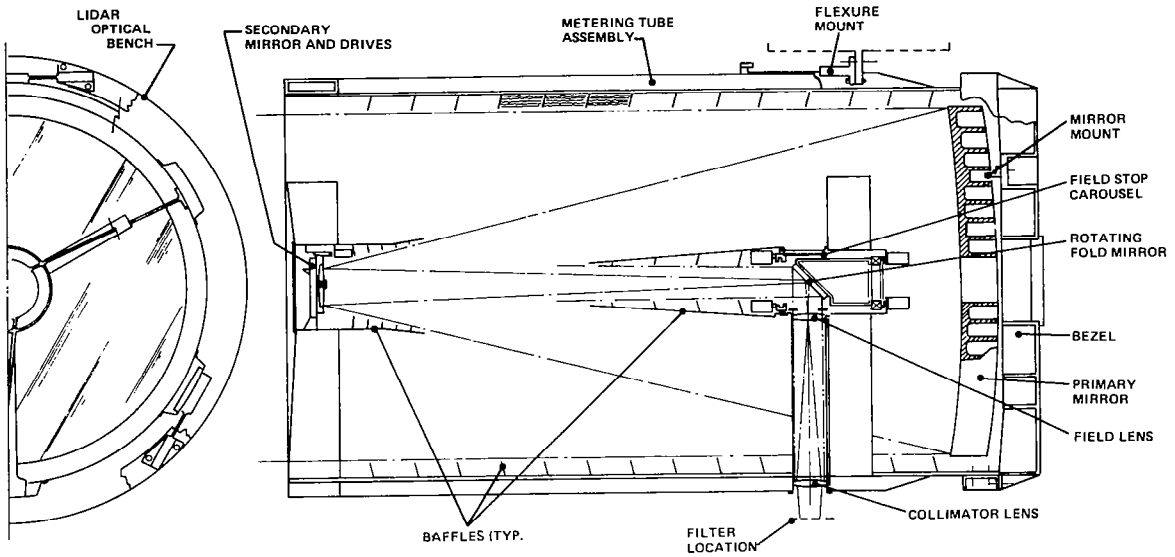

Figure 5-18. Lidar Receiver Telescope Baseline Design Layout.

- BASIC OPTICAL DESIGN: CLASSICAL CASSEGRAIN
- LAYOUT: NASMYTH WITH FOLD FLAT ROTATED TO FEED ALTERNATE EXPERIMENTS
- PRIMARY MIRROR: 1.25 METER DIA., F/2.0 FOCAL RATIO
- MIRROR FORM: MONOLITHIC BLANK, CORED TO 50% OF MASS
- MATERIAL: ULE
- SECONDARY MIRROR: 16 CM. DIA., F/14 SYSTEM FOCAL RATIO
- IMAGE QUALITY: DIFFRACTION LIMITED AT 10.6 MICROMETERS
- FIELD STOPS: 0.1 – 6.0 MRAD AS REQUIRED BY EXPERIMENTS
- FOCAL PLANE OPTICS: COLLIMATING, FIELD LENS AT STOP, COLLIMATOR NEAR FILTER
- MIRROR COATINGS: AL + MgF_2 OR PROTECTED AG DEPENDING ON MISSION SCIENCE REQUIREMENTS
- STRAY LIGHT CONTROL: CONVENTIONAL CASSEGRAIN-TYPE BAFFLING IS ADEQUATE
- STRUCTURE/METERING CONCEPT: MONOCOQUE SHELL ASSY
- MATERIAL: INVAR
- TELESCOPE THERMAL CONTROL: PASSIVE

Figure 5-19. Lidar Receiver Telescope Baseline Design Parameters.

SECONDARY MIRROR DRIVE	REQUIRED: TRANSLATE SECONDARY MIRROR LATERALLY IN TWO AXES TO BIAS LINE OF SIGHT ± 2 MR CONCEPT: BIDIRECTIONAL STEPPER MOTOR/LEAD SCREW DRIVE FOR EACH AXIS WITH PROVISION FOR EXTERNALLY PROGRAMMED CONTROL
FOLD MIRROR DRIVE	REQUIRED: PLACE FOLD MIRROR TO FEED EACH OF THREE DETECTORS IN SEQUENCE CONCEPT: DC MOTOR/CLUTCH TO DRIVE DETENTED ROTARY TABLE; ALTERNATE MOTOR CLUTCH COMMANDABLE
FIELD STOP DRIVE	REQUIRED: SELECTED SIZE STOP TO BE PLACED IN DESIRED DETECTOR BEAM CONCEPT: STOPS ON DETENTED DRUM; DC MOTOR/CLUTCH DRIVE WITH ALTERNATE AS ABOVE; SIX EVENLY SPACED STOP POSITIONS

Figure 5-20. Active Electromechanical Devices.

The electronic design associated with the receiver has been carried out in sufficient detail to establish the system elements and their operational characteristics. Figure 5-21 is a block diagram of the system and shows the secondary mirror drive, fold mirror drive and field stop drives already described earlier. Also shown are two additional electrical assemblies (solar caution and warning and temperature sensor).

The purpose of the solar caution and warning subsystem is to provide signals to the Lidar system relating to the direction of the sun with respect to the telescope line of sight. A set of phototransistor sensors with shrouds defining their fields of view will be mounted at the front of the telescope. A "caution" flag will be issued when the solar vector approaches to within 90° of the telescope axis and a "warning" flag when there is risk of direct illumination of any portion of the primary mirror. In

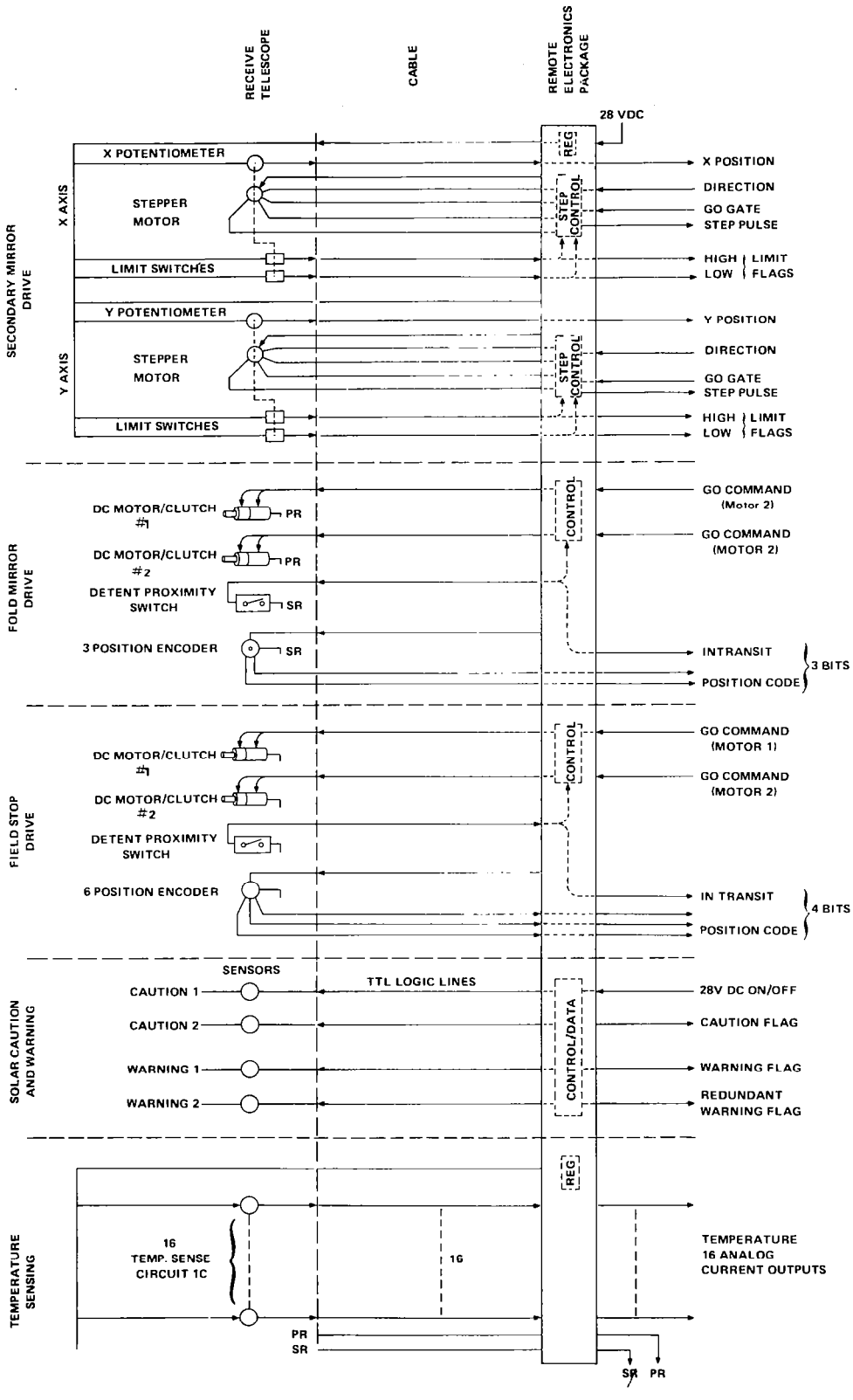

Figure 5-21. Receiver Electrical Block Diagram.

the latter case, the signal will be used to initiate door closure on the Lidar system so as to prevent potential detector damage. The temperature sensing system is to provide thermal housekeeping data for the mirrors, metering structure and drive motors.

It should be noted that the electronics system requires a small remote electronics package mounted external to the receive telescope, a short cable length away. This package will contain the power supplies and regulators, stepper motor controllers and power amplifiers, and the other required logic circuits and data processing equipment to be compatible with the Lidar system/Spacelab interface.

Figure 5-22 summarizes the interface properties of the receiver baseline design which have been described. The receiver power and command and data handling requirements are a very minor fraction of the Lidar system capability; the size and weight have been factored into the system design.

POWER (28V DC)		
STANDBY		
TELESCOPE	0.1	
REMOTE ELECTRONICS	3.0	
		3.1 WATTS
PEAK POWER		
TELESCOPE	25	
REMOTE ELECTRONICS	5	
DUTY CYCLE < 1%		30. WATTS
AVERAGE INTEGRATED POWER		< 3.5 WATTS

SIZE:	
TELESCOPE	
DIAMETER:	1.50 METERS MAX
LENGTH:	2.65 METERS MAX
REMOTE ELECTRONICS PKG	
APPROX. 30 X 30 X 30 CM	

CDHS	
COMMANDS	
PULSE	4
LEVEL	4
DATA	
ANALOG	8 CHANNELS
PCM 16 BITS X 0.55 =	32 bps.

WEIGHT	
MAIN STRUCTURE	256 KG
PRIMARY MIRROR, MOUNTS, BEZEL	221
SEC. MIRROR, MOUNT, DRIVE, SPIDER	39
FOLD MIRROR, STOPS, DRIVES, BAFFLES, SPIDER	49
RELAY LENSES, BAFFLES, MISC. HDWRE.	58
MAIN FLEXURES & MOUNTS	65
TELESCOPE ASSY	688 KG
REMOTE ELECTRONICS PKG	5
RECEIVER TOTAL	693 KG (1528 LBS)

Figure 5-22. Interface Definition.

5.5 GROWTH OPTIONS

A number of growth options exist for the receiver as part of an evolutionary Lidar system. Major ones that have been alluded to earlier are depicted in Figure 5-23.

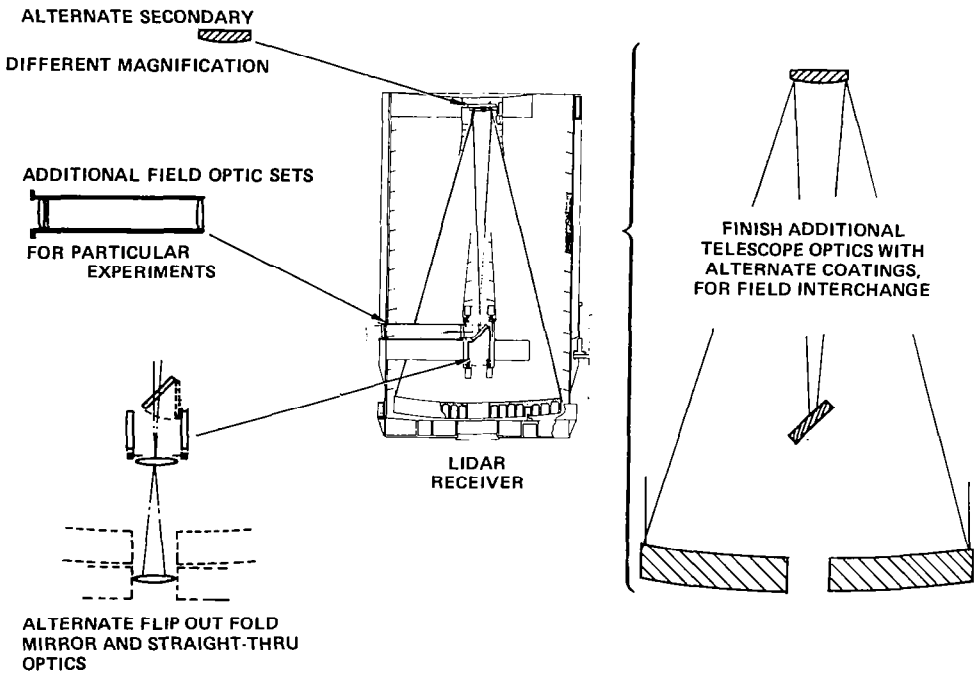

Figure 5-23. Growth Options.

An alternate secondary mirror can be used with the existing primary mirror to provide a change in telescope magnification without shifting the position of the output image. This would allow, for example, a revision of filter size and field of view without any other change in the optical system thereby tailoring these to the requirements of a unique experiment. Likewise, and perhaps at the same time, additional field optic sets can be fitted that are specially designed for unusual wavelength or filter requirements.

If an extreme degree of apolarization is required, space will permit the fitting of a

retracting fold mirror, thus providing a straight-through optical path to a detector package behind the already-perforated primary mirror. Finally, the telescope optics can be returned to the factory for the application of other coatings throughout or, alternatively, a complete additional set of optics can be fabricated with different coatings matched to special experiment needs. System tolerance adjustment and construction details are such that, with appropriate special alignment equipment, an interchange of optics could be accomplished at the NASA integration facility.

5.6 RISK ASSESSMENT

Overall, the development of the receiver entails little risk. Several areas will require special care during the course of the program although not unusually so compared to similar programs. Control of the thermal environment and subsystems requirements will be conducted at the system level; good communication will be required here to assure that optimum balance of tolerance and performance is achieved. Optical fabrication activities always incur a level of risk; this can be reduced by procedural means and the availability of spare blanks, but not completely eliminated. Likewise, lead times for optical elements are long although this should not be a problem within the presently projected schedule.

On the whole, however, in these and all other areas, the development and operation of the Lidar receiver can be considered to involve low risk, available technology, and there is a history of comparable systems which provide enhanced confidence.

6.0 SOURCES SUBSYSTEM

6.1 INTRODUCTION

The purpose of this part of the study is to define a modular laser sources system suitable for conducting the experiments contemplated for a Space Shuttle Orbiter Multiuser Lidar System in the early 1980's. To these ends, the science working group Science Objectives, Experiment Description, And Evolutionary Flow Document (SEED) was analyzed, and from it functional requirements for the sources were identified. This is discussed in paragraph 6.2.1. Based on these functional requirements and knowledge of laser properties, a set of evaluation criteria for potential candidate sources was developed and is discussed in paragraph 6.2.2. The functional requirements led to natural groupings of the laser sources; how this occurs is also discussed in this section.

In Section 6.2.3 the potential candidate lasers and frequency conversion devices presently commercially available or demonstrated in the laboratory are considered. Their performance figures are compared to the Lidar source requirements. Engineering considerations such as their complexity, size, and extent to which they have been engineered for field use are considered, i.e., the state of their technology is assessed.

As a result of this analysis, a modular Neodymium:YAG (Nd:YAG) based system using a dye laser is found to be the best choice for accommodation of the visible and near visible source requirements. How such a system accommodates many experiments is shown in Section 6.10, following a detailed discussion of system definition and conceptual design. Requirements in the far infrared are met by CW and pulsed CO_2 laser sources, for which similar discussions are presented. In addition, several of the experiments require what are called special sources; these are sources where performance exceeds that attainable with the Nd:YAG based system, or any other system using existing

engineering technology, although such performance has been achieved in the laboratory.

The most detailed discussion is given to the modular neodymium based system, since it represents the most advanced state of development. In particular, the Nd:YAG laser part of the system uses technology that has undergone a great deal of engineering development. Based on this experience, detailed knowledge of the problems that can be expected in the construction of a space qualified system is available. These critical engineering issues, many of which will almost certainly be relevant in the engineering of other laser and optical systems for flight use, are discussed in Section 6.4.1.

6.2 LASER SOURCE SELECTION

6.2.1 REQUIREMENTS

Performance figures for the visible and near visible lasers that were assumed by the experiment descriptions in the updated SEED are shown in the chart of Figure 6-1. Requirements for the CO_2 lasers necessary for experiments 10, 13, 18, and 24 are deferred to Sections 6.11 and 6.12.

Because the SEED assumed a neodymium based system as a standard hardware set, the experiments and calculations were to some extent designed around such a source system. Other possible sources were suggested by the experimenters where appropriate. Of course, any laser that meets the functional requirements presented in this section is a candidate. Indeed, the potential scientific benefits from the expriments are so great that any laser is a candidate if it can be used to perform some experiment that fulfills a scientific objective. Realistically, the optimum laser system for meeting the goals of the program must be selected with the overall scientific and mission requirements in mind: first flight success, maximum probability of acquiring data,

ASSUMED PERFORMANCE \ SEED EXPERIMENT NUMBER			1	2	3	4	6	7	8	9a	9b	9c	11a	11b	11c	12a	12b	14	15, 16, 17	19	20	21	22	23	25	26
SEED ASSUMED HARDWARE SET	1064 nm	E PRF τ	1J 10 Hz 15 ns	1J 10 Hz 15 ns	1J 10 Hz 15 ns	2J 10 Hz 15 ns	1J 10 Hz 15 ns	30 Hz 15 ns	30 Hz 15 ns	10 Hz 15 ns			10 Hz 15 ns			10 Hz 15 ns		10 Hz 15 ns	10 Hz 15 ns	1J 1 μs	1J 7 μs	2J 10 Hz 15 ns	30 Hz 15 ns	10 Hz 15 ns	10 Hz 15 ns	20 ps
	532 nm	E Δλ	350mJ	350mJ	350mJ	1J	350mJ													300 mJ 0.1 pm	300 mJ 0.1 pm					
SODIUM LINES	590 nm	E Δλ						20 mJ 1.2 pm					20 mJ 1 pm					100 mJ 1 pm								
OZONE AT LOW ALTITUDES	280 nm TO 300 nm	E Δλ														10 mJ 100 pm										
Mg^+	279.6 nm	E Δλ							1 mJ 0.6 pm														1 mJ 1 pm			
OH	LINES NEAR 300 nm	E Δλ																				20 mJ 1 pm				
Mg	285.2 nm	E Δλ																					1 mJ 1 pm			
H_2O TROPOSPHERE	TWO NEAR 720 nm	E Δλ								60 mJ 5 pm																
H_2O TROPOSPHERE	TWO NEAR 820 nm	E Δλ									40 mJ 5 μm															
H_2O TROPOPAUSE OR STRATOSPHERE	940 nm	E Δλ										20 mJ 5 pm														
OZONE AT HIGHER ALTITUDES	265 nm	E Δλ															100 mJ 100 pm									
Ba^+	493 nm	E Δλ													20 mJ 1 pm											
Ba	455 nm	E Δλ												20 mJ 1 pm												
MgO	500 nm	E Δλ																					20 mJ 1 pm			
NO_2	TWO NEAR 450 nm	E Δλ																						10 mJ 100 pm		
NO	LINES NEAR 215 nm	E Δλ																							1 mJ 0.5 pm	
ATOMIC O	225.6 nm	E Δλ																								1 mJ 10 pm
O_2 A-BAND	TWO NEAR 760 nm	E Δλ																	30 mJ 5 pm							

Figure 6-1. Identification of Functional Requirements for Visible and Near Visible Sources From SEED.

and continued mission and experiment success throughout the evolutionary development.

Special Sources. Several special sources (for experiments marked by asterisks) may immediately be identified:

1. The very narrow band (transform limited) sources used for the velocity measurements of experiments 14, 19, and 20 are identified as special sources. Note that experiment 14, although assuming only a 1 pm linewidth source for some of its sodium measurements, requires ±5m/sec accuracy for velocity measurements.

2. Experiment 26 discusses the use of a 20 ps pulse length source in order to produce two photon fluorescence; this also requires a special source.

Further discussion of these and the far infrared sources is deferred until Section 6.13.

DIAL Requirements. Several experients use Differential Absorption Lidar (DIAL) techniques. Those species for which two lines are used are indicated in the left-hand column. Other experiments require different wavelengths at different times, these are indicated by the column below the experiment number having more than one entry.

6.2.2 EVALUATION CRITERIA FOR CANDIDATE SOURCES

The chart (Figure 6-1) presents the functional requirements for the visible and near visible sources subsystem, as extracted from the experiment descriptions presented in the SEED, and as refined through interaction with GE and NASA. Initially, the requirements were considered from a purely functional standpoint, without regard to the type of laser system used to obtain the particular wavelengths and other parameters. Most writers of the experiment descriptions assumed a standard hardware set in their experiment analyses so there was of course a tendency to orient, adapt, or select experiments compatible with neodymium based sources; however, many experimenters considered other sources - much work in the past has been done with other sources for various reasons. Careful consideration must therefore be given to assessing the suitability and adaptability of all available or potentially available sources to the functional, evolutionary, and engineering requirements for the sources

subsystem, and ultimately to providing an optimally adaptable and capable system for the maximum variety of Lidar experiments.

The suitability of a potential source is determined by considering how well it meets the functional requirements of the SEED. From the laser viewpoint, these requirements may be divided into specifications of: (1) wavelength, (2) linewidth, (3) output power, (4) pulse length, and (5) beam divergence. Each of these parameters, and how it affects the choice and design of the system and the grouping of the experiments, will be discussed in the next several paragraphs. For each of the functional requirements of the SEED, questions and issues concerning the suitability of potential sources arise. Also, certain logical groupings of the experiments can be made, and the source candidates must also be evaluated on their compatibility with these groupings.

Wavelength. The SEED source requirements allow a natural grouping of Lidar experiments according to wavelength region, source linewidth/stability, and single versus multiple wavelength output. First, a large subset of Lidar experiments (1-6) are relatively indifferent to wavelength, and merely require a plentiful and efficient source of photons meeting relatively broad spectral requirements for atmospheric transmission, scattering strength, detector sensitivity, safety, and so on. All the remaining experiments, except 19 and 20, require that the source be tuned to a precise line of the particular species under study. There is often a choice of species for a particular objective and a choice of spectral lines for each species, but the laser must in each case be precisely tuned and stabilized to the line. The wavelength used depends on which species are of interest and which give detectable returns. It also depends on the availability and cost of strong laser sources that can access these lines. Thus, this second class of experiments is further subdivided into those spectral regions that are accessible with a particular set of laser

hardware. A third class of experiments is distinguished as those of the above that use the DIAL technique (experiments 9, 15-17, 23). These require the source to produce two wavelengths simultaneously, or nearly so, so that the differential absorption for each resolution element of the atmosphere may be ascertained. Often only one of them need be set precisely on a given wavelength. A fourth class consists of experiments that require outputs in different spectral regions, but not necessarily during the same mission (11, 12, and 22). From the sources point of view, these four classes require increasingly more complex systems, and this fact must be taken into account in the design of a system that allows evolutionary development.

Linewidth. Requirements for precise tuning to a spectral line are usually coupled with the requirement that the linewidth of the source be comparable to that of the species to be studied, and thus the linewidth requirement produces a similar grouping of experiment classes and system complexity.

In some cases the species of interest have relatively broad spectral lines (those of classes 12 and 23 and to a lesser extent 9 and 26), forming a grouping that would not require as complex a spectral control system as those species studied in other classes (7, 8, 11, 15, 16, 17, 21, 22, and 25). A precisely controlled grating would probably suffice for the former group. The latter group would require additional line narrowing with, perhaps, an etalon, and a more complex control system, including some form of closed loop spectral control. Closed loop control would also be very desirable for the former to ensure with absolute certainty that the laser is on the desired line.

A third group of experiments, those that make wind velocity measurements, place the most stringent requirements on laser linewidth. These experiments require "special sources", that is, sources with transform limited linewidth - the narrowest linewidth physically possible with a given pulse length. The requirement for transform limited

performance can be justified with simple, order of magnitude calculations which ignore numerical factors relating to lineshape, velocity distribution, etc. A laser pulse of wavelength, λ , and pulse length, τ , is said to be transform limited when its linewidth, $\Delta\lambda$, is given by $\Delta\lambda = \lambda^2/c\tau$, where c is the velocity of light. Now, the Doppler shift from a scattering medium moving with velocity v is $\Delta\lambda/\lambda = v/c$. If $\Delta\lambda$ is substituted from the above formula, $v = \lambda/\tau$ is obtained as the smallest velocity that can be measured using a laser operating at wavelength, λ , and pulse length, τ . Again, note that this formula does not include factors such as a factor of two in the Doppler shift of a returned signal, and other factors relating to the exact definition of pulse length and transform limit. In addition, factors relating to the exact experimental conditions have been ignored, such as the practical difficulty of obtaining and measuring transform limited performance, the angle of the wind to the Lidar beam, and its velocity spread in the measurement cell. However, the formula may be used to establish upper limits to the measurement accuracy obtainable with a given laser.

Output Power. The accuracy and quantity of data obtained for each experiment always increases with increasing source power, and the signal to noise ratio improves with increasing pulse energy. It is clearly desirable to maximize these parameters. Greater available source power can also ease other systems requirements. An example would be the possibility of obtaining the same signal to noise ratio with smaller receiver optics size. However, output power cannot be made arbitrarily large because of the constraint to stay within the available power and cooling capabilities of the Shuttle. Clearly, in view of these considerations, efficiency is a very important criterion for selection of the sources system - it is a direct factor in the success of the experiments, and has direct bearing on the degree to which all Shuttle facilities are taxed. Apart from considerations of available power, other factors also limit maximum output power. Eye safety requirements limit the possible output

power indirectly by limiting the irradiance (power per area) on the ground. The power limit is determined by the diameter on the ground of the largest spot that can be allowed the system while still obtaining the desired horizontal resolution. Finally, for example, some experiments measuring sodium concentrations by resonant fluorescence, become inaccurate at higher laser energies (and low specie concentration) per sample volume because of signal saturation due to excitation of all available atoms in the atmospheric cell being irradiated.

Pulse Length. Pulse length affects the overall performance of the system in several ways. First, resolution is limited to a distance of the same order of magnitude as the distance light travels during the pulse length; for example, a laser with a ten nanosecond (ns) long pulse will allow the Lidar system to have on the order of three meters resolution. Second, depending on how the received signal is processed, pulse length, in combination with receiver parameters such as bandwidth and/or range bin size, detector response time, and the nature and source of the noise, enters into the overall system signal to noise ratio equations; shorter pulses generally allow improved signal to noise. Eye safety criteria are generally indifferent to pulse lengths differing by the orders of magnitude in the regime of concern here.

Most of the experiments have relatively large (1 km) range bins. The smallest is 10 m. A single laser that can accommodate the maximum number of experiments must therefore have a pulse length on the order of tens of nanoseconds by the range resolution criterion. Accurate velocity measurements require longer pulses, as indicated above in the discussion of linewidths. Q-switched laser systems with pulse lengths up to 500 ns meet the range resolution requirement, but at best allow marginal velocity measurement accuracy (with luck a meter per second accuracy could be achieved with 500 ns pulses).

Beam Divergence. Because any desired beam divergence can be obtained from even a very poor quality laser beam by the use of sufficiently large optics, beam divergence is not a direct criterion in the selection of the laser. Beam uniformity and consistency are of some importance for experimental data quality and eye safety reasons; all the lasers under consideration are sufficiently well characterized that we may conclude they are usable. The principal effect of the beam divergence requirements is in the grouping of the experiments according to the output optics they require. In all cases mentioned in the SEED, the beam expansion is quite moderate; lasers with near diffraction limited performance, such as laser-pumped dye and low order mode Nd and Ruby lasers, need the least beam expansion and the smallest optics.

Lasers that have larger beam divergence would require proportionately larger optics. Explanation of this requires a slight digression into beam optics theory. The far field angular diameter (beam divergence) of a light beam of wavelength λ passing through a limiting aperture of diameter D, is given by $\beta = 2.44n\lambda/D$, where n is the factor by which the beam quality is greater than diffraction limited. The exact value of the number in front varies with the beam spatial profile and the definition of beam size. For example, for a uniformly illuminated circular aperture of diameter D the angular diameter of the first dark ring in the far field diffraction pattern is $2.44\lambda/D$, while for a Gaussian beam of diameter D, the far field beam diameter is given by $4\lambda/\pi D$ (the radius of a Gaussian beam is defined as the radial distance to the point where the beam intensity has dropped to $1/e^2$ of its value at the beam center). Very few real beams fit either of these situations exactly. A multimode neodymium system can be designed to have approximately three times diffraction limited beam divergence; existing efficient multimode 2 joule output designs have somewhat larger divergence. The main point of this digression is that the angular size of a given optical beam can be made small enough to meet system requirements by increasing the diameter of limiting optical elements. A practical limit to this

procedure is set by size, weight, and cost factors of the optics.

6.2.3 TECHNOLOGICAL EVALUATION OF CANDIDATE LASERS

Mindful of the preceeding discussion, let us consider some potential laser candidates. Those shown in Table 6-1 are not all that were considered but are the most advanced in development; most have been used for Lidar applications in the past, and all have performance parameters that are at least close to the required range. The table has been divided into basic source lasers, some of which are tunable as indicated, and frequency conversion techniques. These can be used to convert any of the basic source lasers to other desired wavelengths and also to improve other specifications. Parameters relevant to engineering criteria are presented in the columns.

Basic Source Laser. Starting at the bottom: the copper vapor laser may be eliminated from consideration because it is not scalable to pulse energies of more than a few mJ. Nitrogen lasers have a similar problem. Excimer lasers are very promising in meeting all the requirements with good efficiency; in addition, they are somewhat tunable in narrow bands. Narrowing of the higher energy versions at good efficiency must be demonstrated, however, as well as efficient operation with the gasses that would give the desired wavelengths. Essentially only laboratory devices have been built. Commercial devices require recharging of the corrosive gas approximately every several hundred thousand shots. Similar to other lasers that involve fast discharges, these devices use electronic tube switches with finite life.

Flash-pumped dye lasers look very promising; they are tunable, so they would not require additional complexity to achieve a range of wavelengths. Flashlamp pumped dye lasers, however, characteristically have dye degradation problems due to UV emission by the flashlamp. In addition, the dye does not operate at maximum efficiency because the flashlamp pump pulse is long compared to the dye fluorescence lifetimes; excited

TABLE 6-1. VISIBLE AND

	Order of Magnitude Performance Figures					Engineering				
	Wavelength(s) μm	Approximate Efficiency (Wall Plug) percent	Approximate Pulse Energy	Approximate Repetition Rate	Tunable?	Overall Complexity of System	Require Tight Temperature or Pressure Control Other Than for Frequency Stability?	High Voltage?	EMI or RFI?	Fluid Handling
BASIC SOURCE LASERS										
Neodymium	1.06 (0.96 - 1.4)	2.0 (YAG) 0.5 (Glass)	Wide range has been done	Wide range has been done	Lines & Slightly With Temp	Moderate	No	2 kV	Have been built with Sensitive Receivers	Only Coolant
Ruby	0.69	0.1	Up to many joules	Up to ~10 Hz	Slightly with temperature	Moderate	No	2 kV	Have been built with sensitive receivers	Only Coolant
Flash Pumped Dye	0.22 - 0.96	0.5 (coax) 0.25 (linear)	Up to 100 joules in special cases also, (Not all λ's)	Up to ~100 Hz	Continuous	Low (much higher if tuned)	No	10 kV	Yes (fast discharge)	Dye & Solvent
Excimer	Dep. on Gas Several Bands in UV and Vis.	Up to several	Up to 300 J	Up to ~20 Hz	Over Band	Moderate to High: Potentially Low	Yes	20-100 kV	Yes (Fast discharge)	Corrosive Gas
Nitrogen	0.34		Up to 100 mJ	Up to ~500 Hz	No	Low	Yes	20 kV	Yes (Fast discharge)	Gas Lasing Medium
Cu Vapor	0.51, 0.58	1.5	Few mJ	Up to ~10 kHz	Line Tunable	Moderate to High	Yes		Yes (Fast discharge)	High Temp Gas
FREQUENCY CONVERSION TECHNIQUES										
		(Conversion Efficiency)								
Frequency Doubling, Mixing	0.217 - 10	Up to 50	Up to joules	Any	No	Low	Yes	No	No	No
OPO (Optical Parametric Oscillator)	Common for IR, usable for visible	few tens	Less than one joule	Any	Yes	Moderate	Yes	No	No	No
Laser Pumped Dye Lasers	Soft UV to Near IR	Up to 50	Up to joules	Any	Yes	If tuned moderate to high	No	No	No	In most cases
Stimulated Raman (or Brillouin) Scattering	Essentially Any	Up to 50	Any	Less than ~10 Hz in gas, 10 kHz in solids	Line Tunable	Very low	No	No	No	In some cases

NEAR-VISIBLE CANDIDATES

Considerations							
Standby (Warmup)?	Maintenance? Limited Life Components?	Size and Weight	State of Technological Development	Reliability	Systems Exist Which Meet All Functional Requirements Simultaneously?	Experiment Accommodation (Visible and Near Visible)	Comments
None	Flashlamp -10^7 Shots	Has been miniaturized for military applications	Excellent	Tested 50 hrs MTBF for 2w device	Yes	With Doublers: 1-6, 19, 20 As Dye Pump: 7, 4-7, 11, 21-23 Doubled Dye: All Remaining	All solid state. Many flown in aircraft.
None	Flashlamp	Has been miniaturized for military applications. Somewhat larger than Nd.	Excellent	Demonstrated in Hands-Off Device	Almost	As is: 1-6 – As Dye Pump: 9, 15-17 Doubled, As Dye Pump 7, 11, 14, 21-23 Doubled Dye - Remainder	All solid state
None	Flashlamp: 10^6 shots. Dye solution - varies with dye.	Lab device: reasonably compact	Good, but not at high PRF (coax) and energy (linear)	Good (less for coaxial)	In many cases	Poor for near IR. For UV would have to be doubled	Dye exposed to broad band UV. Efficiency limited for 500 nsec pulses by triplet state bottleneck; fast flashing lamps difficult.
	Lasing Medium 10^5 Shots Electronic Switch	Lab device, relatively large gas volume	Lab Device	Fair	No – a few	Most, as dye pump. Some need two stages or doubling Narrowing to be demonstrated.	Corrosive gas needing periodic recharging
	Spark Gap Switch	--	Good		No – too little energy	Weak in near IR as dye pump. Low power. Can get all wavelengths.	Low pulse energy
Yes	Tube life, HV and I switch	Lab device, large power supplies at present.	Lab Device	Good	No – too little energy	Will achieve wavelengths (as dye pump and doubled) of all but 11 & 22.	Warmup required. Limited energy per pulse.
Needs precise temp control	None	Has been miniaturized for military applications	Excellent	Mil. qual. 3w device	Yes	--	Many crystals, useful at many wavelengths available; most require bright source
Needs precise temp control	None	Compact	Very Good but Lab Device	Good	No	See text	
No	Dye solution (at much longer intervals than flash pumped)	Lab Device, compact size dominated by circulation system, reservoirs.	Excellent	Good	Almost (energy low)	See text	
No	None	Compact	Lab device	Good	No	--	Fixed shifts in wavelength by up to 4000 cm^{-1} in various materials - high average power difficult at present.

electrons fall to the (slightly) longer lived triplet state, removing them from the possibility of lasing and thereby lowering the efficiency. Flashlamp pulse length would also limit flashlamp pumped dye lasers to those experiments not requiring accurate range resolution. Cavity dumping could be used to obtain shorter pulses from a flashlamp pumped dye laser, with some loss in efficiency and increase in complexity; this would also require some developmental work. Moderate shortening of the pulse by using shorter flashlamp pulses at the expense, generally, of lamp life could also be achieved; again, this would require development.

Dye lasers pumped by Q-switched lasers (pulse lengths shorter than 100 ns) avoid all of the flashlamp pumped dye laser problems mentioned above. In addition, spectral narrowing is easier with laser pumped dye lasers.

Finally, two solid state lasers are shown. The neodymium and ruby systems are to be considered as representative of four- and three-level lasing medium solid state systems, respectively. Note the poor efficiency of ruby; it has proven to be difficult to operate these systems at a repetition rate over ten hertz. Other rare-earth lasers are of course possible; the fact that neodymium is so common today is testament to its superior efficiency and the relative ease of manufacturing good quality lasing crystals (particularly YAG) and glasses.

Study of the matrix shows that the neodymium laser based system has the most desirable properties, especially for the SEED experiment classes having the highest feasibility rating. The neodymium laser was chosen for the visible and near visible experiments because it demonstrated outstanding reliability, particularly in the advanced state of development of systems that meet all the experiment functional requirements simultaneously. It is also superior in efficiency, tolerance to environment, compact size and weight, lack of corrosive or limited shelf life components, limited number of components requiring maintenance, and simplicity.

Frequency Conversion Techniques. To cover the entire spectrum of required wavelengths, some frequency conversion of the neodymium laser output must be performed. Processes that make use of the nonlinear optical susceptibility of crystaline materials are represented in the chart by frequency doubling, a very common method of obtaining shorter wavelengths, mixing and Optical Parametric Oscillation or Amplification (OPO or OPA). Other frequency conversion techniques utilize laser pumped dye lasers or stimulated Raman scattering.

OPO is a completely tunable technique often used in the laboratory for obtaining IR wavelengths. Narrow-band sources of shorter wavelength than any of the desired wavelengths are required for narrowband output, and suitable nonlinear materials must be identified; a technique that has not been investigated very much in the visible. Mixing is a technique where a nonlinear material is used to obtain a laser frequency which is the sum of the frequencies of the two input lasers. Frequency doubling is the case where the two input frequencies are the same (e.g., 1064 nm plus 1064 nm mixed produce 532 nm); frequency tripling is the case where one of the two input frequencies is double the other (e.g., 1064 nm plus 532 nm mixed produce 355 nm).

Optical mixing should also be considered as an alternative to frequency doubling of dye outputs, pumping IR dyes with the third harmonic (354.7 nm) of Nd:YAG to reach the region of wavelengths shorter than 532 nm. Table 6-2 lists the experiments to which mixing is applicable, and the required output wavelength and bandwidth. The next column describes the mixing method(s) by which the desired output may be generated, indicating the dye laser wavelength and the Nd:YAG harmonic with which it is to be mixed (F is the fundamental, SH is the second harmonic, TH is the third harmonic). Where known, the nonlinear crystal to be used is given. The Nd:YAG laser bandwidth (at 1064 nm) needed to yield the desired bandwidth at the output wavelength is calculated and shown in the next column, with the assumption that the dye laser

Table 6-2. Mixing: Applicable Experiments

Experiment	Output λ(nm)	Output Δλ(pm)	Mixing*	Crystal	Nd: YAG Bandwidth† Required (pm)	Alternative	Advantages of Mixing	Disadvantages of Mixing
8	279.6	0.6	379.2 nm w/F	ADP	0.81	double 559	uses leftovers at 1.06 μm	uses UV dye needs narrowband Nd: YAG
			589.3 nm w/SH	ADP	2.7			needs narrowband Nd:YAG
9a	720	3.0	429 nm w/F		0.41	dye pumped by SH	uses visible dye	two additional steps needs narrowband Nd: YAG
			699 nm w/TH		1.3			two additional steps needs narrowband Nd: YAG
9b	940	1.0	499 nm w/TH	ADP	0.93††	dye pumped by SH	uses visible dye	two additional steps needs narrowband Nd: YAG
			570 nm w/TH		0.58††		uses visible dye	two additional steps needs narrowband Nd: YAG
11b	455	1.0	794.9 nm w/F		3.7	dye pumped by TH	uses leftovers at 1.06 μm	uses IR dye needs narrowband Nd: YAG
11c	493	1.0	918.6 nm w/F		3.3	dye pumped by TH	uses leftovers at 1.06 μm	uses IR dye needs narrowband Nd: YAG
12	280 to 300		380 nm to 418 nm w/F	ADP	any	double 560 to 600	uses leftovers at 1.06 μm	additional step needs UV dye needs more than one dye
			591 nm to 688 nm w/SH	ADP or ADA	any			needs more than one dye
15	760	5.0	433 nm w/F		4.1	dye pumped by SH	uses visible dye	two additional steps needs narrowband Nd: YAG
			665 nm w/TH		2.4		uses visible dye	two additional steps needs narrowband Nd: YAG
16	760	5.0	433 nm w/F		4.1	dye pumped by SH	uses visible dye	two additional steps needs narrowband Nd: YAG
			665 nm w/TH		2.4		uses visible dye	two additional steps needs narrowband Nd: YAG
17	770	5.0	447 nm w/F		3.8	dye pumped by SH	uses visible dye	two additional steps needs narrowband Nd: YAG
			658 nm w/TH		2.3		uses visible dye	two additional steps needs narrowband Nd: YAG
21	300	1.0	418 nm w/F	ADP	6.1	double 600	uses leftovers at 1.06 μm	additional step needs UV dye needs narrowband Nd: YAG
			688 nm w/SH	ADA	5.1			needs IR dye needs narrowband Nd: YAG
22a	279.6	1.0	379.2 nm w/F	ADP	6.6	double 559	uses leftovers at 1.06 μm	needs narrowband Nd: YAG
			589.3 nm w/SH	ADP	5.6			needs narrowband Nd: YAG
22b	285.2	1.0	389.6 nm w/F	ADA	6.5	double 570	uses leftovers at 1.06 μm	needs narrowband Nd: YAG
			614.7 nm w/SH	ADA	5.7			needs narrowband Nd: YAG
22c	500	1.0	943.2 nm w/F		any	dye pumped by TH	uses leftovers at 1.06 μm	needs IR dye
23	450		776.8 nm w/F		any	dye pumped by TH	uses leftovers at 1.06 μm	needs IR dye
25	215	0.5	503.9 nm w/375 nm	KB_5O_8(90°)	any	none	90° phase matched	needs 2 dye lasers needs UV dye
			TH of 645 nm	RDP/KB_5O_8	any		simplest	
			SH of 721.6 nm w/SH	RDA/KB_5O_8	1.9			needs IR dye needs narrowband Nd: YAG
			545.9 nm w/TH	KB_5O_8	2.8		uses leftovers at 532 nm	needs narrowband Nd: YAG
			SH of 539 nm w/F	ADP/KB_5O_8	4.4		uses leftovers at 1.06 μm	needs narrowband Nd: YAG
			SH of 572.6 nm w/G	ADA/KB_5O_8		double 451.2 nm or triple 676.8 nm	uses leftovers at 1.06 μm	
26	225.6		493.4 nm w/SH	KB_5O_8			uses leftovers at 532 nm	
			619.9 nm w/TH	KB_5O_8			uses leftovers at 532 nm	

Notes:

* – dye wavelength given followed by F(1064 nm), SH(532 nm) or TH(355 nm) from Nd: YAG
† – 1 pm dye laser bandwidth assumed (except †† indicates 0.1 pm dye laser bandwidth assumed)

bandwidth is 1 pm. (This calculation is described in the next paragraph.) The alternative to mixing is the straightforward dye laser or frequency doubled dye laser indicated in the next column, and finally the advantages/disadvantages of each mixing method as compared with the "alternative" are given.

The determination of the required Nd:YAG fundamental bandwidth is very simple. The wavelengths involved in frequency mixing obey $1/\lambda_3 = 1/\lambda_1 + 1/\lambda_2$ (sum generation) or $1/\lambda_3 = \left| 1/\lambda_1 - 1/\lambda_2 \right|$ (difference generation) where λ_1, λ_2 and λ_3 are the two input and single output wavelengths, respectively. If the desired output bandwidth is $\Delta\lambda_3$ and the assumed dye laser bandwidth is $\Delta\lambda_2$ (1 pm for Table 6-2), the required bandwidth of the Nd:YAG harmonic (F, SH, or TH) is

$$\Delta\lambda_1 = \lambda_1^2 \left(\frac{\Delta\lambda_3}{\lambda_3^2} - \frac{\Delta\lambda_2}{\lambda_2^2} \right)$$

If the mixing is done with the nth harmonic, then the entry in the "Nd:YAG bandwidth required" column is simply $n\,\Delta\lambda_1$.

The main disadvantage in mixing with Nd:YAG harmonics is the bandwidth requirement. Without addition of an etalon to the oscillator, the bandwidth will be 10 to 30 pm. Reducing the linewidth involves an additional optical element and operation of the oscillator near threshold, thus reducing efficiency and total laser output power (unless another amplifier stage is used). Variations of Nd:YAG output wavelength could be detected and corrected by the dye laser control system if the mixer output wavelength (and not just the dye laser wavelength) is measured. Otherwise, a separate spectral control system for the Nd:YAG laser is required.

There is one advantage in mixing dye laser output with Nd:YAG laser output to generate blue or UV light; overall efficiency is improved because some energy at 1064 nm (left over from doubling and possibly not used for anything else) is used in the mixing process. A more significant advantage is apparent for experiments requiring IR

output (numbers 9, 15, 16, 17), for which mixing eliminates the IR dyes that are generally short-lived and inefficient. However, the mixing approach is more complex, requiring two mixing steps in addition to a narrowband Nd:YAG laser.

In summary, the Nd:YAG laser bandwidth requirement severely reduces the attractiveness of mixing for most experiments. Since frequency doubling has not been demonstrated below 217 nm, one of the five candidate mixing processes listed will have to be used for experiment 25. They are represented schematically in Figure 6-2. Third harmonic generation of a 645 nm dye laser is by far the simplest method, and probably as efficient as the others.

Another class of nonlinear interactions used to obtain additional wavelengths is represented by stimulated Raman scattering (SRS). Only fixed shifts in wavelength are possible, the precise value of which is characteristic of the particular Raman medium used, so continuous tuning is not possible. This makes the technique of limited use for a versatile instrument, although the inherent simplicity makes it appealing where a fortuitous match with a desired line exists. It may also be useful in shifting the output of a tunable source, such as a dye laser, from a wavelength region where stable and reliable dyes exist into regions of the near IR where such dyes are unavailable.

Laser pumped dye lasers provide the most versatile method of frequency conversion. A study of all the techniques showed that by the use of only frequency doubled or tripled 1064 nm radiation to pump a dye laser, the least technologically risky and most versatile source meeting all the specifications was obtained, without the necessity for using any other conversion techniques. In some cases, to obtain UV, the dye laser output must be frequency doubled. The only truly tunable element required in this scheme is the dye laser. The spectral control and tuning of dye lasers is the best understood and most technologically advanced of the frequency conversion methods

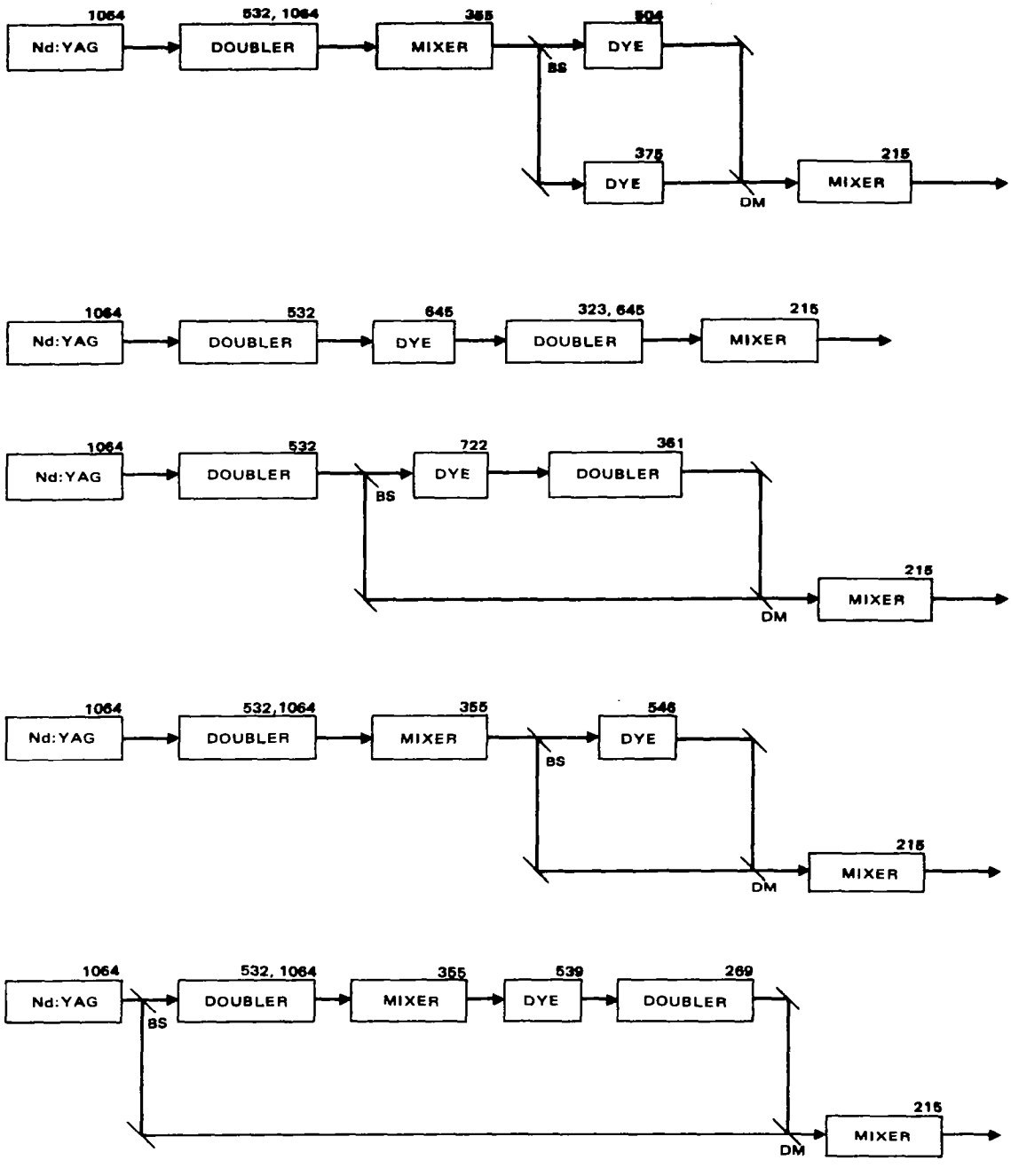

Figure 6-2. Methods of obtaining the 215 nm wavelength for Experiment 25. BS indicates a beamsplitter, DM indicates a dichronic mirror. All wavelengths are given in nanometers.

discussed. Essentially total coverage from the UV to the near infrared is obtained.

6.3 VISIBLE AND NEAR VISIBLE SOURCE DEFINITION

6.3.1 MODULAR NEODYMIUM LASER BASED SYSTEM

The most promising source for experiments in the visible and near visible is a modular system using a neodymium laser as the basic source and a tunable dye laser, frequency doublers, and mixers for conversion to all the wavelengths required for the experiments. This concept allows utilization of hardware building blocks that are, for the most part, already technically mature to build a source system that can be flight qualified in the early 1980's. Modularity allows maximum flexibiilty in producing the variety of required wavelengths, allowing several experiments to be done with one system. It is more amenable to the evolution of the system into one that can accommodate the maximum number of the presently proposed experiments. It also would be the most accommodating for future experiments requiring wavelengths accessible by a neodymium based system. The system may be used over more than the presently proposed spectrum of wavelengths. By use of dye lasers, frequency doubling and other conversion techniques, wavelengths far out into the infrared may be produced. By use of repeated doubling and mixing, wavelengths into the vacuum ultraviolet may be accessed. Potentially in future modules, optical parametric interactions, other mixing techniques and Raman frequency conversion could also be used.

Some specific examples of the versatility possible with the modular system are shown in Table 6-3. The list may easily be extended to create a system that will produce a large number of wavelengths simultaneously. How much of each of the various wavelengths is obtained depends on the efficiencies of all the steps used; it is therefore desirable to minimize the number of steps. Referring to the table: first,

Table 6-3. Examples of Wavelength Flexibility with Modular System

TO OBTAIN SIMULTANEOUS OUTPUT AT

	WAVELENGTH(S):	WITH ENERGY:	REQUIRES THE MODULES:
a)	1060 nanometers	2 joules	PUMP LASER + OUTPUT OPTICS
b)	1060 530	1.4 0.7	PUMP LASER + DOUBLER + OUTPUT OPTICS
c)	1060 λ_{gp}	1.4 VARIOUS	PUMP LASER + DOUBLER +(BEAMSPLITTER)+ DYE LASER + OUTPUT OPTICS
d)	1060 λ_{gp} λ_{gp}	1.4 VARIOUS VARIOUS	PUMP LASER + DOUBLER +(POWER BEAM-SPLITTER)+ TWO DYE LASERS + OUTPUT OPTICS
e)	1060 530 λ_{gp}	0.8 0.45 VARIOUS	PUMP LASER + DOUBLER +(BEAMSPLITTER)+ 2nd DOUBLER +(BEAMSPLITTER)+ DYE LASER + OPTICS
f)	1060 λ_{gp} λ_{gp}	0.8 VARIOUS VARIOUS	PUMP LASER + DOUBLER +(BEAMSPLITTER)+ 2nd DOUBLER +(BEAMSPLITTER)+ TWO DYE LASERS + OUTPUT OPTICS
g)	1060 λ_{gp}^{FD}	1.4 VARIOUS	c) + DYE LASER DOUBLER
	. . .		
h)	1060 λ_{gp} OR λ_{gp}^{FD} λ_{gp}^{FD}	0.8 VARIOUS VARIOUS	f) + ONE OR TWO DYE LASER DOUBLERS
i)	1060 530 355	1.1 0.55 0.20	LASER + DOUBLER + TRIPLER + OPTICS
j)	1060 530 λ_{uvp}	1.1 0.55 VARIOUS	LASER + DOUBLER + TRIPLER +(BEAMSPLITTERS)+ DYE LASER + OUTPUT OPTICS
k)	1060 λ_{gp} λ_{uvp}	1.1 VARIOUS VARIOUS	LASER + DOUBLER + TRIPLER +(BEAMSPLITTERS)+ TWO DYE LASERS + OUTPUT OPTICS
	. . .		

Abbreviations:

λ_{gp} = dye laser wavelength accessible by pumping with 530 nm (green)

λ_{uvp} = dye laser wavelength accessible by pumping with 355 nm (uv)

$\lambda_{gp}^{FD}, \lambda_{uvp}^{FD}$ = wavelengths accessible by doubling above

the power of the neodymium laser may be used by itself, a), frequency doubled, b), or with a dye laser, c). Next, d), e), and f) illustrate methods for obtaining two different visible wavelength outputs. In d), the frequency doubled output of the 1060 nm laser is split by what is labeled a power beamsplitter; half of the energy is used to pump each of two dye lasers. Greater total output energy may be obtained by using the method of f). In this case, all the output of the doubler is used to pump one of the dye lasers; 1060 nm radiation left over from the first doubler is passed through another doubler, and the additional 530 nm radiation obtained is used to pump the second dye laser. In e), only one dye laser is used, and the 530 nm is one of the output wavelengths. In g) a doubler is added to the dye laser so that ultraviolet may be obtained. The same may be done to configurations c) through f), and as suggested for f) in line h). Lines i) on down show some of the possiblities that arise if a tripler is introduced.

The modular neodymium based system is divided into two basic subsystems (as shown in Figure 6-3). The first subsystem is a green or ultraviolet source consisting of a frequency doubled, or tripled, Nd:YAG laser and associated power supplies and other hardware. The second subsystem consists of one or more dye lasers which use either of the above sources as the optical pump for their lasing medium. A tunable doubler module may be added as part of the dye laser subsystem in order to access UV wavelengths by frequency doubling the dye laser output. The outputs from the above subsystems and modules are fed into the output optics module. The beam may be conditioned in beam divergence as required for the particular day or night time experimental conditions. Explicit layout of the system showing experiment accommodation will be deferred to Section 6.10.

The division of the sources system into the two laser subsystem blocks emphasizes the important fact that there are fundamentally two lasers in the sytem. They are

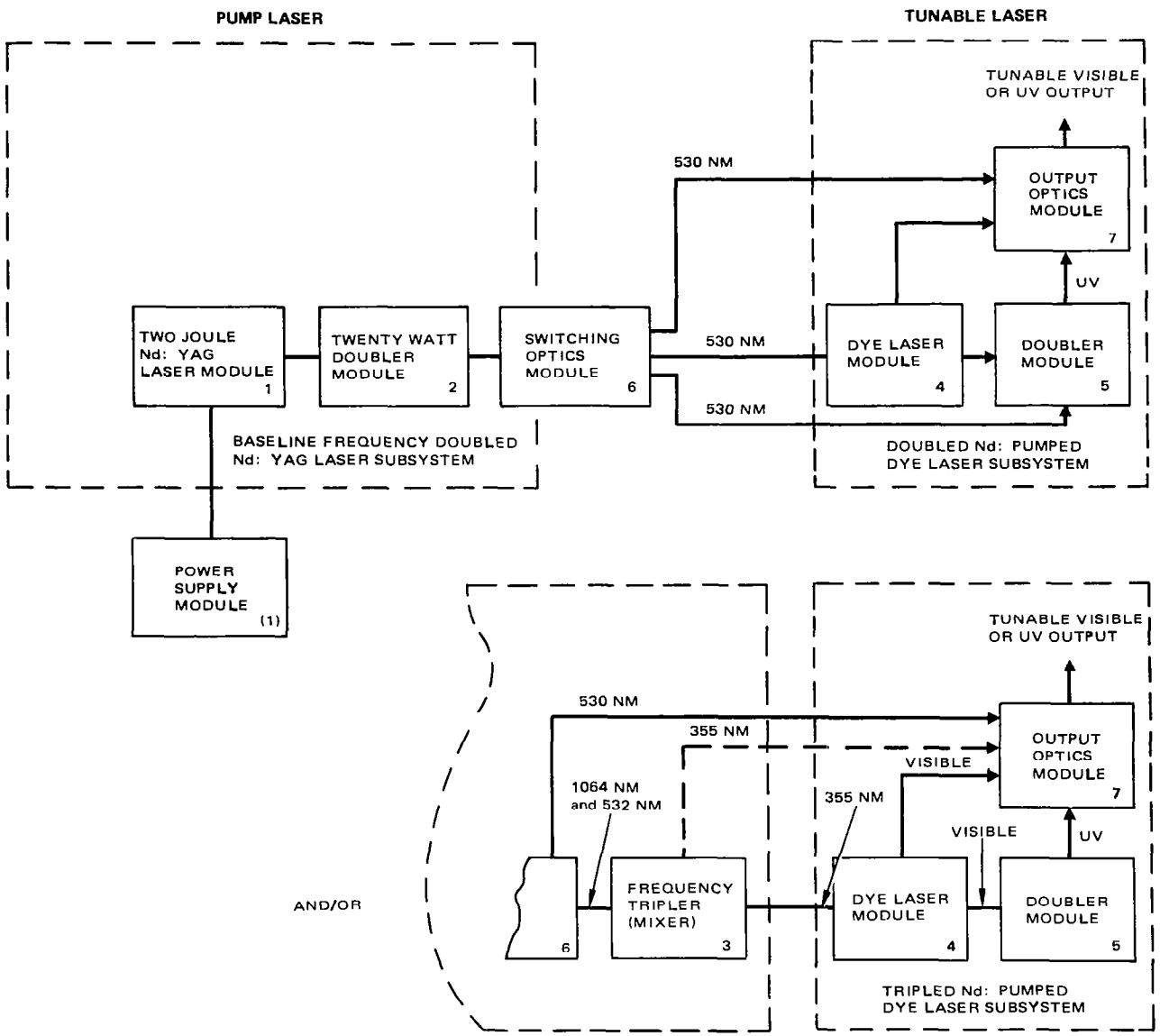

Figure 6-3. Visible and Near Visible Sources System.

related in pulse length and timing because the dye laser, not being able to store optical energy for more than a few nanoseconds, will lase only precisely when pumped by the neodymium laser. It is important to realize that other performance parameters are essentially independent and are determined for each laser by its own resonator and optics configurations. As far as the dye laser is concerned, the neodymium laser is merely a high intensity source of photons; therefore, the output wavelength of the dye laser is a function of what dye is used, and what wavelength selecting elements, such as diffraction gratings, prisms, and etalons, are in its resonator. The 530 nm pump laser affects this performance parameter only by establishing an upper photon energy bound. Only wavelengths longer (i.e., of less energy) than that of the pump laser may be attained. (Actually, this simple rule is complicated by the fact that, in order to obtain high efficiency, a certain separation must exist between the absorption and fluorescence bands of the dye used. A 530 nm pump laser allows wavelengths of longer than about 540 nm to be obtained.)

As an additional example of the independence of the two lasers, the spectral purity and mode quality are determined entirely by the dye laser optics and the degree of spectral control given it, and are quite independent of (although sometimes made easier by) the mode- and spectral-properties of the pump laser. Provided the pump laser has sufficient brightness to achieve the required population inversion in a sufficient volume and correct geometry of dye lasing medium, high efficiency and good output mode quality will be obtained for the dye laser. The mode quality of the neodymium laser has only a secondary effect on dye laser performance. This effect is greater in the case of longitudinal pumping, as is discussed in Section 6.4.2.

One important result of this subsystem independence on the total system is that no particularly stringent performance requirements with respect to beam quality and spectral purity are placed on the 530 nm green source. None of the experiment

classes, with the exception of those proposing to use the green for velocity measurements on aerosols, require that the green have an extremely narrow line width; this property of the green laser is also not required by the dye laser.

The individual modules comprising the visible and near visible sources system are defined and described in Sections 6.4-6.9. Important designs will be presented, and preferred designs will be selected. First, it is appropriate to consider engineering issues that affect virtually all of the modules to a greater or lesser extent.

6.3.2 CRITICAL ENGINEERING ISSUES

For all of the modules in the system, performance approaching that required has been demonstrated in laboratory versions. Thus, all concepts except for some in the dye laser frequency control (see Section 6.7) have undergone at least this much development; this is why they were chosen for the system. Commercial systems are available that meet or approach the performance required. The total mission and environment must be considered to determine suitability of those systems for the Shuttle multiuser Lidar instrument. The Shuttle mission and environment is quite different from that for which commercial systems were designed and engineered. The system must be vibration hardened to withstand launch. Once in space it must be capable of hands-off, unattended operation during the mission. It should have sufficient reliability to ensure that some data will be obtained on every mission, and minimum maintenance will be required between missions. Operation in space requires efficiency and conservative use of all resources: the system should be lightweight and compact, power consumption should be minimized by selecting sources of high efficiency, and use of data handling signal processor and communications facilities should be minimal. A system with multifunction operation is desirable. Experience has shown that to achieve these features requires significant engineering development, as distinguished from, and in addition to, the type of development and

design undergone by laboratory and quasifieldable systems. This essential development is a major factor in the increased cost of flight qualified systems.

Neodymium systems have completed this development cycle; many problems were encountered and solved, and many systems are now fielded or flying in military systems. The extent to which the seven modules of the visible and near visible sources system have undergone this kind of engineering is summarized in Figure 6-4. The first four columns are specific problems that have been encountered in the engineering development of Nd:YAG lasers and frequency doublers for field/flight use. It is reasonable to expect that analogous problems will be encountered in the engineering of the dye laser system. On Figure 6-4, the circles indicate that engineering development is in process or completed; a blank indicates that development effort is needed.

6.4 NEODYMIUM LASER SUBSYSTEM, MODULE 1: NEODYMIUM LASER

A modular neodymium laser based system has been identified as the preferred approach to providing a reliable, flyable Lidar source. The state of development of neodymium lasers is the subject of this section: engineering issues are identified, transverse mode quality requirements are discussed, and existing lasers are evaluated.

6.4.1 ENGINEERING ISSUES

As was mentioned in Section 6.3.2, the major engineering issues concerning neodymium lasers have been identified and solved, leading to the production of reliable, military qualified hardware. It is valuable to list the major areas where problems occurred, and to present the solutions. This is not only for historical orientation, but also to provide the reader with realistic examples of what problems might arise in converting any laboratory or commercial laser concept to a viable piece of hardware.

MODULE	HEAT EXCHANGE	THERMAL EFFECTS	ALIGNMENT STABILITY	CONTAMINATION	EFFICIENCY IN POWER CONSUMPTION	LIGHT WEIGHT/SMALL SIZE ENGINEERING	EFFICIENCY IN DATA PROCESSING REQUIREMENTS	AUTOMATION	FLIGHT/FIELD HARDENING	RELIABILITY ENGINEERING
1. TWO JOULE NEODYMIUM LASER	O	O	O	O	O	O	O	O	O	O
2. TWENTY WATT DOUBLER	O	O	O	O	O	O	O	O	O	O
3. TWENTY WATT TRIPLER (MIXER)	O			O	O	O	O			
4. NARROW LINEWIDTH DYE LASER										
5. TUNABLE DOUBLER	O				O					
6. SWITCHING OPTICS	O			O	O	O	O			
7. OUTPUT OPTICS	O	O	O	O	O	O	O		O	O

O – NEEDS ENGINEERING DEVELOPMENT OR NOTHING

BLANK – NEEDS ADVANCED DEVELOPMENT

Figure 6-4. Visible and Near Visible Sources System - Flight Engineering Status.

Heat Exchange Method. For a neodymium laser, the lasing medium is a solid (most commonly Yttrium Aluminum Garnet (YAG) or some kind of glass) doped with the neodymium ions. These ions are optically pumped into the state from which they lase by, typically, some sort of flashlamp, usually a quartz tube filled with a few hundred torr of a noble gas. Several percent of the electrical energy input to the flashlamp emerges as the laser output energy; the remainder of the energy appears as heat in the rod, in the reflecting cavity that directs and filters the light from the lamp to the rod, and especially in the lamp. In gaseous or liquid lasing media, the heated medium itself is typically circulated, by either passive or forced convection, at a fast enough rate to remove the deposited heat. The circulation system in this

case must be designed with the chemical and physical properties, sensitivities and requirements of the flowing lasing medium in mind. This is the case, for example, for the dye laser. For the solid state laser, on the other hand, heat is removed from the medium by conduction to the edge of the medium, and then by conduction or convection away from the medium to the outside world. Thus, more freedom is allowed in the choice of cooling technique and coolant, and a simpler system is possible.

The use of large volumes of a liquid coolant such as water, ethylene glycol, alcohol or a fluorocarbon has been the most common method for cooling laboratory and industrial flashlamp pumped lasers. However, several problems occur when similar systems are attempted for completely closed loop, sealed flyable hardware. Leakage, freezing, boiling and expansion problems for the coolant must be eliminated. Precipitation, dissociation, or other chemical reactions of the coolant caused by the ultraviolet flashlamp radiation or simply the passage of time must be avoided. Corrosion of the optical, electronic, or mechanical components and seals by the coolant must be prevented. Discoloration of the coolant, coolant channel walls or optical components with attendant laser pump light loss must be averted.

The systems that have been most successfully fielded have used the inert gas cooling technique developed by Hughes. This technique allows a lightweight, compact and completely self contained unit that solves all the above mentioned problems. At the same time, periodic flash tube replacement is simplified through the use of a simple dry process, avoiding complex liquid handling.

Misalignment Tolerance. A laser resonator consists of a number of optical components that must be kept in alignment for the device to function. Various components, depending on the complexity of the design, require different degrees of alignment precision in order that the laser operate with the specified efficiency, beam

quality, and beam pointing throughout its operating and shelf life. These design problems, distinct from but related to the problems of co-aligning several optical systems, will now be discussed. They have been solved for solid state lasers now being manufactured and operating in severe physical environments; therefore, there is no reason to incorporate active alignment control loops (internal to the laser) within the Shuttle-borne sources system. Such additions should be avoided in any case because of their complexity and the burden put on the data collection and control systems.

The causes and types of alignment problems that have been encountered may be classified as follows:

1. Maintaining alignment during storage. The slow creepage or relaxation of structural materials (castings and so forth) simply due to the passage of time or caused by hysteresis in temperature, shock or vibration cycles can cause the laser to become misaligned.

2. Maintaining alignment during operation in a changing external environment. The spacecraft environment is quite benign during operation of the Lidar system. However, tolerance of the alignment and beam quality to a certain temperature range is very desirable.

3. Maintaining alignment during operation and a changing internal environment. To clarify, this includes preventing misalignment caused, for example, by the distortion of optical elements during operation due to uneven heating or cooling. This is especially a problem in the lasing medium itself. It also includes misalignment caused by distortions in the structure due to thermal gradients introduced during operation.

The solutions to these problems are twofold. The first solution is the selection of laser designs that are relatively alignment insensitive. As an example, lasers with narrow beam divergence are generally more alignment sensitive. Curvature of the mirrors - how "stable" the resonator is - has an effect. The use of a retroreflecting porro prism instead of a mirror as an end reflector is a very common design feature. This gives alignment insensitivity in one plane. The use of a folded resonator, with the two end mirrors placed mechanically close together (and thus, easier to keep aligned with each other), and the beam folding done using a section of a corner cube

have both proven to be effective solutions. The second solution, is to build very stable structures. A large amount of structural stability with the careful design and selection of materials has always been found necessary, and difficult in the presence of weight and size constraints, and becoming progressively more difficult for larger systems.

Correct design philosophy must be extended to problems such as thermal distortions in the solid state lasing medium. These also require careful mechanical/thermal design, with uniform heat removal, so that wedging and consequent resonator misalignment do not occur. This is discussed in more detail below.

Operation Over a Range of Pulse Repetition Frequencies. If the laser is required to operate over a range of pulse repetition frequencies, the above problems are aggravated. Thermal effects, in particular, must be given careful consideration in the laser design. As mentioned above, the operation of the laser results in a certain amount of heat being deposited in the lasing material; this heat is removed from the interior by conduction to the edges of the material. As a result of this heat flow, a temperature gradient causes corresponding variations in the refractive index of the material. In laser rods, for example, the heat flow causes the rod to become a lens and, if heating or cooling is nonuniform, it becomes a wedge. The stability of this lens depends on the amount of heat being deposited in the rod, and is directly related to the repetition frequency at which the laser is being operated. This lens affects the divergence of the laser and must be compensated precisely at the design repetition frequency using a negative lens or defocused one power telescope. If the laser is to be operated at several repetition frequencies, or if best performance is demanded within a few seconds after turn-on during the transient period, before the temperature gradients have stabilized, some compromise in the laser specifications must be made, or an elaborate dynamic compensator must be developed.

Contamination. Contamination of optical surfaces is a classic problem occurring in the engineering of optical systems, and in many cases elaborate precautions have had to be taken in the cleaning and handling of the optical components used for these systems. With some optical systems the problem may hardly be noticed; there is merely a speck on a lens or a haze on a window. However, with lasers, because of the high intensities of radiation involved, the problem can be very critical, to the point that the device will no longer operate and, indeed, destroy its optics. Inside the laser resonator, the laser flux interacts with the contaminants, causing spots of optics damage that enlarge until laser oscillation ceases. Outside the resonator, spots of damage will continue to enlarge and spread as long as the laser remains on.

In laboratory systems, the optics may be continually monitored for cleanliness and protected from contamination. A free circulation of clean air usually exists, and the temperature is relatively constant, so that there is little likelihood of condensation occurring. In a flyable system, on the other hand, the optics must be enclosed in a sealed box, and any volatile materials that are also in the same compartment are almost certain to eventually creep or condense onto the optics. Any loose particles that are in the chamber, also, may be shaken or fall onto the optics.

In practice, it has been found that the most difficult problems occur for optics inside the laser resonator. This is the case for several reasons. First, it is common practice to expand the beam immediately after it leaves the resonator. This results in lower flux levels on the optics and, therefore, less likelihood of damage. In theory, the beam may be made arbitrarily large. Thus, the system can be designed to avoid damage at a given irreducible level of potential contamination of, for example, the exit window. Second, the highest flux levels are typically found inside the laser resonator, and are necessary for efficient operation. Sensitive components, such as Q-switches and polarizers,must be placed inside.

The problem has been solved for production military systems by placing the resonator optics in a hermetically sealed compartment that has been carefully cleaned of all potential contaminants. Only specially qualified and prepared materials are used inside the chamber and in sealing it. The intensity levels are designed to be well within the tolerance of the optical components. Tests have demonstrated that such units survive millions of laser shots operating at elevated temperatures after being stored at even higher temperatures.

6.4.2 LASER MODE QUALITY

The issue of laser mode quality has been given much discussion and is affected by many factors. To clarify this issue, and also present an example of how engineering issues can drive a design, a detailed discussion of this issue is given here. A single mode laser is more complex and difficult to engineer, and more costly than a multimode design. It must be strongly emphasized that there are not only two distinct choices, single or multimode. Multimode designs vary widely in output beam quality, as single mode performance is approached, more and more design engineering precautions are required, until the laser approaches the complexity of, and in fact becomes, a single mode laser. Therefore, unless there is an overwhelming performance requirement demanding use of the single mode laser, it is more reliable, economical, somewhat more efficient, smaller, and less power consuming, to design to some level of multimode performance. Alternatively, a single mode design may be made the goal, as is usual in commercial or laboratory systems.

Several system considerations and performance requirements drive the decision:

1. Beam Divergence. Every laser beam has an intrinsic beam divergence. Single mode beams have the smallest divergence that the laws of physics allow for beams of their spot diameter, i.e., diffraction limited divergence.

$$\beta \cong 2.4\lambda/D$$

where

β = beam divergence

λ = wavelength

D = characteristic beam or optics diameters

They represent the ultimate in laser performance; calculations involving lasers usually assume single mode behavior because it is well characterized by the theory of Gaussian beams. Multimode beams have larger divergence and are more complicated to analyze theoretically. The divergence of multimode beams is usually expressed as multiples of the diffraction limited performance. To decrease its divergence, any beam may be expanded and recollimated to a larger diameter; there is a simple rule that states that the product of the beam divergence and the beam diameter is a constant. Theoretically, therefore, any desired beam divergence may be obtained with a sufficiently large beam expanding telescope. Multimode beams will require proportionately larger optics. The difficulty and expense of the larger telescope must be traded against the difference in expense and difficulty of producing lower beam divergence lasers.

The most stringent 530 nm laser divergence requirement discussed in the SEED requires only a moderate beam expansion. The telescope would be less than 20 cm in diameter even with a relatively poor divergence multimode

beam. However, if co-alignment and signal to noise requirements for the system drive the laser beam divergence requirement downward, the output telescope size becomes unwieldy unless some care is taken in designing the laser for low beam divergence. Totally single mode performance would probably not be required except to ease telescope dimension problems; however, care must be taken to ensure that the correspondingly narrower beam divergence does not impact eye safety constraints.

2. Hot Spots. A single-mode beam characteristically has a smooth Gaussian (or, in the case of unstable resonators, a top hat) spatial intensity profile. As they become more multimode, lasers have a progressively more complicated intensity profile, with the possibility of a larger peak to average intensity ratio than for the single-mode beams. This is important in the calculation of eye-safety criteria. It is also important, although not always a limiting factor in the laser optics design, where a low ratio of peak to average intensity level allows higher average flux at components without damage caused by localized high peak flux. This may, for example, allow better amplifier utilization in a single mode oscillator-amplifier if it contains elements with marginal damage tolerance. Unless the beam quality of the multimode laser is quite poor, however, this is not an overriding consideration.

3. Doubler and Mixer Considerations. In addition to the damage considerations related to hot spots, which also apply in the case of devices using nonlinear crystals, there is another aspect of the laser brightness issue that affects the efficiency of the nonlinear processes used to produce 530 and 355 nm radiation from the 1060 nm neodymium laser output. The efficiency of the nonlinear processes is directly proportional to the

brightness of the pulsed fundamental beams (1064 nm in the case of the first doubler, 1064 and 532 nm in the case of the tripler, and the dye laser output wavelength in the case of the doubler used to produce UV from visible). A single mode beam is brighter than a multimode beam of the same size. This would lead to a conclusion that more efficient doubling could be achieved with single mode lasers. Since the doubling efficiency tends to saturate at a certain brightness level, however, any sufficiently bright laser can produce the maximum efficiency available from the nonlinear material. That is to say, in practice, the efficiency of the nonlinear process is limited by the quality and tolerance of the lasers. The brightness needed is a strong function of the particular nonlinear material used. An order of magnitude less brightness is adequate if a material can be found for which the nonlinear process is "90 degree phase matched".

4. Spectral Purity. Single mode lasers have better spectral purity than multimode lasers. The output has a narrower linewidth. None of the SEED experiments which require the 530 nm laser source need to have a narrow enough linewidth to force it to single mode; however, the velocity measuring experiments at 1060 nm require such a narrow linewidth that a special laser must be used. The dye laser is relatively indifferent to the spectral quality of the laser used to optically pump it. The only case where a narrow linewidth would be required of the neodymium laser is its possible use in a mixing process with the dye laser output. If it were desirable in the future to do mixing of the dye laser output with the doubled, tripled or quadrupled neodymium laser output, or to use, instead of the dye laser, optical parametric oscillator or amplifier techniques (a general category of nonlinear processes of which frequency doubling, tripling and mixing are examples; see Section 6.2.3) to obtain a narrow

linewidth output, tunable through the visible and infrared, a narrow linewidth source would be necessary.

5. Dye Laser Considerations. The characteristics of the outputs of single-mode and multi (transverse) mode frequency-doubled Nd:YAG lasers differ only in beam divergence and spatial uniformity. Beam divergence (β) of a single-mode laser is "diffraction-limited"; equaling a small multiple of λ/D where D is the diameter of the beam and λ the wavelength; a typical multi-mode frequency-doubled Nd:YAG laser has $\beta = 10\ \lambda/D$. Note for reference here that if a beam is focussed by a lens and its minimum spot size occurs at a distance f from the lens, then the spot diameter at that point is $f\beta$. This equation is often used to define the measurement of β. For transverse pumping of dye laser oscillators or amplifiers (see Figure 6-5a), the pump radiation must be focussed to a line in the dye cell. With the high peak power available from a frequency-doubled, Q-switched Nd:YAG laser, it is not necessary to focus very tightly to achieve the desired intensity. However, very often a tightly focussed pump beam is required to match it to the diameter of the dye laser beam in the dye cell, and thus use the pump light efficiently. This can be accomplished with either single- or multi-mode lasers and appropriate optics. For example, if a dye laser requires focussing of a 1 mm diameter single mode laser beam to a 0.3 mm thick line, and a 30 cm focal length lens is used, a line focus with the same thickness may be obtained even with a $30\lambda/D$ multi-mode laser, with a beam diameter of 10 mm and a 10 cm focal length lens. Thus, the optical system used for multi-mode pumping will be generally different (but not more complex) than that used in a dye laser designed for single mode pumping. The dye pumping optics should be tailored to accommodate the specific pump source used.

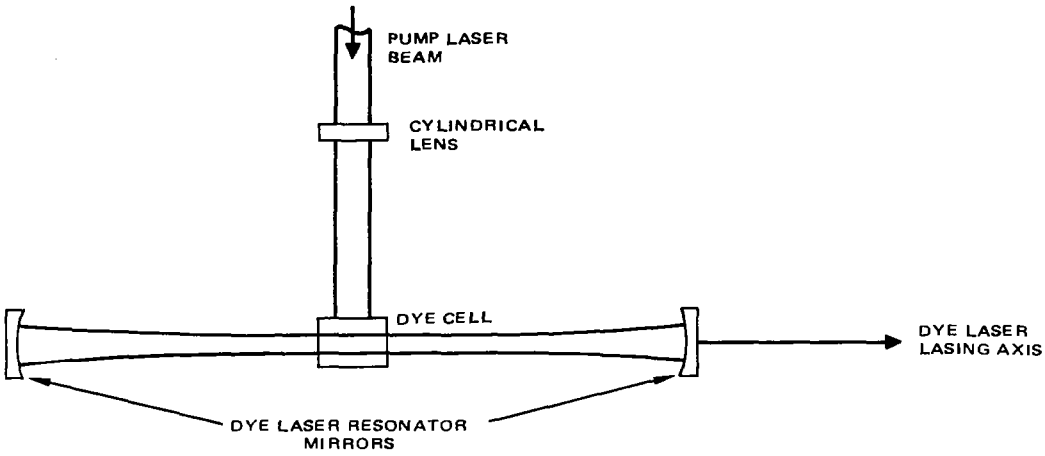

Figure 6-5a. Transverse pumping of dye laser.

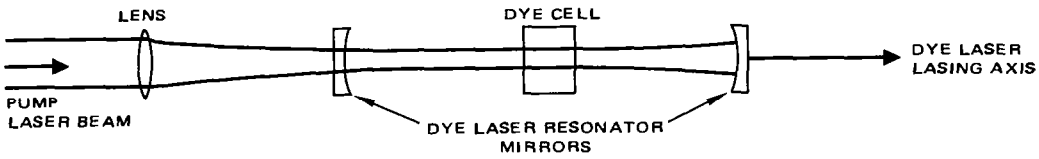

Figure 6-5b. Longitudinal Pumping of Dye Laser.

A method to achieve efficient coupling of pump light into a transversely pumped dye cell is incorporated in some commercial dye laser system designs. This technique uses a capillary tube for the dye cell so that the volume of excited dye is circular in cross-section and matches that of the dye laser beam in the cell. The increased efficiency applies to both single- and multi-mode pumping. In addition, use of a diffusely illuminated cell ensures uniform dye excitation and, in multi-mode pumping, eliminates any possible difficulties due to poor beam uniformity.

In the case of longitudinal pumping (Figure 6-5b), the spatial profile of the pump laser is more important, and the use of a single mode pump may

indeed result in better mode quality for the dye laser, depending on the care which is taken in focussing the beam into the dye cell.

6.4.3 EXISTING NEODYMIUM LASERS

All of the above issues, as well as the performance specifications, must be taken into account in the selection of the laser design and construction. A comparison matrix showing trades between several representative designs of existing operating lasers was constructed (Figure 6-6), in order to assist in selection of a preliminary Strawman design for an engineered system. Although not intended to be a comprehensive survey, the data in Figure 6-6 provides several examples of laser designs for existing systems, with performance in the range desired, that were selected from the literature, commercial brochures, and our data. In particular, the efficiency figures are those quoted, and have various degrees of credibility. Some design features can be interchanged; for example, presurized gas cooling or features of the power supply, can be incorporated into any of the other designs; whatever is shown in the matrix happens to be what was used by each worker. Not all possibilities have been shown; (only those that have actually operated) for example, the last design can be done with the oscillator in a polarization output coupled design - a different version of the second design - instead of the conventional resonator shown. The lower energy output designs would require more amplifiers. Any of the designs can use porro prisms, where feasible, instead of flat mirrors. As discussed previously, this would improve alignment tolerance. In sum, the designs are representative; some refinement can be suggested for any of them, although it may not be required for the present application.

The variety of designs possible emphasizes an important point. Careful distinction must be made between using a particular optical design to achieve the performance

	REPRESENTATIVE OPTICAL SCHEMATIC SYMBOLS) OR - MIRROR (M) P - POLARIZER λ - WAVEPLATE Q - Q-SWITCH R - ROD T - BEAM EXPANDER TELESCOPE I - ISOLATON E - ETALON	EFFICIENCY (WALL PLUG)	COMPLEXITY				APPROXIMATE SIZE AND WEIGHT (INCLUDING PFN AND POWER SUPPLY)	COOLING SYSTEM	RELATIVE ALIGNMENT SENSITIVITY	BEAM QUALITY	DEVELOPMENTAL STATUS OF SYSTEM SHOWN
			NO. OF RODS	NO. OF OTHER OPTICS	NO. OF LAMPS	NO. OF PFNS AND POWER SUPPS					
STRAIGHT FORWARD SINGLE MODE Nd YAG LASER, OSCILLATOR AMPLIFIER	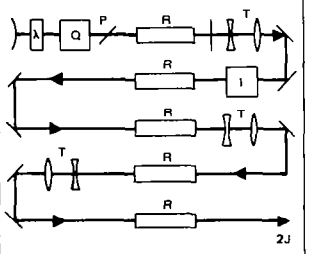	~ 1.8%	5	20	5	3.5	90 kg	LIQUID LOOPS	HIGH	CLOSE TO DIFFRACTION LIMITED	HAS BEEN BREADBOARDED FROM FIELDABLE PARTS
MORE SOPHISTICATED LOW ORDER/ MODE Nd:YAG LASER OSCILLATOR AMPLIFIER	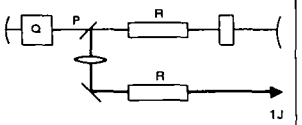	~ 1%	2	7	2	2	LASER HEAD PLUS EQUIPMENT RACK POWER SUPPLIES	LIQUID LOOPS	MODERATELY HIGH	CLOSE TO DIFF LIM	CAN BE CONFIGURED FROM COMMERCIAL MODULES
Nd:GLASS SLAB	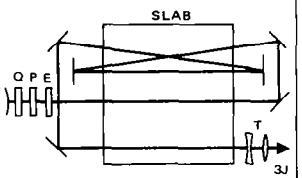	~ 0.5%	1	15	1.2	1.2	100 kg	LIQUID LOOPS	MODERATE	~5X DIFF LIM	BREADBOARD OF DESIGN INTENDED FOR FIELD USE
UNSTABLE RESONATOR	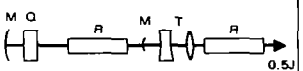	0.5%	2	5	2	2	LABORATORY OPTICAL TABLE PLUS EQUIPMENT RACK POWER SUPPLIES	LIQUID LOOPS	MODERATE (AFFECTS BORESIGHT)	CLOSE TO DIFF LIM (ANNULAR BEAM)	CAPABLE OF LABORATORY CONSTRUCTION
HIGH BRIGHTNESS MULTIMODE	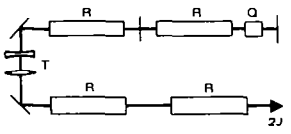	~ 1.3%	4	8	2	1	36 kg	PRESSURIZED GAS LOOPS	LOW MODERATE	~8X DIFF LIM	HAS BEEN BREADBOARDED FROM FLIGHT QUALIFIED MODULES

Figure 6-6. Neodymium Laser: Representative Existing Design Examples.

specifications, and selcting a design to solve engineering difficulties of the type discussed in Section 6.4.1. In the laboratory, through the use of the great variety of very convenient optical breadboarding systems, that have evolved over the years to serve the scientific community, great freedom in optical design and layout is possible. Hardened versions of such systems have been fielded in the pseudolaboratory environment of vans or airplanes where they are almost continuously accessible to adjustment and trouble shooting; thereby, avoiding many of the previously mentioned engineering difficulties. However, a different design philosophy in overall layout, components and their mountings, classes of allowed materials, the use of adjustable mechanical gimbals, the allowed level of contaminants such as oils and greases, environmental control and many other factors, as enumerated earlier, has evolved in the engineering phases of flyable and fieldable systems for military applications. These systems are required to operate "hands-off" under severe storage and field conditions. Similar conditions and "hands-off" requirements relative to Space Shuttle environments and missions, respectively, do not allow the engineering problems to be avoided, and the laser design must be selected with this in mind.

From the above discussion it is apparent that, any one design which has been evaluated and selected as to its superiority over the many other possible basic laser designs meeting the scientific performance requirements, must also be evaluated on the basis of amenability to resolving the engineering issues. Designs that require precise alignment of a large number of widely spaced components, or that have a large number of damage sensitive optical components, or that require extensive engineering to remove sources of contamination, or that require complex cooling engineering are not desirable. For this reason, the complexity and development status columns in Figure 6-6 were included.

6.4.4 TWO JOULE NEODYMIUM LASER - DETAILED DESCRIPTION

Of the several existing designs shown in Figure 6-6, the bottom concept was selected for a detailed description. Figure 6-7 is a photograph of a breadboard setup of this design with a multi-mode oscillator. The flashlamp pulse forming network is in the rear, the two large objects in the foreground are militarized self contained internally pressurized gas cooled laser heads, each containing two rods and one lamp. Integral to them are pressurized gas-to-ambient-air heat exchangers. Other resonator optics are mounted on the bench. To the right is the energy measurement instrumentation and a tubular beam dump.

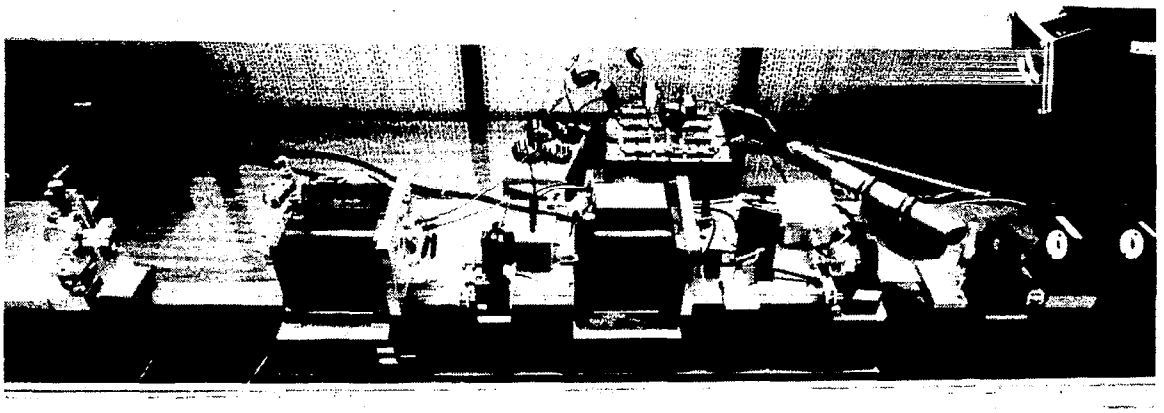

Figure 6-7. Two Joule Breadboard Laser.

An existing Hughes 2 Joule laser was modified to bring its performance from 1.6 percent efficiency at 5 Hz to 1.9 percent efficiency at 10 Hz. It uses two identical pressurized gas (21 Kg/cm^2) pumping/cooling High Power Illuminator program modules, each adapted to hold one 7.6 cm long 0.8 cm diameter rod, and one 7.6 cm long 0.95 cm diameter rod, pumped by a zenon flashlamp located in the space between them. This configuration uses an asymmetrical Sm^{3+} glass insert in conjunction with a diffusely reflecting pump cavity coated with $BaSO_4$, a highly reflecting material.

The oscillator/amplifier layout is shown in Figure 6-8. The oscillator is a conventional Q-switched resonator, using a KD*P pockels cell and a thin-film polarizer. The output of this stage (≃ 400 mj) is passed through the first amplifier (≃ 800 mj output) then folded back and enlarged by a beam expander before being amplified by the two 3 x 3/8 inch rods. Output energy is calibrated and

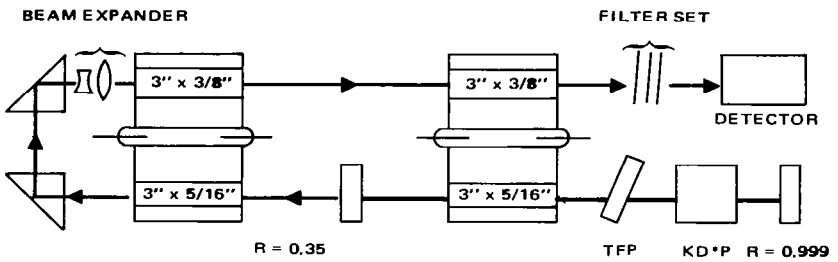

Figure 6-8. 2J Nd:YAG Oscillator/Amplifier Layout.

measured by use of a bi-planar vacuum diode placed behind calibrated neutral density filters. At 10 Hz, a multi-element stack of glass plates was calibrated and placed in front of the filter set to prevent damage to the filter coatings during the enegy measurement/calibration. Absorption by the SM^{3+} glass insert reduces the effect of parasitic modes and superfluorescence losses, so that saturation conditions are determined mainly by the longitudinal photon flux. In the present case, however, the system operates slightly below the longitudinal saturation level of the rods, and no interstage buffers are needed to obtain the maximum output and the desired high efficiency. Originally the insert was designed to divide the lamp energy between the 5/16 and 3/8 inch rods approximately in the ratio of 0.33/0.67. However, to improve the overall efficiency, some of the reflector paint was removed to increase the laser output of the 5/16 inch stages and improve extraction from the 3/8-inch rods. The efficiency increased as intended, and the pumping ratio for the two rods changed to 0.46/0.54. A series of operational tests was made after laser upgrading, and an extra

fan was added to the power supply to avoid transformer overheating during continuous 10 pps operation over long periods. The performance characteristics of the Hughes 2 J 1060 nm laser are given in Table 6-4.

Table 6-4. 2J Nd:YAG Laser Characteristics

COOLING	PRESSURIZED NITROGEN,
OUTPUT ENERGY	2 J
PULSEWIDTH	20 ns
PULSE REPETITION FREQUENCY	10 PPS
PFN INPUT POWER	1080 W (10 PPS)
EFFICIENCY	1.9 PERCENT
BEAM DIVERGENCE X DIAMETER PRODUCT	~ 30 MRAD-MM

Although the emphasis of the laboratory 2 joule laser was not placed on field adaptability, the optical system, power supply and PFN could be made into fieldable modules of minimal size and weight to produce what may be the smallest laser of this type to date. The overall unit, in principle, could be fitted into a volume of 40 liters, with a total weight of 31.5 kg.

Figure 6-9 is a photograph of the 2 kW power supply used for this laser. It uses Hughes patented switching circuitry to achieve high power, extremely efficient operation in a compact design and operated on a 400 Hz AC input. Figure 6-10 depicts a 1 kW power supply using a decade older technology that operates on 28 VDC.

Figure 6-9. Two Kilowatt Power Supply.

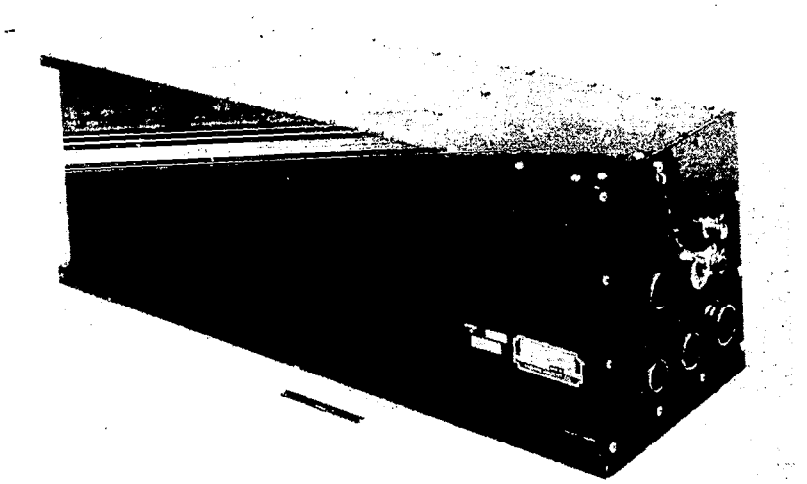

Figure 6-10. One Kilowatt Power Supply.

6.5 NEODYMIUM LASER SUBSYSTEM, MODULE 2: TWENTY WATT DOUBLER

There are many issues that affect the design of the neodymium laser subsystem frequency doubler; the specific design that is selected is driven by several performance and engineering requirements. The assumed requirement of high energy per pulse, as we have seen, drives the design to one in which an oscillator-amplifier chain neodymium laser must be used. The pulses from this laser must then be frequency doubled in a nonlinear crystal to obtain the required 530 nm output. Although higher doubling efficiencies have been achieved in the laboratory, efficiencies of less than, very optimistically, 50 percent are all that can be expected at the present time for practical devices. Since the 1060 nm radiation is not used for any of the Lidar experiments, maximum conversion to 530 nm is very desirable. There are several methods of increasing the conversion efficiency; two are discussed below as trades. The preferred design will then be described.

6.5.1 ENGINEERING ISSUES

Power Limits. A critical issue in the frequency doubling system is its power handling capability. All crystals absorb some of the light passing through them. When the transmitted flux is high, localized heating of the crystal in the region of the beam will occur to the point where different regions of the crystal will be at sufficiently different temperatures to destroy the phase matched condition. Historically this has limited the average power obtainable from devices using frequency doubling to less than 10 or 20 watts. This phenomenon has been quantified[1] and is represented by the equation

$$\bar{P} = \frac{8K\Delta T}{b} \cdot \frac{w}{h}$$

where

$\bar{P}$ = average power obtainable

K = crystal thermal conductivity

ΔT = temperature difference in the crystal between the center and the edge of the beam; this T must be kept small enough so that phase matching is not destroyed; the acceptable T is called the temperature tolerance of the particular crystal

b = absorption coefficient

w, h = width and height dimensions of the beam, respectively

The last term (w/h) has recently been exploited to achieve heretofore unobtainable average 530 nm powers. In the past, and in many existing systems, emphasis was directed toward reducing the absorption term. Thus, high quality, low absorption, large crystals of KD*P have been used, despite their disadvantages: that they may have lower nonlinear coefficients, and they require single mode or very high brightness beams because they must use angle-tuned phase matching and have a narrow acceptance angle (which gets narrower for longer crystals).

Phase Matching Considerations. For some experiments, the 1060 nm and 530 nm energy out of the doubler are mixed in a subsequent crystal to obtain 355 nm (frequency tripled) radiation. For any nonlinear process, in particular frequency tripling, maximum efficiency requires the incident radiation to have well defined polarization. If type-II phase matching is used for the doubling process, the radiation emerges from the crystal elliptically polarized. This, the beam walkoff, always occurs for an optical beam propagating through a birefringent crystal except for propogation directions and beam polarizations having special symmetry. (Beam walkoff is the propagation of the two orthogonal polarizations of a beam at slightly different angles in a birefringent medium; it occurs because the two polarizations see different indices of refraction). For type-I phase matching, the emerging 1060 nm and 530 nm beams are linearly polarized and colinear. This makes it relatively easy to arrange their polarizations to be correct for introduction into the tripling crystal. Typically, all that is required is a crystal quartz polarization rotator of the correct length. For elliptically polarized beams, somewhat more elaborate

polarization manipulating optics would be required. For this reason, type-I phase matching (90 degree phase matching is a special, more preferred case, since it also eliminates walkoff between the 530 and 1060 nm beams) is generally preferred in laboratory systems that are to be frequency tripled. Note that it is also more convenient to do subsequent doubling of the beams.

6.5.2 OPTIONAL TECHNIQUES TO IMPROVE CONVERSION EFFICIENCY

Intracavity Doubling. If the doubling crystal is placed inside the neodymium laser cavity, theoretically essentially 100 percent conversion efficiency may be obtained; that is, the laser will produce as much radiation, at 530 nm only, as at 1060 nm, had the usual partially reflecting mirror instead of the doubling crystal provided the output coupling for the laser.[2] By its nature, this technique is only applicable if the neodymium laser is entirely an oscillator - it will not work for the oscillator-amplifier configurations necessary for achieving pulse energies in excess of about half a joule (limited by available high quality Nd:YAG crystal size). However, the method would be quite tempting - and a factor of two more efficient than the extracavity method - if the laser were specified at less than approximately a quarter joule green output at around a hundred hertz repetition rate (to give equal average output power). Other system parameters, indeed, the whole issue of optimal repetition rate, would be affected. Smaller beam divergence for the laser and a narrower field of view for the receiver (greater resolution per shot, within coalignment considerations) could be used while still meeting the eye safety criteria, but the accuracy of data obtained per shot would be lower due to the lower per shot energy; this would be offset by the greater number of pulses. The laser resonator using the intracavity crystal can also be designed to produce any ratio of 530 nm to 1060 nm output. These direct to green output lasers have not undergone extensive commercial development in the past (except for a few relatively low power sources that are

marketed) because there has been little demand. It is, however, also worth emphasizing that the highest average 530 nm powers so far obtained in the laboratory (in excess of 35 watts) were obtained with an intracavity device. Most research users needing moderate peak powers want the flexibility of having both wavelengths available in addition to the option of adding amplifiers to the 1060 nm laser. It is therefore more convenient and straightforward to have the doubling unit as an add on. In addition, as previously mentioned, greater per shot energies are obtainable.

Two Successive Doubling Crystals. The above fact suggests another class of methods for obtaining higher net green conversion. If maximum conversion efficiency is desired in the nonlinear (doubling and tripling) processes a succession of two crystals may be used. For example, when using a non-linear crystal that allows 90 degree phase matching, the green produced in the crystal is linearly polarized in a plane perpendicular to that of the (linearly polarized) 1060 nm radiation. Therefore, after the crystal, the green may be easily split off using a polarizer. The remaining 1060 nm radiation may then be refocused into another doubling crystal to produce more green. It is detrimental to allow the green produced in the first crystal to pass through the second; since it will be out of phase with the other beams it interferes with further conversion in the second crystal. The green produced in the second crystal may again be separated from the 1060 nm light by the use of polarizer. There are now two polarized green beams. These may be recombined with only small loss in a polarizer to produce a single unpolarized beam. No more than two beams may be combined in this way, so that the use of more than two successive crystals will result in more than one output beam. Note that the use of two successive crystals produces an eliptically polarized output when the beams are recombined.

6.5.3 SELECTED DOUBLER DESIGN

The selected doubler design will utilize extracavity doubling in a 90 degree phase matched, temperature turned CD*A crystal, with some beam shaping to handle the moderately high average power. This device, shown in Figure 6-11, has already been built and tested with performance near the required specifications. For the doubling step, a practically achievable doubling efficiency of 35 percent is assumed. Although efficiencies of twice this have been achieved in the laboratory, reliable and consistent results at these high average powers without taking special precautions or risking damage to the doubling material have been demonstrated in fieldable devices only at these conservative conversion efficiencies.

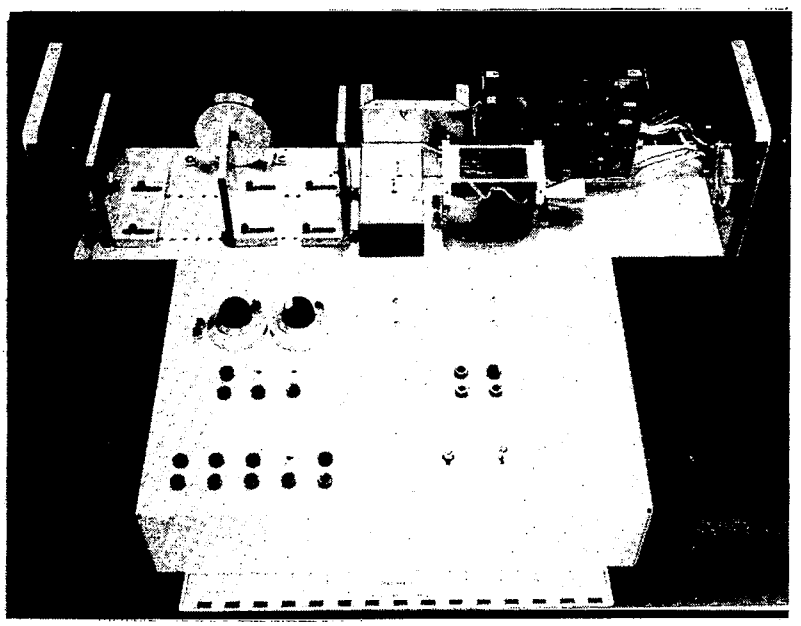

Figure 6-11. High Average Power Frequency Doubling Module.

6.6 NEODYMIUM LASER SUBSYSTEM, MODULE 3: TWENTY WATT MIXER

The most efficient available technique for generation of the third harmonic of Nd:YAG radiation at 354.7 nm is sum frequency generation. The efficiency of this process, requiring input at 1060 nm and 530 nm, is similar to that of frequency doubling. However, at present no known nonlinear crystals can generate 354.7 nm light with noncritical (90 degree) phase matching. The crystals that have been used in this application (KDP, KD*P, ADP, $LiIO_3$, RDA and RDP) are angle-tuned, and have small acceptance angles. This places upper limits on the allowable divergence of the beams focused in the crystal. Commercial systems generally obtain high mixing efficiency by pumping with inefficient single-mode Nd:YAG laser systems. As described in the following paragraph, comparable efficiency may be obtained with a high-brightness multi-mode Nd:YAG laser.

The most widely used crystal for generation of 354.7 nm output is KD*P with Type II phase-matching. The acceptance angle-crystal length product, as measured by Okada and Ieriri[3] is 2.7 mrad-cm. Typically, power densities of 50 to 100 MW/cm^2 are required to obtain 12 percent to 14 percent conversion efficiency from 1060 nm to 354.7 nm is a 3.5 cm long KD*P crystal.

The MUIS baseline two joule Nd:YAG system has the following characteristics after frequency doubling: 1.2J at 1060 nm (60 MW) and 0.7J at 530 nm (44 MW). For a conservative worst case calculation assume both beams have 3.5 mrad divergence and are 1 cm in diameter. The effective power density ($\sqrt{I_1 I_2}$) for mixing is 51 MW/cm^2 before focusing. Thus, even without focusing to achieve higher intensity, the laser beam divergence exceeds the acceptance angle of a 3 cm KD*P crystal (0.9 mrad). However, this problem may be circumvented by taking advantage of the fact that the small acceptance angle applies only to the θ direction; the divergence in the ϕ direction is not subject to this constraint. Therefore, it is helpful to expand the

beam in one direction (θ) and shrink it in the other (ϕ) to maintain the same intensity in an elliptical beam. Expanding to 3.9 cm reduces the divergence to < 0.9 mrad in the θ direction, and a beam thickness of 0.33 cm keeps the intensity near 50 MW/cm^2. This design permits efficient output at 354.7 nm from a multi-mode Nd:YAG laser. In mechanical configuration, this module is very similar to the twenty watt doubler module.

6.7 DYE LASER SUBSYSTEM, MODULE 4: DYE LASER

Figure 6-12 shows a generic dye laser block diagram to assist in conceptualization of the primary dye laser issues. These issues are:

1. Pointing stability or beam wander
2. Configuration, particularly for the DIAL sources
3. Spectral control problems and implementation
4. Relative performance with respect to pump laser mode quality
5. High average power, high pulse energy capability
6. Dye and optics changes to cover a wide wavelength range
7. Fluid handling problems in space

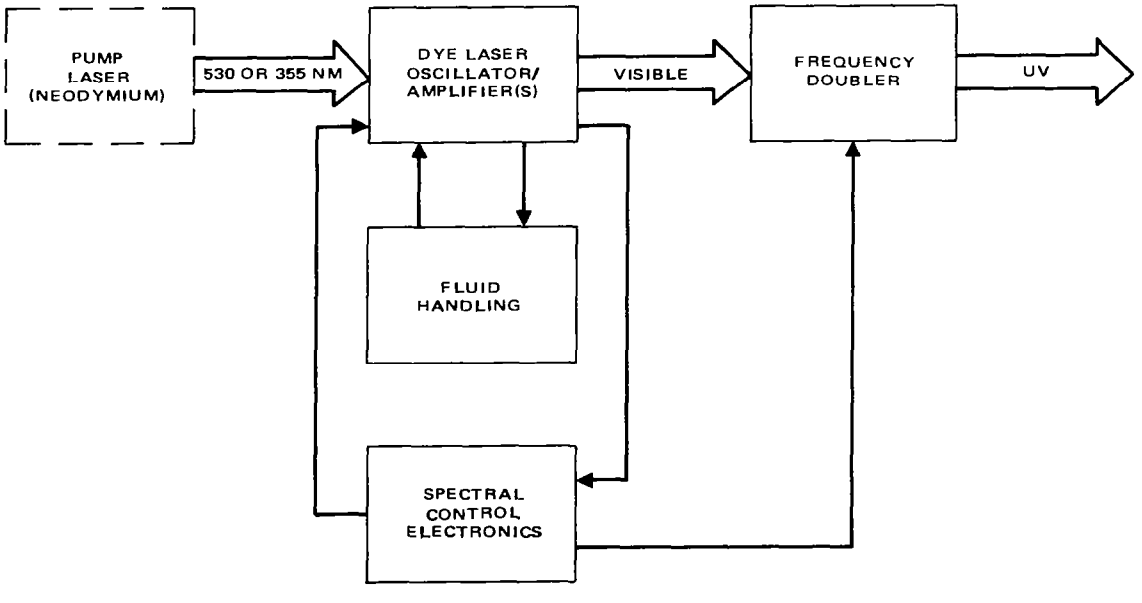

Figure 6-12. Generic Dye Laser Block Diagram.

Dye laser beam wander will be discussed first, because that discussion will introduce the reader to dye laser oscillator concepts. The two issues that most affect the design of the dye laser system are the requirement for DIAL sources and the degree of spectral control demanded. Accordingly these issues are discussed in more detail. The pump laser mode quality issue was already addressed in Section 6.4.2. Certain engineering and development issues are raised by requirements for high average power and high per pulse energy. Issue 6 is subordinate to the spectral control problem. Once the decision is made not to change wavelengths during a mission because of spectral control problems, Issue 6 simply means making dye and optics changes on the ground where it is relatively simple to perform thorough flushing, optics changes, and required readjustments. Issue 7 is one of sound engineering of the dye fluid system.

6.7.1 DYE LASER BEAM WANDER

Dye lasers are more prone to exhibit beam wander than other lasers because their resonator cavities generally include mechanical tuning elements. The drawing at the top of Figure 6-13 is an illustration of a commonly used dye laser cavity design. Tuning and line narrowing are provided by the grating, which may be rotated about an axis parallel to its grooves. Because the resolution obtainable with a grating is proportional to the number of illuminated grooves, a telescope is inserted in the cavity to expand the laser beam before it impinges on the grating. The telescope also decreases the divergence of the light striking the grating, which further serves to narrow the dye laser bandwidth.

As mentioned previously, the laser is tuned by rotating the grating about an axis parallel to its grooves. Any incidental rotation of the grating about the axis perpendicular to the grooves and laser beam (hereafter referred to as "tilt") is equivalent to a cavity misalignment, just as if a laser end mirror were rotated. This

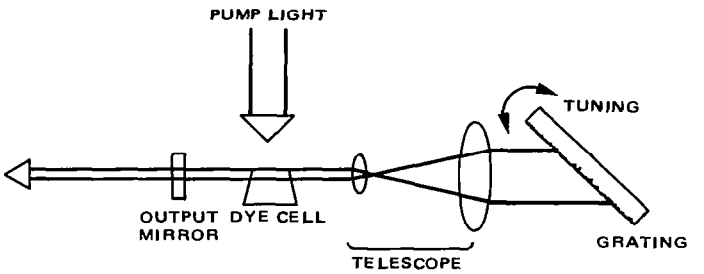

COMMONLY USED DYE LASER CONFIGURATION

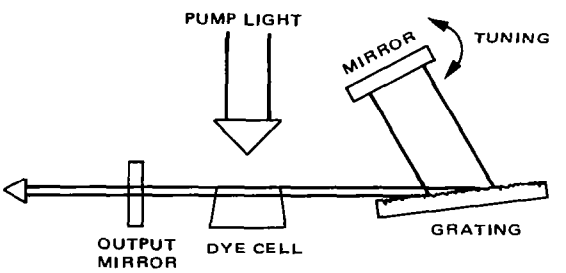

GRAZING INCIDENCE DYE LASER CONFIGURATION

Figure 6-13 Dye Laser Configuration.

unwanted rotation both decreases the laser output and causes beam steering. The telescope also aggravates the sensitivity to misalignment. For example, if the telescope magnification is 20, then a grating tilt of 1 μrad is equivalent to a misalignment of 20 μrad in an ordinary laser cavity.

Another factor contributing to dye laser beam wander is the dispersion of optical elements external to the dye laser cavity. If there are any prisms, wedged windows or wedged mirrors in the beam, the laser output will wander as the laser is tuned. For all the reasons enumerated above, many dye lasers have in the past exhibited beam steering problems.

Sensitivity of output beam direction to grating tilt can be greatly reduced by using one dimensional beam expansion instead of the usual (two-dimensional) telescope. This maintains high grating resolution while reducing both tilt sensitivity and the size of the required grating. It may be implemented with cylindrical lenses (rather than

spherical lenses) to expand the beam perpendicular to the grating grooves, or with a clever design described by Littman and Metcalf[4] and Shosham and Oppenheim.[5]. This design, shown at the bottom of Figure 6-13, uses a grating at grazing incidence to provide beam expansion as well as spectral selectivity. The cavity has fewer optical elements and thus can have low losses and compact construction. The shorter cavity allows more efficient operation with short pump pulses, such as the harmonics of an Nd:YAG laser.

A possible method to further reduce beam wander is to replace the tuning mirror with a porro prism. The prism apex must be accurately cut and polished, and carefully aligned perpendicular to the grating grooves because in this application the apex is the only part of the prism in use. Tuning is accomplished by rotation of the porro prism just as before; accidental rotation about an axis parallel to the apex has no effect. However, gross misalignment causing prism rotation about the incident laser beam axis would result in poor laser efficiency.

Expansion of the dye laser beam by the Lidar output optics assembly will further reduce beam steering by an amount roughly equal to the magnification. This is true even if the telescope output is not perfectly collimated as may be required for reasons of eye safety.

6.7.2 SOURCES FOR DIAL EXPERIMENTS

For differential absorption Lidar, output at two wavelengths is required. All DIAL experiments need one output accurately tuned to an absorption line and the other output at a nearby wavelength that is not abosrbed. Wavelength separations must be between 0.1 and 1.0 nm for some experiments (15 and 17) and may be larger for others. For the latter experiments (e.g., No. 9) one dye laser wavelength and perhaps the fundamental or a harmonic of Nd:YAG may be sufficient, as suggested by the SEED.

Several alternative techniques were considered for generating the two wavelengths. The most straightforward approach is to use two dye lasers independently tuned to the desired wavelengths. For typical DIAL experiments only one of the lasers must be narrowband and well stabilized.

The second alternative relies on the existence of a Raman medium which will shift a harmonic of YAG to a wavelength near that of the desired absorption line. This stimulated Raman oscillator, simpler and more rugged than a dye system, would replace the second dye laser, representing a moderate simplification, perhaps at the expense of DIAL measurement accuracy if the Raman-shifted wavelength is not optimal. In addition some development work, now underway, is required for operation of the Raman oscillator at 10 or 30 pulses per second.

The straightforward approach that was slected involves the use of two entirely independent dye laser systems. This eliminates the requirement for rapid switching between wavelengths, but adds an entire dye laser, frequency control system, and pump laser. It does mean, however, that only one type of relatively simple dye laser need be designed; the second laser could be obtained at only the recurring cost and with no additional development effort. The use of two separate laser systems also allows, within electronic limitations, the arbitrarily close simultaneity important in some types of DIAL measurements (those that have small resolution elements).

6.7.3 SPECTRAL CONTROL

To maintain the narrowband dye laser output on a particular spectral line, a system capable of precise wavelength tuning is required. Clearly the laser spectral stability must be at least as good as the desired laser bandwidth. The extremely broad tuning range of a dye laser, the strict tolerances on laser bandwidth imposed by the spectral feature under study, and the strong dependence of the dye laser

output wavelength on temperature, pressure and mechanical misalignment combine to make spectral control a very difficult problem.

Regardless of the mechanical stability of the dye laser, the only way to ensure that the output is at the desired wavelength during the mission is by comparison with a reliable, on board wavelength standard. Standards provided by molecular transitions are very insensitive to environmental conditions, as compared with a laser cavity or an independent Fabry-Perot cavity. There are two ways in which a molecular resonance may be used as a laser frequency reference. The simplest way is to provide an absorption cell and a servo system that "locks" the laser frequency at an absorption peak. The second method is to compare the dye laser, frequency with that of a narrow band fixed-frequency laser the output of which is determined by a molecular transition.

For locking the dye laser to resonance lines of certain species, such as sodium, an absorption cell is the easiest type of frequency reference. This approach is schematically indicated in the right-hand diagram of Figure 6-14. As illustrated in the figure, imposing a small wavelength dither on the laser output allows the generation of a correction signal to bring the laser wavelength back to the resonance line if it begins to drift. Laser wavelength adjustment is accomplished by changing the pressure in the laser cavity or by piezoelectric tuning of the etalon(s). In this example, pressure changes are used to tune the laser, while the piezoelectric device on the etalon is used for the rapid shot to shot dither. A disadvantage of this technique is that a different absorption cell would be required for each species; in many cases, a high temperature oven or an ion source would be needed. The weak absorbers, such as the O_2 and H_2O lines, need a very long optical path length cell; this is impractical on the Shuttle, even if a multi-pass White cell arrangement 6 is used. In addition, unless the cell pressures and temperatures are similar to those in

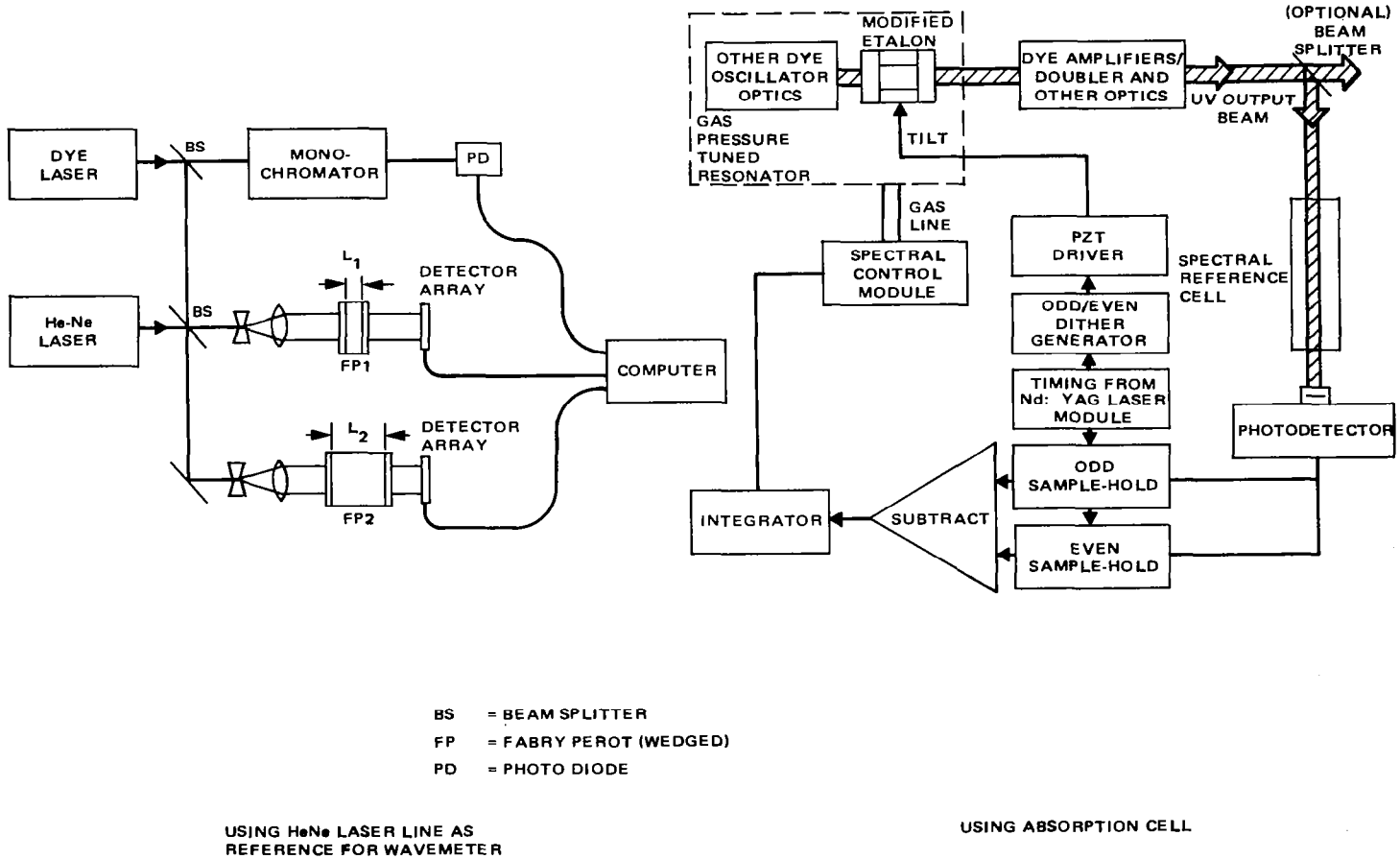

Figure 6-14. Examples of Spectral Control Loops.

the atmospheric layer under study, errors may be caused by broadening and shifting of the spectral reference lines in the cell.

Using a non-tunable laser whose wavelength is accurately known, it is possible to measure the dye laser wavelength and maintain it on a desired spectral feature. When both lasers are cw (cw dye and He-Ne lasers, for example), the wavelength measurement can be done relatively easily with a simple scanning Michelson interferometer and a fringe counter. Hall and Lee[7] describe a more sophisticated device capable of 0.06 pm resolution with a measurement time of 0.25 second. However, a system useful with the short pulse dye lasers of the present system must complete the measurement in about 10 ns. This may be accomplished with Fabry-Perot etalons and array detectors, and again, a stable cw He-Ne laser. A possible spectral control system is shown in the left of Figure 6-14. Assuming a reasonable Fabry-Perot finesse of 100, and a monochromator or thin film filter that has a 0.5 nm bandpass, two Fabry-Perot interferometers are needed to obtain 0.05 pm accuracy. Their lengths would be 0.3 mm and 30 mm. To set up the desired fringe pattern on the detector array, either the Fabry-Perot is wedged slightly or the incident light beams are made slightly diverging. For most efficient use of the detector array, there should be exactly two fringes from each beam on the array. If the divergences of the He-Ne and dye laser beams are nearly identical, the distance between the two sets of fringes, compared to the separation between each pair, indicates the wavelength relationship.

The fringe shift dependence on the deviation from normal incidence is quadratic for small angles. Thus, if a plane-parallel Fabry-Perot is used with diverging beams, the transformation from wavelength separation to fringe separation is nonlinear. Furthermore, the accuracy is strongly dependent on the degree to which the two beams have identical divergence.

For these reasons, it is desirable to use well collimated beams and a wedged Fabry-Perot. This scheme avoids both the nonlinearity and the sensitivity to divergence. It is also unaffected by small changes in etalon plate separation and wedge angle.

For real-time spectral control of the dye laser, a computer would process the information from the detector array, compare the measured wavelength with the desired preprogrammed wavelength, and generate an error signal proportional to the difference. The correction is then applied to the laser cavity pressure control system. If the required correction is outside the pressure control range, the grating is mechanically rotated. Examples of spectral control loops for the lasers are shown in Figure 6-14.

6.7.4 HIGH ENERGY/POWER DYE LASER PROBLEMS

A major problem encountered with dye oscillator/amplifiers lies in parasitic losses and loss of spectral fidelity (due to amplified spontaneous emission or spurious oscillation along the beam line) when using high gain, closely spaced, unsaturated amplifiers. The appropriate solutions to such problems, including optical delay between gain media, polarization rotation isolators, spatial filters, and operation in a heavily saturated, low gain (10 - 25X) medium, are well known and have been proven effective in repeated cases reported in the technical literature. [8-12].

6.7.5 DYE LASER HOST ALTERNATIVES

The dye solution reservoir and flow system comprise a major part of the volume, weight, and complexity of a dye laser. Special precautions will have to be taken to qualify the dye system for the space environment. In addition, a mechanism for changing dye solutions during flight is likely to be complicated, aggravated by the fact (even on the ground) that the flow system will have to be thoroughly flushed before new dye is added.

Hughes' experience in developing a solid host dye laser may be directly applicable to the Shuttle Lidar lasers. This would replace the liquid flow system and dye cell with a rotating solid plastic disc impregnated with dye. Many dyes have been incorporated in such discs and successfully tested by pumping at power levels required for this program. Problems which remain to be considered include dye laser amplitude and frequency stability. Good lifetime has been demonstrated.

6.7.6 ALTERNATIVES TO IR DYES

Dyes that lase in the near infrared from 700 nm to 950 nm are generally inefficient and short-lived. Stable dyes like the rhodamines may be used with stimulated Raman scattering (SRS) to reach the same wavelengths. While the overall efficiency would probably not be improved and the system would be more complex, the dye lifetime problem would be greatly alleviated. The stable, efficient dyes, Rhodamine 6G, 110, and B can be used with SRS in CH_4 and H_2 to cover the range from 650 nm to 850 nm. Oxazine 720 with SRS in H_2 can access the 940 nm region required in Experiment 9; dyes which operate at this wavelength are very inefficient and need further development.

Before a final decision between IR dyes and SRS can be made, work must be done to determine the linewidth of the Raman-shifted radiation and its dependence on dye laser linewidth and Raman oscillator design.

6.7.7 EXISTING DYE LASERS

<u>Commercial Systems</u> Pulsed dye laser technology is quite well developed, as evidenced by the large number of commercially available systems. With the appropriate pump wavelength and dye solution, any visible wavelength can be generated.

As an example of this technology status, Figure 6-15 was compiled to illustrate the peak powers available from commercial systems. The manufacturer specified peak powers

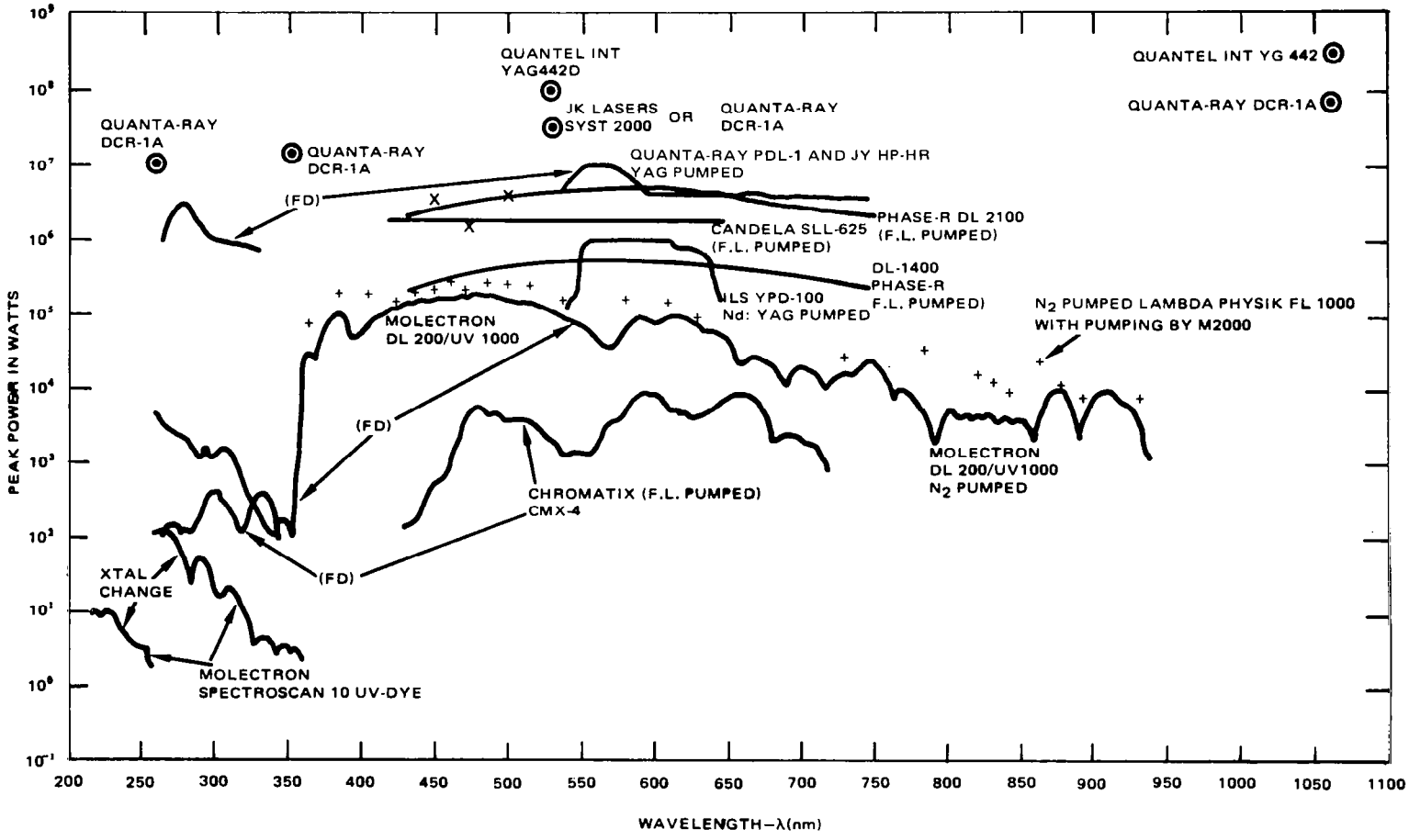

Figure 6-15. Typical Commercial Systems Capabilities.

attainable at wavelengths between 200 and 1100 nm are plotted for systems pumped by flashlamps (F.L.), nitrogen (N_2) lasers, and frequency doubled neodymium YAG lasers (frequency doubled Nd:YAG), as annotated on the figure. Peak power is a good comparison criterion because it also shows the relative efficiencies obtainable in producing the wavelengths. Each hump in the curves for the laser pumped dye lasers represents the optimal spectral region for a specific dye. Distinct falloffs in available power can be seen at wavelengths just shorter than those for the pumps (these are unobtainable by those pumps) - for example at around 350 nm for both tripled neodymium and nitrogen pumped lasers, and at 530 nm for doubled neodymium. Most of the wavelengths in the UV are obtained by doubling visible wavelengths. The peak powers for the fundamental, second, and third harmonics for some of the commercial pump lasers used in these systems are also shown for reference. Rough calculations of the relative efficiencies of the systems at different wavelengths may be made; note that wavelengths far from that of the pump laser are relatively more difficult to obtain.

Generally, the highest peak powers are available from flashlamp-pumped and frequency doubled Nd:YAG pumped dye lasers. Flashlamp pumped dye lasers have 0.5 to 1.5 μs pulse lengths, making them unsuitable for high range resolution purposes, for which the short 5 to 12 ns pulses obtained with frequency doubled Nd:YAG pumping are better.

A figure of merit that incorporates several of the most important and difficult to achieve performance parameters other than efficiency is the peak spectral brightness. This is a measure of the peak optical power per unit solid angle, unit emitting area, and bandwidth, given by

$$B = \frac{4\,P}{(\pi d \beta)^2 \Delta\tilde{\nu}}$$

where P is the peak power, d is the beam diameter (cm), β is the half-angle divergence, and $\Delta\tilde{\nu}$ is the bandwidth (cm^{-1}). A comparison of the brightness of commercial pulsed dye lasers, together with other relevant data, is given in Table 6-5. The high brightness available from frequency doubled Nd:YAG systems is immediately apparent.

Laser pumping allows excitation of a small active region and is therefore more suitable than flashlamp pumping for low order mode oscillation and good beam quality. In addition, laser pumped dye lasers can be easily used in the oscillator-amplifier configuration with little increase in complexity. Two of the frequency doubled Nd:YAG-pumped systems in the table utilize both of these advantages and are the birghtest dye lasers commercially available. A frequency doubled Nd:YAG pumped dye laser was chosen for the Lidar system, it was discussed in Section 6.4.

Laboratory Systems. Many high brightness dye laser systems have been reported, a few of which are listed in Table 6-6. The brightest are those that use either an oscillator-amplifier system or injection locking. In both techniques, the key component is a low power, low divergence, narrowband oscillator, which may be either CW or pulsed. The oscillator output is greatly amplified either by a sequence of single pass amplifiers or by an injection-locked oscillator (which is, in effect, a multi-pass amplifier). As indicated in the table, extremely high brightness dye systems have been built for flashlamp, N_2 laser and frequency doubled Nd:YAG pumping.

6.7.8 NARROW BAND DYE LASER DESIGN

Figure 6-16 shows a schematic layout of a dye laser conceptual design that would meet the specifications shown in Table 6-5. A single 532 nm beam pumps the oscillator and all three amplifiers. The folding optics add appropriate time delays to the amplifiers so they may be at a condition of maximum gain when the oscillator pulse arrives. As discussed in Section 6.7.4, proper attention must be paid to potential

Table 6-5. Commercial Systems Comparison Data

Manufacturer	Model	Pump	Peak λ(nm)	d Beam dia (cm)	β 1/2α Div (Mr)	Δν̃ BW (cm^{-1})	Rep Rate (pps)	E Energy (mJ)	P Peak Power(W)	B Peak Brightness, (w/cm^2 - $ster/cm^{-1}$)
Quanta-Ray	PDL-1	FD Nd:YAG	560	0.6	$5x10^{-4}$	0.5	10	50	10^7	$9.0x10^{13}$
Phase-R	DL-2100B	F.L.	590	1.5	$7.5x10^{-4}$	40.0	0.33	1500	$5x10^6$	$4.0x10^{10}$
Chromatix	CMX-4	F.L.	600	0.3	10^{-3}	0.15	30	7	$3.5x10^3$	$2.6x10^{16}$
Molectron	DL-200	N_2	460	0.06	$1.5x10^{-3}$	0.8	10	1	$1.2x10^5$	$7.5x10^{12}$
Candela	SLL-625	F.L.	un	1.6	$2x10^{-3}$	240.0	1	1250	$1.8x10^6$	$3.0x10^8$
	Custom	F.L.	610	1.6	10^{-3}	3.2	un	1000	$1.4x10^6$	$6.9x10^{10}$
ILS	YPD-100	FD Nd:YAG	600	un	un	2.0	10	4	10^6	
Electro-Photonics	23	F.L.	600	0.2	$5x10^{-4}$	3.0	15	15	$1.3x10^4$	$1.8x10^{11}$
Lambda-Physik	FL 1000	N_2	460	0.6	$1.5x10^{-3}$	0.6	500	1	$2x10^5$	$1.7x10^{11}$
Quantel Int.	TDL	FD Nd:YAG	565	0.7	$1.2x10^{-4}$	0.1	10	130	$1.3x10^7$	$7 x 10^{15}$
Instruments S.A. (JY OPT. DIV)	HP-HR	FD Nd:YAG	590	0.6	$2x10^4$	0.03	UN	135	$1.1 x 10^7$	$N 10^{16}$

(un = unspecified)

Table 6-6. Laboratory Systems Comparison Data

Reference	Dye Laser System Type	Pump	Peak λ(nm)	d dia (cm)	β 1/2 Div	$\Delta\tilde{\nu}$ BW (cm^{-1})	Rep Rate (pps)	E Energy (mJ)	P Peak Power (W)	B Peak Brightness (W/cm^2 - ster/cm^{-1})
S Blit, et al. Appl Phys. 12, 69 (1977)	Injection	F.L.	585	0.5	2×10^{-4}	10^{-3}	un	50	10^5	4.1×10^{15}
A. Moriarty, et al. Opt. Comm 16, 324 (1976)	Osc-amp	FD Nd:YAG	564	0.2	10^{-4}	0.12	10	55	6×10^6	5.1×10^{16}
C. Moore, et al. J. Appl. Phys. 49, 47 (1978)	Osc	FD Nd:YAG	558	0.6	2×10^{-3}	240.0	10	250	2.4×10^7	2.8×10^{10}
M. Salour, Opt. Comm 22, 202 (1977)	Osc-amp-amp-amp	N_2		"near" diff. limited		2×10^{-3}	un	0.4	10^5	3.2×10^{15}
R. Wallenstein, et al. Opt. Comm 14, 353 (1975)	Osc-amp-amp	N_2	460	"near" diff. limited		2.8×10^{-3}	un	0.5	5×10^4	1.1×10^{15}
A. Gibson, et al. J. Phys. D. 11, L59 (1978)	Injection	F.L.	647	un	un	10^{-3}	un	100	3×10^5	

(un = unspecified)

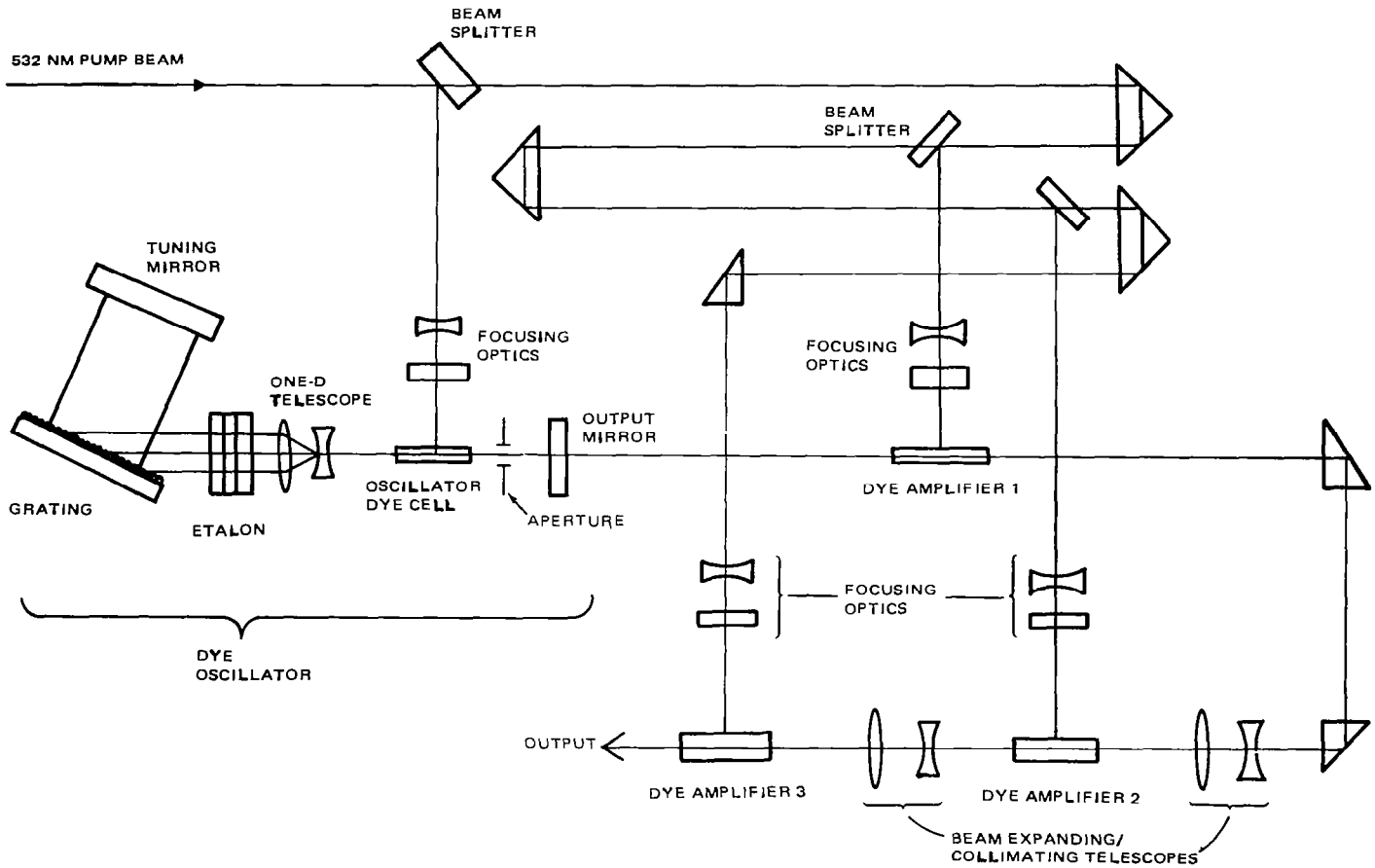

Figure 6-16. Optical Schematic of Dye Laser.

problems of parasitic losses and loss of spectral fidelity.

Of the two methods of implementing closed-loop spectral control that were described in Section 6.7.3, the method using an atomic transition (a Helium-Neon laser) as a reference is preferred because it is applicable to all wavelengths of interest. However, although the method has been demonstrated, engineering development is necessary before it can be incorporated into a reliable hardware design.

The predicted size of a packaged version of the dye laser is indicated in Figure 6-19. The weight of the module is estimated at 30 kg, with an additional 16 kg each for the dye circulator and the stabilization and wavelength monitor electronics package, parts of which are mounted in the central bay of the system structure. The DIAL experiments would require two dye laser modules.

6.8 DYE LASER SUBSYSTEM, MODULE 5: TUNABLE DOUBLER

Dye Laser Doubler. The frequency doubler module to obtain UV from the dye laser output has essentially the same technical issues associated with it as the mixer module. However it does not need to handle as high an average power, so it would not require as elaborate a set of beam shaping optics as the twenty watt doubler and mixer modules. Angle tuned crystals of KDP isomorphs will be used in a physical configuration again similar to, but considerably smaller than, the doubler.

6.9 ANCILLARY OPTICS: MODULES 6 AND 7

The ancillary optics subsystem of the visible and near visible sources system comprises the output optics, any necessary switching optics for the particular mission, a zoom mechanism for controlling the output beam divergence, and the structure supporting the other subsystems. All the possible output telescopes are well within the present state of the art, including those for the UV. Since all of

the laser beams are close to diffraction limited, relatively modest size output optics are required to achieve the necessary beam divergence; the minimum requirement of 0.1 mr beam divergence will never require more than approximately 5-10 cm output aperture, even by conservative estimates (beam divergence for the laser is defined as the full width to the $\frac{1}{e^2}$ point or approximately 87.5% of the peak intensity).

Refractive optics are therefore very convenient, giving no central obscuration. The optics must be anti-reflection coated to transmit all of the beams for the experiments contemplated on a particular mission; the small size makes changing of optics relatively simple. The possibility of using separate apertures for the 532 nm and the UV and dye laser outputs is desirable. The physical conceptualization of Figure 6-19 shows only one output telescope, mounted in the central bay of the system.

Switching optics, for example for alternatively deflecting the 532 nm laser output into the output optics or the dye laser, are located in the lower bay of the system. These can be arranged in such a manner that boresight misalignment will not take place. For the example above, the switching optics would be arranged so that the 532 nm beam is coaligned with the receiver with no movable optics in the path of the 532 nm beam. When dye laser output is desired, a mirror intercepting and deflecting the 532 nm beam into the dye subsystem is actuated. It is important to recall here that the dye laser has its own alignment and boresight, determined by its own optics, and the output beam of this laser may be independently coaligned, through its own output telescope, to the receiver. Any slight misalignment of the 532 nm beam caused by imperfections of the beam switching would have only second order effects on the dye laser output alignment. Beam switching schemes such as that described have already been incorporated into flying military laser systems for alternatively obtaining 1064 nm or 532 nm output from the system.

All three subsystems are mounted on a rigid structure. Experimentation has shown that with careful design, structures of this size can have coalignment between various parts on the order of 10 μr. Coalignment of each of the two output beams, namely the 532 nm beam and the dye laser output beam (possibly frequency doubled to the μv) to the mounting structure of Figure 6-19 is estimated at 30 μr. Their alignment with each other would therefore be on the order of 40-50 μr.

In several experiments, and depending on whether it is day or night, the output beam divergence must be adjusted. The most advantageous location for such an adjustment is just ahead of the output telescope. Several means of performing this function have been considered. If only a few distinct beam divergences are required, a solenoid actuated device for inserting weak negative lenses into the beam path is simplest. It has been demonstrated that such devices can be indexed with sufficient accuracy to maintain the above specified boresight tolerance. The degree to which decentering of the lens results in loss of pointing (boresight) accuracy depends upon the focal length of the lens; stronger lenses are more sensitive to decentering. This is counteracted, on the other hand, by the fact that the stronger lenses produced larger output beam divergence, and correspondingly larger pointing accurary tolerances.

Another method of controlling output beam divergence is defocussing of the output telescope. A continuous range of divergence would be obtainable using this method. Variable telescopes of this kind have been built for hardware systems, and have demonstrated misalignment through their range on the order of 500 μr. (This misalignment would be reduced to 50 μr for the output beam by the ten power telescope). A variety of mechanisms with stepper motor drivers are used for controlling the lens position.

6.10 EXPERIMENT ACCOMMODATION WITH MODULAR VISIBLE AND NEAR VISIBLE SOURCES SYSTEM

As discussed in Section 6.3, a modular sources system was chosen because it is most amenable to the Lidar Multiuser Instrument goals. This modular system consists of two primary subsystems: (1) the neodymium laser and its associated modules; and (2) the dye laser and its associated modules; including also, the output and switching optics modules which have been grouped in Figure 6-17 as the ancillary optics. The grouping of the modules into subsystems was also shown earlier in Figure 6-3.

All these and many other possibilities were given consideration. Through interaction with GE and NASA personnel, a baseline sources system, built from a minimal inventory of modules, was chosen. Figure 6-17 shows how the seven module system is configured to accommodate the SEED experiments. The output energies that would be obtained by a conservative estimate are shown. These energy estimates are for a field engineered system and are generally lower, perhaps by as much as a factor of two, than output energies typically reported for laboratory lasers. The baseline system is a two joule output neodymium laser. Laser linewidths and pulse lengths are also shown. The chart is intended to convey a great deal of information in compact form. The boxes heavily outlined in the matrix indicate the source properties that will serve the experiment number labeling the column. These are the performance specifications that the system will provide; in many cases they exceed requirements. The information at the left identifies, successively, the particular atmospheric species of interest for this experiment, the dye that would be used, the solvent, and the set of dye laser optics. Other filled boxes of a particular experiment number column indicate the performance that could be obtained with this particular laser configuration in doing other experiments or studying another specie. In addition, in all cases the 530 nm radiation would be available for experiment classes 1-6. The numbers at the top of each column indicate the quantity required, as a minimum, of each type of module to

PERFORMANCE PROVIDED BY SYSTEM \ SEED EXPERIMENT NUMBER					1-6	7	8[d]	9a	9b	9c
MODULES REQUIRED	NEODYMIUM SOURCE SUBSYSTEM	TWO JOULE NEODYMIUM LASER		1	1	1	1	2	2	2
		TWENTY WATT DOUBLER MODULE		2	1(2)[a]	1	1	2	2	2
		TWENTY WATT MIXER (TRIPLER)		3						
	DYE LASER SUBSYSTEM	NARROW LINEWIDTH DYE LASER (OSC/AMP)		4		1	1	2	2	2
		TUNABLE DOUBLER MODULE		5			1			
	ANCILLARY OPTICS	SWITCHING OPTICS		6			[2][b]	[1][b]		
		OUTPUT OPTICS SETS[g]		7	1	1	1	2	2	2
		1064 nm	PRF		10	10	10	10^c	10^c	10^c
			E (mJ)		1200(700)		1200	1200	1200	1200
			Δλ (pm)		30					
			τ (ns)		20					
		530 nm	E (mJ)		700(1120)		[700][b]	[700][b]	[700][b]	
			Δλ (pm)		15					
			τ (ns)		16					
		265 nm	E (mJ)							
			Δλ (pm)							
			τ (ns)							
SET OF OPTICS FOR 550-650 nm OPERATION	RHODAMINE 6G DYE IN METHANOL	Na	589.9 nm	E (mJ)		200	[200]			
				Δλ (pm)		1	1			
				τ (ns)		13	~13			
		OZONE AT LOW ALTITUDES	280-300 nm	E			30			
				Δλ			0.5			
				τ			10			
		Mg+	279.6 nm	E			30			
				Δλ			0.5			
				τ			10			
		Mg	285.2 nm	E			30			
				Δλ			0.5			
				τ			10			
		OH	LINES NEAR 300 nm	E			30			
				Δλ			0.5			
				τ			~10			
	CRESYL VIOLET DYE[k] IN METHANOL	NO	LINES NEAR 215 nm	E						
				Δλ						
				τ						
SET OF OPTICS FOR 450-550 nm OPERATION	COUMARIN 500 DYE IN METHANOL	MgO	500 nm	E						
				Δλ						
				τ						
		Ba+	493 nm	E						
				Δλ						
				τ						
	STILBENE 3 DYE IN ETHANOL	Ba	455 nm	E						
				Δλ						
				τ						
		NO_2	TWO NEAR 450 nm	E						
				Δλ						
				τ						
SET OF OPTICS FOR 720-770 nm OPERATION	OXAZINE 725 DYE IN ETHANOL	O_2 A-BAND	TWO NEAR 760 nm	E						
				Δλ						
				τ						
	OXAZINE 725 DYE IN METHANOL	H_2O (TROPOSPHERE)	TWO NEAR 720 nm	E				70		
				Δλ				1		
				τ				~10		
SET OF OPTICS FOR OPERATION NEAR 820 nm	DTTC IN METHANOL	H_2O (TROPOSPHERE)	TWO NEAR 820 nm	E					15	
				Δλ					1	
				τ					~10	
SET OF OPTICS FOR OPERATION NEAR 940 nm	IR125 DYE IN DMSO	H_2O (TROPOSPHERE OR STRATOSPHERE)	TWO NEAR 940 nm	E						1
				Δλ						~10
				τ						
CONFIGURATION (SEE FIGURE 6-18)					6-18a	6-18b	6-18c	6-18b		

(Figure explained in text,

Figure 6-17. Performance Provided

11a	11b[d]	11c[d]	12a[d]	12b[d]	14[f]	15, 16, 17	19[f]	20[f]	21[d]	22[d,h]	23[d]	25	26[j]
1 1	1 1 1	1 1 1	1[e] 1(2)	1 1		2 2			1 1	3 3 1	1-2 2 2	1 1	
1	1 [1]	1	1[e] 1(2)	1		2			1 1	3 2	2 [2]	1 2[k]	
[1] 1	[2] 1	[1] 1	[2] 1	1		[2] 2			[2] 1	[1-3] 3	2	[2] 1	
10 1200 [700]	10 1200 [700]	10 1200 [700]	10 1200(700) [700]			10[c] 1200 [700]			 [700]	10[c] 1200		10 1200 [700]	
			[b,e] [(70)](40) 7 13	70 7 13									
200 1 13			[200][b] 1 13						[200][b] 1 13	[200][b]×2 1 13			
			30 0.5 ~10						30 0.5 ~10	30 x 2 0.3 ~10			
			30 0.5 ~10						30 0.5 ~10	30 0.5 ~10			
			30 0.5 ~10						30 0.5 ~10	30 0.5 ~10			
			30 0.5 ~10						30 0.5 ~10	30x2 0.5 ~10			
												5 0.5 ~8	
		50 1 ~10								50 1 ~10			
		40 1 ~10								40 1 ~10			
	30 1 ~10										30 1 ~10		
	30[i] 1 ~10										30 each 1 ~10		
						50 1 13							
6-18b	6-18d	6-18d	6-18c	6-18e	SPECIAL	6-18b	SPECIAL	SPECIAL	6-18c	6-18c,d	6-18d	6-18f	SPECIAL

superscripts are notes.)

by Seven Module System.

NOTES FOR FIGURE 6-17

a. AN EXAMPLE IS SHOWN OF HOW MORE 530 nm OUTPUT MAY BE OBTAINED BY USING TWO SUCCESSIVE DOUBLERS.

b. OBTAINING OUTPUTS IN BRACKETS REQUIRES ONE [ ] OR TWO [[ ]] SETS OF SWITCHING OPTICS AS INDICATED. THE NUMBER OF DIFFERENT SWITCHING OPTICS IS GIVEN IN THE BRACKETS AT THE TOP.

c. EACH OF THE SYSTEMS CAN OPERATE AT 10 Hz, WITH ANY DESIRED ASYNCHRONICITY OF THE OUTPUTS. ALTERNATIVELY, TO CONSERVE POWER, EACH OF THE SYSTEMS COULD BE MODIFIED TO RUN AT 5 OR 3.3 Hz.

d. THE WAVELENGTH(S) SPECIFICALLY REQUIRED FOR THE EXPERIMENT NUMBER AT THE HEAD OF THE COLUMN ARE IN THE HEAVY BOX, OTHER WAVELENGTHS AVAILABLE FROM THE CONFIGURATION BY TUNING THE DYE LASER AND/OR USING SWITCHING OPTICS (INDICATED BY BRACKETS [ ] { }) ARE ALSO SHOWN. WHETHER A DYE OR OPTICS CHANGE IS NECESSARY CAN BE DEDUCED BY OBSERVING LISTS AT LEFT.

e. IF THE REMAINING 1.2 JOULES OF 1060 nm RADIATION IS FED INTO ANOTHER DOUBLER, PRODUCING MORE GREEN, WHICH IS THEN DOUBLED AGAIN TO PRODUCE 265, BOTH 12a AND 12b MAY BE DONE WITH THE SAME HARDWARE SET, ENERGIES AS SHOWN, WITH NO SWITCHING OPTICS.

f. THE VELOCITY MEASUREMENT OF EXPERIMENTS 14, 19 AND 20 REQUIRE A SPECIAL LASER HAVING LONGER PULSEWIDTHS SO THAT NARROW LINE OUTPUT CAN BE OBTAINED. MEASUREMENTS OF LIMITED ACCURACY (500 M/SEC) MAY BE MADE WITH THE SET OF MODULES SHOWN HERE. MAXIMUM ACCURACY THEORETICALLY POSSIBLE WITH LASERS OF THIS PULSEWIDTH THAT HAVE TRANSFORM LIMITED BANDWIDTH IS 20 M/SEC.

g. AN OUTPUT OPTICS SET MAY INCLUDE MORE THAN ONE TELESCOPE.

h. THE USE OF THREE SYSTEMS ASSUMES THAT THE LASERS ARE NOT TUNABLE BETWEEN SHOTS. IF THIS FEATURE IS INCLUDED IN THE DYE LASER, ONLY TWO SYSTEMS WOULD BE NEEDED. IN ADDITION, THERE IS THE OPTION, BY DOUBLING OF RESIDUAL 1064 nm RADIATION, OF USING ONLY ONE OR TWO NEODYMIUM LASERS TO PUMP THE DYE LASERS.

i. ONLY ONE WAVELENGTH IS AVAILABLE AT A TIME.

j. EXPERIMENT 26 REQUIRES A MODE LOCKED (IN ORDER TO OBTAIN HIGH PEAK POWERS) LASER SOURCE. THIS COULD BE ACHIEVED THROUGH MODIFICATION OF THE EXISTING NEODYMIUM AND DYE LASER SYSTEMS.

k. TWO DOUBLER MODULES, OF WHICH ONE IS USED AS A MIXER, FOR GENERATION OF THE THIRD HARMONIC OF THE DYE OUTPUT (645 nm).

do the experiment of that column. Some other subtilties of the chart are explained in the notes. A more explicity layout of the system as configured for each of the experiments is given in Figure 6-18.

Figure 6-19 shows the physical/optical conceptualization of the modular laser. The primary specifications for the modular laser are listed on Figure 6-20.

As summarized earlier in Figure 6-4, the various modules have undergone differing amounts of development and engineering. Several of the modules consist of relatively standard assemblies whose general design and engineering are well understood, but which must be specifically designed and qualified for this application. The output optics and the switching optics fall in this category. Some design areas, which were indicated in Figure 6-4, must be resolved. For the 2 joule laser, the 20-watt doubler, the mixer, and the tunable doubler, sufficient design data and experience from previous programs exist to allow high confidence that all critical engineering issues are resolvable. For the narrow linewidth dye laser, issues of spectral control, peak and average output power exist which have not been resolved even for laboratory systems. Commercial and laboratory systems exist which have come close to the required performance, as is discussed in Section 6.7.7.

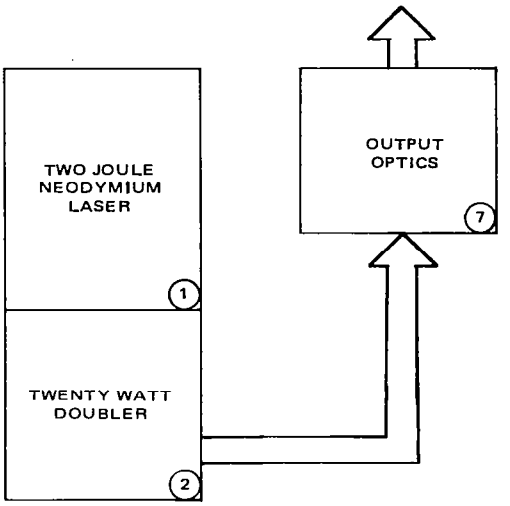

Figure 6-18a. System Configuration for Experiments 1-6.

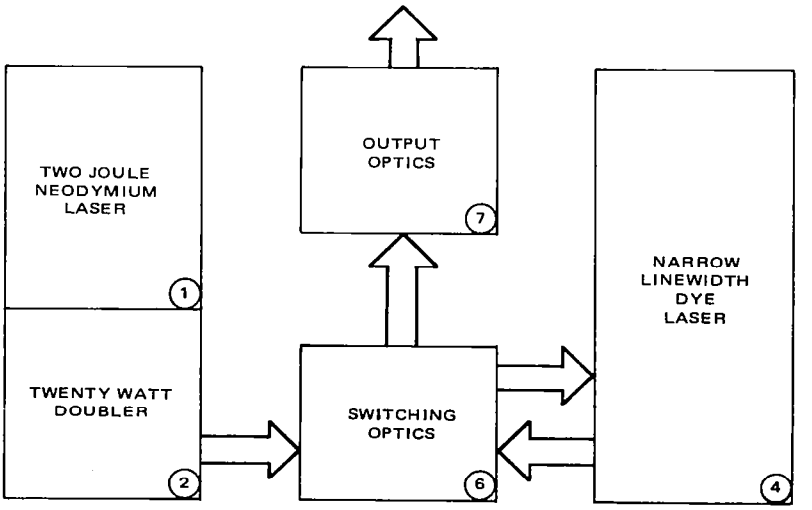

Figure 6-18b. System Configuration for Experiments 7,11a. With Two Such Systems Experiments 9,15,16 and 17 May be Performed.

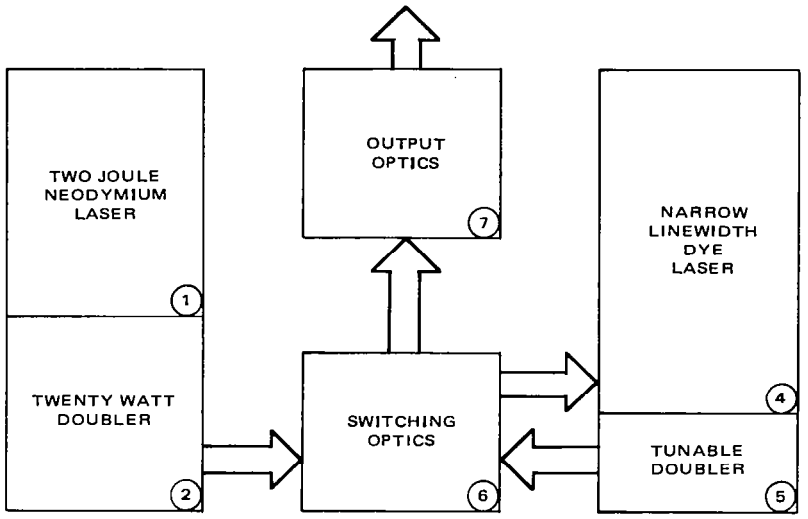

Figure 6-18c. System Configuration for Experiments 8, 12a, 21. Two systems each in this Configuration will Perform Experiment 22.

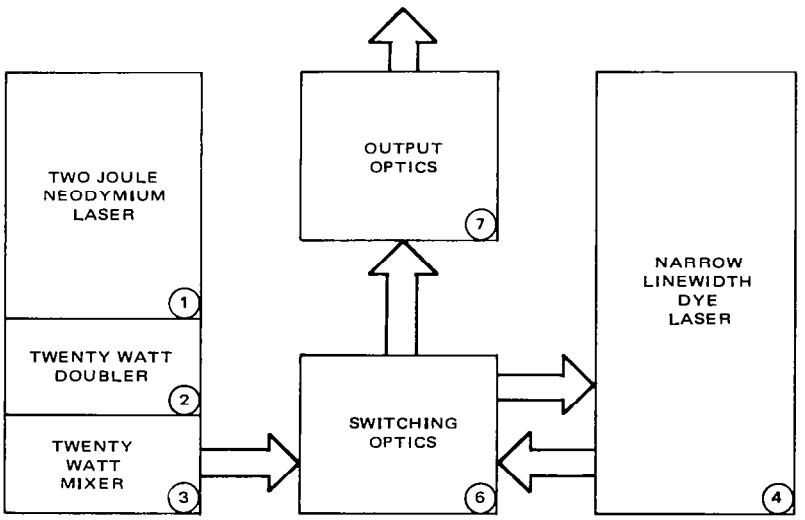

Figure 6-18d. System Configuration for Experiments 11b,11c, two will do 23.

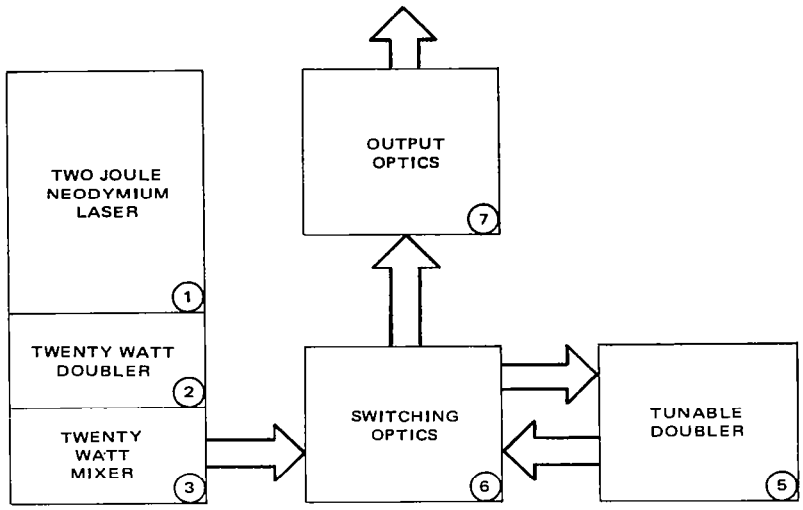

Figure 6-18e. System Configuration For Experiment 12b.

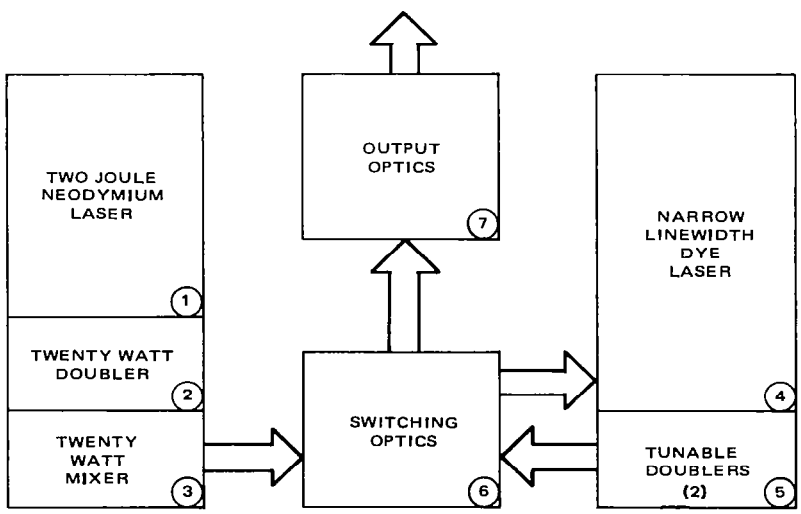

Figure 6-18f. System Configuration for Experiment 25.

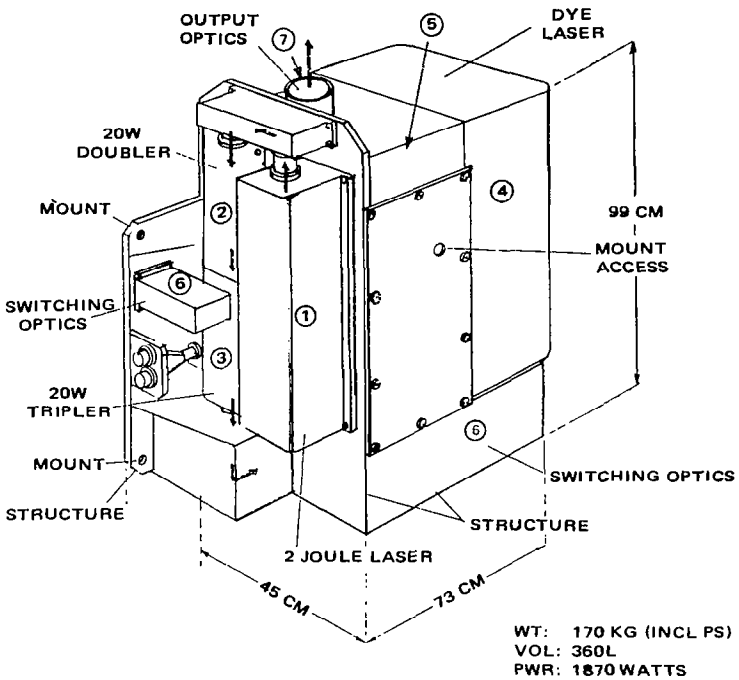

Figure 6-19. Physical/Optical Conceptualization for Seven Module System.

NEODYMIUM SUBSYSTEM	1. NEODYMIUM LASER MODULE 2. HIGH POWER DOUBLER MODULE 3. FREQUENCY TRIPLER MODULE	WAVELENGTH ENERGY PULSE RATE INPUT POWER	532 nm ± 100 pm 700 mJ 10 Hz 1.5 kW	355 nm ± 70 pm 200 mJ 10 Hz 1.5 kW
DYE LASER SUBSYSTEM	4. DYE LASER MODULE 5. TUNABLE DOUBLER MODULE	WAVELENGTH LINE WIDTH ENERGY LIFE	TUNABLE 215 TO 940 nm ± 0.5 pm 0.5 TO 1.0 pm 5 TO 200 mJ 10^6 PULSES	DEPENDING ON WAVELENGTH
ANCILLARY OPTICS	6. SWITCHING OPTICS MODULE 7. OUTPUT OPTICS MODULE	TO ACCOMMODATE EXPERIMENTS ON MISSION TO GIVE	0.1 TO 6.0 mrad OUT OF INSTRUMENT	

Figure 6-20. Requirements Specification for Seven Module System.

6.11 CW CO_2 SOURCE

6.11.1 REQUIREMENTS AND CANDIDATE SELECTION

The CW CO_2 laser sources that are required for Experiment classes 10 and 13 are listed in Table 6-7. Experiment class 10 uses the DIAL method which requires two simultaneous laser outputs at different wavelengths. The technique for accomplishing this in both CW and pulsed CO_2 lasers is described in section 6.12.1 of this report. This very general specification will allow heterodyne detection at the appropriate resolution as determined by the experimenter.

Table 6-7. CW CO_2 Laser Source Requirement

Power output	10 watts
Wavelength	10.6 μm — line tunable
Frequency stability	±5 MHz
Life	250 hours

Currently, three CW CO_2 laser types are candidates for use as 10 W transmitters.

1. The conventional low pressure, DC excited large bore laser
2. The longitudinally excited DC waveguide laser
3. The transversely excited RF waveguide laser

The DC conventional (DCC) type laser refers to a larger bore (typically greater than 5 mm) and lower pressure laser, in which the discharge is excited longitudinally and the propagating wave has negligible interaction with the walls. The DC waveguide (DCWG) laser is a smaller bore device (typically 2 mm bore) with higher gas pressure in which, again, the discharge is excited longitudinally. In this case, the propagating wave is guided by the walls. The RF excited waveguide laser (RFWG) is

similar to the DCWG in bore size, gas pressure, and guiding properties, but differs from the DCWG in that the discharge is sustained by an RF field rather than a DC field, and the discharge runs transversely, as opposed to longitudinally.

A comparison of the three lasers is shown in Table 6-8. No military specification CO_2 laser, of any type, exists to date. Of the three lasers, the DC conventional laser was fabricated first; it was developed most extensively for the commercial market. The RF waveguide laser, on the other hand, is the newest and least understood. This laser was invented at Hughes in 1976 and has since been under development, funded by an internal research and development program. The DC waveguide laser has been the most thoroughly developed into a rugged-type configuration by both Hughes and others. Hughes believes the RFWG it to be the most promising laser overall for a 10 W multifunctional Lidar transmitter. Its characteristics are outlined below:

1. Ruggedness and mode quality associated with the waveguide structure
2. Easiest scalability to the higher output powers, even to the 20 W range
3. Highest overall efficiency
4. Potential for the highest reliability and life
5. Smallest package size and weight for a given output power
6. Most versatility in terms of use as a Lidar transmitter.

<u>Scalability Issue: Longitudinal vs. Transverse Discharge.</u> CW output powers in the 10 to 20 W range infer device lengths in the 50 to 200 cm range. As a rule of thumb, when the power output is maximized both with respect to gas mix and gas pressure, between 0.1 W/cm and 0.2 W/cm output can be expected for all CW CO_2 devices when operated sealed-off. At the optimum gas pressure of 70 Torr and with the optimum gas mix, the sustaining E-field value is equal to roughly 0.6 kV/cm for a 2.0 mm DCWG. Because of difficulties in handling supply voltages much greater than 10 kV for nonlaboratory type environments, the longitudenally excited DCC or DCWG lasers need a

Table 6-8. CW CO_2 Laser Comparison

Parameter	RF Waveguide	DC Waveguide	DC Conventional
Power/Unit Length, W/cm	0.20	0.13	0.1
Laser Head Efficiency, percent	10	10	10
Overall Efficiency, percent	8	4.7	5
Lifetime, hours			
Best	240 (limited by leak)	6000	30,000
Nominal	–	270	2,000
Per CC Ballast	–	20 to 30	2 to 3 (typical)
State-of-Development	One commercial manufacturer	Commercial unit	Commercial unit
Potential			
Advantages	Higher efficiency Higher output power or lower weight and size Readily scalable Longer life	Furthest along in development	Demonstrated maximum life
Disadvantages	Limited sealed-off experience	Scalability difficult	Mode control Larger size

number of independent discharge sections. With a 10 kV supply, the optimum 2.0 mm device requires a separate discharge every 8.3 cm. For a 50 cm device, six discharge sections are implied; for a 100 cm device, 12 discharge sections must be used.

Hughes has had considerable experience in handling the multiple discharge problem and has tried a number of different approaches. One approach is to have pairs of discharge sections stacked, one upon another, with each pair consisting of two grounded anodes at each end, and in the center two independently ballasted cathodes separated by a centimeter spacing. This approach has two problems:

1. Difficulty in lighting and maintaining the separate discharges independently, even with starting circuitry.
2. Tendency for the discharge to occur between the two 1 cm spaced cathodes.

Variations of this approach to solve these problems include 1) ballasting the anodes individually and separating the anodes with a spacing between the adjoining discharge pairs and 2) interchanging the anodes and cathodes. The difficulties in lighting the discharge and maintaining the discharge only between the desired points are still present.

An alternative approach is to use common anodes and cathodes and also to alternate between cathode and anode along the length. Through the use of current regulators and current limiters, the discharge problem may be entirely solved. Discharges valued as equal to roughly 0.6 kV/cm for a 2.0 mm DCWG are obtained.

The discharge problem is somewhat easier for the large bore, lower pressure DCC, primarily because of the lower sustaining E-field required. However, mode quality considerations limit the maximum allowable bore size to 3 mm. To maintain the optimum power output per unit length, the gas pressure must scale inversely to the bore size. Hence, for a 3 mm device, the optimum gas pressure is of the order of 45 Torr. Under

these conditions, the sustaining E-field is approximately 0.4 kV/cm. For a maximum drive voltage of 10 kV, the discharge length is thus limited to 12.5 cm. For a 1 m long device, eight separate discharge sections are still required. Also the entire problem of maintaining and lighting numerous discharge sections is still present. It appears therefore that within the constraints of maintaining good mode quality, device compactness, and high efficiency, the longitudinally excited devices, DCC or DCWG, are practically limited to output powers of about 6 W or less. This figure is equivalent to a maximum number of four separate discharges.

Transverse RF excitation, as used in the Hughes RFWG, eliminates the discharge problems. Because the discharge is transverse, the design of a longer length discharge section does not require an increase in discharge voltage but simply an increase in discharge current. Further, because the discharge is transverse, the drive voltage is reduced from roughly 10 kV as in longitudinally excited devices to a mere 100 V rms. Thus, corona or unintentional discharges are no longer present or, at least, are easy to eliminate. Finally, since the starting voltage is generally about equal to the drive voltage, starting difficulties are entirely eliminated. In conclusion, Hughes believes that transverse RF excitation, as in the Hughes RFWG, is the only practical method of achieving a 10 W, efficient, compact, good mode quality laser.

Efficiency and Reliability. Hughes believes the RFWG has the potential for the overall highest reliability and life, although to date the DCC has shown the best life data. To date, the RFWG has shown a tested life of 240 hours, where the life has been limited solely by an air leak. The air leak in the RFWG may easily be eliminated, and longer lives are anticipated. The higher reliability of the RFWG is based on:

1. The cathodeless discharge of the RFWG.

2. The absence of high voltage in the RFWG.

3. The absence of starting problems and other related discharge difficulties.

The last two features of RFWG were discussed earlier; however, the first requires more explanation. In the DCWG and the DCC, both cathode and cathode fall are frequently the major sources of contamination and failure. These reliability problems are caused by 1) gas breakdown in the high electric field region of the cathode fall, 2) electrode erosion, and 3) subsequent deposition of the erosion products on laser cavity mirrors and windows.

Versatility. Hughes believes the RFWG is the most versatile of the three lasers for applications as a Lidar transmitter. This versatility is due to 1) the relative ease of building a "quiet" laser and 2) the large pressure broadened bandwidth. Because of the negative impedance of the DCC or DCWG, even slight stray capacities can lead to both an AM and FM modulation of the output. This problem does not exist in the RFWG because of positive impedance. Theoretical work at Hughes has indicated that the RF field induces a negligible amount of FM or AM modulation. The large pressure broadened bandwidth of the RFWG is a result of its ability to operate at high pressure. Clearly, the small bore of either the RFWG or DCWG permits considerably higher pressures, and, hence, broader bandwidth, than the DCC permits. In addition, because of corona and other discharge difficulties, maintaining discharges with gas pressures much greater than 200 Torr is cumbersome in the DCWG but not in the RFWG.

6.11.2 WEIGHT AND VOLUME

The RFWG has the potential for being made in the smallest package of the three types because of:1) elimination of large high voltage filtering capacitors and also high voltage transformers, and 2) elimination of ballast circuitry. A 40 W RF supply

available commercially is an example of the small size possible with the RF supply. Here, the dimensions are approximately 10 x 10 x 3.8 cm and the efficiency is 60 percent. No attempt was made in these devices at achieving either a higher efficiency or a smaller package size.

One final note is included on the power output per unit length of comparative package size. With the RFWG, output powers of 0.2 W/cm are readily achievable; whereas for the DCC and DCWG, output powers typically run closer to 0.1 to 0.15 W/cm, when operating at a 10 percent laser head efficiency.

6.11.3 FREQUENCY STABILIZATION

Frequency changes within an oscillator are due to optical path length changes. The frequency change is directly related to the length change by the relation

$$\frac{\Delta f}{f} = \frac{\Delta \ell}{\ell}$$

where f is the frequency and ℓ is the resonator length. Changes are either physical length changes due to heating, acoustical coupling, or actual vibration of the laser structure, or refractive index changes due to variations in resonant susceptibility due to gain or electron density changes. Compensation for physical length changes is made in the laser mechanical design. Refractive index changes are inherent and must be kept to acceptable levels by careful engineering design.

With CW lasers, the predominant mechanisms causing frequency variation and chirping are physical length changes of the optical cavity. In pulsed lasers, physical length changes occur over times long compared to a pulse effecting long term stability. The refractive index changes that take place during a pulse contribute to short term frequency chirps; changes in these parameters may cause long term frequency variation.

The required five MHz stability means that $\Delta \ell / \ell \leq 2 \times 10^{-7}$. Vibration coupling to the optics need not be very large before large frequency variations are caused. Very minor thermal expansion within the cavity leads to large frequency variations. There are two categories of techniques, that compensate for these changes - passive or active. Some passive techniques are

1. Make the laser of temperature stable materials
2. Cool the laser with temperature controlled coolant
3. Make the structure massive
4. Shock mount the laser
5. Environmentally isolate the laser
6. Use a highly stable discharge supply.

Active techniques include dither stabilization and Stark cell stabilization. Various passive techniques and an active technique to ensure long term stability, should be incorporated into the design. A description of two active stabilization techniques is shown below.

Dither Stabilization. Dither stabilization of the output frequency of a laser oscillator is achieved by a single-loop feedback control system, or simple regulator, generally referred to as a type-0 system. The various methods of achieving laser frequency stabilization differ in their manner of obtaining the frequency discriminant. Ideally, the discriminant would be obtained by comparing the laser output with a reference oscillator. Lacking an ideal reference oscillator, the discriminant must be obtained by other means. The basic control circuit resembles that shown in Figure 6-21.

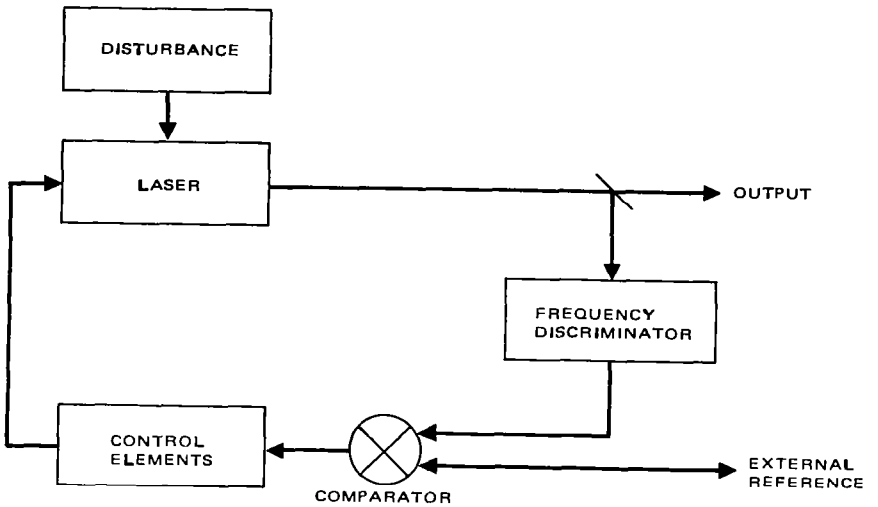

Figure 6-21. Basic Control Circuit for Stabilized Laser.

The dither method of laser frequency stabilization utilizes the laser line itself as a reference in the control system, thereby eliminating the need of an external frequency reference in the control system. The dither method also has been called FM stabilization, phase modulation stabilization, or active frequency stabilization. In any case, the method relies on the rounded pressure-broadened gain curve and the synchronous amplitude-demodulation of the output power of the laser at the dither frequency.

The operation of the dither stabilization method is shown in Figure 6-22. As the laser cavity optical length is dithered by a modulator, such as a piezoelectric crystal or electro-optical crystal, the output power of the laser varies across the doppler linewidth of the laser gas. The synchronous detector generates a discriminant which is the frequency error signal. The polarity of the signal is chosen to cause the modulator to scan the frequency back to line center.

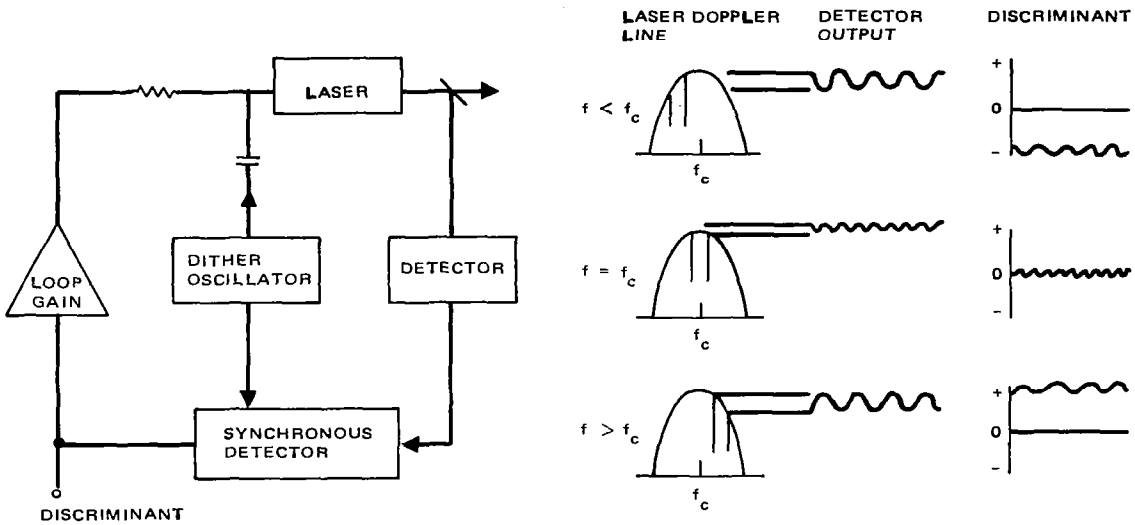

Figure 6-22. Dither Method of Obtaining Frequency Discriminant for Stabilizing Laser Frequency.

Because the dither method relies on the rounded homogeneous gain curve, the shape of the line must be considered. Repeated measurements of the line shape for high performance lasers have yeilded the empirical relationship near line center of

$$P = P_o e^{-\left((f-f_c)^2/(\Delta f)^2\right)}$$

where f is the laser frequency, f_c is line center, and Δf the laser bandwidth. For very small excursions from line center, the modulation depth (δP) of the laser power is

$$\frac{\delta P}{P_o} = \frac{2(f_o - f_c)\,\delta f}{\Delta f^2}$$

where $f_o - f_c$ is the excursion from line center, and δf the amount of laser frequency dither.

The power detector in the circuit must be able to detect the modulation δP in the presence of a steady P_o on the detector. Because cooled photoconductors are saturated at fairly low flux levels, an optimum flux level exists at which the maximum signal-

to-noise output is obtained. Other types of detectors, such as thermopiles and thermistors, do not saturate as the power is increased but will eventually suffer damage. From the above equation, it can be seen that the modulation depth can be increased by setting the laser frequency f away from line center f_c. Although this technique offers some enhancement in the theoretical stability, the system is not independent of the laser amplitude of the laser power. To be completely independent of the laser amplitude, the laser frequency should be positioned at line center.

Stark Absorption Cell Stabilization. Many approaches to the problem of laser frequency stabilization have been demonstrated, including frequency lock to a fixed absorption line in an external gas cell[13] (which may be either the same or a different molecule as the lasing species), and dither stabilization to the center of a Lamb dip in the power tuning curve[14] (which results in stabilization of the laser to line center). Most of the previously demonstrated techniques are designed for very accurate fixed frequency operation of gas lasers, for use as frequency standards and for spectroscopic applications. These approaches lack the versatility of continuous frequency control and, in most cases, require some form of laser frequency modulation to generate control signals. For many applications in optical communications and radar, frequency control of gas lasers over their complete tuning range is needed with moderate precision (on the order of 1 MHz). In particular, the recently developed GHz tunable waveguide CO_2 laser[15] probably will become very useful for heterodyne optical communications systems, but no simple technique has been devised for frequency control within this tuning range. The Stark absorption cell frequency stabilization technique utilizes an external gas cell whose resonant frequency is controlled by the linear Stark effect. Error signals are generated by dither modulation of the Stark cell voltage rather than dithering of the laser, eliminating the sometimes troublesome frequency modulation of the laser output. Stabilization of

a waveguide CO_2 laser to the Stark cell is accomplished with continuously programmable frequency tracking over the laser tuning range. Long-term frequency stability and measurements of precision of frequency reproducibility are described below.

Stark tuning of molecular absorption lines has been studied extensively and has been used by several investigators.[16,17]. A resonance absorption[18,19] deuterated ammonia (NH_2D) cell was used by Nussmeier and Abrams[20] to stabilize the P(20) 10.6μm CO_2 laser transition. The reasonably high absorption and fortuitous location of this transition make it an ideal choice for the present investigation. The spectroscopic characteristics of the Stark-tuned absorption have been described by references 17, 18, and 19.

The components of a typical control loop are shown in Figure 6-23. One Stark electrode is DC biased with a voltage from a precision high-voltage power supply, and the second electrode is driven by an audio oscillator. The signal from the optical detector is phase-sensitively detected with respect to the modulating signal in a lock-in amplifier. The lock-in output, which becomes the laser frequency discriminant, is amplified and fed back to the laser modulator to complete the frequency control servo loop. As the AC drive voltage to the Stark cell is increased, the peak absorption frequency deviation increases so that it becomes an appreciable fraction of the absorption linewidth. Further increases cause harmonic distortion and a loss of fundamental signal strength, thus, optimum AC voltage exists for a given linewidth. When the Stark cell is tuned near the edge of the laser tuning range, the discriminant becomes asymmetric because of the variation of laser power with frequency. The zero crossing, however, depends only on the Stark cell voltage and not on the slope of the laser power tuning curve. This fact would not be true, however, if the discriminant were generated by frequency modulation of the laser, as required for stabilization to a fixed absorption line.

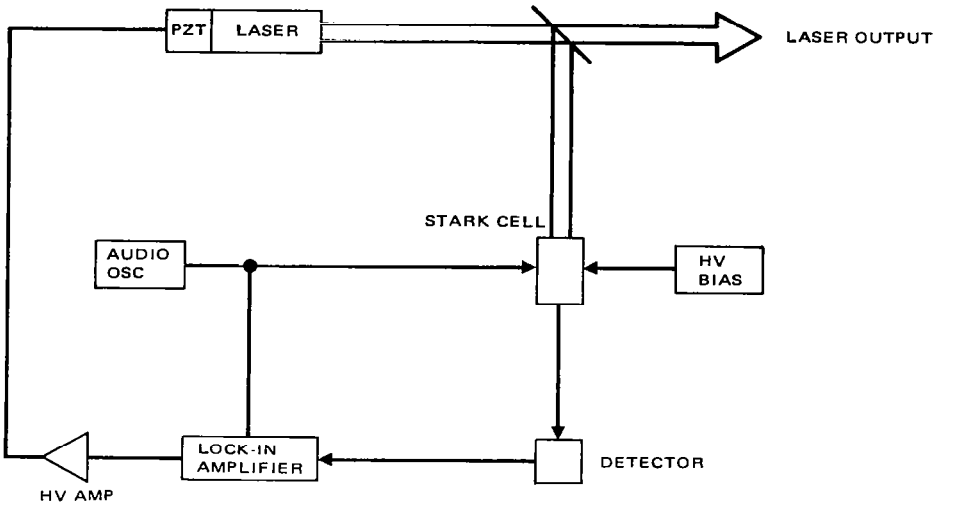

Figure 6-23. Stark Cell Frequency Stabilization.

6.11.4 CONCEPTUALIZATION OF CW CO_2 LASER

A CW CO_2 laser of the required output will generally appear as the one shown in Figure 6-24. Inside the laser housing will be a multiple pass cavity with stabilization and line tuning elements and the optical cavity internally mounted. Mounted atop the laser housing will be the RF power supply with impedance matching circuits and the electrical feedthrough into the laser. Mounted beside the laser housing is the stabilization electronics package which will be PZT control and feedback circuitry. The mechanical and optical detection elements are mounted internally in the laser housing.

Not shown in the sketch are the control box for any line tuning which would be necessary. This device could weigh as much as 2 kg (conservative estimate), have a volume of 4 liters, and require 200 watts of DC power to drive it. This required power allows for 5 percent overall efficiency. Similar packages with only a single pass cavity are now being ruggedized for various military applications.

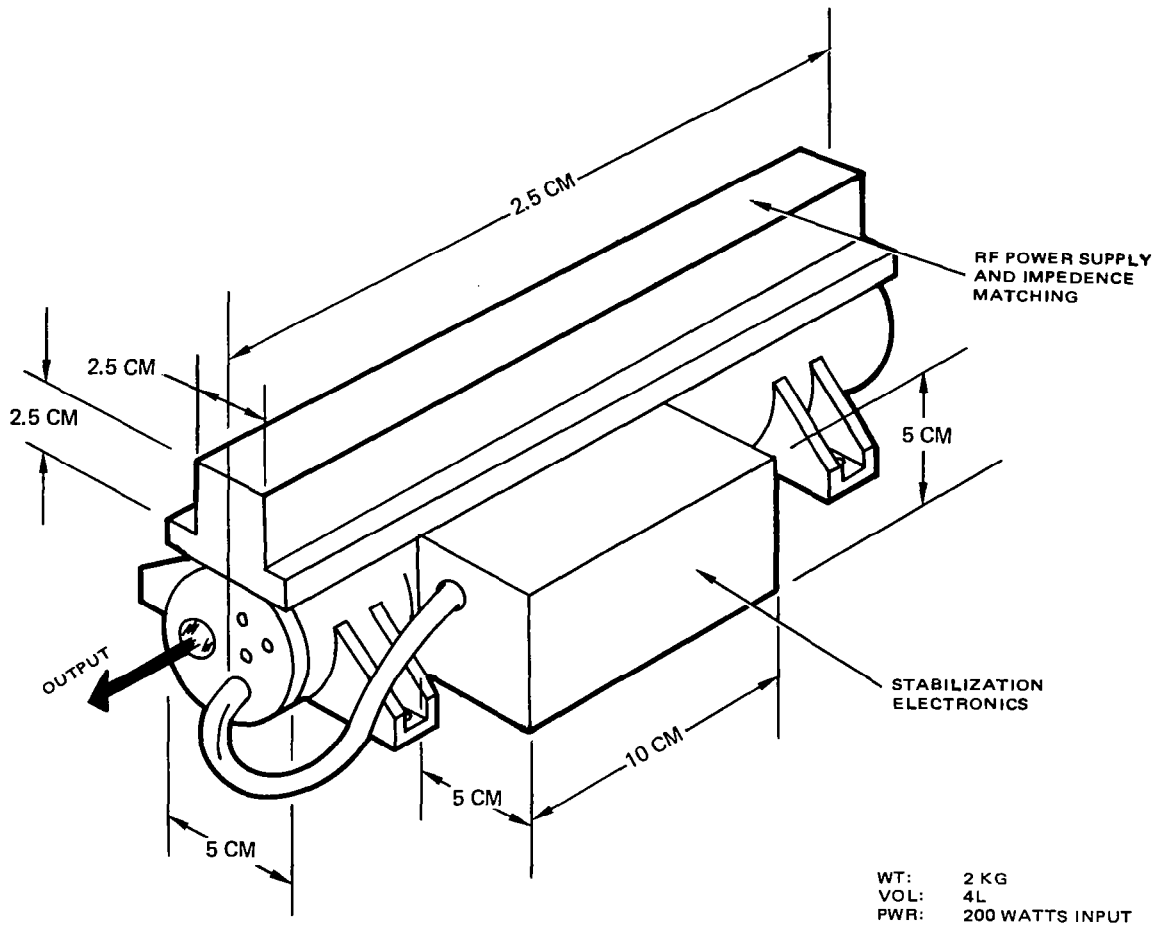

Figure 6-24. Conceptualization of CW CO_2 Laser.

6.12 PULSED CO_2 LASER SOURCE

6.12.1 REQUIREMENTS AND TRADES

The general requirements for the pulsed CO_2 laser are

Energy	- 10 J per pulse
Pulse Rate	- 15 Hz
Wavelength	- 9-11 micrometers (line tuneable)
Stability	- $\pm$5MHz
Pulse Width	- 200-10,000 ns.
Amplitude Stability	- 0.01-0.1 percent short term.

A laser with these specifications will allow the constituent concentration and velocity measurement experiments to be performed. A DIAL Source is also required for Experiment 18.

Excitation Method. Only two basic device designs existing today will meet the 10 J/pulse output requirement. Both are transversely excited, atmospheric pressure (TEA) devices; they differ in the method of exciting the active medium. The two methods are described followed by a discussion of areas requiring trades: efficiency, ease of varying pulse length, and gas handling.

One type of TEA device uses a UV preionizing signal to generate a low level background electron density so that breakdown becomes possible at a somewhat reduced field. Once breakdown occurs, the discharge proceeds toward an arc condition; removing the UV source does not terminate the discharge. The optical output of a TEA device is composed of a gain switched spike followed by a longer, lower powered pulse caused by additional transfer of energy from nitrogen to CO_2. The longer pulse can contain as much energy as the gain switched pulse. To obtain short pulses with most of the pulse energy in the gain switched spike, the gas mix must be nitrogen lean. To

obtain long pulses in a TEA device, a high background electron density is generated by the addition of a low ionization potential seed gas.[21]. With this technique the potential is kept below that required for avalanche ionization (6 kV/cm). With the UV preionization devices, specific outputs up to 20 J/l have been obtained with normal preionization and up to 60 J/l for long pulsed operation.[22,23].

An e-beam sustained electric discharge laser (EDL) uses a high voltage e-beam to generate the high background electron density ($7 \times 10^{12}/cm^3$); the breakdown field is again held to less than the avalanche ionization field. If voltage is now applied to the cavity, the discharge can be controlled by pulsing the e-beam current. This controls the discharge and optical output to any pulse length required by merely changing the e-beam pulse length. Also, by adjusting the background electron density, the device can operate at the most efficient portion of the pumping curve. The optimum pumping occurs when the field is approximately 4.4 kV/cm compared to 10 kV/cm for UV preionized devices of comparable efficiency. Also, since electron density is controlled by the e-beam, it tends not to vary during the pulse. The specific output of these devices ranges from 50 J/l to 20 J/l for pulse lengths greater than 20 μs. Comparison of the two types of devices is summarized in Table 6-9. The wire ion plasma (WIP) version of the electron gun, developed at Hughes, consists of an ion source, an extraction grid, and a high voltage cold cathode. Positive ions extracted from the plasma strike the high voltage cathode and produce secondary electrons which are then accelerated through the ion source to the thin metallic window. The electron beam distribution is thus the same as that of the ion beam falling on the cathode. This makes it possible to use the ion source to generate, control, and regulate the electron beam. This is unique to the WIP, and simplifies engineering. It is very advantageous because control can be accomplished at ground potential rather than having control electronics operating at 200 kV.

TEA e-gun technology is now being developed at Hughes in a higher powered (on the order of a few kW) version that will be completed in 1979. The e-gun for the contemplated Lidar source is therefore within the present state of the art since its average power is only a few watts.

Table 6-9. Pulsed CO_2 Device Comparison

Parameter	Conventional TEA	EDL TEA
Specific Energy		
(Short Pulse)	5-20 J/l	
(Long Pulse)	0-60 J/l	50-200 J/l
Extraction Efficiency	10 percent	30 percent
Wall Plug Efficiency	4 percent	10 percent
Cavity Potential	10 kV/cm	4.4 kV/cm
Ionization Mechanism	UV	e-beam
Large Volume Discharge Uniformity	Not good	Good
Switching Required	High power Thyratron	Low power e-beam switch
State of Development	Commercial cavity length plus CAS mix	Controlled by e-gun

Efficiency. Efficiency is a key element in the choice of the device. The following elements are directly related to system efficiency.

1. Power supply size and weight
2. Heat exchanger size and weight
3. Flow rate of coolant needed for heat exchanger
4. Gas flow system size and weight
5. Contamination effects on output power - also dependent on voltages in the high power discharge.

In view of the premium paid for size and weight, the e-beam sustained EDL is preferable for the Shuttle mission on the basis of efficiency.

Pulse Length Control. One requirement considered in the design choice is pulse length variability. Experiment 18 requires pulse lengths on the order of a few hundred μs while experiments 19 and 20 require pulse lengths on the order of a few μs. It is difficult to vary pulse length in conventional TEA lasers; extensive changes in the high power circuitry and gas would be required. This would probably not be possible as a spaceborne operation; it would be accomplished on the ground; both types of experiments would be done on different Shuttle flights. However, changes with an e-beam sustained EDL are made in the pulse length of the e-beam control signal. Because this is done at low voltage and power it is accomplished much more easily. With a variable pulse length capability, both classes of pulsed expeirments could be run during the same mission. An e-beam sustained EDL is thus favored for the pulsed device in this trade.

Gas Handling. The last issue is that of gas handling. The gas may either be recycled or discarded after use. For the operation times required during a mission, running the open loop laser would required prohibitive amounts of gas. The question that must therefore be addressed is whether contamination in a closed cycle system will be sufficient to severely degrade the laser performance. Chemical reactions, related to gas contaminants, taking place in the discharge cause breakdown of the gas and consequently degradation of output and more contamination. High discharge fields and operating powers aggravate the problem. For this reason efficient devices with low operating voltages, like the e-gun sustained discharge, are preferable to conventional UV preionized devices. The long pulse conventional devices also require continuous replenishment of the seed gasses.

Long term contamination has been studied by C. Freed at MIT Lincoln Labs. In his studies, it was found how contamination affects the discharge and therefore the output power. For constant e-beam current cavity sustaining voltage, the discharge current dropped by a factor of 2 in the first hour of operation and leveled off with no significant decreases in output thereafter. This decrease is thought to be due to the immeasurably small amounts of HNO_x invariably present even in a super clean system. In an e-beam system, current could be increased throughout the first hour of run time to counteract the effects of this contamination, or a burn-in period could be specified.

Stabilization. At atmospheric pressure, the pressure broadened gain bandwidth of a typical TEA CO_2 laser gas mix is approximately 3 GHz FWHM. For a 1 m long laser resonator, the longitudinal mode spacing is 150 MHz. Depending on system losses, then, 10-20 modes can be present simultaneously competing for gain. This gives rise to a wide spectrum output with spiked mode-beating. Current frequency stability techniques concentrate on forcing the system to operate in a single longitudinal mode (SLM). The techniques and relevant journal articles are listed below.

1. Intracavity saturable absorber (Stiehl and Hoff[24])
2. Injection of low pressure laser into the cavity
   a. Intracavity low pressure cw laser (Girad,[25] Gondhalehar,[26] Hamilton,[27])
   b. Extracavity low pressure laser (Lachambre,[28] Izatt[29])
3. Intracavity etalon (Lee[30])

The intracavity low pressure CW laser is the most widely used method for obtaining SLM, see Figure 6-25. A low pressure laser is practically limited to small bore diameter by cooling constraints. This apertures the useful gain volume for the pulsed device causing a decrease in efficiency. An intracavity etalon, on the other hand,

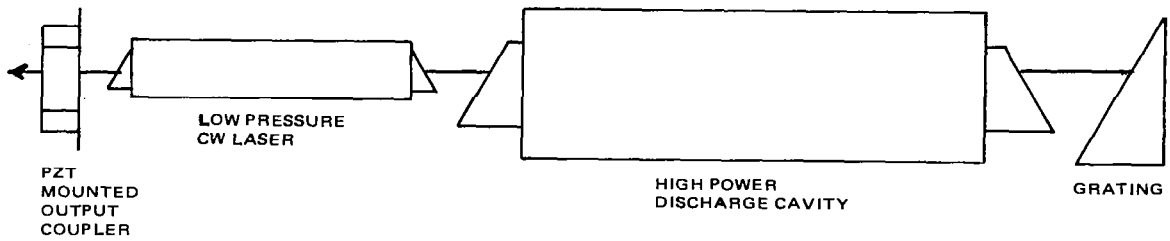

Figure 6-25. Intracavity Low Pressure CW Model Selection Scheme.

can be made to cover the total aperture; therefore, the gain volume is completely used. This technique uses the most efficient device and should therefore be considered a prime candidate for SLM selection. It could also be used for lone selection by appropriate tilting of the etalon.

One problem that etalons suffer is the change in index of refraction with temperature, causing an output frequency shift. Temperature control of a solid piece of ZnSe, for instance, would probably be prohibitive; however, substituting a gas filled etalon would only require simpler control of a low expansion spacer material.

Even with the use of these methods the laser output is still subject to frequency chirping during the pulse due to refractive index changes. The refractive index from the resonant susceptibility is given by

$$n_{\nu_{gain}} = \frac{g(\nu_o)\ \left[(\nu - \nu_o)/(\Delta\nu/2)\right]}{2\ \left\{1 + \left[(\nu - \nu_o)/\Delta\nu/2\right]^2\right\}}$$

where g is the incremental gain, $k = 2\pi/\lambda$, ν_o is the oscillator frequency and is the Lorentzian FWHM pressure broadened linewidth. The chirp due to this susceptibility is:

$$\frac{(\Delta\nu)_{chirp}}{\nu} = \Delta n_{gain} \approx \frac{\Delta g(\nu_o)\ \left[(\nu_i - \nu_o)/(\Delta\nu/2)\right]}{2k}$$

where Δg is the change in gain from some during the pulse, ν_i ; is the initial

oscillator. The farther off line center the laser operates, the worse the chirp will be. Chirps as great as 100 MHz/μs have been measured. By controlling the laser to operate near line center, chirps as low as 0.4 MHz/μs have been achieved. The laser must run on line center to operate as an oscillator. The refractive index due to the plasma is given by

$$n_{electron} = -\frac{\omega_p^2}{\omega^2} = -\frac{\epsilon_o N_e e^2}{2 m \omega^2}$$

where N_e is the electron density, e the electron charge, ω the resonator angular frequency, m the electron mass, and ω_p the plasma frequency. If the maximum allowable chirp is 5 MHz then

$$\Delta N_e \leq 8 \times 10^{11}/cm^3$$

is the allowed electron density change.

The refractive index change due to gas susceptibility is caused by a change in gas density through expansion. Since

$$n_{gas} = 1 + \kappa\rho$$

where κ is the Gladstone-Dale constant and ρ is the density.

$$\Delta n_{gas} = \kappa \Delta \rho$$

Deposition of power into the gas causes gas density disturbances which travel at the speed of sound (~300 m/sec). If the pulse length is less than 10 μs in a 3 mm bore device, density changes will not affect the frequency stability.

Assuring that the laser cavity length is constant shot to shot is important to keeping the laser operating on the same longitudinal mode. One technique[31] uses the

laser resonator as an etalon with a stable reference laser. The cavity length is precisely set between shots; the reference laser is blocked during the shot. If an unstable resonator is used, a partially transparent output coupler is required. Figure 6-26 is a block diagram showing how this is accomplished.

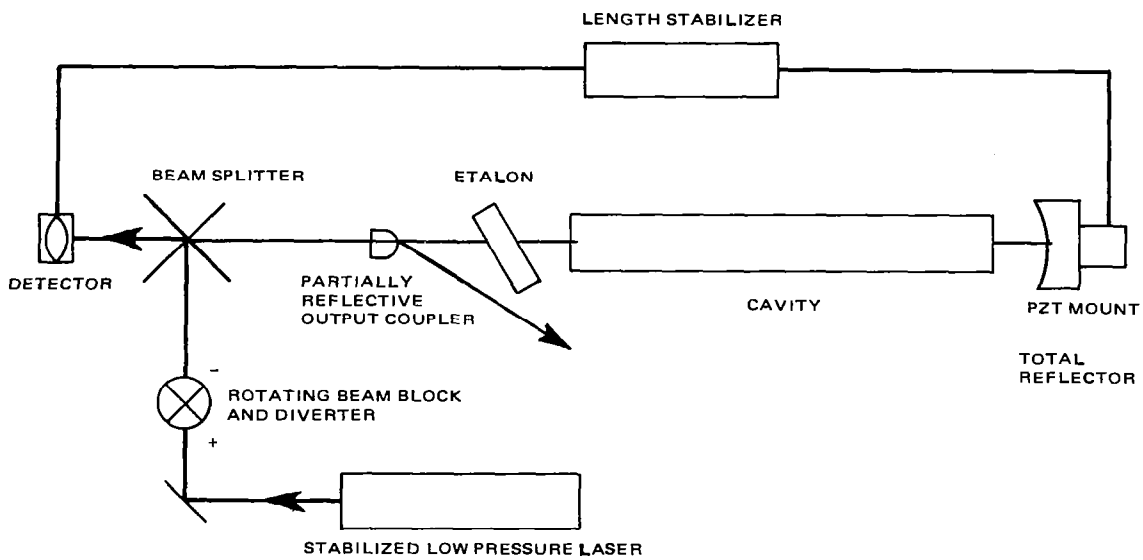

Figure 6-26. Etalon Method of SLM Selection With Length Control.

Pulsed CO_2 Dial Experiment. To handle CO_2 DIAL experiments it is necessary to provide two laser lines, one on the spectral line associated with the specie in question and the other off the line. Several alternatives, as discussed for the visible and near visible sources, are available for accomplishing this. First, two complete laser systems, including the transmitter, the local oscillator and the detector, could be provided, each controlled to a different wavelength. This would be difficult not only from the standpoint of combining the beams, but also from the standpoint of providing sufficient pallet space, cooling, and power to include two pulsed CO_2 lasers without halving the pulse repetition rate. Another possibility would be to utilize an active

tuning system whereby one flight tunable laser is used. This approach would require that the laser system alternately operate on and off the species line for short times. This method could be implemented from a laser technology viewpoint in a manner similar to that discussed for the visible system. Different sample volumes would be probed at each wavelength giving rise to large measurement uncertainties depending on the field of view and resolution element size. A third method, which appears best from not only the technology and cost viewpoint, but also offers the capability of probing the same sample volume at both wavelengths is to operate the laser system at two simultaneous wavelengths.

A CO_2 laser, either pulsed or CW, can be made to operate in a mode which provides two or more simultaneous wavelengths in the output. This is easiest to do if the wavelengths arise from different rotational lines in the lasing gas. In this case, the laser would operate at two wavelengths, both stable and of limited noise bandwidth so that heterodyning could be done on the returning signal. The diagram in Figure 6-27 shows how this system might be implemented. The power output of the CW laser would be such that each line contained sufficient power for the experiment. In the pulsed laser, the energy per pulse per line can be made equal to that required by the experiment. The pulse rate, however, may have to be reduced in order to keep the average power required within Shuttle capability.

The implementation of this method is within the present state of the art of laser and detector technology. The impact on the Atmospheric Multi-User Instrument System is that the CO_2 laser transmitter will become slightly more complex while the detector for that laser will be almost doubled in complexity.

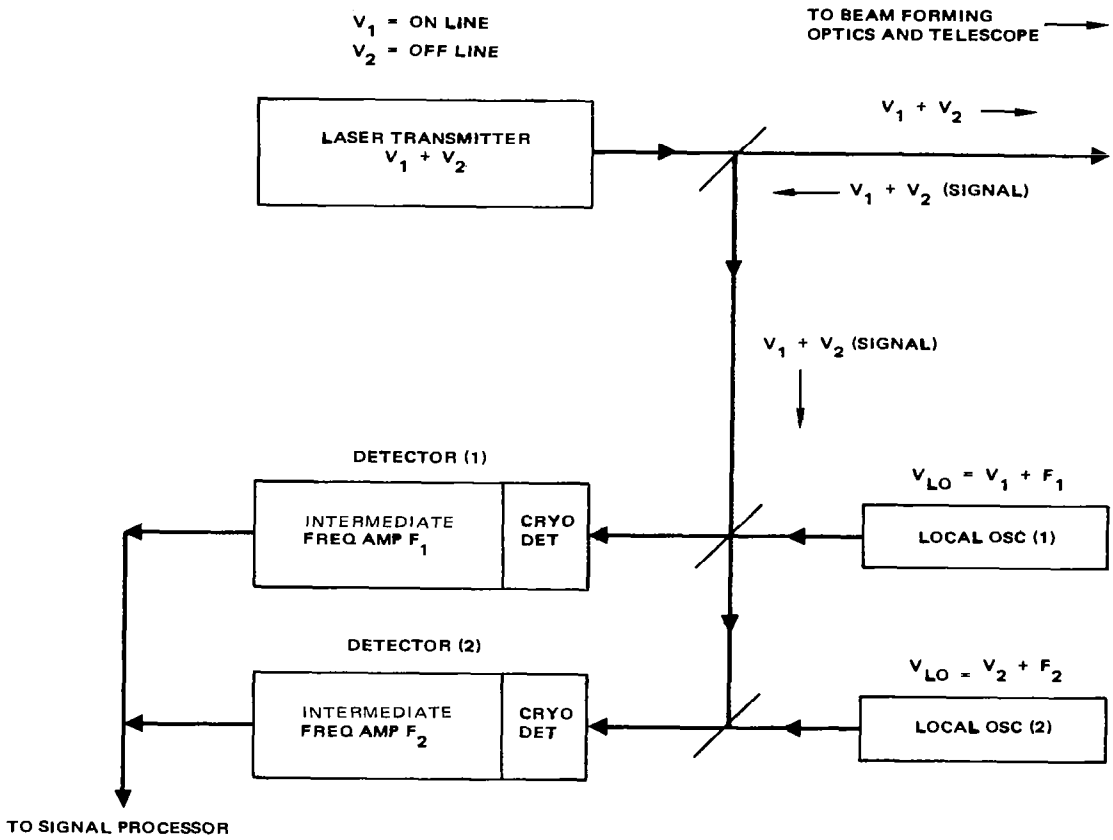

Figure 6-27. Possible System Block Diagram for CO_2 DIAL Experiments.

6.12.2 CONCEPTUALIZATION

A pulsed CO_2 laser with the required performance will look similar to the drawing in Figure 6-28. This drawing shows the major components of a 10 J/pulse laser. Stabilization components are not shown; these would fit within the opening of the flow loop. This laser consists of a laser resonator cavity, rigid optical bench for passive cavity stabilization, e-gun, flow loop with flow smoothing transitions, a fan to circulate the gases and a heat exchanger. Such a device would weigh ~210 kg, have a volume of 330 liters, require 3750 watts of power, and will operate at 4 percent efficiency.

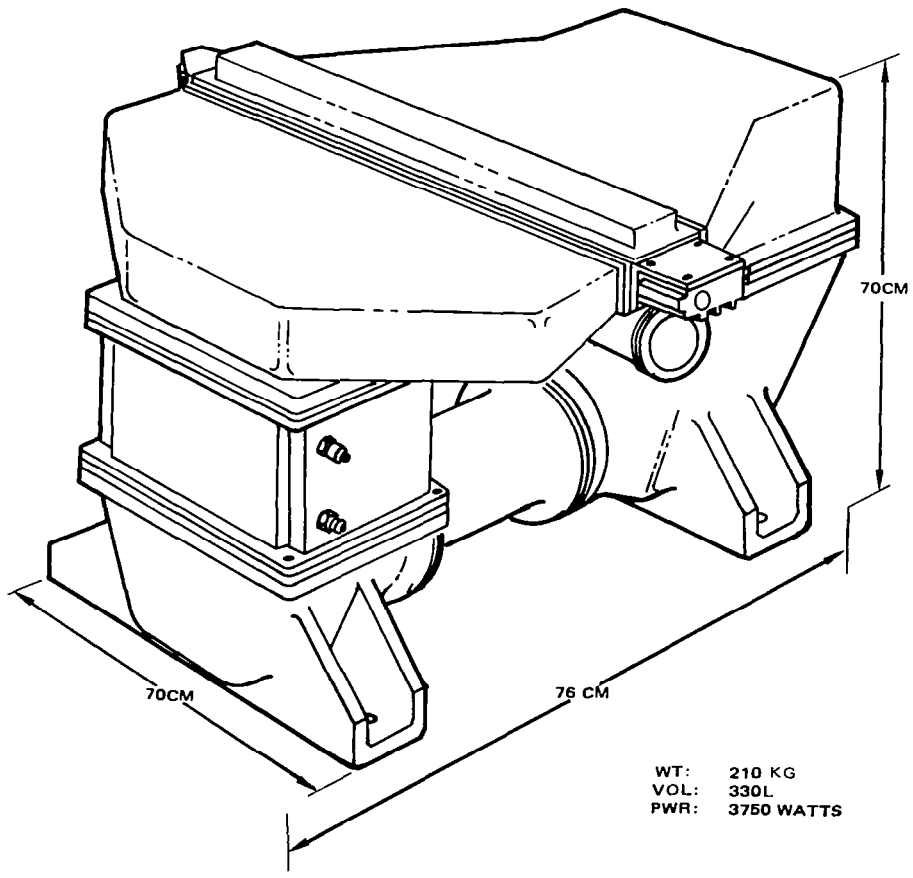

Figure 6-28. Conceptualization of Pulsed CO_2 Laser.

6.13 SPECIAL SOURCES

6.13.1 NARROW LINEWIDTH SOURCES

The purpose of some experiments is to use the Doppler shift of light backscattered by aerosols or atoms to measure wind velocities with typical accuracies of 3 m/s. For light at 500 nm, the backscatter Doppler shift resulting from 5 m/s particles is 20 MHz. In order to obtain such velocity resolution, the laser bandwidth must be smaller than 20 MHz, implying (for transform-limited Gaussian pulses) a pulse length no shorter than 16 ns. Since typical frequency doubled Nd:YAG pulses are about this long, they would have to be transform-limited in order to achieve the accuracy desired. No commercial laser systems of any type can produce pulses with transform-limited bandwidths. For example, the narrowband Quantel TDL dye laser has a bandwidth of 30 GHz, about 100 times the transform limit. Two Nd-pumped dye laser systems (Salour,[32] Wallenstein[33]) with nearly transform limited pulses have been reported recently in research laboratories, but their output energies are less than 1 mJ. Flash-pumped dye lasers may obtain the required bandwidth without being near the transform limit due to their long pulses; however, no commercial systems, and only two laboratory systems, have been operated with the necessary spectral purity. Thus, it is apparent that considerable development is required before a laser with capabilities suitable for these experiments is ready for the Space Shuttle Lidar system.

A possible approach to this problem is to use the injection-locking techniques demonstrated by Blit, et al[34]. A single mode CW argon ion laser pumped dye laser was used as the injection source for a flash-pumped dye laser. Injection-locked output with a 30 MHz bandwidth was obtained, the bandwidth being attributed entirely to jitter in the CW dye laser. Such a laser, properly engineered for use on the Shuttle, would almost meet the experiment requirements. Further linewidth reduction could

easily be achieved by active stabilization of the CW dye laser (due to the inefficient CW ion laser pump source that is required) and space qualification of this additional laser.

6.13.2 HIGH BRIGHTNESS SOURCE

The generation of high intensity laser pulses for two photon excitation of atomic oxygen (Exp. 26) requires the use of a mode-locked laser system.[35] Mode-locking is a technique for generating a train, or regular succession, of ultrashort laser pulses. Although the Nd:YAG based system proposed for the other Space Shuttle Lidar experiments may be used as a baseline for the mode-locked laser design, there are many modifications and additions which must be incorporated if ultrashort, 215.6 nm pulses with energies approaching 1 mJ are to be produced.

A convenient source of tunable, picosecond duration, laser pulses is a short pulse, organic dye laser. Using the baseline Nd:YAG laser system, two principal approaches may be employed to generate ultrashort dye laser pulses which may in turn be frequency doubled or mixed with Nd:YAG pulses to produce high intensity radiation at 225.6 nm. The first approach involves synchronous pumping of a dye laser by a mode-locked train of frequency-doubled or tripled Nd:YAG pulses.[36,37,38] Synchronous mode-locking requires careful matching of the dye laser cavity length to the optical length of the Nd:YAG resonator, to provide the appropriate fluctuating gain condition in the dye laser. A single dye laser pulse must then be selected from the mode-locked pulse train, amplified and frequency converted in order to produce a 1 mJ, ultrashort pulse at 226.5 nm. However, significant amplification of the single dye laser pulse is difficult because of the low energy content associated with each frequency tripled Nd:YAG pulse in the laser train which would be used to pump the dye laser amplifier. This problem may be obviated by either: (1) cavity, dumping a single high intensity pulse from a very high Q, synchronously mode-locked dye laser cavity or (2) using a

single Nd:YAG pulse amplified and frequency tripled to pump a short dye laser oscillator and an external dye amplifier.

The former technique would require excitation of the dye laser by a mode-locked train of frequency tripled Nd:YAG pulses. As before, the cavity lengths would be matched to provide the necessary gain condition for buildup of the dye laser pulse. Instead of allowing a fraction of the circulating pulse to be coupled out on each traversal of the cavity, however, the pulse would be confined to oscillate in a high Q resonator. Interaction of the pulse with each subsequent pump pulse would produce further amplification until all of the pump radiation has interacted with the dye medium. The dye laser pulse is then switched out of the cavity, by an electro-optic cavity dumper, and frequency doubled to produce the ultraviolet pulse required for the experiment. Tuning of the dye laser is accomplished by adjustment of a grating and/or an intracavity etalon.

The second approach involves use of a single Nd:YAG laser pulse selected from the mode-locked train, amplified and frequency tripled to pump both a very short dye laser cavity and a dye amplifier. The Nd:YAG laser is passively mode-locked by a standard saturable absorbing solution (Kodak 9860 or 9740) to produce a train of mode-locked pulses with an interpulse spacing equal to the round trip transit time of light in the optical cavity. An optically actuated single pulse selector removes one pulse from the train, and a Nd:YAG amplifier increases the single pulse energy from ~1 mJ to 10-15 mJ. A second amplifier stage increases the energy to ~40 mJ. The pulse is then frequency tripled and pumps the short dye laser. The dye laser cavity should be less than 1 mm in length to allow significant dye laser pulse buildup to occur during transit of the pump through the cell. Tuning of the short dye laser by adjustment of the cavity length, and by varying the angle between the pump pulse propagation direction and the dye resonator axis has been demonstrated.[8]. The dye

laser output may be amplified by using a portion of the original pump pulse as a pump for a dye amplifier. The ultraviolet pulse is generated by frequency doubling the dye amplifier output.

Other techniques may be employed for frequency conversion to the UV. For example, frequency doubled Nd:YAG radiation may be used to pump a dye laser operating at ~575 nm. The output of the dye laser is then frequency doubled and mixed with the residual 1060 nm fundamental source radiation to produce the required UV output. Since an efficient laser dye is used for tunable pulse production, and the residual 1060 nm radiation is used for sum frequency generation, this process offers the potential for high efficiency UV pulse generation. Other alternatives employing optical mixing of pump and dye laser radiation may also be considered. These include, for example, sum frequency generation of frequency doubled YAG pumped dye laser output at 620 nm with 355 nm frequency tripled Nd:YAG radiation, and optical mixing of the output of a dye laser pumped by frequency tripled Nd:YAG radiation with the frequency doubled Nd:YAG pulse which was used for tripling.

An important issue in the development of a mode-locked laser system for UV ultrashort pulse production is the extent of amplification required in the fundamental Nd:YAG pulse train or single mode-locked pulse. Amplification of picosecond duration pulses in Nd:YAG amplifiers can be accompanied by intensity dependent refractive index changes in the amplifier rods. Since the nonlinear index (n_2) is higher in Nd:YAG than in glass systems, single pulse amplification will be limited in the former compared to the latter. The problem becomes more severe as entire pulse trains are amplified; therefore, careful analysis of this nonlinear effect must be made for the baseline Nd:YAG system.

The eventual upgrade of the 1 mJ, 225.6 nm, ultrashort pulse system to a 1 J/pulse level will require the use of an excimer laser amplifier. Development of an efficient excimer system operating near 226 nm is necessary before this technique may be implemented.

6.14 SUMMARY

The purpose of this part of the study was to define a laser sources system suitable for conducting the experiments contemplated for a Space Shuttle Orbiter Multiuser Lidar System in the early 1980's. To these ends, the science working group Science Objectives, Experiment Description, and Evolutionary Flow Document (SEED) was analyzed, and from it functional requirements for the sources were identified. Based on these functional requirements and knowledge of laser properties, a set of evaluation criteria for potential candidate sources were developed. The functional requirements lead to natural groupings of the laser sources; the major groups are (1) sources designed to perform in the visible and near visible, (2) far infrared sources, and (3) "special" sources.

6.14.1 VISIBLE AND NEAR VISIBLE SOURCES SYSTEM

Potential candidate lasers and frequency conversion techniques were evaluted for utilization in the sources system. A modular system based on the neodymium laser was selected. The neodymium laser was the choice as the basic source laser because of its demonstrated outstanding reliability, its advanced state of engineering development, its efficiency, tolerance to environment, compact size and weight, lack of corrosive or limited shelf life components, limited number of components requiring maintenance, and relative simplicity. Other modules in the neodymium subsystem are a frequency doubler and a mixer (frequency tripler). The selected doubler design is an existing hardened breadboard built for military applications. The mixer is very similar to the doubler except for the use of a different nonlinear crystal.

The second subsystem is a laser pumped dye laser with a spectral control module and a tunable doubler. Pumped by the frequency doubled neodymium laser, the dye laser presents low risk while meeting all specifications. Although engineering development is necessary to transform the dye laser from a commercial or laboratory device to flyable hardware, dye laser spectral control and tuning are well understood and are among the most technologically advanced frequency conversion concepts.

In addition to the two primary laser subsystems are the ancillary optics modules to switch from one wavelength to another and to direct beams to the correct output aperture.

The flight engineering status of each of the seven modules was assessed, and detailed designs of various modules were presented when available. Experiment accommodation was discussed, and in all cases the proposed system meets or exceeds the performance required by the SEED.

6.14.2 FAR INFRARED SOURCES

A review of far infrared sources indicated that CW and pulsed CO_2 lasers would provide the require performance. Although CO_2 engineering is not as advanced as neodymium engineering, an objective assessment indicates that existing efforts to harden breadboard designs will likely succeed in the next few years. Technical discussions of CO_2 laser pumping techniques were presented. In addition, several methods of maintaining spectral control were discussed.

6.14.3 SPECIAL SOURCES

Several experiments require "special" sources, that is, sources that are not readily available today and are not likely to exist in flyable form in the near future. The relevant experiments are those that require transform limited pulses to measure wind velocities, and the experiment requiring mode-locked pulses for two photon excitation

of atomic oxygen. Recent studies show these "special" sources are possible to build, but not practical for near term Shuttle applications.

6.14.4 SUMMARY OF SELECTED SOURCES

The choice of lasers for the various spectral and application areas are:

1. Visible and near visible sources
   a. Neodymium:YAG laser (doubled, tripled, quadrupled)
   b. Dye laser (doubled, with spectral control)
2. CW CO_2 laser
3. Pulsed CO_2 Laser
4. Special Lasers
   a. High Peak Power
   b. Very Narrow Line - Long Pulse

6.14.5 RISK ASSESSMENT

During the course of the study a risk assessment was made for each of the laser sources considered. These assessments are listed below for the lasers of choice for each application area.

1. Neodymium

   Mature technology - ready for direct application to flight now.

2. Dye

   Engineering required, particularly in area of unattended, closed loop spectral control.

3. CW CO_2 - Maturing technology - ready in 1980 time period.
4. Pulsed CO_2 - Component technologies available, integration needed.
5. Special sources - Research and development required for space application.

A source development timeline is shown in Figure 6-29.

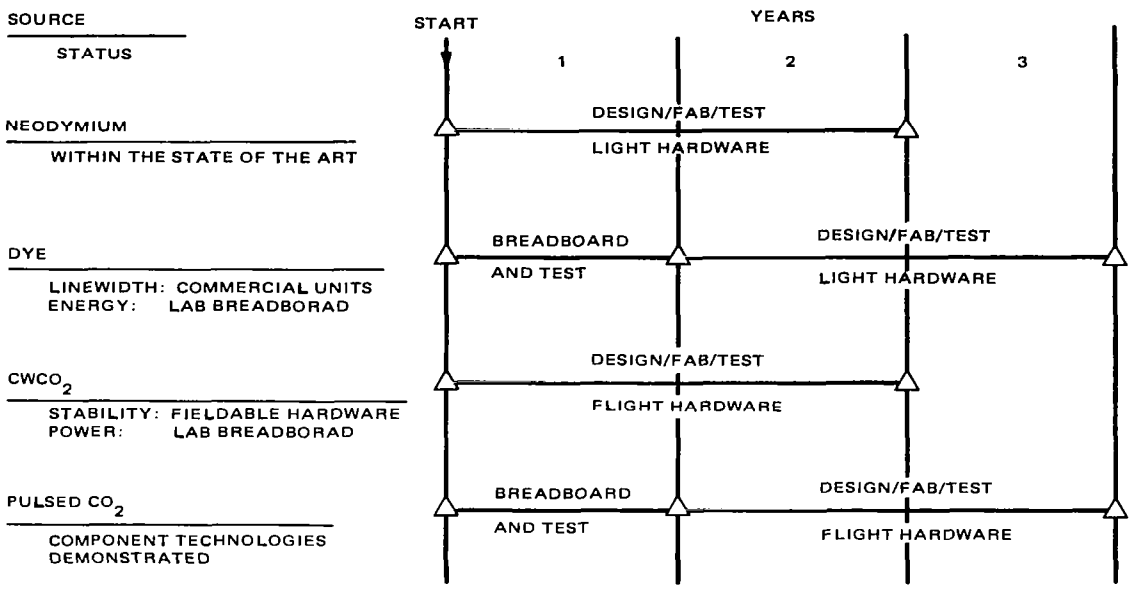

Figure 6-29. Source Development Timeline.

6.15 REFERENCES

1. D. T. Hon, H. W. Bruesselbach, E. J. Woodbury, SPIE Proc. 122 Advances in Laser Engineering, p. 95 (1977).
2. A. Yariv, Intro. to Optical Electronics (New York: Holt Rinehart and Winston, 1971), p.194.
3. Okada, and Ieriri, Jap. J. of Appl. Physics 10, 808 (1971).
4. M. G. Littman and H. J. Metcalf, Applied Optics 17, 2224 (1978).
5. I. Shoshan and U. P. Oppenheim, Optics Communications 25, 375 (1978).
6. J. U. White, J. Opt. Soc. Am. 32, 285 (1942).
7. J. L. Hall and S. A. Lee, Appl. Phys. Lett. 29, 367 (1976).
8. G. W. Scott and A. J. Cox, SPIE Laser Spectrosc. 113, 25 (1977).
9. R. Wallenstein and T. W. Hansch, Opt. Commun. 14, 353 (1975).
10. J. Pinard and S. Liberman, Opt. Commun. 20, 344 (1977).
11. C. Loth, Y. H. Meyer, and F. Bos, Opt. Commun. 16, 310 (1976).
12. R. Wallenstein, Opt. Acta 23, 887 (1976).
13. C. Freed and A. Javan, Appl. Phys. Lett. 17, 53 (1970).
14. C. Borde and L. Henry, IEEE J. Quantum Electron. QE-4, 874 (1968).
15. R. L. Abrams, Appl. Phys. Lett. 25, 304 (1974).
16. A. Landman and H. Marantz, IEEE J. of Quantum Electron. QE-5, 137 (1969).
17. P. C. Claspy and Y. H. Pao, IEEE J. Quantum Electron. QE-7, 512 (1971).
18. R. G. Brewer, M. J. Kelly, and A. Javan, Phys, Rev. Lett. 23, 559 (1969).
19. M. J. Kelly, R. E. Francke, and M. S. Feld, J. Chem. Phys. 53, 2979 (1970).
20. T. A. Nussmeir and R. L. Abrams, Appl. Phys. Letters, 25, 615 (1974)
21. R. C. Lind et al, IEEE J. Quantum Electron. QE-10, 818 (1974).
22. J. Beaulieu, Proc. IEEE 59, 667 (1971).
23. J. D. Daugherty, Bull. Am. Phys. Soc. 17, 399 (1972).
24. W. Stiehl and P. Hoff, Appl. Phys. Lett. 22, 15 (1973).
25. A. Girard, Op. Comm. 11, 4 (1974).

26. A. Gondehalehar, N. Heckenberg, E. Holzhauer, IEEE J. Quantum Electron. QE-11, 3 (1975).

27. D. Hamilton, D. James, S. Ramsden, J. of Phys. E. 8, (1975).

28. J. Lachambre, P. Lavigne, G. Otis, M. Nod, IEEE J. Quantum Electron. QE-12 (1976).

29. J. Izatt, C. Budhirajar, P. Mathieu, IEEE, J. Quantum Electron QE-13, 118 (1977).

30. Lee and R. L. Aggarwall, Applied Optics 16, 2620 (1977).

31. W. Lipchan, Optics Comm. 19, 205 (1976).

32. M. Salour, Opt. Comm. 22, 202 (1977).

33. R. Wallenstein, et. al., Opt. Comm. 14, 353 (1975).

34. S. Blit, et. al., Appl. Phys. 12, 69 (1977).

35. For a review of laser mode-locking see P. W. Smith, M. A. Duguay, Ippen, Mode-Locking of Lasers (Pergamon Press Ltd., 1974).

36. W. H. Glenn, M. J. Brienza, and A. J. DeMaria, Appl. Phys. Lett. 12, 54 (1968).

37. T. R. Royt, W. L. Faust, L. S. Goldberg, and C. H. Lee, Appl. Phys. Lett. 25, 514 (1974).

38. L. S. Goldberg and C. A. Moore, Appl. Phys. Lett. 27, 217 (1975).

7.0 DETECTOR SUBSYSTEM

7.1 INTRODUCTION

During the Task 1 Experiment Evolutionary Analysis the basic detector requirements were established from the analysis of the SEED. These were refined as the analysis continued with inputs from published material, NASA, and the Science Working Group. As the iterative system design process began to unfold, detector configurations and descriptions were developed which would meet those requirements. The definition of the detector subsystem includes the detector processor electronic package, the power supplies, and all the items necessary to interface between the Receiving Telescope Subsystem and the Command and Data Handling Subsystem.

7.2 DETECTOR REQUIREMENTS AND TYPES

The detector requirements which were identified from the SEED are shown on the matrix of Figure 7-1. The detectors are shown on the right side of the matrix with the experiment class numbers up the right hand edge. The form of this matrix was evolved through the course of the study and in the form shown it contains much information, in addition to the detector requirements; for example, the grouping of detectors into six basic types is indicated on the matrix. The detector grouping came out of the system design process in order to accommodate the use of three primary laser positions and three detector positions located around the body of the receiver. Since at least three wavelengths can be obtained simultaneously from one laser, i.e. the fundamental at 1060 nm, the second harmonic at 532 nm and the third harmonic at 353 nm, then the detector must be capable of simultaneously detecting the return from all three wavelengths. In addition, Experiment Class 22, which is the simultaneous measurement of metal atom, ion, and oxides with three different dye laser wavelengths, is easier to accomplish from an operational standpoint with a three element detector package. In experiment classes 10 and 18, which are the CW and pulsed infra-red Dial

EXPERIMENTS	LASERS														DETECTORS							EXPERIMENTS
	EXPERIMENT SUBSET NO	VIII	VII	VI	VA	V	IV	IIIA	III	IIB	IIA	II	IA	I	IA II IIA IIB III IIIA VIII	I	IV V	VA	VI	VII	EXPERIMENT SUBSET NO	
			Nd X 2 VERY NARROW LONG PULSE (3μs)	TWO EACH OF IIA AND ONE OF IIB	Nd X 2 POL 1000:1	TUNABLE PULSED CO_2 HET DET	TUNABLE CW CO_2 HET DET	TWO EACH OF IIB	TWO EACH OF II	Nd X 2 X 3 + D N	Nd X 2 + D N X 2	Nd X 2 + D N	Nd X 4	Nd X 2	1 P M T	2 P M T (INCLUDES 1060 COOLED)	9-11 nm CRYO HET	2 PMT + POL	3 PMT	FAB PER.		
26		226.8								225.6					225.6							26
25										215					215							25
24						o9-11 nm											9-11 nm					24
23								*442 2 448 6								442.2 448.6						23
22				279.6 285.2 500															279.6 285.2 500			22
21										300					300							21
20			530			9-11 nm											9-11 nm			530		20
19			530			9-11 nm											9-11 nm			530		19
18						*9-11 nm											9-11 nm					18
17									*TWO NEAR 760						760							17
16															760							16
15															760							15
14												589								589		14
13						*9-11 nm	*9-11 nm										9 11 nm					13
12											280 300		265		265-300							12
11										455.4 493 4		589			455.4 493.4 589							11
10						*9-11 nm	*9-11 nm										9-11 nm					10
9									*TWO NEAR 720 OR 940						940 720							9
8											279 6				279.6							8
7												589 770 671			589 770 671							7
6														530 + 1060		530 + 1060						6
4																						4
3					530 1000:1 POLARIZED													530				3
2														530 + 1060		530 + 1060						2
1																						1

*TWO SIMULTANEOUS OR NEAR SIMULTANEOUS WAVELENGTHS
oMULTIPLE WAVELENGTHS
EXPERIMENT NO 5 IS INCLUDED AS PART OF EXPERIMENT NO 2
WAVELENGTHS ARE IN NANOMETERS EXCEPT AS INDICATED

Figure 7-1. Experiment Hardware Requirements

experiments, a more complex problem is presented. In order to handle CO_2 DIAL experiments it is necessary to provide two laser lines, one on the spectral line associated with the specie in question and the other off the line. Several methods are available for accomplishing this. First, two complete laser systems, including the transmitter, the local oscillator, and the detector, could be provided, each operating on a different wavelength. This would be difficult not only from the standpoint of combining the beams but there is insufficient space within the pallet to include two pulsed CO_2 lasers; nor is there power enough to operate them without halving the pulse repetition rate. Another possibility would be to utilize an active tuning system whereby one laser is used which can be tuned in flight from one wavelength to another. This system would require that the laser system operate on the specie line for a short time then be retuned to operate off the specie wavelength for a short time. This method could be implemented from a laser technology viewpoint but different sample volumes would be probed at each wavelength giving rise to large measurement uncertainties. A third method which appears best from both the technology and cost viewpoint and also offers the capability of probing the same sample volume at both wavelengths is to operate the laser system at two simultaneous wavelengths.

A CO_2 laser, either pulsed or CW, can be made to operate in a mode which provides two or more simultaneous wavelengths in the output. This is easiest to do if the wavelengths arise from different rotational lines in the lasing gas. In this case, the laser would operate at two wavelengths, both stable and of limited noise bandwidth so that heterodyning could be done on both the returning signals. The power output of the CW laser would be such that each line contained the power output required by the experiment. In the pulsed laser, the energy per pulse per line can be made equal to that required by the experiment. The pulse rate, however, may have to be reduced in order to keep the average power required from the shuttle within the bounds of availability. In all cases, however, both the on and off line wavelengths

do probe the same volume of aerosol. The modular design of the system also allows for the inclusion of lasers and detectors not yet identified to fit the descriptions given in the SEED for experiment class 13, which discusses absorption measurements in the 3.5 to 15 μm spectral range.

The detector types shown on the matrix of Figure 7-1 represent the minimum configurations required to meet the requirements of the SEED document. It is conceivable and perhaps desirable that other or more complicated configurations will be needed as the capabilities of the system become known and expanded experiments are proposed. The three basic wavelengths from the neodymium laser mentioned above are a good example of this. While not mentioned in the SEED, it has become apparent through interactions with the Science Working Group that it would be highly desirable to utilize those three wavelengths in order to expand the quantity and quality of science data obtainable in Experiment Class 6, which involves the measurement of stratospheric aerosols. There is sufficient space available around each detector location so that the detector packages can take a large variety of shapes and volumes.

Figure 7-2 gives a detailed description of the minimum detector types identified in the SEED. This Figure shows 6 basic detector packages and indicates that 5 types of photomultipliers will be required to cover the wavelength range. The wavelengths are identified, as are the experiment classes from the SEED which are performed by each detector package. A more detailed description of the contents of each detector package is given on the chart of Figure 7-3. A summary of the characteristics of the packages is shown in Figure 7-4.

NO.	DETECTOR PACKAGE	PMT	WAVELENGTH (NM)	EXPERIMENT CLASS
1	SINGLE PMT	A	215	25
		A	265	12
		A	279.6	8
		A	297	12
		A	300	21
		B	455.4	11
		B	493.4	11
		B	589	7,11
		C	844.9	26
		C	720	9
		C	760	15,16,17
		C	940	9
2	TWO PMT	B	442.2	23
		B	444.6	23
		B	530	1,2,4,6
		D	1060(REQUIRES PHOTOCATHODE COOLING)	
3	TWO PMT WITH POLARIZATION SEPARATION	B	530	3
		B	530	
4	THREE PMT	A	285.2	
		A	279.6	22
		B	500	
5	FABRY-PEROT INTERFEROMETER	E	530	19,20
		E	589	14
6	TWO FAR INFRA RED CYROGENIC	NONE	9-11μm	10,13,18,19,20,24

PMT LETTERS INDICATE GENERAL WAVE LENGTH RANGE

Figure 7-2. Detector Types

- SINGLE PMT
  - MULTIPLE PMT TYPES
  - MULTIPLE FILTER WAVELENGTH
- DOUBLE PMT
  - MULTIPLE PMT TYPES INCLUDING COOLED NEAR IR TUBE
  - MULTIPLE FILTER WAVELENGTHS
  - DICHROIC BEAM SPLITTER
- DOUBLE PMT WITH POLARIZATION SEPARATION
  - SINGLE FILTER
  - MOUNTS ON AXIS OF TELESCOPE
- TRIPLE PMT
  - MULTIPLE PMT TYPES
  - MULTIPLE FILTER WAVELENGTHS
  - DICHROIC BEAM SPLITTERS
- FABRY-PEROT INTERFEROMETER
  - MULTIPLE RING DETECTOR
  - MOUNTS ON AXIS OF TELESCOPE
- FAR INFRA-RED CRYOGENIC (TWO EACH)
  - HETERODYNE DETECTION
  - MOUNTS ON LASER OPTICAL BENCH
  - TRANSMIT/RECEIVE IDENTICAL PATH THROUGH TELESCOPE
  - INFLIGHT TUNABLE LOCAL OSCILLATOR

Figure 7-3. Detector Type Descriptions.

- SIX DETECTOR PACKAGE TYPES
  - 4 TYPES OF PHOTOMULTIPLIERS - BY WAVELENGTH
  - 10^5 DYNAMIC RANGE
  - PHOTON COUNTING CAPABILITY
  - 24 FILTER WAVELENGTHS - OVEN CONTROLLED
  - POLARIZATION SEPARATION
  - HIGH DISPERSION ELEMENT AND MULTIPLE RING DETECTOR
  - HETERODYNE INFRA-RED DETECTORS
  - RUGGEDIZED FOR ENVIRONMENT
  - REGULATED HVPS FOR PMT'S

Figure 7-4. Detector Type Requirements.

7.3 DETECTOR SUBSYSTEM AND COMPONENTS

A block diagram of the detector subsystem is shown on Figure 7-5. This diagram shows one each of the single, double, and triple photomultiplier detector packages and how they interface with the remainder of the subsystem. In practice any combination of detector packages can be assembled into the subsystem to meet the needs of a particular flight profile. The block diagram shows that light from the receiver subsystem enters any one of the detector packages where it is converted in the detector or detectors to an electrical signal which is then sent to the detector processor. Other on-axis detector packages can also be fed into the processor. The Detector Processor Unit is the electrical interface between the detectors and the Command and Data Handling subsystem. This component will be discussed later in this section.

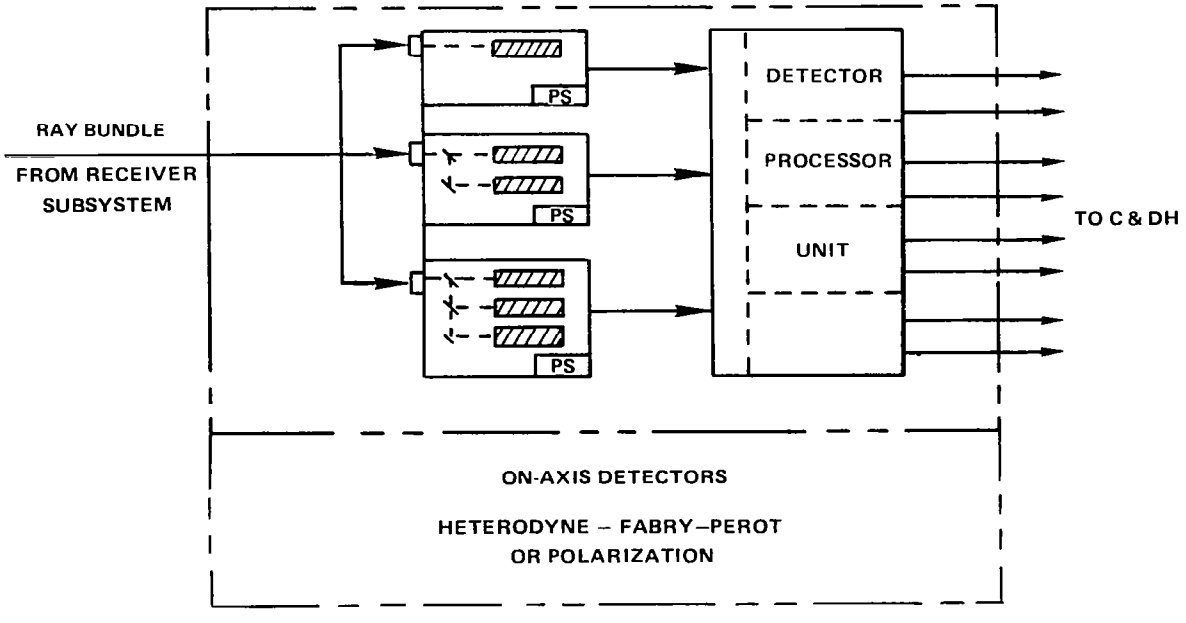

Figure 7-5. Detector Subsystem Block Diagram.

Figure 7-6 shows a detail block diagram of the contents of the single photomultiplier detector package and how it interfaces with the remainder of the subsystem.

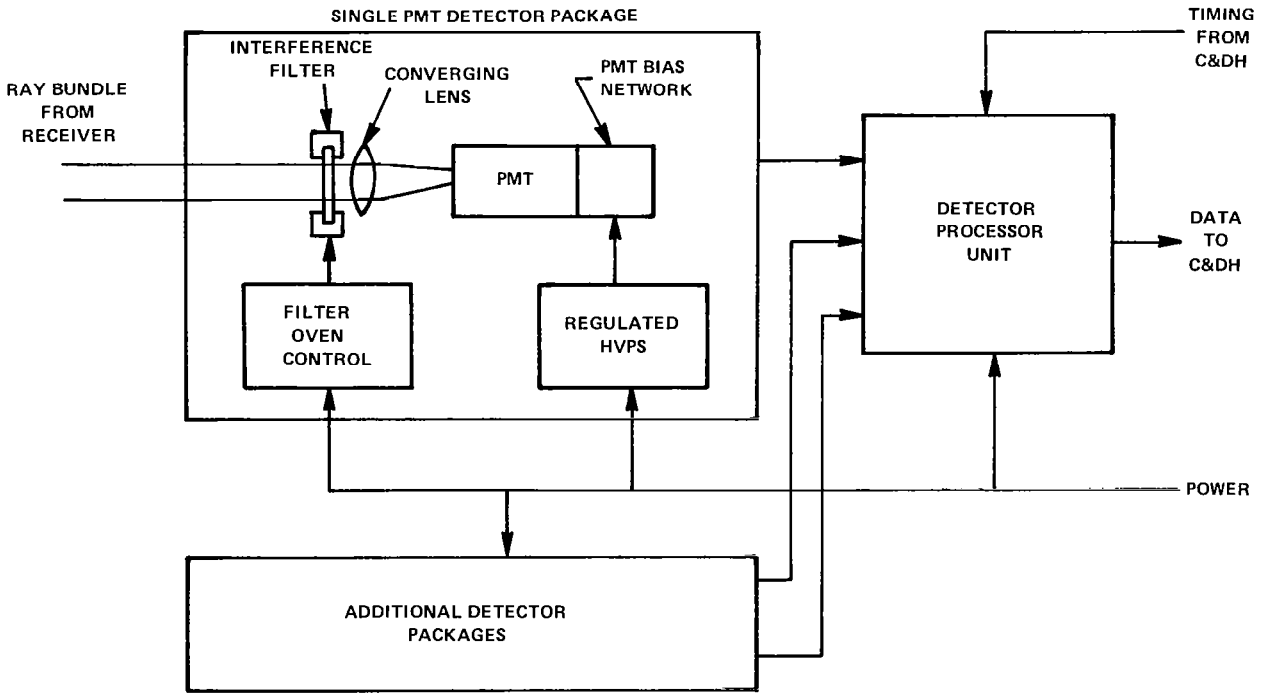

Figure 7-6. Detector Package Detail Block Diagram.

The narrow band filter, which is included in the detector package, receives the collimated ray bundle from the receiver. The clear aperture at this point is 45 mm in diameter. The narrow band filters are temperature controlled by an oven in order to maintain their passband centered on the desired wavelength. An assessment of narrow band interference filter availability was made. The results of that assessment are shown in Figure 7-7. This graph shows a plot of filter bandwidth in nm plotted against wavelength in nm. On the graph is a curve of the approximate filter

bandwidths presently available at wavelengths between 200 and 1000 nm. Filters of two general types are illustrated in the chart. Down to about 400 nm, solid spacer layer filters are available with bandwidths ranging down to 0.01 nm. Below about 400 nm it becomes necessary to go to evaporated spacer layers and the minimum available bandwidth rises sharply in the ultraviolet. Other filter types such as air spaced etalons may be available for flight use and should be examined nearer to the system flight time. Also presented in Figure 7-7 are the bandwidth requirements from selected experiment classes to indicate where the present availability curve covers the requirements stated in the SEED.

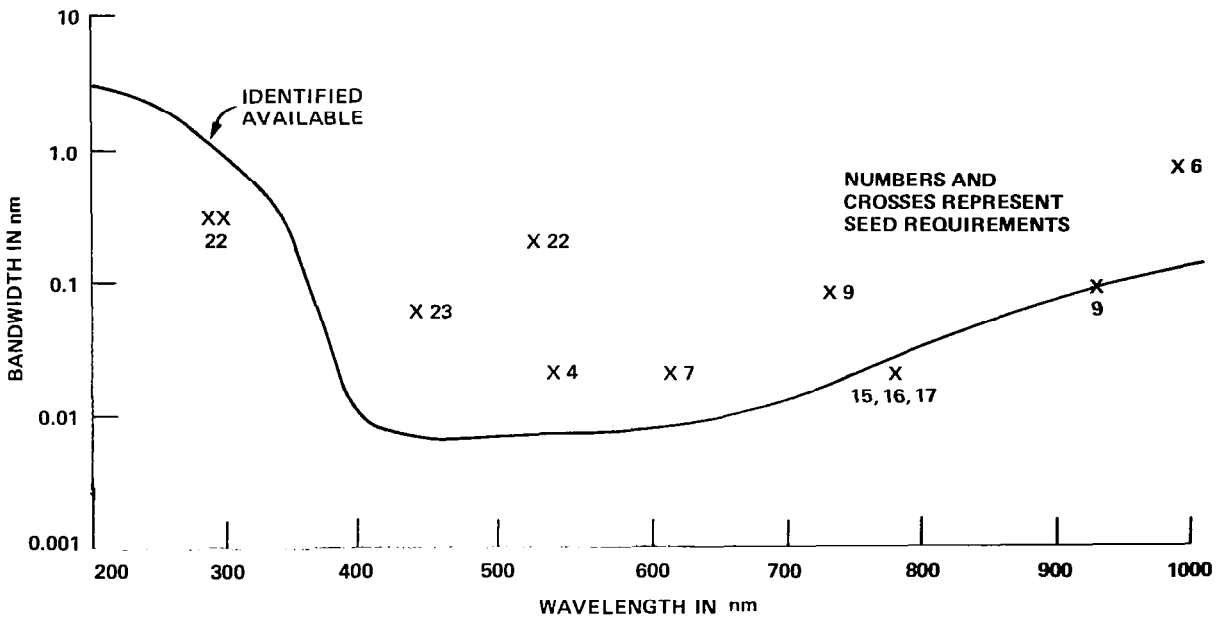

Figure 7-7. Initial Narrow Band Interference Filter Bandwidth Assessment.

After the ray bundle passes through the filter it is converged by a lens so that the light falls on the photocathode of the photomultiplier tube in an area about 1 cm in diameter. In the near IR tube this is about the total diameter of the photocathode. In many types of photomultiplier tubes, the photocathode is not uniform across the

face of the tube, generally having a broad maximum in sensitivity near the center. This should be evaluated on the tubes chosen for use by mapping the photocathodes to insure that they are illuminated in the most sensitive area.

A large variety of photomultiplier tubes are available in ruggedized versions which could be used for the Lidar system application. Another requirement on the tubes is, of course, that they have the highest quantum efficiency available at a given wavelength. The graph on the right of Figure 7-8 shows the approximate quantum efficiencies which are available as a function of wavelength. The second graph of Figure 7-8 shows another required feature of the tubes for this application. It is a graph of the typical pulse height spectrum for photomultiplier tubes of the class which exhibit very high gains (in the order of 20 to 60) at the first dynode. This is often accomplished by using a gallium-phosphide first dynode with high voltage (600 to 1000 volts) between the photocathode and the first dynode. The effect of this

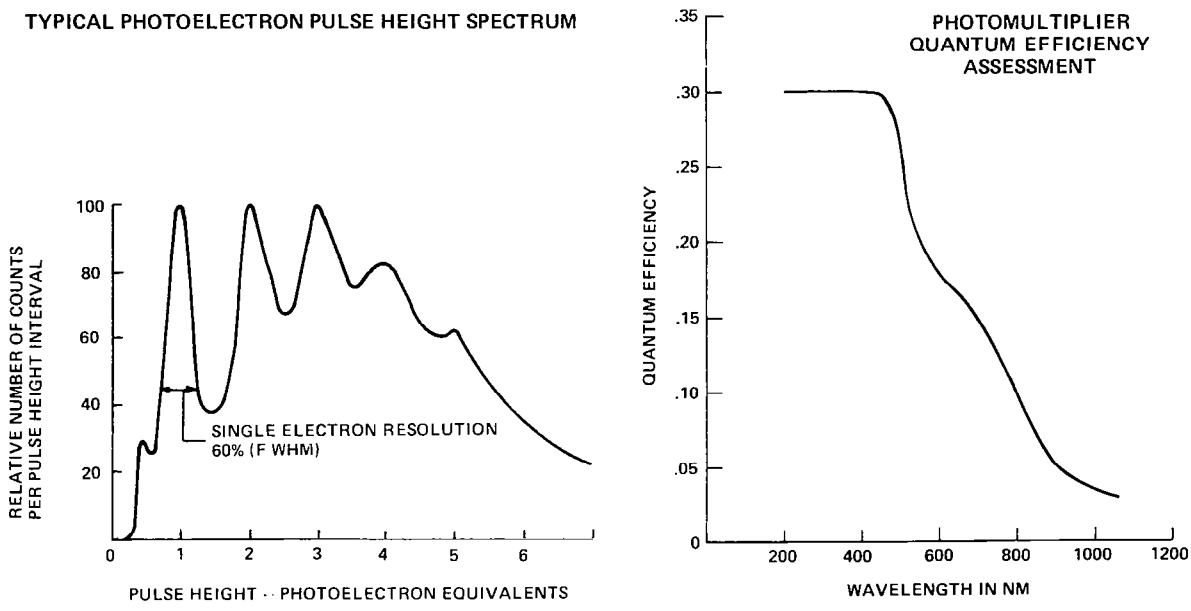

PMT AVAILABILITY SURVEY INDICATES PMT'S ARE AVAILABLE IN RUGGEDIZED VERSIONS WITH HIGH QUANTUM EFFICIENCY, DESIRED COUNTING STATISTICS AND WIDE DYNAMIC RANGE.

Figure 7-8. Requirements for Photomultiplier Tubes.

combination is to preferentially amplify photoelectrons from the photocathode, as shown on the graph, to produce the characteristic peaks for single, double, and triple photoelectron events. When more than 3 simultaneous photoelectrons are emitted by the photocathode the variations in pulse width caused by multiple amplifications in the dynode string begin to widen the pulse and resolution is lost. The result is that tubes of this type, when used with very simple amplitude gating at the anode, exhibit dark currents which are in the region of only 300 to 600 counts per second. This will provide only about 10^{-3} dark counts per one km range bin while the tube is in operation. This effectively removes the photomultiplier dark current as a major source of noise in the system.

The near infra-red photomultiplier tube identified for use at 1060 nm is a recent development by Varian which provides photocathode quantum efficiencies of up to 5% at the neodymium laser fundamental wavelength. This class of tubes is ruggedized for flight use and exhibit excellent electron multiplication characteristics and very low dark current. The only disadvantage of tubes of this type is that for optimum results the photocathode must be kept at or below $-20^{\circ}C$ during the entire useful life of the tube, not only in operation but during non-operating times as well. This is accomplished with a thermoelectric cooler attached to the tube. The design of the Atmospheric Lidar Multi-User Instrument System includes a nickel-cadmium battery to provide power to the cooler during times that Shuttle power is not available.

7.4 DETECTOR PROCESSOR

The detector signal processor is the electronic interface between the photomultiplier anode and the Command and Data Handling Subsystem. Practically, it is a complicated element of electronic circuits which generates the range bins and digitizes the information in each range bin. An outline of the requirements for the detector processor unit is shown in Figure 7-9.

- 2000 RANGE BINS
- MINIMUM RANGE BIN SIZE 10 METERS (66.7 NS)
  - TOTAL RANGE COVERED AT MINIMUM BIN SIZE – 20 KM
  - CAN LOOK AT ANY 20 KM SEGMENT OF ATMOSPHERE
- MAXIMUM RANGE BIN SIZE UNLIMITED
  - FOR EXAMPLE IF MAXIMUM BIN SIZE IS 50 METER (333 NS)
  - TOTAL RANGE COVERED AT MAXIMUM BIN SIZE = 100 KM
  - LARGER BIN SIZES (1-2 KM) OBTAINED ON GROUND BY PROCESSING DATA
- OVERALL AMPLITUDE ACCURACY GOAL FOR DETECTOR IS 1% OR ± BIT WHICHEVER IS LARGER FROM OUTPUT SIGNAL THROUGH DIGITIZED DATA
- OVERALL DYNAMIC RANGE OF DETECTOR SYSTEM 10^5 WITH AUTO GAIN CONTROL
- AUTOMATIC GAIN CHARGE CAN LOSE MAXIMUM OF 100 NANOSECONDS OF DATA
- RANGE ACCURACY ± 0.5 μsec
- INCREMENTAL RANGE ACCURACY ± 0.03 μsec

Figure 7-9. Processor Unit Requirements.

The study results indicated that an analog sample and hold range bin storage should be used. The reason for this was that the count rates calculated for the maximum signal case and the daytime case (due to background noise) were so high that large numbers of pulses would not be counted because of overlap in the pulses at the anode of the photomultiplier tube. Calculations of pulse rates at the anode of the

photomultiplier for selected experiments using the system parameters, which have been described, and daytime operation indicate that pulse rates of the order of 10^8 per second will be encountered. A nominal value for the pulse width at the anode for a single photoelectron event is about 2.7 nanoseconds. The pulses are randomly spaced in time so that at this count rate significant numbers of pulses would be lost if a simple pulse counting technique were used. The analog sample and hold system, on the other hand, can handle the high count rates and can also provide accurate data in the one count per range bin area.

A block diagram of the detector processor is shown in Figure 7-10. The processor consists of an automatic gain changing amplifier followed by 2000 range bins which are contained on 100 large scale integration (LSI) circuit chips. These range bins

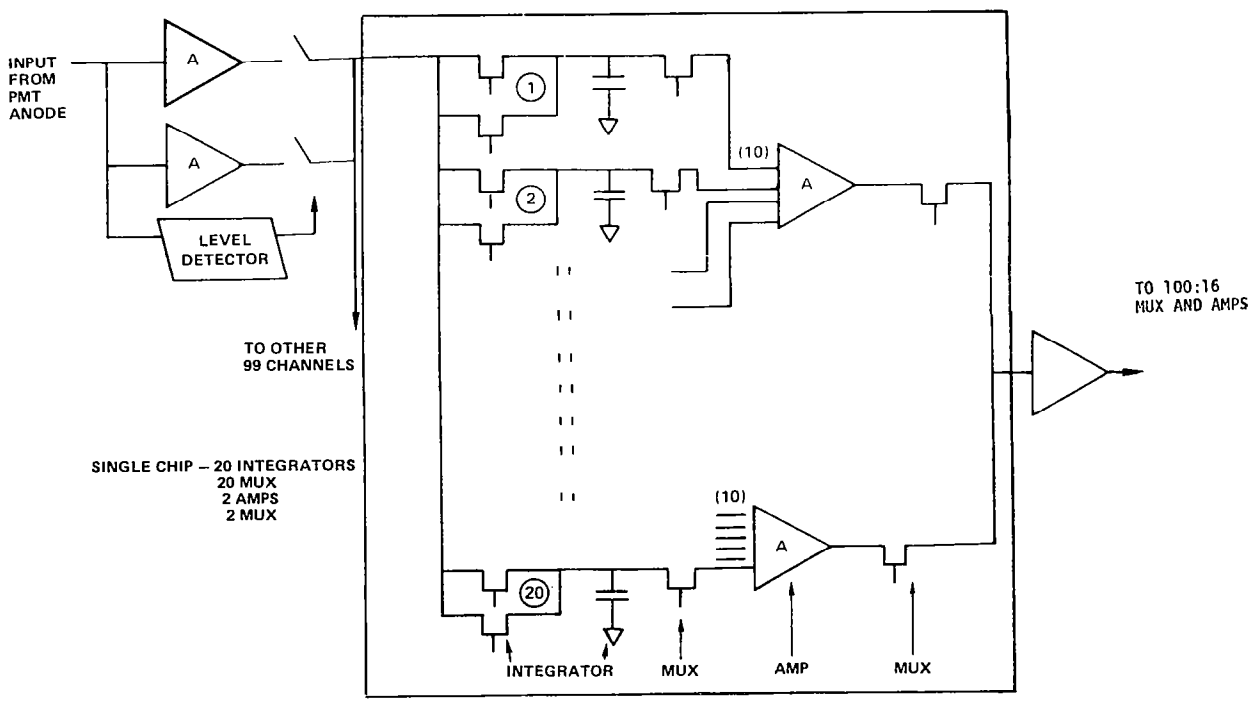

Figure 7-10. Detector Processor Channel Block Diagram.

are followed by isolation amplifiers and multiplexers and finally the analog to digital converter which sends the digital data to the Command and Data Handling Subsystem. A more detailed block diagram of one of the LSI chips which contains 20 sample and hold range bins, two buffers, and the multiplexers required to go to the next buffer amplifier, is shown in Figure 7-11.

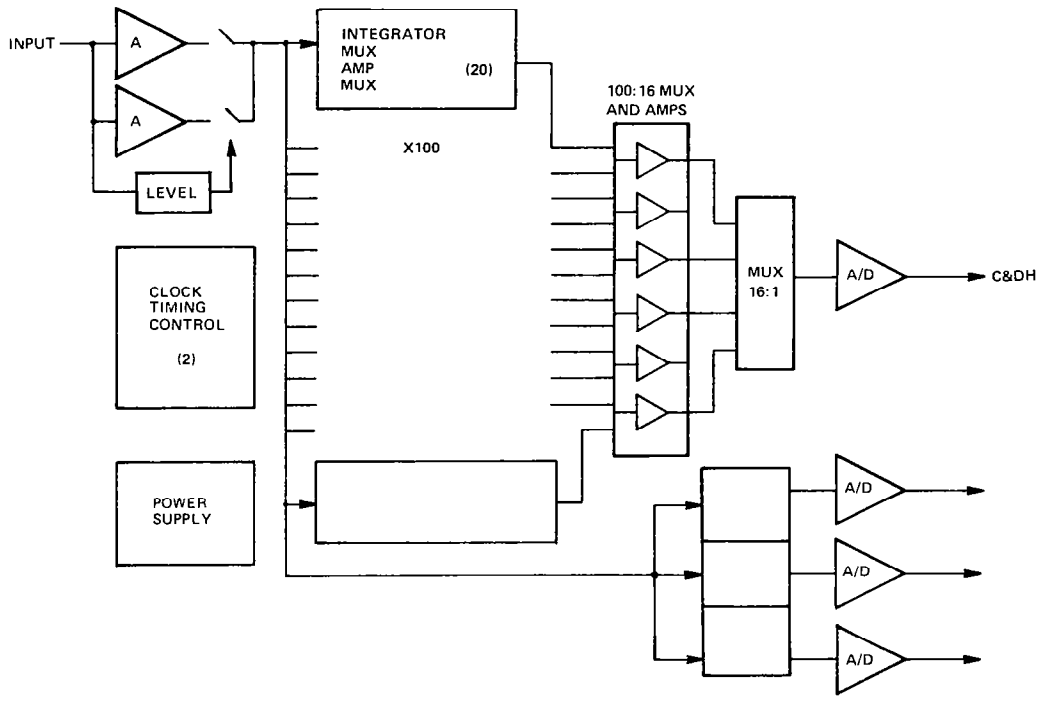

Figure 7-11. Detector Processor Block Diagram.

There are four detector processor units used in the detector subsystem. Three may be required at any one time with the fourth unit used as a spare to improve reliability. The details of the switching matrix which switches the processors between detectors is not shown on the block diagrams.

7.5 DETECTOR SUBSYSTEM PHYSICAL SUMMARY

A summary of the volume, weight and power requirements of various components which go to make up the detector subsystem is shown in Figure 7-12. The detector components are of reasonable size except for the Fabry-Perot detector. It must be remembered that its volume includes all the optics and thermal control enclosure for the interferometer in addition to the interferometer components. It is expected that the Fabry-Perot interferometer will be of the type which is currently under development by NASA for use in satellites.

DETECTOR ITEM	VOLUME (LITERS)	WEIGHT (Kg)	POWER (WATTS)
SINGLE PMT	3	4	35
TWO PMT	6	8	70
TWO PMT WITH POLARIZATION	6	8	70
THREE PMT	9	12	110
FABRY-PEROT (1) INTERFEROMETER ASSEMBLY	340	16	60
DETECTOR	10	3	30
SUPPORT PACKAGE	330	13	30
CRYOGENIC HETERODYNE (2) DETECTORS	1	2	SMALL
DETECTOR PROCESSOR UNIT	17	14	60

(1) FABRY-PEROT INTERFERFEROMETER VOLUME IS ABOUT 10 LITERS AND MAY NEED LARGE INSULATED SUPPORT PACKAGE. THIS DETECTOR IS USED ON-AXIS AND NOT ON THE RING BENCH.
(2) LOCATED INSIDE LASER PACKAGE OUTLINE

Figure 7-12. Detector Subsystem Physical Characteristics Summary.

7.6 RISK ASSESSMENT

The risk assessment indicates that detectors present a mature technology and the components are available. The signal processor/digitizer technology is available in semiconductor LSI format. Some specialized chip design, development, and integration needs to be done but the technology is ready and in use. The Fabry-Perot interferometer and cryogenic heterodyne detector component technologies do need to be integrated before these items can be considered flight worthy.

8.0 COMMAND AND DATA HANDLING SUBSYSTEM

This section discusses the Lidar Command and Data Handling (C&DH) Subsystem. This subsystem is responsible for the handling and processing of science data, both prime and correlative, commands, ancillary data, and housekeeping information. The extent of processing and the methods of handling the various data are discussed in the following paragraphs. The initial portion of this section defines the terms used and the requirements, imposed on the data system by the scientific and functional requirements and the science parameters. In the later portion, tradeoffs and analyses that were performed are identified, and the Lidar C&DH subsystem, as designed on the conceptual level, is presented and discussed.

8.1 INTRODUCTION

An overview of the entire end-to-end Space Transportation Data System is required in order to understand the terms used in the following discussions as well as to obtain an overall perspective of the role of the data handling subsystem. The data originated by the experiment hardware in the Spacelab are transmitted via the Orbiter, as shown in Figure 8-1, to the TDRS relay satellite, then to the TDRS ground station at White Sands, New Mexico, then via DOMSAT to other locations. The Spacelab

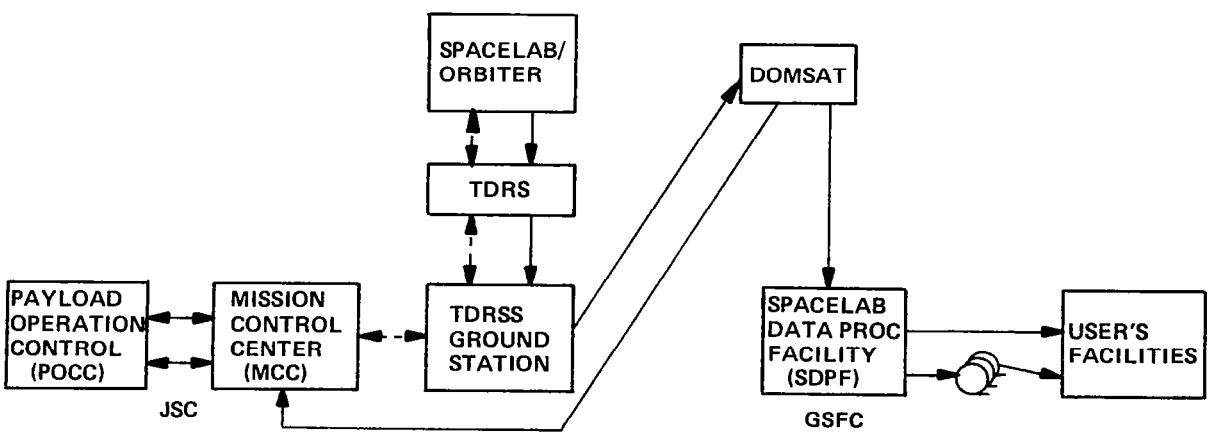

Figure 8-1. The End to End STS Data System.

Data Processing Facility (SDPF), located at Goddard Space Flight Center, will process the data into a standard format, remove overlaps caused by onboard tape recorders (which will be discussed later), annotate the data as required, and deliver the data to the experimenter for his use within one month after the flight. At the same time, the data is transmitted to the Mission Control Center and into the Payload Operation Control Center (POCC) located at Johnson Space Center in Houston. Presumably the Principal Investigator (PI) will be resident at the POCC during the flight mission and will control and/or monitor the operation of the experiment either directly via commands from the POCC or in conjunction with the Payload Specialist onboard the Spacelab via voice communication.

8.2 REQUIREMENTS

The basis for the design of the C&DH Subsystem is derived from requirements. These are imposed by the science needs, which define data rates, accuracies, and repetition rates, and the functional requirements which define the functions to be performed by the data handling subsystem. The functional requirements include collecting, formatting, and transmitting the data to the POCC and the SDPF via the links available to the Space Transportation System (STS), and displaying of the detector output to the Payload Specialist to enable him to perform certain functions based on the data he is observing (in particular the output of the photomultiplier tubes will be displayed as co-alignment routines are performed). The functional requirements also include programming the receiver and transmitter co-alignment devices, performing housekeeping functions, and evaluating system operating performance and displaying the operating parameters to the Payload Specialist. These parameters include laser energy, temperatures, pressures, voltages and other functions of interest to the operation of the experiment. The C&DH subsystem must also be capable of recognizing anomalous operating modes and alert the Payload Specialist to these

modes; it must also allow the Payload Specialist to reconfigure the system so that he may reestablish new configurations which work around defective components such that, if not the Prime experiments, at least some experiments can still be performed. Overall the Lidar C&DH subsystem must support the flight operation during the mission. It must also support instrument integration and test prior to the mission and support the integration of the Lidar system with Spacelab.

The requirements imposed by science on the C&DH subsystem are shown in Figure 8-2 and are tabulated in terms of modes, according to the height of the measurement in the atmosphere and the range resolution requirement in meters. Figure 8-2 relates the timed intervals to the specific portions of the laser and detector waveshapes. Typical experiment classes corresponding to each of these modes are indicated in Figure 8-3.

MODE	TOTAL HEIGHT (KM)	RESOLUTION (M)	ACCURACY $\frac{\Delta S}{S}$	DYNAMIC RANGE	T_1 (MS) (FROM	T_2 (μS) 300 KM	T_3 (MS) ALTITUDE)	NO. BINS	READ-IN SAMPLE RATE (SAMPLES /SEC)	READ-OUT SAMPLE RATE (SAMPLES /SEC)	READ-OUT RATE (Kbps)
A	20	10	1%	10^5	1.87	133	100	2000	15M	21K	253
B	20	50	1%	10^5	1.87	133	100	400	3M	4.2K	51
C	20	150	1%	10^5	1.87	133	100	133	1M	1.4K	17
D	100	150	1%	10^5	1.33	666	100	667	11M	7.0K	84
E	400	1000	1%	10^5	0	1334	100	200	150M	2.1K	25

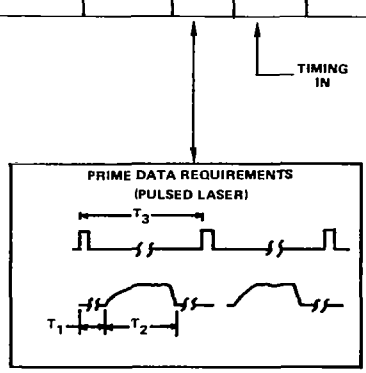

Figure 8-2. Science Requirements.

MODE	TOTAL HEIGHT (KM)	RESOLUTION (M)	TYPICAL EXPERIMENT CLASS
A	20	10	15 - SURFACE PRESSURE, CLOUD TOP PRESSURE, AND HEIGHT MEASUREMENT
B	20	50	11 - CLOUD TOP HEIGHT
C	20	150	2 - TROPOSPHERIC CLOUDS AND AEROSOL, AND SURFACE REFLECTANCE
D	100	150	14 - SODIUM TEMPERATURE AND WINDS
E	400	1000	11 - CHEMICAL RELEASE

Figure 8-3. Experiment Grouping By Requirements.

The total height in kilometers and the resolution in meters define the number of bins required. The most demanding mode establishes the upper bounds for the C&DH subsystem. In particular this mode requires 2000 bins and results in a readout rate of 253 kilobits per second. All the other modes, which require fewer bins and a lower readout rate, can readily be satisfied by the same system. These data are based on the assumptions of an altitude of 300 km, a pulse repetition period (T3) of 100 milliseconds, and that buffering is provided in the detector electronics subsystem such that the data which is read into the Lidar system in a relatively short period (T2) of the order of 100 microseconds is read out into the C&DH subsystem in 95 milliseconds. This buffering results in a readout rate of 21,000 samples per second, and on the basis of 12 bits per sample (to maintain dynamic range and accuracy requirements), results in a maximum readout rate of 253 kilobits per second for mode A. The other modes are correspondingly lower. T1 is the period between transmission of the laser pulse and the start of the returned energy sensed by the detectors.

8.3 DESIGN

Processes are performed on the various data, as shown in Figure 8-4, at three different locations: On-Board and during integration, at the POCC, and at the SDPF.

DATA TYPE	INTEGRATION/ONBOARD	POCC (JSC)	SDPF (GSFC)
SCIENCE DATA – PRIME	FORMAT, BUFFER, MERGE OSCILLOSCOPE DISPLAY TO PAYLOAD SPECIALIST	EXTRACT TBD FOR P.I. QUICK-LOOK	TIME SEQUENCE ORDER, REMOVE OVERLAP, TIME TAG, FORMAT, QUALITY CHECK.
– CORRELATIVE	FORMAT, BUFFER, MERGE	EXTRACT TBD FOR P.I. QUICK-LOOK	SAME AS ABOVE
COMMANDS	ISSUE VIA KEY BOARD ISSUE VIA PRE-STORED PROGRAM DECODE DISTRIBUTE	ISSUE VIA KEYBOARD	N/A
ANCILLARY DATA	FORMAT (MERGE) DISPLAY	EXTRACT DISPLAY INCLUDE IN PRIME DATA PROCESSES (AS REQ'D) FOR QUICK LOOK	SAME AS SCIENCE DATA
HOUSEKEEPING	FORMAT (MERGE) HI-LO LIMIT CHECKS CONVERSION TO ENGINEERING UNIT DISPLAY	EXTRACT HI-LO LIMIT CHECKS CONVERSION TO ENGINEERING UNIT DISPLAY INCLUDE IN PRIME DATA PROCESSES (AS REQ'D) FOR QUICK LOOK	SAME AS SCIENCE DATA

Figure 8-4. Lidar Data Processes.

8.3.1 The End-To-End System

The design of the Lidar C&DH must be made within the context of the overall end-to-end system and must consider the Lidar instrument parameters, the capabilities available on Spacelab and the Orbiter, as well as the links and the operation of the ground facilities. For example, the equipment (and its capabilities) which is available at the POCC will determine if certain processes should be performed by the C&DH subsystem or on the ground by this equipment. As will be discussed later the

Spacelab Command and Data Management System (CDMS) offers significant data processing facilities and capabilities, as do various elements in the Orbiter avionics. A major issue is the extent which the C&DH subsystem should make use of the Spacelab CDMS and of the Orbiter avionics.

Less direct to the design of the Lidar C&DH but somewhat pertinent is the extent of the use that is made of the general purpose facilities at the POCC versus use of dedicated equipment such as the Lidar Electrical Ground Support Equipment (EGSE). The design of the Lidar C&DH must also consider the complexity of the interfaces that it has with the Lidar instruments and of those with the Spacelab CDMS. A judicious architecture and choice of functions can minimize the complexities of these interfaces and enable a simpler and more cost effective integration both at the instrument level and at level IV, III, and II integration. The resolution of these issues then, to a large extent, determine the functions which will be performed by the Lidar C&DH as well as some aspects of its architecture.

Performance of the trade-offs identified earlier require some understanding of the capabilities of the equipment of the Spacelab CDMS and the Orbiter Avionics which are applicable to the Lidar C&DH functions. The block diagram of Figure 8-5 shows the elements of the Spacelab CDMS which are pertinent to this trade-off with respect to the Lidar C&DH Subsystem. There are several other elements within the Spacelab CDMS which are not indicated on this diagram.

A complete description of the entire Spacelab CDMS and of each of the blocks shown on Figure 8-6 is contained in the Spacelab Payload Accommodation Handbook, ESA document SLP 2104, Section 4.4. The Orbiter avionics equipment description is contained in JSC Document 07700 Volume XIV, Section 14.

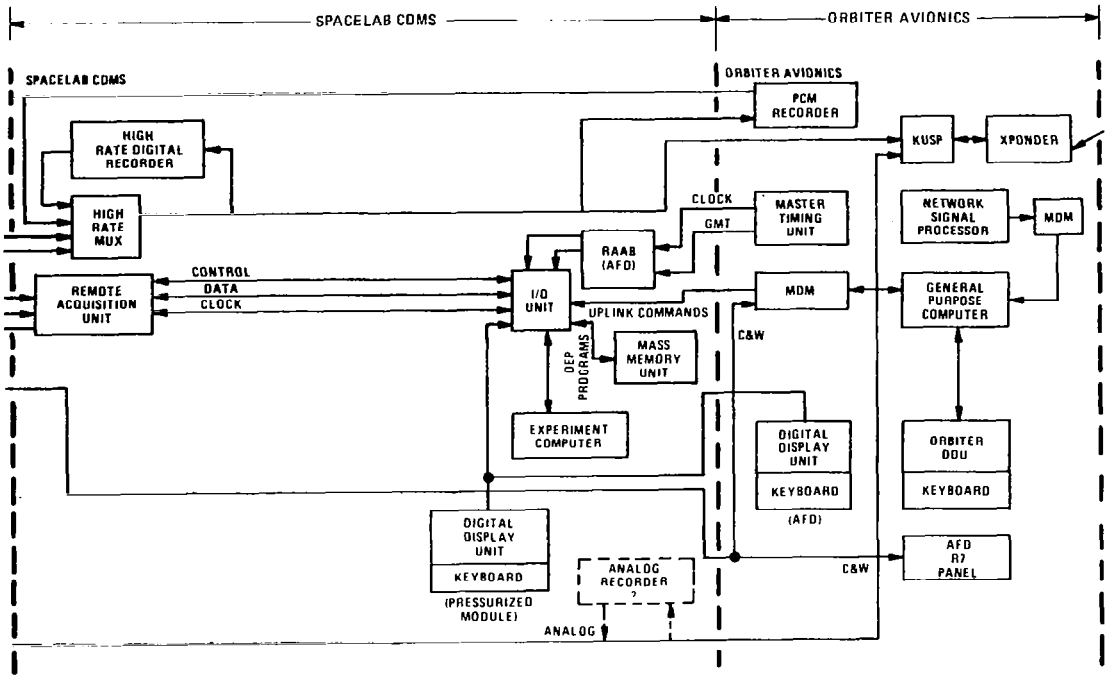

Figure 8-5. Spacelab CDMS and Orbiter Avionics.

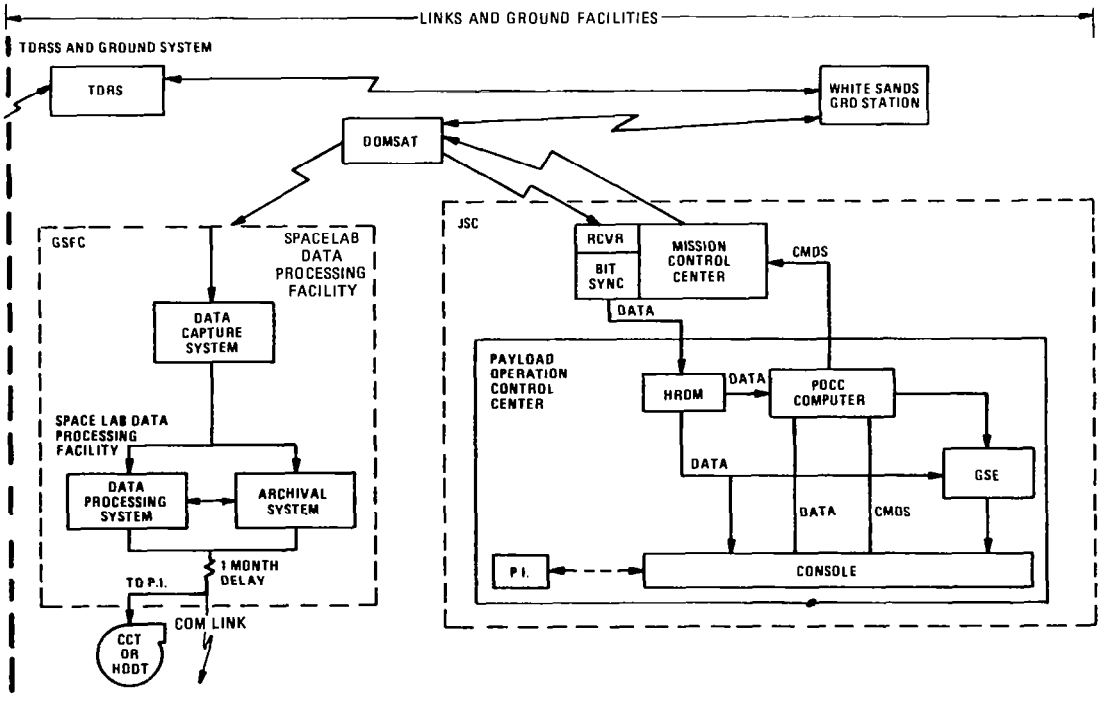

Figure 8-6. STS Data System Links and Ground Facilities - Block Diagram.

Experiments or experiment facilities have two major interfaces with the Spacelab CDMS. One is to the High Rate Multiplexer (HRM) which has 16 channels for use by experiments. Each of these channels has a data rate capability of up to 16 megabits per second. The output of the HRM is a single data stream of up to 48 megabits per second which is transmitted to the ground via the Ku-band signal Processor in the Orbiter. To buffer this data during TDRS occultations there is a 32 megabit-per-second tape recorder operated by the crew during these occultations (Note that if the HRM output exceeds this rate during occultations, the excess data will be lost). A 1-megabit per second tape recorder, the Pulse Code Modulation (PCM) recorder, is also provided by the orbiter avionics to fulfill a similar buffering function when the HRM output data bandwidth is 1 Mbps or less.

The second major interface with the CDMS is through Remote Acquisition Units (RAU). RAU's provide four serial PCM inputs to the Spacelab CDMS system, four serial PCM outputs to the experiment, 128 low bandwidth analog or discrete inputs to the Spacelab CDMS, and 64 discrete outputs for use as commands to the experiments. The RAU connects with the input/output (I/O) unit associated with the Spacelab Experiment Computer. Each RAU is polled sequencially by the Experiment Computer and a maximum of 32 words can be sent to the Spacelab CDMS, or received from the Spacelab CDMS, with each poll. Note that there is only one HRM but there can be as many RAU as there are experiment facilities, up to a maximum of 32 (although initially, at least, there will only be a total of 8 RAU's, implying some sharing if there are more than 8 experiments).

The Experiment Computer is a mini-computer capable of performing approximately 350,000 operations per second and has 64,000 16-bit words of memory. There is, however, some drawback in that the operating system uses approximately 54,000 words of that memory leaving only 10,000 words for experiment application software to be

shared among all the experimenters using the computer. Of particular interest is the Mass Memory Unit (MMU) which is a tape recorder capable of storing large amounts of data and, in particular, various programs for dedicated experiment computers contained within the experiments. These programs can be fed to the dedicated experiment computers via the RAU on demand. The use of the MMU for storing experiment data is discouraged.

The Spacelab CDMS also provides GMT and clocks derived from the Master Timing Unit of the Orbiter avionics. The GMT provided to the experiment has an accuracy of 10 milliseconds. A Digital Display Unit and a keyboard are available on the Aft Flight Deck for pallet experiments. An additional unit is provided in the pressurized module when it is present. The Digital Display Unit is a full alpha-numeric graphic display which also must be shared between the various experimenters. The Operating System of the Experiment Computer contains subroutines which perform high-low limit checks and conversion to engineering units; however a certain amount of Experiment Computer Application Software (ECAS) is required for tables and formats.

An analog transmission capability exists via direct transmission of analog signals to the KU-Band processor, however, when this link is used (4.5 MHZ) the digital link can be only 2 megabits per second. A direct connection to an Aft Flight Deck panel must be made for Caution and Warning signals if any are required. Uplink commands are received by the Ku-band transponder, fed to the Network Signal Processor, then to the Orbiter General Purpose Computer where they are decoded and checked and, when identified as being Spacelab commands, transmitted through the Multiplexer-Demultiplexer (MDM) to the Experiment Computer via the Input/Output unit. There they are again decoded in terms of specific experiment address and sent via the RAU to the indicated experiment, or stored for subsequent issue as a function of the indicated code.

The block diagram of Figure 8-6 depicts the Links and Ground Facilities of the STS data system. The TDRS has 3 digital channels: 50 Mbps, 2 Mbps, and 192 Kbps, or as indicated previously; 4 1/2 MHZ analog, 2 megabits per second digital, and 192 Kbps digital. The 192 Kbps link is for engineering data. An 8 kilobit per second uplink capability provides for 2 kilobits per second of command data. These 2 kilobits per second include addresses for use by the Orbiter computer and by the Spacelab computer. The downlink data is relayed to the White Sands ground station where a "bent pipe" retransmits it through a domestic satellite to the Spacelab Data Processing Facility (SDPF) at GSFC and the Mission Control Center (MCC) and Payload Operation Ceontrol Center (POCC) at JSC in Houston.

At the POCC, facilities include a 370/168 computer and seven experimenter rooms each having access to the High Rate Demultiplexer (HRDM) outputs, and consoles. Capability is also provided to accommodate the Electrical Ground Support Equipment (EGSE) of the experimenter provided it fits within the volumetric constraints of the experimenter's room. At any one time the POCC provides capabilities to process the data of any four out of the 16 experimenter channels from the demultiplexer. Computations performed in the POCC computer require development of software and the integration of this software with other experimenters' software.

Since the decision whether or not to use the POCC computer or the experimenters' EGSE for processing of this data does have impact on the choice of function performed by the on-board Spacelab C&DH and Spacelab CDMS systems, a preliminary decision was made that the POCC computer would not be used and that all processing required by the Lidar experimenter on the ground would be done in the EGSE. This preliminary decision assumes that the EGSE will inherently contain all the equipment needed to perform the processes required at the POCC since these same functions will be required during the various stages of checkout and integration and test.

8.3.2 Data Processes

The basic processes performed at the Spacelab Data Processing Facility consist mainly of removing the overlaps caused by the recording of data during TDRS occultations and reordering the various time sequences un-ordered by the recording and playback processes. At the POCC, science data may be processed to extract information for quick-look by the Principal Investigator. This processing can be performed either by the POCC computer or by an experiment EGSE which can be brought into the experimenters' rooms at the POCC.

The processes performed on-board are identical to those performed during integration. They do not at this time include information extraction from the science data. Basically the science data will be formatted, buffered, and merged with ancillary and housekeeping data to form complete packets which will allow the processing of the data as an entity. The raw output of the photomultipliers will also be displayed to the Payload Specialist via an oscilloscope.

Commands can be issued to the system via the keyboard in the Payload Specialist station on the Aft Flight Deck, or issued via pre-stored programs contained within the C&DH system. The C&DH will also decode commands which are uplinked from the ground and distribute these commands to the appropriate units within the Lidar system.

Ancillary data which consists of such items as GMT, state vector, ephemeris, or any other extraneous data needed to identify and characterize the science data will also be formatted and merged with the science data and can be displayed to the Payload Specialist.

Housekeeping data, which basically indicates the operating status of the various elements of the Lidar system, will also be formatted and merged with the science data

and can be displayed to the Payload Specialist.

Additionally, limit checks will be performed using pre-stored instructions to assure that each of the parameters is within its allowable limits. Housekeeping data will be converted to engineering units and can be displayed to the Payload Specialist on demand or automatically upon detection of an anomaly. Data displayed to the Payload Specialist will be in a pre-defined set of formats called "skeletons" which will be pre-stored in the C&DH Subsystem.

There are certain considerations which impact not only the operating modes of the experiments but also the design of the C&DH Subsystem. In particular, TDRSS is periodically occulted from the Shuttle due to two mechanisms: One is the interposition of the earth between the Shuttle and the TDRS; the other is the interposition of the Shuttle body between the antenna on the Shuttle and the TDRS Satellite. These occultations can vary in duration up to a maximum of 60% over a 24 hour period for a 55° inclination with the Shuttle in an earth-viewing attitude.

Although the data link from the ground to the orbiter is 8 kilobits per seconds, the data is BCH (Bose - Chaudhuri-Hocquenghem: An error-correcting code used as an error - detecting code on Shuttle) encoded, effectively limiting the actual data transfer rate to 2 kilobits per second. When commands are transmitted they are checked on the orbiter for errors using the BCH code then transmitted to the address indicated in the format of the command. Commands can be sent only one at a time and there are several check points along the way such that the effective uplink command rate is something less than 100 bits per second. Additionally, since commands are sent up one at a time they must wait in line to be transmitted.

Each experimenter will share the link with several other experimenters and, although prioritization will be effected by the various working groups, even the highest

priority experimenter will still incur delays before his commands are transmitted. This is particularly true because Orbiter commands, which use the same link, will have priority over all payload commands. These factors have significant implications with respect to the operation of the experiment and, therefore, on the design of the data system.

The Payload Specialist will need to assume greater responsibility with respect to the operation of the instruments since the PI will periodically be out of contact with the experiment from the point of view of receiving data which he can evaluate, sending commands, or consulting with the Payload Specialist. The greater responsibility of the Payload Specialist, in turn, implies that certain data must be displayed to him so that he can make proper decisions.

The low data rate associated with uplink commands from the ground as well as the delays which may be incurred in sending these commands and the fact that they may not be sent 50% of the time implies that the commands must be originated on-board either by the Payload Specialist or through an autonomous system whereby the commands or command sequences are contained within the C&DH System.

In general, greater experiment autonomy is indicated. This autonomy need not be independent of the Payload Specialist participation but can certainly consist of sets of pre-sequenced commands which are initiated by either the Payload Specialist or recognized events such as GMT. In general, experiment "Command Strategy" will need to be planned well in advance on a case by case basis.

8.3.3 Tradeoffs

Figure 8-7 shows the rationale for choosing the selected approach. Four criteria, each with subsets, were used to perform the trade-offs determining the extent of the use of Spacelab CDMS versus a fully autonomous Lidar Command and Data Handling subsystem with minimum utilization of the Spacelab CDMS or the Orbiter avionics. The trade-offs resulted in the selection of a fully autonomous subsystem. The autonomous Lidar C&DH will have its own microcomputer obviating the need to depend on a polling with limited data rate transfer to the Spacelab CDMS computer, as well as avoiding an early delivery of software for integration with other experiments' software within the Spacelab CDMS computer.

CRITERIA	BASIC APPROACH	
	AUTONOMOUS LIDAR C&DH	MIXED LIDAR C&DH AND SPACELAB CDMS
LIFE CYCLE COST		
– HARDWARE/SOFTWARE	KB & DISPLAY S/W DEVELOPMENT	ECAS DEV'MT AND INTEGRATION
– INTEGRATION & TEST	MINIMAL GSE – RELATIVELY SIMPLE – DONE ONCE	REQUIRES EXTENSIVE EGSE, REPEAT FULL CYCLE EACH FLIGHT
TECHNICAL INTEGRITY		
– CAPABILITY	TAILORED TO REQUIREMENTS	LIMITED BY RAU I/F, EC AVAILABILITY
– GROWTH	DEPENDENT ON SELECTED ARCHITECTURE	FIXED BY CDMS
INTEGRATION AND TEST		
– SCHEDULE	TOTAL DATA SYSTEM DELIVERED WITH LIDAR	ECAS DELIVERED TBD MONTHS BEFORE LIDAR
– FIDELITY	ACTUAL HARDWARE/SOFTWARE USED	SIMULATORS USED UNTIL LEVEL IV
OPERATION		
– SHARING RESOURCES	100% DEDICATED TO LIDAR ADDS EQUIPMENT TO AFD	SHARED WITH TBD OTHER EXPERIMENTS CHANGES FROM FLIGHT-TO-FLIGHT
– FLEXIBILITY	DETERMINED BY ARCHITECTURE AND DESIGN	MINIMAL IN CDMS, RIGID FORMATS AND PROTOCOL

Figure 8-7. Rationale for Selected Approach.

The fully autonomous Lidar C&DH will also have its own keyboard and display unit. A penalty is paid in the cost of the initial hardware procurement and the utilization of additional power on the Aft Flight Deck. This is, however, offset by the elimination of (Spacelab) Experiment Computer Application Software (ECAS) and of the Spacelab CDMS simulators in the EGSE which would be required during checkout and integration. The major advantage of a totally autonomous Lidar C&DH with minimum

interfaces to the Spacelab CDMS is the availability of all of the C&DH components during integration and checkout. Further, these components are the actual hardware and software which will be used during flight, as opposed to simulators which would run at less than real time speed and would provide lower fidelity until actual integration is made with the Spacelab CDMS at Integration Level II. Although more software development is required for the autonomous Lidar C&DH since it makes minimal use of the Spacelab CDMS Operating System, this software will be developed on the Lidar computer at significantly lower costs than would be required to develop a lesser amount of ECAS using the larger IBM 360 or 370 machines for which the Spacelab CDMS computer cross-compilers and-assemblers have been developed; further the savings effected during the Level IV, III, and II integration are repeated for each flight whereas the original cost of the keyboard and display unit and the software is a one time cost.

8.3.4 Subsystem Design

The block diagram of Figure 8-8 shows the Lidar C&DH subsystem, as it was developed, and its interfaces with the Lidar system and the Spacelab facilities. The actual C&DH subsystem on the pallet is shown within the dotted lines. The Lidar display and keyboard and the Lidar oscillosocpe located on the Aft Flight Deck are also part of the Lidar C&DH subsystem. The basic architecture of the subsystem is based on hardware units controlled by the Lidar computer.

The computer is used primarily for control and does not handle the science data itself. Simple functions such as high/low limit checks, decoding of commands, and conversion to engineering units are the only processes performed by the computer on data.

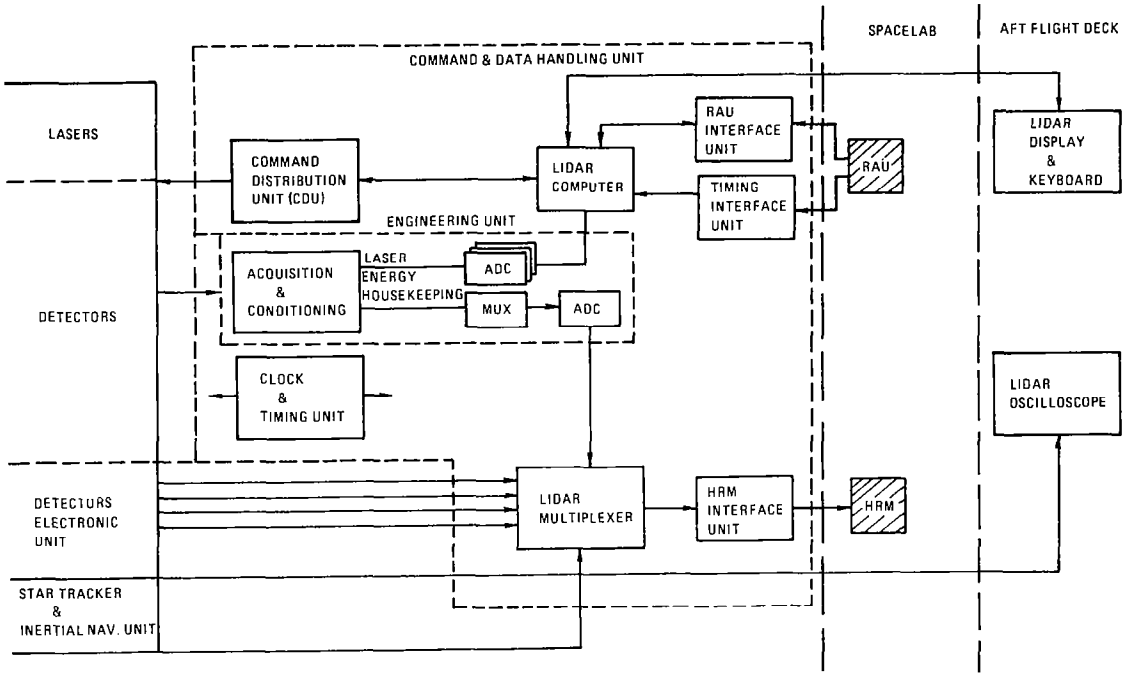

Figure 8-8. Lidar C&DH Subsystem.

The Command Distribution Unit accepts serial commands from the computer and distributes them as discretes or coded words to the various subsystems and units within the Lidar system. At this time it is anticipated that 100 commands will be required.

The Engineering Unit acquires and conditions signals associated with housekeeping functions. These signals are primarily analog although some may be discretes. It is assumed that approximately 200 signals will be acquired; further it is assumed that 50 of these will be sampled ten times per second, 100 once per second and 50 once every ten seconds. In particular the measured laser energy will be converted to digital data and fed to the computer where the status and health of the lasers will be determined.

The Clock and Timing Unit provides all clocks and counts required by various Lidar subsystems and establishes all timing intervals required. This clock operates at 100 megahertz providing 10 nanosecond granularity. All units of the Lidar system will be synchronized to this clock which is asynchronous with the Spacelab CDMS and Orbiter clock.

The Lidar Multiplexer multiplexes together the science data, the housekeeping data, the corelative sensors data, ancillary data, and additional information as required from the Lidar computer indicating status and performance.

The data will be multiplexed in such a way that they are compatible with the Instrument Telemetry Packet concept. Interfaces to the Spacelab are minimized and consist only of a RAU interface to provide the various ancillary data on request and GMT to an accuracy of 10 millisecond provided by the Timing Interface Unit in conjunction with the clock update provided by the RAU.

The entire Lidar C&DH subsystem is modular with respect to both hardware and software. This architecture provides growth in all respects. As an example, although processing of science data is not proposed in the initial version, this can readily be provided subsequently by adding a hardware box which will perform the required processing, and a software module to the computer, controlling this process. All elements of the Lidar C&DH are well within the state of the art and present no technical challenge. The architecture is also fully compatible with the CAMAC concept and could be implemented using the Spacelab Payloads Standard Modular Electronics (SPSME) being developed by MSFC specifically for such applications, should this prove desirable and cost-effective. CAMAC is a standard system with modules and bus systems having standardized interfaces and protocols. It is produced by over 100 companies worldwide. SPSME is a Spacelab-qualified set of modules functionally and electrically compatible with the CAMAC standard.

Figure 8-9 summarizes the functions that the Lidar C&DH will perform. The co-alignment routine shown under Command and Control will be a preset pattern by which the transmitter and receiver are displaced relative to each other. The computer will automatically issue commands to these subsystems in a set of predefined commands. Simultaneous display of the photomultiplier tube output to the Payload Specialist will enable him to determine when maximum coincidence exists, at which time he will direct the computer to switch to a mode which repeats the co-alignment routine on a, perhaps, 10:1 reduced range of motion providing for optimization of the co-alignment.

1. FORMATTING
   - INTEGRATE SCIENCE DATA
   - ANNOTATE HOUSEKEEPING AND ANCILLARY DATA
   - INTERFACE TO HRM AND RAU
2. SIGNAL CONDITIONING AND PROCESSING
   - PRE-AMPLIFICATION
   - ADC
   - FILTERING
   - BUFFERING
   - MULTIPLEXING
   - MEASURING
   - MONITORING
3. COMMAND AND CONTROL
   - PRE-STORED SEQUENCES
   - COMMAND DISTRIBUTION
   - CONTROL
   - ROUTING
   - CO-ALIGNMENT ROUTINE
4. TIMING
   - SUPPLY CLOCKS
   - MEASURE INTERVALS
   - ANNOTATE
5. DISPLAYS
   - HI-LO LIMIT CHECKS
   - SKELETONS
   - FORMAT
   - ENGINEERING UNITS CONVERSION
   - PMT OUTPUT ON OSCILLOSCOPE (QUICK-LOOK)

Figure 8-9. Lidar C&DM Functions.

Figure 8-10 summarizes quantitatively the capabilities of the Lidar C&MD. Although no commitment is made at this time as to the specific computer to be used as the Lidar C&DH computer, a microcomputer is indicated provided it has sufficient word length and sufficient directly addressable memory. The LSI-11 appears to satisfy the requirements and has the advantage of being compatible with most of the PDP-11 software library. Additionally, the LSI-11M, produced by Norden Systems, has been

developed as a militarized and vibration- hardened version of the LSI-11. A recent study conducted by Norden Systems for GSFC indicates the feasibility of readily converting this computer to be qualified for flight on a Spacelab pallet. The other capabilities indicated on the chart have been discussed previously.

- 16 BITS MICRO-COMPUTER
- 64 K WORDS DIRECTLY ADDRESSABLE MEMORY
- ACCEPTS PROGRAM LOADS FROM MMU VIA RAU
- 200 KOPS
- COMPATIBLE WITH PDP 11 SOFTWARE

} EQUIVALENT TO LSI-II

- 12 BIT WORDS FOR SCIENCE DATA
- 8 BIT WORDS FOR HOUSEKEEPING DATA
- 16 BIT WORDS FOR RAU INTERFACE
- COUNTS UP TO 1 SECOND INTERVALS
- 10 NS CLOCK ACCURACY
- 10 MS GMT ACCURACY
- 90 DISCRETE, 10 SERIAL COMMANDS - UP TO 10 COMMANDS/SEC
- 200 ANALOG HOUSEKEEPING CHANNEL
  50 SAMPLED ONCE/SEC, 100 ONCE/10 SECONDS, 50 10/SEC
- 7 CHANNEL MULTIPLEXER
  500 Kbps FOR SCIENCE DATA
- FULL ALPHA-NUMERIC PLASMA PANEL DISPLAY AND KEYBOARD
- VARIABLE PERSISTENCE 100 MHz OSCILLOSCOPE WITH VARIABLE DELAYED SWEEP

Figure 8-10. Lidar C&DM Capability.

8.3.5 Software

Figure 8-11 shows the Lidar software family tree. The modularity of the software is readily apparent. The executive programs and applications programs will be the only programs resident during flight. The support software and diagnostic software will be provided for development of the executive programs and applications software during software development; however, diagnostic software could be available on-board, stored in the mass memory unit of the Spacelab CDMS as would alternate application programs. The executive and application programs total approximately 10,000 instructions.

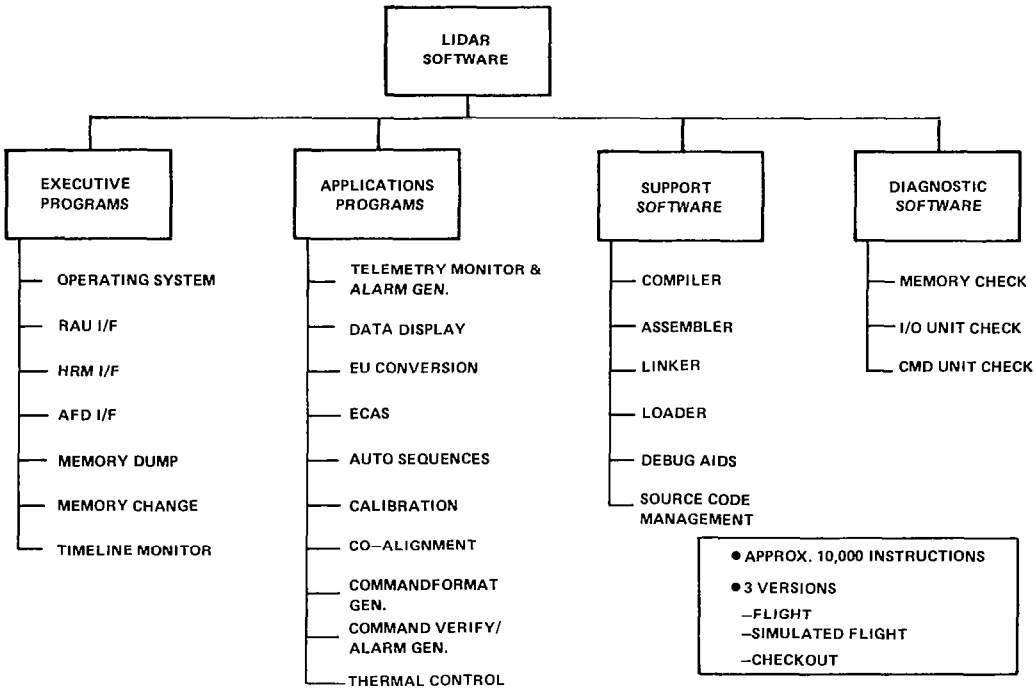

Figure 8-11. Lidar Software.

Three versions of the software will be required: The Flight version used during actual operations, a Simulated Flight version which varies the procedure to account for actions or operations which cannot be performed in 1-G, and a Check-out version which contains additional routines and diagnostics used during tests.

The simulated Flight software, while hopefully identical to the Flight version, will take into account that certain functions cannot be performed in earth gravity (1 G) and will either modify command sequences or take differing results into account. The Checkout version of the software will include routines to verify proper operation which are not normally performed during actual operation. It is anticipated that the Operating System will be a commercially available version modified as required for the Lidar mission. The support software and the diagnostic software will be standard packages available for the computer selected, as modified for the specific unit

checks of the Lidar components. Note that an ECAS module is indicated under the applications programs. This is a minimal package which will allow the recognition of the Lidar subsystem by the CDMS computer such that it will respond to requests for computer program updates from the Mass Memory Unit and requests for ancillary data. To the greatest extent possible the entire software package will be table-driven, i.e., the program will be structured as tables wherein coefficients or instructions can readily be changed.

8.3.6 SUBSYSTEM CHARACTERISTICS

Figure 8-12 summarizes the characteristics of the Lidar C&DH. A major feature is that, with the exception of the housekeeping data which will be primarily analog, the entire system is digital and its interfaces with both the Lidar Instruments and with the Spacelab CDMS are digital. The science data signals are digitized within the detectors electronics and are acquired by the C&DH subsystem as serial digital streams. To the greatest extent possible timelines and command sequences will be pre-stored in the Lidar computer. The architecture selected and the power of the computer enable maximum autonomous operation. The interfaces to the Spacelab CDMS have been minimized and consist only of connections to the High Rate Multiplexer for transmission of data to the ground, and connections to the RAU to receive computer program changes from the MMU, ancillary data, and Caution and Warning connections as required in response to stated policy. The components on the pallet require approximately 115 watts using present technology. The components on the Aft flight deck require a total active power of 195 watts. This is approximately half of the power available to payload dedicated equipments on the Aft flight deck. The overall capabilities exceed the requirements for envisioned early experiments, and growth is provided readily through the modular structure of the software and the hardware. This system responds to, and meets, all the functional and science requirements identified in paragraph 8.2.

- MAJOR FEATURES
  - ALL DIGITAL SYSTEM (ANALOG DATA DIGITIZED BEFORE CEDH SYSTEM)
  - PRE-STORED TIMELINES AND COMMAND SEQUENCES
  - NO PROCESSING OF SCIENCE DATA ONBOARD
  - PROCESSES REQUIRED AT POCC FOR QUICK-LOOK DONE BY EGSE

- MAXIMUM AUTONOMOUS OPERATION
  - MINI/MICRO-COMPUTER
  - KEYBOARD/DISPLAY UNIT
  - OSCILLOSCOPE

- MINIMUM CDMS INTERFACE
  - HIGH RATE MULTIPLEXER
  - LIDAR COMPUTER PROGRAM CHANGES
  - CAUTION AND WARNING (AS REQUIRED)
  - ANCILLARY DATA (GMT, STATE VECTOR, ETC. . .)

- PHYSICAL CHARACTERISTIC
  - PALLET COMPONENTS: 22,653 cm^3 (0.8 CU. FT.), 17 Kg (38 LBS.), 115/WATTS
  - AFD COMPONENTS: 56,634 cm^3 (2 CU. FT.), 26 Kg (58 LBS.), 195 WATTS

- CAPABILITY
  - COLLECTS, FORMATS, AND TRANSMITS DATA TO HIGH RATE MULTIPLEXER
  - MONITOR, AND DISPLAY STATUS AND HEALTH OF LIDAR EQUIPMENT
  - OPERATE AND CONTROL INSTRUMENTS VIA SIMPLE KEYBOARD COMMANDS AND PRESTORED SEQUENCES
  - DISPLAY PHOTOMULTIPLIER OUTPUT FOR PAYLOAD SPECIALIST EVALUATION

MEETS OR EXCEEDS REQUIREMENTS FOR ENVISIONED EARLY EXPERIMENTS AND . . .

- GROWTH ADAPTABILITY
  - GRADUAL VIA EXPANSION OF LIDAR COMPUTER MEMORY AND PERIPHERALS
  - DISCRETE VIA REPLACEMENT OF MODULES

COMPATIBLE WITH ADVANCED EXPERIMENTS VIA MODULAR EQUIPMENT ADDITION

Figure 8-12. Characteristics of Lidar C&DM.

9.0 SYSTEM DEFINITION

9.1 GENERAL

Figure 9-1 presents a simplified block diagram for the Lidar system. The design of the directly science related subsystems: Sources, receiver, detector, and command and data handling, have been discussed in the prior sections. The supporting subsystems: Electrical power, thermal control, and structures, which impact the system configuration, are treated in this section as part of the overall configuration definition. This is consistent with the priorities of the system design approach discussed in Section 4.0. The system variables, evaluated in Table 9-1, demonstrate that a science focus has been maintained throughout the trade studies to define the supporting subsystems. This approach assures a balanced system design which is directly related to the science performance requirements.

A system arrangement which illustrates compliance to the overall system constraints introduced by the science requirements and the STS/Spacelab environments is shown in Figures 9-2 and 9-3. A preliminary manufacturing and test flow plan noting the implementation of the system design is shown in Figure 9-4. Possible growth plans of the currently defined system which may be implemented to assure achievement of all the science requirements are listed in Table 9-2.

Preliminary principal investigator interfaces are listed in Table 9-3. Such a listing, when fully developed after a detailed system design will assure the most cost-effective and efficient transfer of laboratory type devices to flight hardware and enhance the productivity of the LIDAR system throughout its useful life.

9.2 SYSTEM CONFIGURATION

The derivation of the system configuration was governed by the priorities noted in Section 4.0. Since the major science-content subsystems have already been discussed

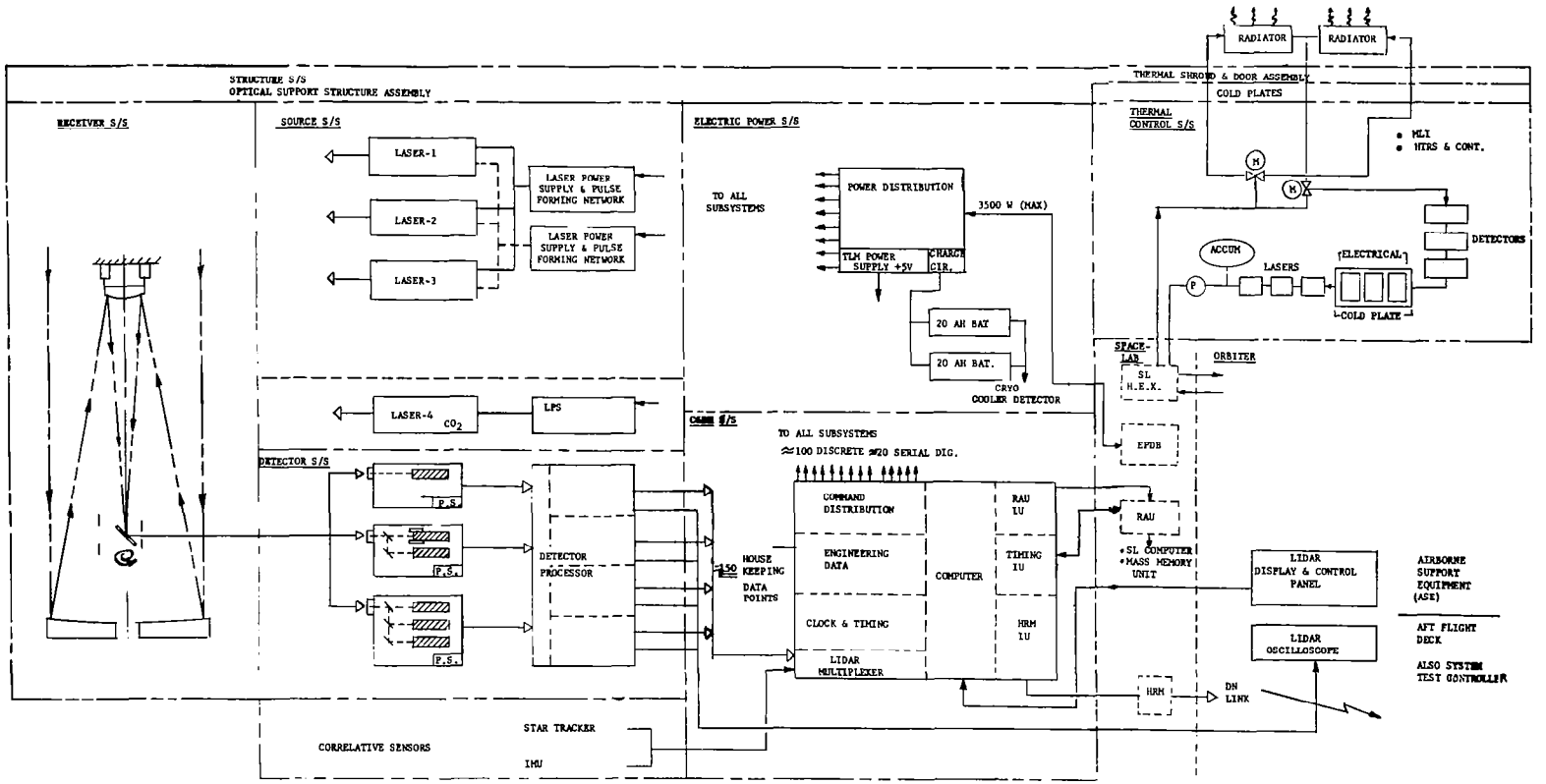

Figure 9-1. System Functions.

Table 9-1. System Performance Trade Summary

TRADES	VARIABLES EVALUATED
TELESCOPE – TYPE – APERTURE – f NO.	– FOV-RANGE – FILTER DIAMETER – ALIGNMENT – ARRANGEMENT – ERROR APPORTIONMENTS – GROWTH
LASER Nd YAG EXCIMER RUBY FLASH PUMPED DYE	– AVAILABILITY – EFFICIENCY – GROWTH – POWER
DETECTOR OPTICAL ACCESS	– TYPES – ARRANGEMENT – GROWTH
COMMAND & DATA AUTONOMOUS/DEPENDENT DIGITAL/ANALOG ONBOARD/GRD.PROCESSING STORED/REAL TIME CMMDS	– TRAINING – DATA RATES – COMPLEXITY – REPEATABILITY – GROWTH – INTEGRATION TIME CYCLES – INTERFACES
THERMAL CONTROL ACTIVE/PASSIVE COLLECTIVE/DISBURSED	– ABSOLUTE TEMP. – FLUXES: INTERNAL & EXTERNAL – GRADIENTS – POWER
ALIGNMENT PASSIVE/ACTIVE RECEIVER/SOURCE	– TOLERANCES/COST – SIGNAL/NOISE – COMPLEXITY/RELIABILITY – THERMAL

at length, only the power, thermal control, and structure subsystems will be treated here. These three subsystems work so closely together, especially the thermal control and structure subsystem, that they were evaluated together in many of the supporting trade studies. An instance of this is the incorporation of the thermal door into the structural shroud of the structural subsystem and the location of the telescope aperture with respect to the structural shroud to guard the telescope from incident solar thermal excitation. The salient trades of each of these subsystems along with various configurational effects are discussed in the following paragraphs.

9.2.1 ELECTRICAL POWER SUBSYSTEM

The block diagram for the electrical power subsystem is shown in Figure 9-2. It consists of a power controller and a pair of 20 AH batteries. The power controller contains a power distribution unit which is supplied by the Spacelab/STS interface with 28V ± 4V D.C. power. The C&DH subsystem activates various relays to provide power to elements of the Lidar system as required by the particular experiment protocol selected. The power controller also provides 5 volt power for all of the telemetry signals required for Lidar. A charge circuit to maintain a full charge state on the 20 AH batteries is also provided.

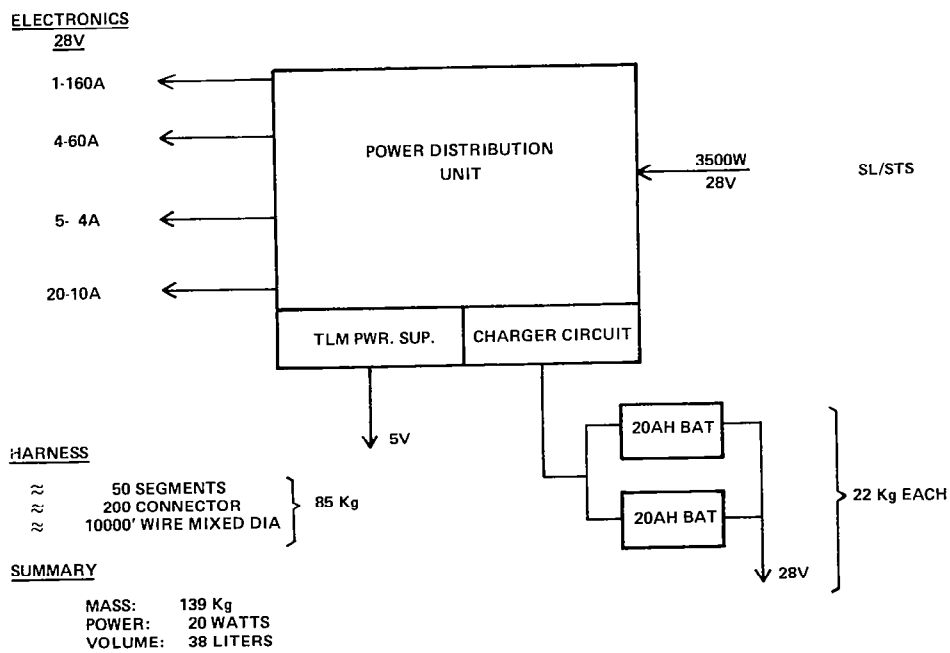

Figure 9-2. System Configuration.

The major considerations in the electrical power subsystem were associated with the use of a regulated or unregulated bus for the Lidar system. The design life of the system coupled with its growth plans makes it difficult, if not impossible, to design

a system which provides adequate power regulated within narrow limits to subsystems whose requirements may not be known for years. The most reasonable approach to regulation indicated that the use of internal regulation with each of those components or portions of components would not compromise the system design with respect to either weight or complexity. The simplification of the component interfaces allows the definition of electrical interfaces with future, to-be-determined, items of equipment that may in time be provided by Principal Investigators.

Normal spacecraft harness disciplines, which require reasonable segregation of power, command, and signal were utilized for the system.

The charger circuit/battery combination provides power to the thermo-electric cooling devices utilized for some of the detectors. Current pre-post, and in-flight planning indicates that power is denied the STS/Spacelab payload for brief periods.

9.2.2 THERMAL CONTROL SUBSYSTEM

The thermal control subsystem is designed to assure adequate thermal protection of the Lidar system under all ground and orbit conditions specified for the STS/Spacelab. Numerous trade studies were performed to determine the optimum design approach to be employed. Figure 9-3 illustrates two basic concepts, separate and collective conditioning which were examined in some detail leading to a selected approach. The separate approach, when evaluated with respect to external environmental variations induced by STS solar attitude and internal variations created by the multiplicity of operating configurations within the Lidar system, demonstrated power demand and thermal gradient control shortcomings. The collective approach was selected for the baseline system as it is capable of accepting prior broad solar attitude and operating configuration variations. It also maximizes the

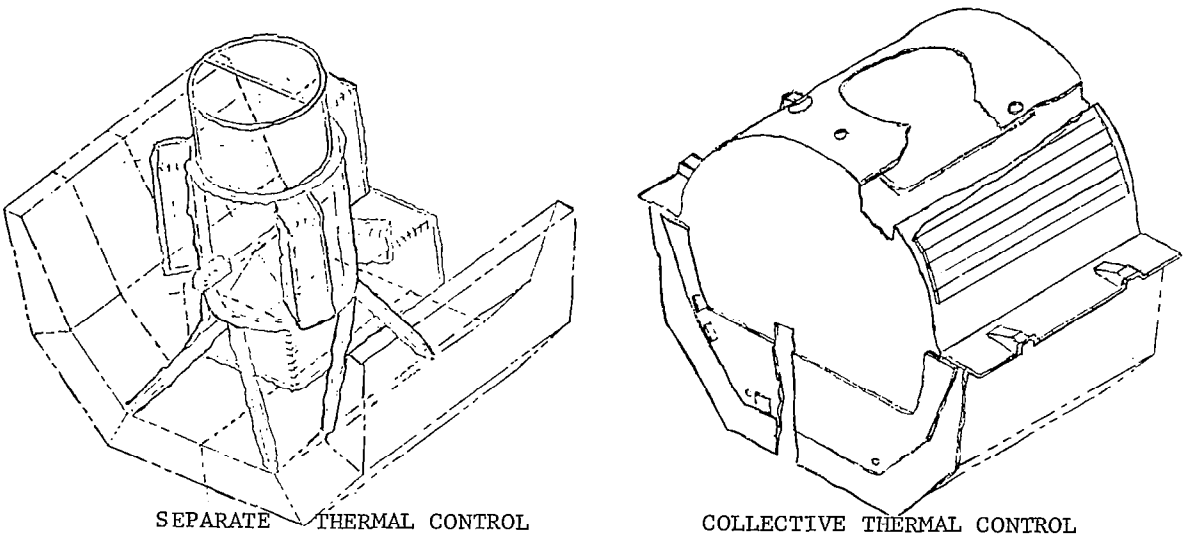

Figure 9-3. Lidar Basic Thermal Control Options.

thermal capacitance of the system and thus provides gradient control with lesser power requirements than the separate approach. As the absolute temperatures required by Lidar can be less than those provided by the Spacelab/STS cooling loop, additional cooling capacity is required. The use of port and starboard auxiliary radiators, carefully positioned to avoid direct coupling to the STS radiators, provide this capability. The entire enclosure is protected with multi-layer insulation to assure minimal heat loss during periods of non-operation and thus maintain the auxillary heater requirements at the 200 watt or less level. The receive telescope has multi-layer insulation within its metering structure and hence is referenced to the bulk temperature of the Lidar system. Figure 9-4 shows the block diagram of the thermal control system. It is interfaced to the Spacelab cooling loop via a liquid to liquid heat exchanger and is capable of modifying the exit temperature of this heat exchanger by means of computer controlled split flow thru and/or around the auxiliary radiators. Sensors within the loop provide signals which modulate the valves to both proportion the flow thru the radiator and to select the appropriate radiator.

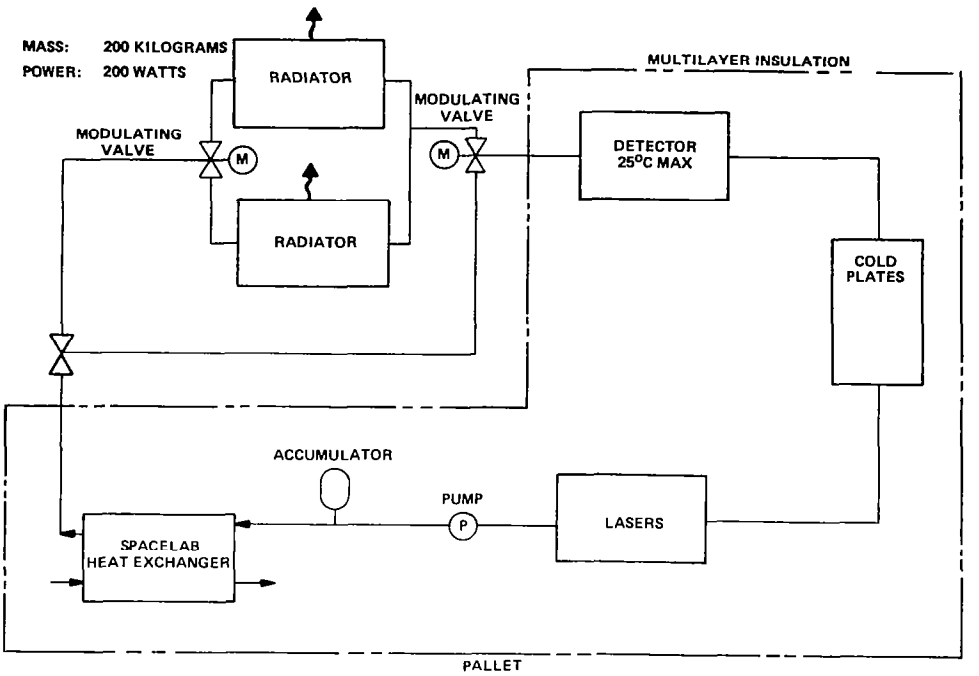

Figure 9-4. Thermal Control Subsystem Block Diagram.

Flow temperatures provide adequate cooling of the detectors to assure that their maximum temperatures will be equal to or less than 25°C at the baseplate and flow volumes will successfully remove 4500 watts of internal dissipation as well as the heat load associated with maximum worst case solar illumination on the enclosure. Conventional materials and assemblies have been identified for use throughout the system. Man rated pumps, accumulators, etc., are available from past NASA programs and will form the basis for specific hardware selection.

9.2.3 STRUCTURE SUBSYSTEM

The structure subsystem, while being the least complex of the Lidar subsystems, is most heavily related to the overall configuration of the system. It is the matrix which adequately binds all of the other system elements into an assembly which can be built, tested, maintained, aligned, and refurbished with minimal impact to the

system. It contains, supports, and protects all the system elements from possible damage throughout the specified range of mechanical environments both on the ground and in flight.

It consists of:

- Optical Support Assembly - Contains the cylindrical support structure and space frame. It supports the lasers, telescope, detectors, and correlative sensors. It interfaces to the pallet.
- Thermal Shroud Assembly - Contains the thermal door, door drive mechanisms, and the radiation baffle assembly. It supports the multilayer insulation assembly and the auxillary radiators. The thermal shroud assembly interfaces to the pallet.
- Cold plate assemblies which mount various system components, not installed on the optical support assembly, to the Spacelab pallet.

The key considerations in the design of the system were associated with the selection of the optical support assembly configuration due to alignment requirements among all of the Lidar optical devices. Two basic approaches to the optical support assembly were examined in detail as shown in Figure 9-5.

The cylindrical support structure was selected over the flat bench approach based on its lesser sensitivity to thermal distortion and its greater mass efficiency for a given natural frequency. The precise natural frequency required is not known at present but based on related Spacelab pallet experience it is expected to fall between 12 and 15 HZ.

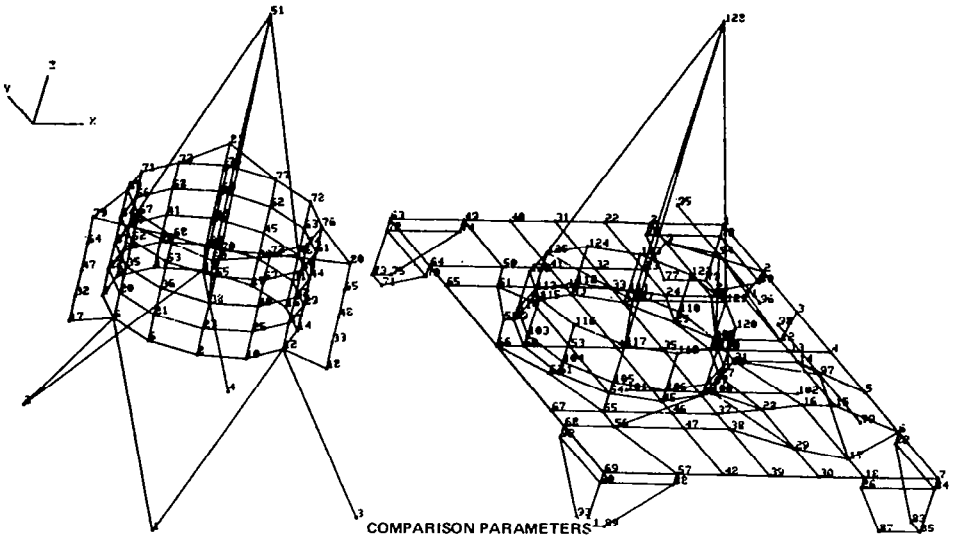

CYLINDRICAL SUPPORT STRUCTURE

COMPARISON PARAMETERS

0.1	THERMAL DEFORMATION - mr $\Delta T = 12^{o}C$	0.5
65	MASS - Kg 15Hz NATURAL FREQUENCY	180

FLAT BENCH SUPPORT STRUCTURE

Figure 9-5. Alternate Configurations.

The use of a cylindrical support structure has other advantages which relate to a simplified telescope installation that allows removal of the primary cell without disassembly of the entire system. A three point support for the telescope assures that deformations introduced by the structure will be minimized. The cylinder also aids in assuring adequate alignment of all the optical elements of the system - telescope, laser modules, detectors, and correlative sensors. The cylinder has mounting provisions for three lasers, three detector assemblies and three correlative sensors. All of the mounting interfaces are identical so that devices can be shifted from point to point as required. Mechanical tolerances are held to nominal values by the judicious use of shims at the time of assembly.

The cylindrical support structure is interfaced to the Spacelab pallet by means of a space-frame assembly which maximizes access to the assembly. The cylindrical support structure connects to the space frame at three points and thus is decoupled from any internal deformation created by pallet motions on orbit. The entire optical support assembly can be assembled and tested as a unit.

The thermal shroud assembly is built-up from conventional aluminum structures and supports the multilayer insulation, radiation baffle assembly, Lidar radiators, and the thermal door. The door is redundantly driven to assure optical access of the Lidar system to its intended target. Door drive mechanisms are based on currently available space qualified solar array drive units.

The cold plate assemblies are Lidar unique. The use of Spacelab cold plates was explored and rejected on the basis that they were of excessive mass and complexity for the Lidar application. Lidar does not expose the cold plates to direct solar illumination hence their mechanical/thermal coupling to the pallet can be simpler than that required for Spacelab.

9.2.4 CORRELATIVE SENSOR SUBSYSTEM

The particular correlative sensors utilized by Lidar will be directed by the science requirements. For the initial Lidar system the use of a NASA Standard Star Sensor and Inertial Reference Unit were defined to meet the 0.5 degree post-flight pointing knowledge requirement specified. Both of the above items are mounted to the optical support assembly and are interfaced to the power and data handling subsystems.

Other correlative sensors may be utilized in the future and the baseline design has acknowledged that eventuality by allocating power and mounting interfaces as defined in the structural subsystem.

9.3 SYSTEM ARRANGEMENT AND TEST

The arrangement for the Phase I Lidar system, which is capable of accommodating rational growth to perform all of the experiment classes contained in the SEED, is shown in Figure 9-7 and 9-8 Table 9-1 summarizes the results of the system/subsystem/configuration trades which were conducted during the study to support and define the configuration.

The system arrangement as shown, meets all of the interface requirements to the Spacelab/STS and can be logically assembled and tested as shown in Figure 9-6.

The test program is designed to make maximum use of the Electrical Ground Support Equipment (EGSE) and the Mechanical General Support Equipment (MGSE), listed in Table 9-2, so that the need for, and the associated cost of, special test equipment is minimized. Portions of EGSE and MGSE are then shipped to KSC to support the pre-Level IV and subsequent integration tasks. The test philosophy, shown in Table 9-3, is based on building early and continued confidence in the Lidar system at the various levels of assembly leading up to a protoflight qualification of the entire system immediately prior to shipment to the launch site.

9.4 SYSTEM DESIGN & CAPABILITIES SUMMARY

9.4.1 DESIGN SUMMARY

A summary of the system design with respect to its compliance to the Spacelab/STS constraints is shown in Table 9-4 for the Phase I system and in Table 9-5 for the maximum accommodation capability of the system. Table 9-6 compares the above values of power and mass to both the full SL/STS capability and to the Lidar system "fair-share" allocations which were developed in Section 3.0 to assure the compatibility of

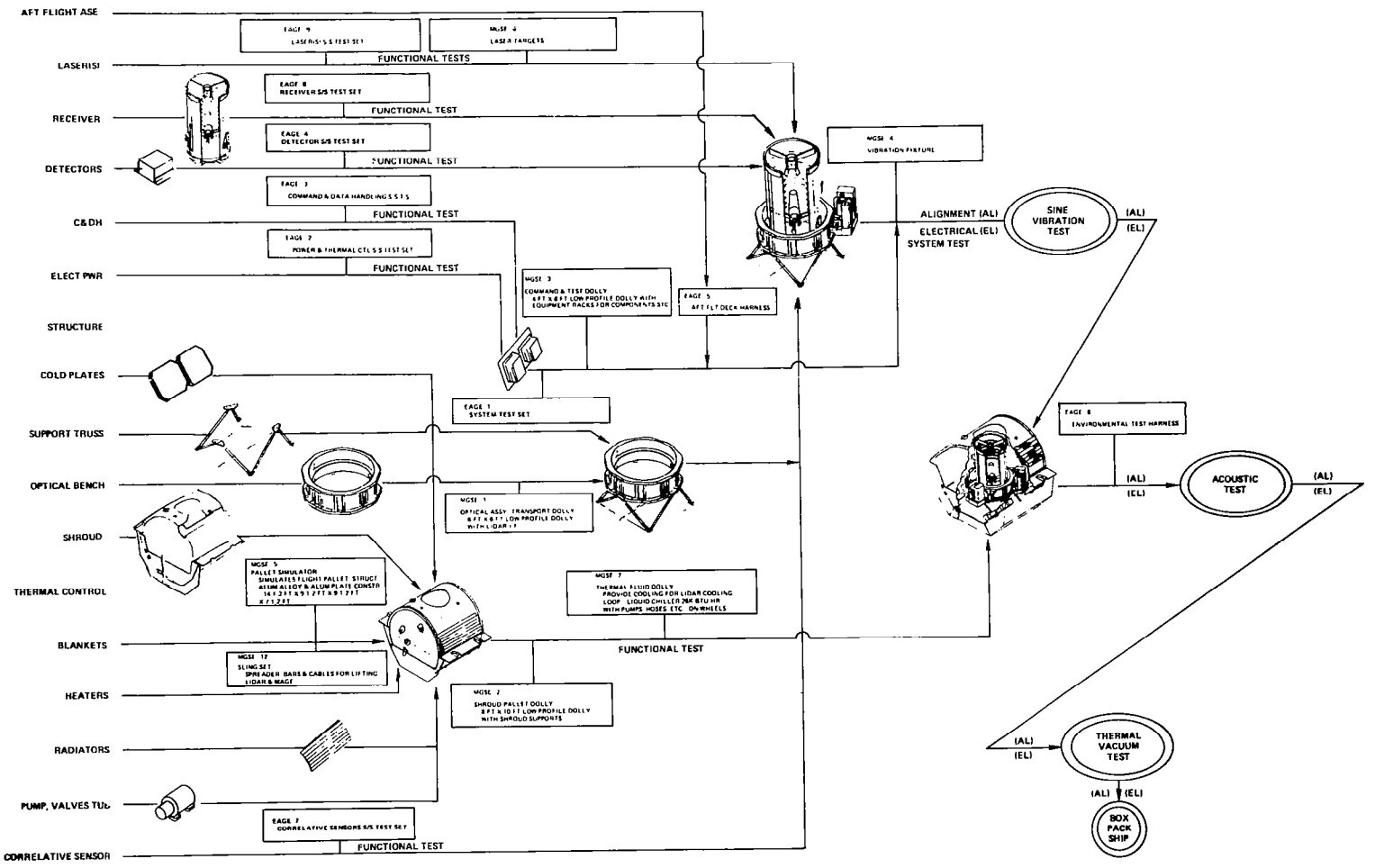

Figure 9-6. System Assembly & Test Flow Plan.

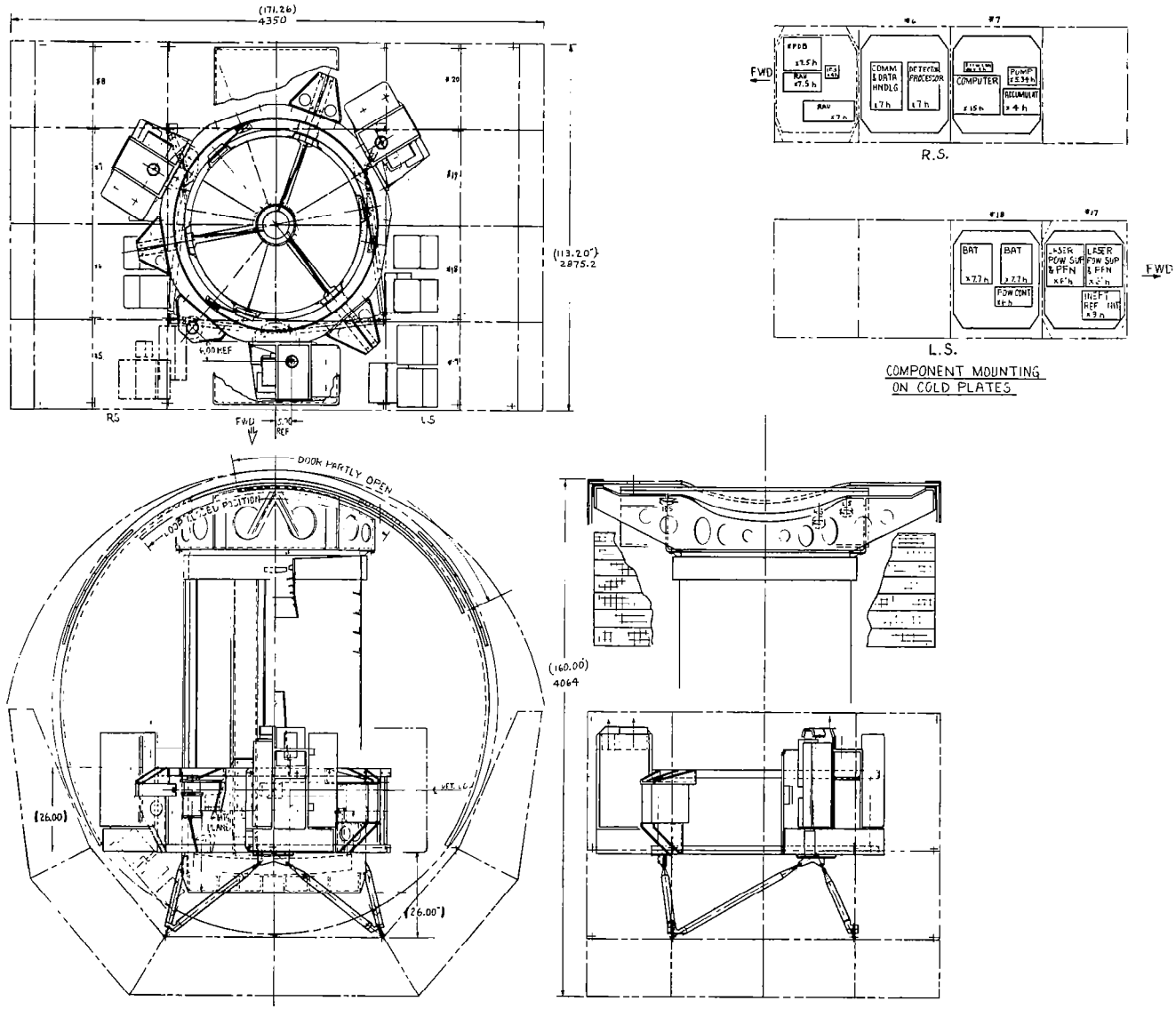

Figure 9-7. Lidar Assembly. (Dimensions are given in mm (in.).

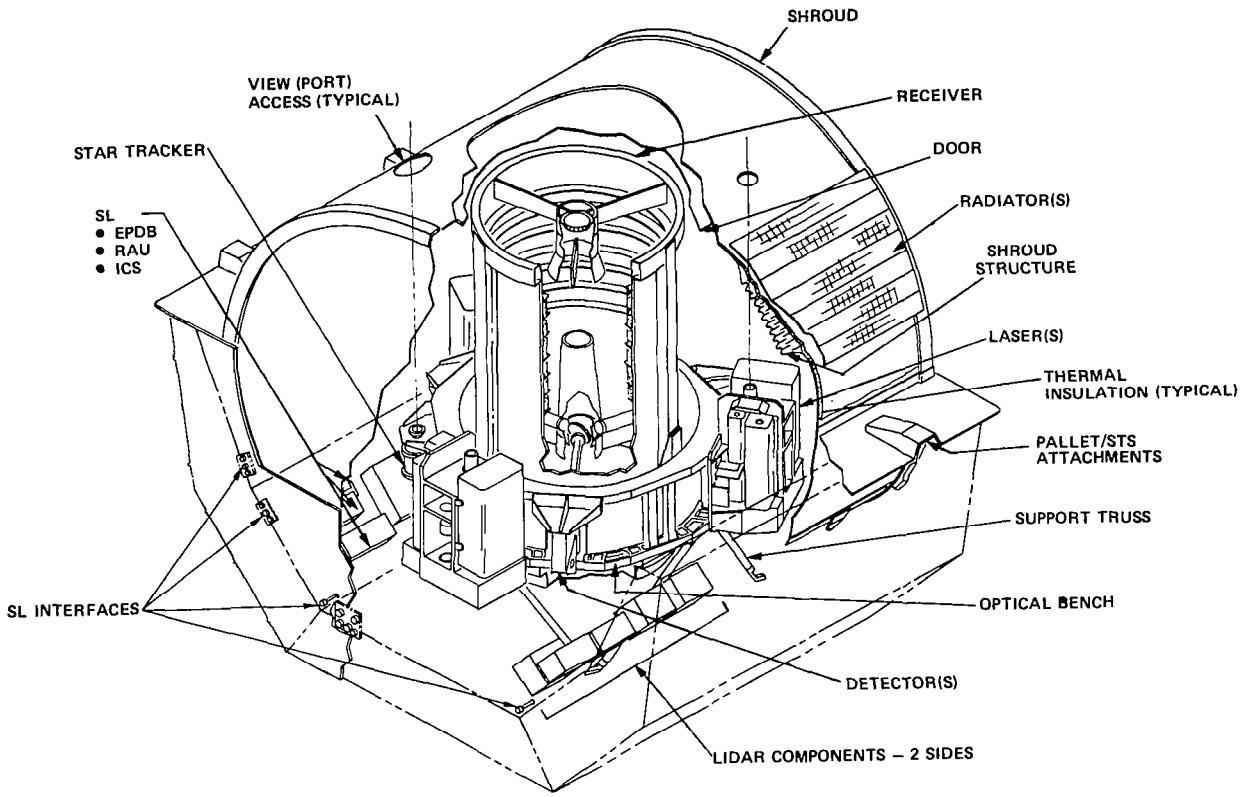

Figure 9-8. System Arrangement.

the Lidar system to the other payloads which will be flown on the same mission. This comparision indicates that a power/energy management problem could exist if the efficiency of the pulsed CO_2 laser cannot be improved from that identified in Section 6.0. Even at the currently forecasted power requirement the problem is manageable but places some constraints upon the operation of the system. It is expected that improvements in technology will remove this restriction at the time a pulsed CO_2 laser is ready for flight.

Table 9-2. GSE Definition

MECHANICAL GROUND SERVICE EQUIPMENT (MGSE)		
	UOE	
ITEM	IN HOUSE	LAUNCH SITE
1. OPTICAL ASSEMBLY/TRANSPORT DOLLY	X	X
2. SHROUD/PALLET DOLLY	X	X
3. CMMD & TEST DOLLY	X	
4. VIBRATION TEST FIXTURE	X	
5. PALLET SIMULATOR	X	
6. LASER TARGETS	X	X
7. FLUID-HANDLING DOLLY	X	X
8. SHIPPING CONTAINERS	X	
9. SHROUD SHIPPING COVER	X	
10. UNIVERSAL SLING SET	X	X

ELECTRICAL GROUND SUPPORT EQUIPMENT (EGSE)		
	UOE	
ITEM	IN HOUSE	LAUNCH SITE
1. SYSTEM TEST SET	X	X
2. POWER & THERMAL CONTROL S/S TEST SET	X	X
3. COMMAND AND DATA HANDLING S/S TEST SET	X	X
4. DETECTOR S/S TEST SET	X	X
5. AFT FLIGHT DECK TEST HARNESS	X	X
6. ENVIRONMENTAL TEST HARNESS	X	
7. CORRELATIVE SENIOR S/S TEST SET	X	X
8. RECRIUER S/S TEST SET	X	X
9. LASER S/S TEST SET	X	X

Table 9-3. System Test Requirements Matrix

TEST CONFIGURATION / SUBSYSTEM	DETAIL, PARTIAL ASSEMBLY PARTIAL COMPONENTS	ASSEMBLY	COMPONENT •VIBRATION •THERMAL	SUBSYSTEM	SYSTEM •VIB •ACOUSTIC •THERMAL VACUUM
LASER	FUNCTIONAL (BREADBOARD)	FUNCTIONAL (ENGINEERING) (MOD.) →	QUALIFICATION & ACCEPTANCE		
DETECTOR	FUNCTIONAL (BREADBOARD)	FUNCTIONAL (ENGINEERING) (MOD.) →	QUALIFICATION & ACCEPTANCE		
RECEIVER	→	IN PROCESS →		FUNCTIONAL PARTIAL – QUAL. & ACCEP.	QUALIFICATION & ACCEPTANCE
C&DH	FUNCTIONAL (BREADBOARD)	FUNCTIONAL (ENGINEERING) (MOD.) ↕ (BIT)	QUALIFICATION & ACCEPTANCE	BENCH INTEGRATED TEST (BIT)	
ELECTRICAL POWER	FUNCTIONAL (BREADBOARD)	FUNCTIONAL (ENGINEERING) (MOD.)	QUALIFICATION & ACCEPTANCE		
THERMAL CONTROL	→	FUNCTIONAL ENGINEERING MODEL →	(PARTIAL) →	FUNCTIONAL	QUALIFICATION & ACCEPTANCE
STRUCTURE		FORM, FIT AND INTERFACE VALIDATION →		→	QUALIFICATION & ACCEPTANCE

Table 9-4. Phase 1-System Design Characteristics Summary

SYSTEM/ SUBSYSTEM	ITEMS	EACH	TOTAL MASS KG	DC POWER WATTS	TOTAL VOLUME LITERS
SOURCE	Nd YAG X 2	1	140	1870	300
	X DYE X 3 X 2				
	POWER SUPPLY	1	30		60
RECEIVER	1.25M F/2	1	635	INTERMITTENT 35	4550
DETECTOR	SINGLE PMT	2	4	35	2.8
	DUAL PMT	1	8	70	5.6
	DETECTOR PROC	1	12	60	17.2
C&DH	CDH UNIT	1	17	100	17.2
ELECTRICAL POWER & DIST	POWER DIST UNIT	1	10	10	7.1
	BATTERY	2	44		30.3
	HARNESS SET	1	85		
STRUCTURE	OPTICAL SUPPORT	1	70		
	COLD PLATES	2	12		56.0
	SHROUD/DOOR	1	85	INTERMITTENT 60	N/A
THERMAL CONTROL	RADIATORS	2	60		300
	MULTILAYER INSULATION SET	1	30		
	PUMP, VALVES TUBE SET HEATERS	1	60	200	
	COOLANT	1	50		
CORRELATIVE SENSORS	STAR TRACKER	1	5	INTERMITTENT 20	10
	IN. REF. UNIT	1	5		
TOTAL			1362 (3003 LBS)	2310	

Table 9-5. Maximum Accommodation-System Design Characteristics Summary

SYSTEM/ SUBSYSTEM	ITEMS	EACH	TOTAL MASS KG	DC POWER WATTS	TOTAL VOLUME
SOURCE	Nd-YAG CO_2PULSE	3 1	510 210	1870 3750	1080 330
RECEIVER	1.25M, F/2 SWING AWAY MIRROR	1	693	INTERMITTENT 40	4550
DETECTOR	SINGLE PMT DUAL PMT TRIPLE PMT DETECTOR PROC	1 1 1 1	4 8 12 12	35 70 110 60	18
C&DH	CDH UNIT	1	17	100	18
ELECTRICAL POWER & DIST	POWER DIST UNIT BATTERY HARNESS SET	1 2 1	10 44 85	10	8 30
STRUCTURE	OPTICAL SUPPORT COLD PLATES SHROUD/DOOR	1 3 1	70 18 85	INTERMITTENT 60	160
THERMAL CONTROL	RADIATORS MULTILAYER INSULATION SET PUMP VALVES TUBE, HEATERS SET COOLANT	2 1 1 1	60 30 70 50	200	300
CORRELATIVE	A/R	A/R	60	INTERMITTENT 100	30
TOTAL			1990 (4375 LB)	2350 - Nd-YAG 4230 - CO_2 PULSE	

Table 9-6. System Power & Mass Margin Summary

STS RESOURCE	LIDAR "FAIR SHARE" ALLOCATION	PHASE 1		MAXIMUM ACCOMMODATION	
		PARAMETER	FAIR SHARE MARGIN %	PARAMETER	FAIR SHARE MARGIN %
MASS 2300 KG	2300 KG (AVERAGE SINGLE PALLET)	1420	+38	1990	+14
POWER 4500 WATTS	3500 WATTS PALLET ONLY (1000 WATTS TO COMPANION PAYLOADS)	2310	+35	4230 - CO_2 2350 Nd-YAG	–20 +34

9.4.2 SYSTEM CAPABILITY

The Lidar system hardware required for the various experiment classes in the SEED is shown in Table 9-7. This table defines a possible, but not the only, evolutionary development of the Lidar system. The first two columns define the experiment classes and the wavelengths required to perform them. The last three columns note the science supporting hardware and its impact on the system design considerations. The arrow-heads in the first column indicate the introduction points of evolutionary system modifications required to accommodate the orderly growth of the system. The modifications need not be made in the order shown. They can be defined by prioritized science goals without negative impact on the evolutionary capability of the system.

Table 9-7. System Evolutionary Capability

EXPERIMENT CLASS	WAVELENGTH – NM	LASER HARDWARE	DETECTOR	SYSTEM CONSIDERATIONS
1 CLOUD TOP HEIGHTS & SURFACE ALBEDO 2 TROPOSPHERIC AEROSOL PROFILES 4 NOCT CLOUD & CIRCUMPOLAR PART LAYER PROFILE 6 STRAT AEROSOL BACKSCAT PROFILE	1060/532	Nd YAG FREQUENCY DOUBLED	DOUBLE PMT (ONE COOLED NEAR IR)	1.25 METER RECEIVER ORBIT ADJUSTABLE SECONDARY - 2 m RANGE 10 Hz REP RATE
7 ALKALI ATOM PROFILES	589.0 (Na) 769.9 (K) 670.7 (Li)	NARROW BAND TUNABLE DYE LASER PUMPED WITH Nd YAG DOUBLED	SINGLE PMT	
8 IONOSPHERIC METAL IONS	279.6 (Mg^+)	NARROW BAND TUNABLE DYE DOUBLED PUMPED WITH Nd YAG DOUBLED	SINGLE PMT	
11 CHEMICAL RELEASE DIAGNOSTICS	589 (Na)	NARROW BAND TUNABLE DYE LASER PUMPED WITH Nd YAG DOUBLED	SINGLE PMT	
	493.4 (Ba)	NARROW BAND TUNABLE DYE LASER PUMPED WITH Nd YAG TRIPLED	SINGLE PMT	
12 STRATOSPHERIC OZONE PROFILES	280 300	NARROW BAND TUNABLE DYE LASER DOUBLED PUMPED WITH Nd YAG DOUBLED	SINGLE PMT	
21 MESOSPHERIC OH PROFILE	300		SINGLE PMT	
25 THERMOSPHERIC NO PROFILE	215		SINGLE PMT	
26 ATOMIC OXYGEN VERTICAL PROFILE	225.6 (TRANSMIT) 844.8 (RECEIVE)		SINGLE PMT	
9 TROPOSPHERIC H_2O PROFILE	720 (2) 940 (2)	TWO NARROW BAND TUNABLE DYE LASERS PUMPED WITH Nd YAG DOUBLED	SINGLE PMT	ORBIT ADJUSTABLE LASER MOUNT NEAR SIMULTANEOUS LASER PULSES
15 SURFACE AND CLOUD TOP PRESSURE 16 TROPOSPHERIC PRESSURE PROFILE 17 TROPOSPHERIC TEMPERATURE PROFILE	760 (2) 760 (2) 760 (2)		SINGLE PMT SINGLE PMT SINGLE PMT	
23 TROPOSPHERIC NO_2 PROFILE	442.2 and 448.6		DOUBLE PMT	
10 COLUMN CONTENT AND ROUGH PROFILES OF FOLLOWING SPECIES O_3 (9.6 μM) NH_3 (10.6 μM) CFM_1 (10.7 μM) C_2H_4 CO_2 C_2H_5Cl H_2O ETC	TWO IN 9-11 μM REGION	C= CO_2 DISCRETELY TUNABLE WITH HETERODYNE DETECTION TWO WAVELENGTHS	CRYOGENIC INTEGRATED WITH LASER (TWO DETECTORS)	SWING AWAY FOLDING MIRROR OR LASER TRANSMIT RECEIVE THROUGH DETECTOR PORT
13 STRATOSPHERIC SPECIES MEASUREMENT AT TANGENT ALTITUDE O_3 NH_3 CFM_1 HNO_3 CO C_2H_4 CO_2 $ClONO_2$ ETC (TWO SATELLITE TECH)				
10 SAME AS 10 ABOVE		PULSED CO_2 DISCRETELY TUNABLE HETERODYNE DETECTION TWO WAVELENGTHS		SWING AWAY FOLDING MIRROR
13 SAME AS 13 ABOVE				
18 ALTITUDE DISTRIBUTION OF ATMOSPHERIC CONSTITUENTS - IR DIAL SAME SPECIES AS 10 13 ABOVE				
24 STRATOSPHERIC AEROSOL COMPOSITION	MULTIPLE IN 9-11 μM REGION			
3 CIRRUS ICE/WATER DISC	532	Nd YAG DOUBLED - POLARIZED	DOUBLE PMT WITH POLARIZATION SEPARATION	
22 THERMOSPHERIC Mg, Mg^+ and MgO PROFILE	279.6 285.2 and 500	THREE NARROW BAND TUNABLE DYE LASERS TWO DOUBLED AND PUMPED WITH Nd YAG TRIPLED AND ONE PUMPED WITH Nd YAG DOUBLED	TRIPLE PMT	
14 SODIUM TEMPERATURE AND WINDS	589	NARROW BAND TUNABLE DYE LASER PUMPED WITH Nd YAG DOUBLED	FABRY PEROT INT WITH MULTIPLE RING DETECTOR	
19 CLOUD TOP WINDS - PROOF OF PRINCIPLE	530	SPECIAL VISIBLE LASER LONG PULSE >30μS VERY NARROW BAND		
20 TROPOSPHERIC AEROSOL WINDS PROOF OF PRINCIPLE	530			
26 VERTICAL PROFILE OF ATOMIC OXYGEN	225.6 (TRANSMIT) 844.9 (RECEIVE)	SPECIAL LASER MODE LOCKED	SINGLE PMT	

The Lidar system, as designed, is capable of interfacing with any laser and detector devices which meet the Preliminary System Interface Requirements shown in Table 9-8. It should be noted that this table is a "guide only" at this time but is the forerunner of an expanded definition which will be the product of the hardware design. It does, however, fully demonstrate the "multi user facility" aspect of the Lidar design in terms which can be related to the requirements of various Principal Investigators.

Table 9-8. Preliminary System Interface Requirements For Principal Investigators

PARAMETER	SOURCES	DETECTORS	REMARKS
WEIGHT – Kg	150	25	• CAN ACCUMULATE CORRELATIVE SENSOR ALIGNED TO SOURCE/ RECEIVER
POWER – WATTS	1500 (28V UNREG.)	50 (28V UNREG.)	
VOLUME – LITERS (1)	300	30	
COOLING REQUIREMENTS	HEAT EXCHANGER TO LIDAR LIQUID	BASE PLATE EXTRACTION	• THREE-POINT MOUNTING OF SOURCE
QUALIFICATION TEMPERATURE	0-100°C 0-50°	0-25°C	• ACTIVE CO-ALIGNMENT OF RECEIVER TO SOURCE .01 mr.
TELEMETRY	15 CHANNELS ANALOG. 0-5 VOLTS. REGULATED		
COMMAND	10 DISCRETE 2 SERIAL 10 CMMD/SEC RATE		(1) SPECIFIC DIMENSIONS TO BE DEFINED BY INTERFACE DRAWINGS
SCIENCE DATA HANDLING	ANALOG INPUT 10 METER RANGE RESOLUTION 2000 RANGE BINS 10^5 DYNAMIC RANGE PHOTON COUNTING (FUNCTION OF DETAIL DESIGN)		
RECEIVE TELESCOPE OPTICAL EFFICIENCY	FUNCTION OF COATINGS		

10.0 PROGRAMMATICS

10.1 PROGRAMMATIC PLANNING RATIONALE

This final section of the report will present the results of the programmatic assessment performed during the Study. The elements of the programmatic assessments are shown in Figure 10-1. The activities conducted were in accordance with the Study guidelines and concentrated primarily on the cost, schedule, and the Lidar Instrument Program definition as portrayed by the Work Breakdown Structure. Additionally a risk assessment and a technology assessment were performed. The programmatic factors all contributed to the conclusions and recommendations formulated for the Study.

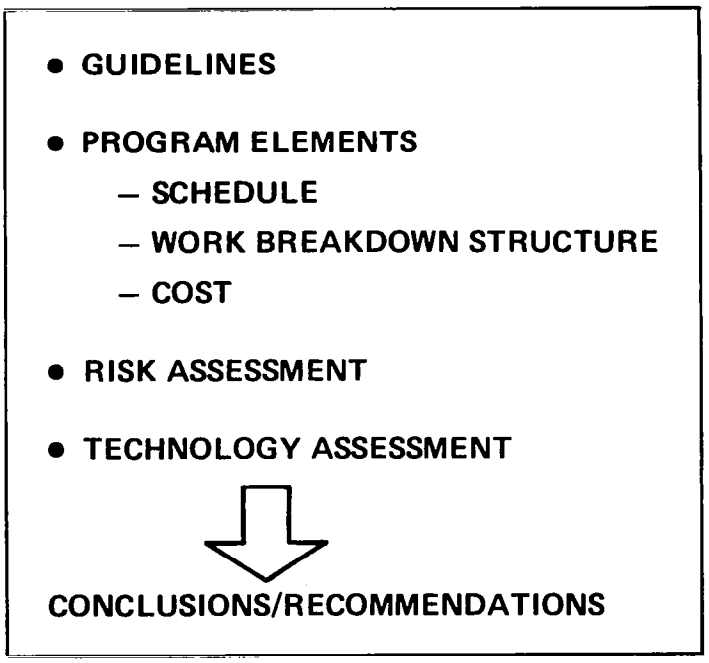

Figure 10-1. Programmatics.

The programmatic evaluations, in addition to their individual treatment were interwoven throughout the scientific, technical, and engineering tasks. The interaction of programmatic factors with the other study elements contributed to the

integrity of the study results. Equipment technology status and development time interact directly with cost, schedule, and risk determination. These interactions were assessed at the Lidar Instrument subsystem or module level (as appropriate) and considered in the "bottoms up" determination of the total program.

The study goal and objectives, and the technical ground rules, identified in Section 1 of this report, were accomodated as appropriate in the program formulation. Specifically the goal to fly the Lidar Instrument in the mid 1980's and the technical ground rule of maximum life at lowest overall cost provided criteria and boundary conditions for the range of viable programmatic options. These criteria and boundary conditions were further supplemented by the detailed technical ground rules enumerating the specific program requirements in the areas of modular design, flexibility, growth, and mission success.

10.2 LIDAR PROGRAM DEFINITION

The scientific and technical elements of the Lidar Instrument have been discussed in the prior sections of this report. For the programmatic determination these scientific and technical elements are summarized and identified in the tabular form of Figure 10-2. The Lidar program, as this figure shows, was divided into several distinct elements. A "base" program was defined and will hereafter be referred to as the "Multi-User Instrument System". This base program consists of the science equipment identified in Figure 10-2, the support subsystems (power, thermal, structural, command and data handling, and correlative sensors) previously described in this report and the necessary programmatic efforts (program management, systems engineering, and integration and system support) to provide a viable, independent Lidar Program.

PROGRAM OPTION	SCIENCE EQUIPMENT
BASE	ND-YAG DYE MODULE 2 DOUBLERS TRIPLER OPTICS MODULE SWITCHING OPTICS MODULE 1.25 METER DIAMETER CASSEGRAIN TELESCOPE – ORBITAL ADJUSTABLE SECONDARY MIRROR 3 SINGLE PMT AND 2 DOUBLE PMT DETECTORS
OPTION 1	ONE LASER SET SAME AS BASELINE SOFTWARE MODIFICATION ACTIVE LASER COALIGNMENT SYST.
OPTION 2	ONE CW CO_2 LASER WITH CRYO DETECTOR ONE SWING-OUT FOLDING MIRROR ASSY. DET. CRYO COOLING ASSY ($77^{o}K$ IN OPERATION WILL TOLERATE ROOM TEMP. NON OPERATE)
OPTION 3	ONE PULSED CO_2 LASER WITH CRYO DETECTOR* (ALSO REQUIRES MIRROR AND DETECTORS AS IN OPTION 2)
OPTION 4	ONE LASER SET SAME AS BASELINE (FOR EXP NO. 22) ONE 3-PHOTOMULTIPLIER DETECTOR PACKAGE
OPTION 5	ONE SPECIAL LONG PULSE VERY NARROW BAND Nd: YAG LASER * ONE FABRY-PEROT INTERFEROMETER DETECTOR

* TECHNOLOGY DEVELOPMENT REQUIRED

Figure 10-2. Lidar Evolution Options Equipment Definition.

In addition to the base program, five options were developed. These options and the scientific equipment associated with each are also listed in Figure 10-2. It should be noted that the options are element groupings that must be added to the base program in the order shown. The numerical designation of the option is provided for identification only and does not reflect any scientific prioritization. Figure 10-2 further shows elements of these options where technology development is required.

The operations for the Lidar instrument defines a separate and distinct program element. This element is not shown in the figure and has been treated in the study as a recurring cost for each flight mission performed. Operation efforts associated with a specific flight will be initiated 18 months prior to launch and will continue for a period of 12 months after mission completion. The activities that necessitate this schedule will be covered in the following sections.

10.3 LIDAR PROGRAM SCHEDULE

The assessment of the Lidar Program is driven by the flight hardware element; i.e. the period of time required to detail design, develop, procure, fabricate, assemble, test, and deliver the flight instrument. This prime driver is moderated by the range of applicable schedule over which the program can be conducted. Schedules can be established for too short a period, one that involves the use of overtime or priority status to meet schedule; similarly the schedule can be so extended and relaxed that fixed program costs (program management) increase and project personnel are not effectively or efficiently used. The objective of the schedule assessment was to avoid these extremes, and establish a schedule with high confidence of adherence at or near minimum cost.

Prior experience, the long lead elements of the Lidar Instrument, and programmatic cost analyses were employed in establishing the selected program schedule, shown in summary form in Figure 10-3. In arriving at this schedule a range of options between 24 months and 48 months from authority to proceed (ATP) to delivery to Kennedy Space Center (KSC) were considered. The variable programmatic fixed and variable costs were assessed, as was consideration of schedule risk.

It was determined that a program schedule in the range of 36 to 40 months was acceptable. This schedule provided little total program cost variation, with the minimum occuring at approximately 37.5 months. Schedule risk analysis showed, however, that significant gains in schedule confidence could be achieved by increasing program schedule within this range. A program schedule of 39 months was therefore chosen. The basic program schedule, identifying the major milestones and the subsystem schedules is shown in Figure 10-4. A period of 12 months from ATP to the Preliminary Design Review was defined. This period was established to provide the highest assurance of design accommodation/satisfaction of scientific requirements

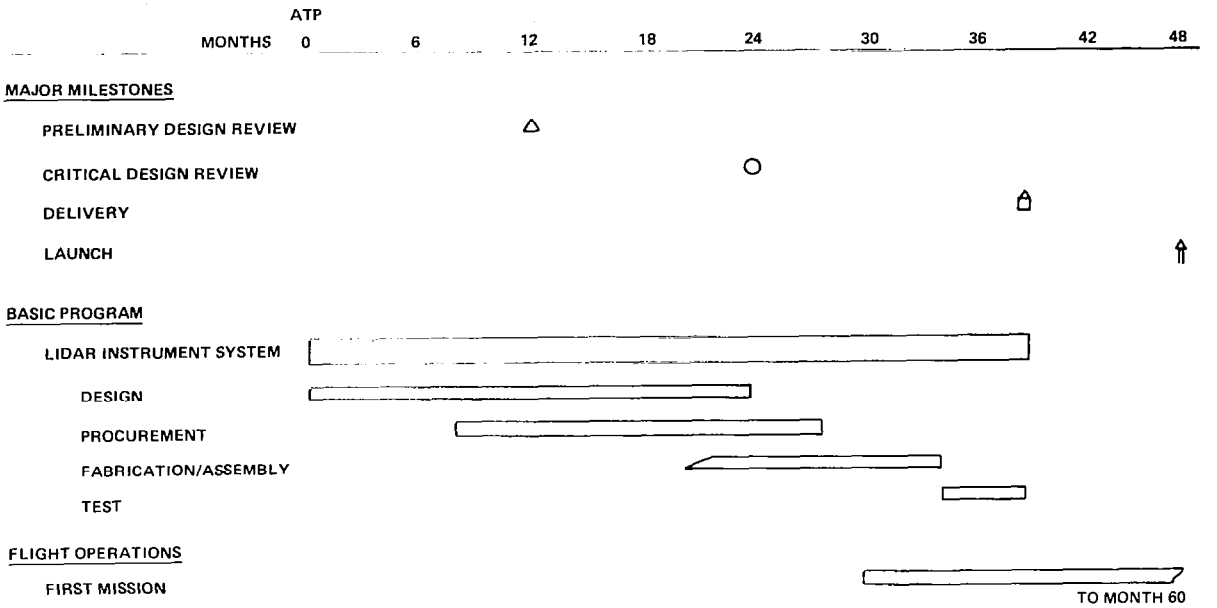

Figure 10-3. Lidar Summary Program Schedule.

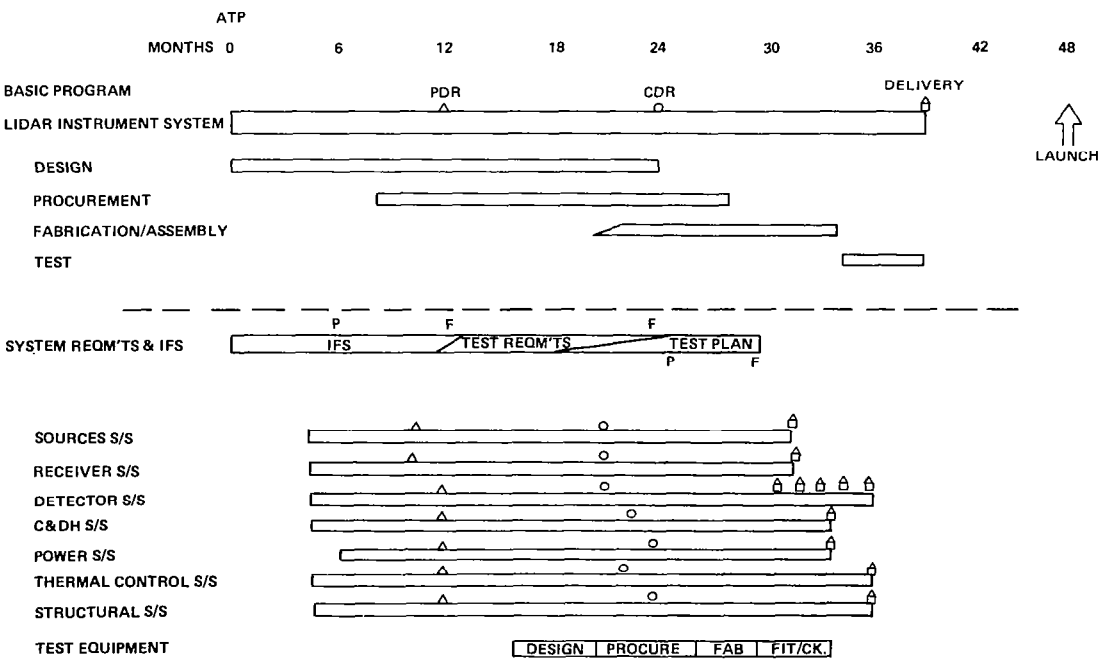

Figure 10-4. Lidar Basic Program Schedule.

prior to major hardware commitment (cost effective approach). The Critical Design Review was established 12 months later, a schedule point sufficient to provide the incorporation of the development test results into the flight design without impacting assurance of meeting the Instrument delivery data.

The subsystem schedules were used to develop the above described scenario. Each subsystem schedule PDR and CDR was established and sequenced with each other to accommodate necessary interactive aspects.

A period of 9 months was allocated for the period between delivery to KSC and the first mission launch. This schedule was formulated on the currently defined scenario for partial Spacelab payloads into an early Shuttle flight mission. It is anticipated that as operational experience is gained for both the Shuttle and the Lidar payload that the envisioned 4 month turn - around time, to accommodate the required 3 flight missions per year, can be achieved.

The results of the previously identified schedule risk assessment are shown in Figure 10-5. In the conduct of this analysis, the desire, as stated previously, was to establish the nominal program schedule for low risk. To accomplish this the critical path elements of instrument definition, instrument development, system integration and system test intervals were established. This model was then subjected to a computerized Monte Carlo simulation of 1000 occurences.

As shown in Figure 10-5 the cumulative probability of schedule adherence increases with increasing schedule. The selected 39 month nominal program schedule provides a 93% schedule confidence. This figure further shows a mean schedule duration (i.e. 50% confidence) at 36.77 months.

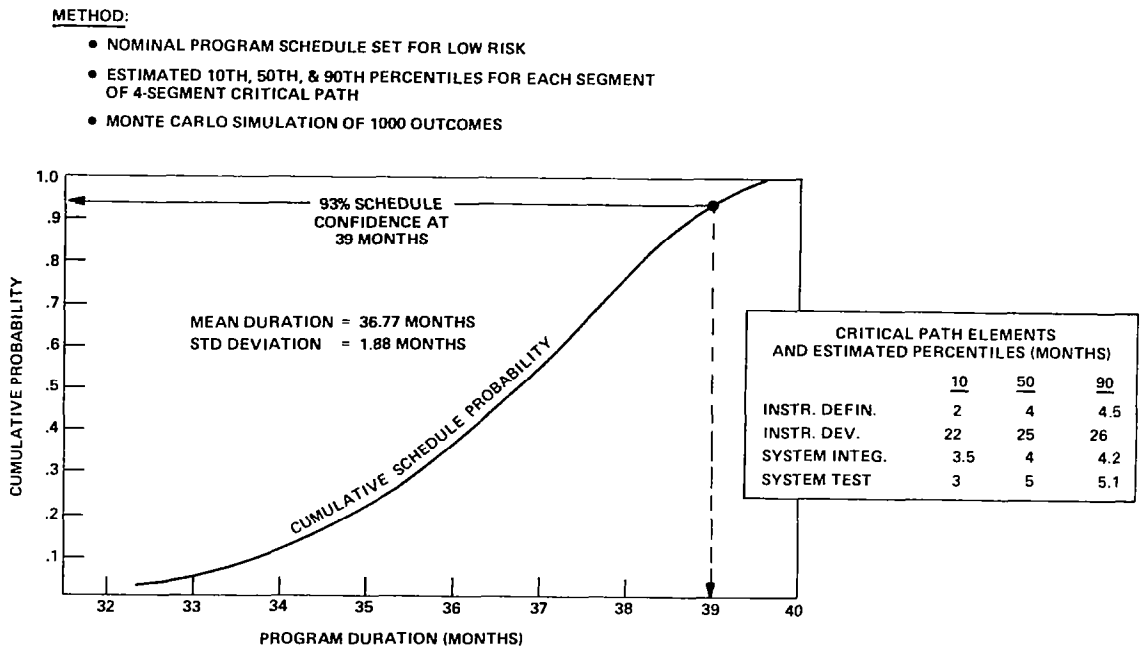

Figure 10-5. Lidar Schedule Risk Assessment.

10.4 WORK BREAKDOWN STRUCTURE

The Work Breakdown Structure (WBS) is the fundamental program management tool for cost analysis of the Lidar program. It does not represent the organizational structure or the management hierarchy for the program implementation phase, but it is an organizational arrangement of project elements to account for all costs incurred in a program. Its purpose is to assure that all cost elements are accounted for and it is structured such that costs are neither overlooked nor accounted for more than once in the program.

The Summary Work Breakdown Structure (WBS) formulated and used in the study costing task is shown in Figures 10-6 and 10-7. The WBS elements 1.0 through 4.0 comprise the top level program elements for the "base" Lidar MUIS. The activities, equipment, functions, etc. contained within each of these WBS elements are identified in Figure 10-6. Each of these elements can be further subdivided. For example, the subsystems

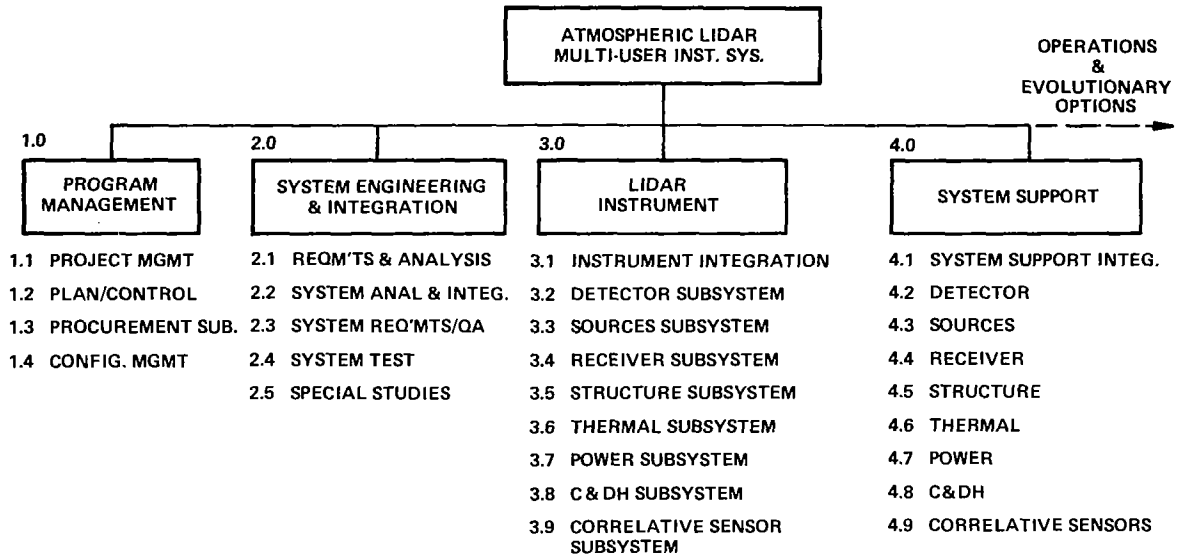

Figure 10-6. Work Breakdown Structure.

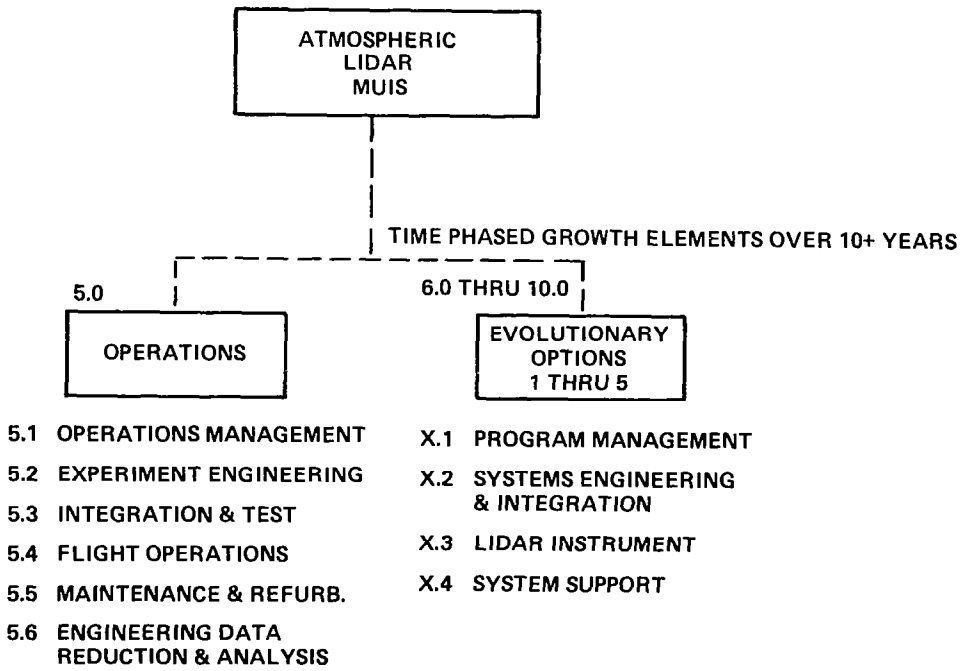

Figure 10-7. Work Breakdown Structure (Continued).

of WBS 3.2 through 3.9 can be divided into assemblies, the assemblies divided into modules, the modules divided into components, and the components into piece parts. Such subdivisions were accomplished in the study, as described in prior sections of this report, and were used in the cost estimating process.

The primary WBS element of the "base" MUIS, shown in Figure 10-6, is the Lidar Instrument (WBS element 3.0). This element contains all the activities, equipment, functions, etc. associated with the flight hardware and software, and in turn provides the basis for the activities, equipment, functions, etc. of the other program WBS element. For example the flight instrument equipment determines the mechanical and electrical ground support equipment and the related software of WBS element 4.0, System Support. Additionally, the Systems Engineering and Integration of WBS 2.0 and the Program Management of WBS 1.0 are directly related to the flight and ground hardware and software.

In addition to the base Lidar MUIS, the Program included 6 additional major WBS elements. These WBS elements are shown on Figure 10-7 and include Operations (WBS 5.0) and the five Evolutionary Growth Options (WBS 6.0 through 10.0).

Operations have been defined, for costing purposes, as the activities/services required for the conduct of a single flight mission. This activity will cover a 30 month duration, from 18 months prior to launch to 12 months after the mission completion. Each flight mission has been defined as being separate and distinct since each will most probably have a distincitive set of scientific, operational, and management activities. Each mission will, under the current NASA plan, have a mission manager for a flight mission with a variable payload mix (Lidar is only one element of the total payload). The Principal Investigator(s) will be different for each mission, as will the payload specialist. The Lidar Instrument flight configuration

can vary from mission to mission depending on the science objectives. These factors and others (including Eastern Test Range launch, Western Test Range launch, available resources of weight, power, volume, payload specialist time, etc.) require initiation of activities near concurrent with flight assignment and continuation through the post flight support of the Principal Investigator(s). The specific WBS elements within Operations are defined in Figure 10-7 and described in detail in Section 3 of this report.

The five Evolutionary Growth Options were established as separate program elements including their individual Program Management, Systems Engineering and Integration, Lidar Instrument (flight equipment) and System Support (ground support equipment). These program elements were scheduled to be conducted in a period of 18 months and include the flight equipment shown in Figure 10-2. They were separately identified and costed to permit Langley Research Center to use the programmatic effort outputs to develop the Lidar Project it desires to pursue.

In summary the WBS was formulated to present all aspects of the envisioned Lidar Project (including growth) in a manner that permits the orderly restructuring of elements. It separates the "base" program from the five individual evolutionary options and treats the individual operations of each flight mission. This WBS is directly correlatable to the cost and schedule definitions.

10.5 LIDAR PROGRAM COST

The cost estimating activity for the study was conducted in accordance with the ground rules identified in Figure 10-8. All costs are reported in constant 1978 dollars. Costs were established for a total Lidar MUIS Program, the Operations for one flight mission, and for each of the five evolutionary options. These seven cost elements were treated as independent program elements involving flight and ground

support equipment and the related program management and systems engineering and integration activities. As described earlier in this section the base Lidar MUIS schedule was established at 39 months. The five evolutionary growth options were defined as independent 18-month activities. A 30-month schedule was identified for the Operations associated with a single flight mission.

LIDAR COST GROUND RULES

- COSTS ARE IN 1978 DOLLARS
- SINGLE PROGRAM FOR ALL HARDWARE, SOFTWARE AND SUPPORT
- A 39 MONTH PROGRAM SCHEDULE (ATP TO DELIVERY)
- PROTOFLIGHT PROGRAM
- "TECHNOLOGICALLY READY" SYSTEMS, SUBSYSTEMS AND ASSEMBLIES
- SHUTTLE ERA PHILOSOPHY/CONCEPTS
- DEVELOPED AT OR BELOW WBS LEVEL SPECIFIED
- TYPICAL GE-SD PRACTICES/PROCEDURES
- ASSUMED 10% FEE

TOTAL COSTS TO GOVERNMENT

NO COSTS ARE INCLUDED FOR:

PRINCIPAL INVESTIGATOR ACTIVITIES
GROUND FACILITIES, SPACELAB ELEMENTS
SHUTTLE TRANSPORTATION AND SUPPORT SERVICE CHARGES
REQUIRED SIMULATORS OF SHUTTLE AND SPACELAB
SCIENCE DATA ANALYSIS
GOVERNMENT PROGRAM MANAGEMENT COSTS

Figure 10-8. Lidar Cost Ground Rules.

In all instances, for the base Lidar MUIS and the evolutionary options, a proto-flight program was selected. This proto-flight program concept is predicated on the use of initial program hardware, with refurbishment, throughout the program. That is, the initial developmental hardware will be designed, built, and tested with the objective that it will be the Lidar instrument flight hardware (maintenance and refurbishment/redesign are provided for in this concept).

The base Lidar MUIS and evolutionary options 1, 2, and 4 were identified as "technologically ready"; that is, none of the equipment identified required advancement in the current state-of-the-art. The evolutionary options 3 and 5 (see Figure 10-2) identified equipment requiring supporting research and technology (SR&T) efforts prior to their incorporation into the flight instrument program.

The cost estimating was conducted using Shuttle era philosophy/concepts. In addition to the protoflight program, Shuttle era concepts with regard to safety, reliability, quality assurance, maintenance, etc., were used. It is, however, recognized that these concepts are still in the formulative stage and have yet to be demonstrated.

The cost estimating procedure used was basically "bottoms up". The Lidar Instrument definition was formulated to at least the assembly level. Costs were established at or below this level and accumulated to the Summary WBS level. Throughout the cost activity, typical General Electric practices and procedures were used. These practices and procedures included but were not limited to make-buy decisions, manufacturing support practices, inspection requirements, overhead rates, and the basic labor category/ratio defined for each activity. In addition, all costs reported include an assumed fee of 10%.

The cost estimates conducted under the study represent the cost to the government by the industrial contractor for the equipment and services defined by the WBS. The cost for activities and equipment not identified in the WBS are assumed to be GFE to the prime contractor or accounted for elsewhere. The costs that are not included are for facilities at the launch site, the Spacelab elements (pallet, remote acquisition unit (RAU), etc.), the Shuttle transportation and support services charges, and any simulators. These were assumed as government furnished equipment (GFE). Principal Investigator activities and science data reduction were assumed as costs to the government not involving the instrument prime contractor.

The Lidar MUIS cost for the base program was estimated at $33.9 million dollars (Figure 10-9). Approximately two-thirds of this value is for the flight hardware, with approximately one-quarter provided for the program management and systems engineering and integration efforts. The remaining percentage (approximately 8 percent) is required for system support. The funding profile associated with the Lidar MUIS is shown in Figure 10-10. This figure shows the time-funding of each major WBS element of the program for the 39 month schedule. As shown, the program expends 65% of the defined resources in the first half (19.5 months) of the schedule. This "front loading" is typical of a proto-flight payload program. The program, as currently defined requires a peak funding level of approximately 4.5 million dollars per quarter and this peak occurs at about the midpoint of the second year.

WBS ELEMENT	TOTAL COST TO GOVERNMENT (M$)
1. — PROGRAM MANAGEMENT	3.1
2. — SYSTEMS ENGINEERING AND INTEGRATION	4.5
3. — LIDAR INSTRUMENT	23.4
4. — SYSTEM SUPPORT	2.9
TOTAL	33.9

Figure 10-9. Lidar MUIS Cost.

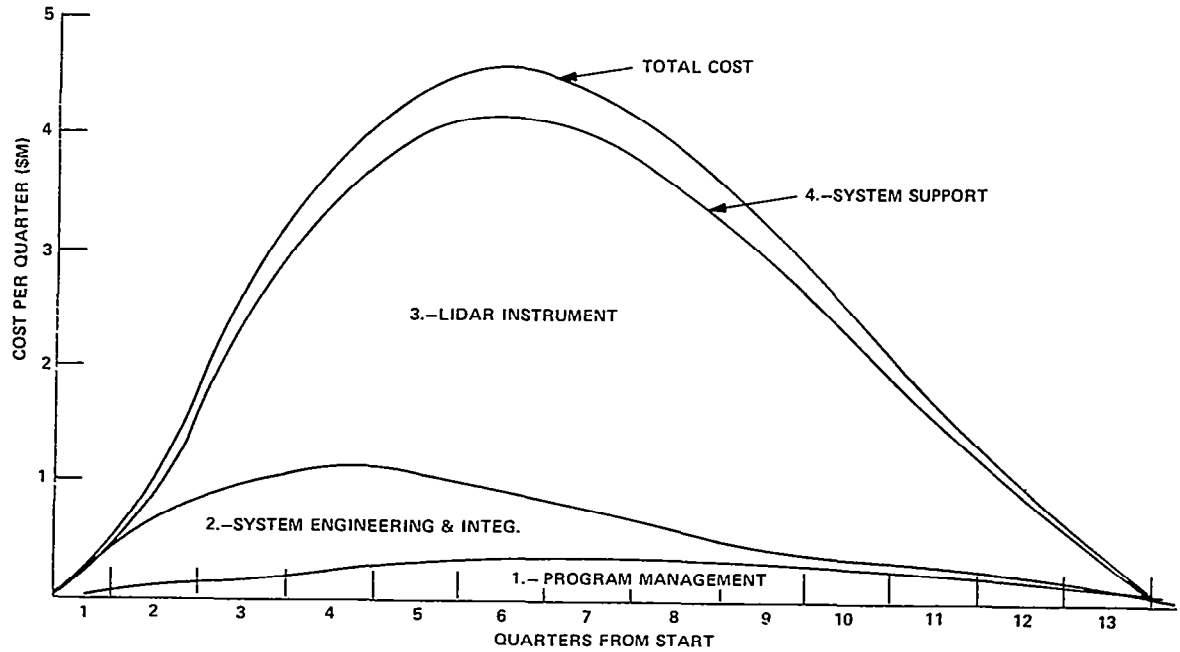

Figure 10-10. Lidar Program Funding Profile (~65% Of Cost in 50% of Time).

The cost risk assessment for the "base" Lidar MUIS program was performed in a manner similar to the schedule risk assessment. The results of this analysis are shown in Figure 10-11. This analysis shows that there is 55% confidence level of meeting the cost estimate of 33.9 million dollars. This result was achieved by the estimation of the 10th, 50th, and 90th percentiles (in millions of dollars) for each of the 4 major WBS elements (tabulated values of FIgure 10-11). These percentiles were used in a Monte Carlo simulation of 1000 cases. The computerized assessment provided the curve shape shown and defined the standard deviation of 2.36 million dollars about the mean cost of 33.9 million dollars.

Cost estimates for the Operations (WBS 5.0) and the Evolutionary Options (WBS 6.0 through 10.0) are presented in Figure 10-12. The cost estimating confidence for Operations and Evolutionary Growth Options 1, 2, and 4 is similar to that presented for the "base" Lidar MUIS program. The Evolutionary Options 3 and 5 contain technology development equipment and are therefore of lower confidence.

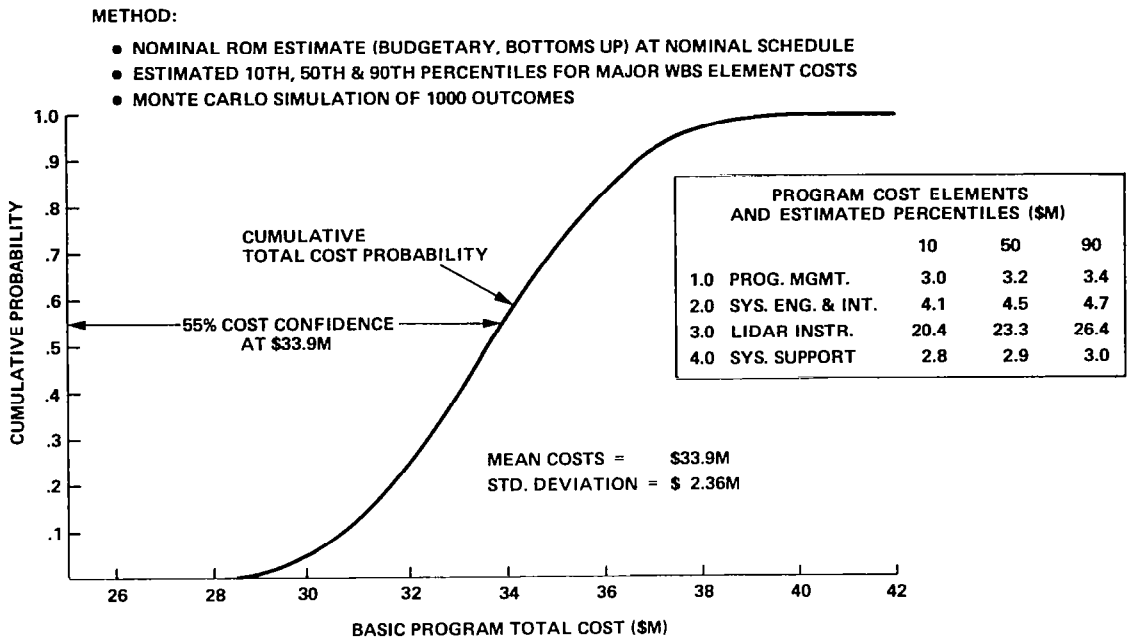

PROGRAM COST ELEMENTS AND ESTIMATED PERCENTILES ($M)

	10	50	90
1.0 PROG. MGMT.	3.0	3.2	3.4
2.0 SYS. ENG. & INT.	4.1	4.5	4.7
3.0 LIDAR INSTR.	20.4	23.3	26.4
4.0 SYS. SUPPORT	2.8	2.9	3.0

Figure 10-11. Lidar Basic Program Cost Risk Assessment.

The Operations cost for each flight mission was estimated at 1.6 million dollars. This value is typical for missions currently anticipated. It was assumed that any learning curve advantage reducing cost would be offset by the introduction of additional equipment/complexity by the evolutionary options.

The costs for each of the evolutionary options was established by the same "bottoms up" cost estimating technique previously described. The level of depth, however, for the evolutionary options is the subsystem level, (with the exception of that equipment which is identical to equipment in the Lidar MUIS). The total cost for the five evolutionary options is 39.9 million dollars with individual options in the range of 6.5 to 9.4 million dollars.

WBS ELEMENT	TOTAL COST TO GOVERNMENT (M$)	TOTAL (M$)
5. - FIRST FLIGHT OPERATIONS	1.6	PER MISSION (TYPICAL)
6. - OPTION 1	6.5	
7. OPTION 2	7.0	
8. OPTION 3	9.1	39.9
9. OPTION 4	7.9	
10. OPTION 5	9.4	

Figure 10-12. Lidar Operations and Evolutionary Options.

10.6 SUPPORTING RESEARCH AND TECHNOLOGY IDENTIFICATION AND LONG LEAD ITEMS

The identification of supporting research and technology items was completed near the end of the study. These are items which are assessed as not being technologically ready for space flight on the Shuttle at this time. Advancements in the state of the art are, of course, being constantly made and at some later date some of these items may be demonstrated to be space flyable and no additional work will have to be done on them. The items identified as needing SR and T funding are:

- The Long Pulse very narrow band Nd:YAG laser. This device is required to have a bandwidth of 10^{-4}nm and similar wavelength stability. This narrow pulse requires a transform limited pulse length of several microseconds.
- Pulsed CO_2 Laser. A narrow band, two line, single mode, pulsed laser required as a source for the heterodyne detector of winds.
- Special Lasers. Special pulsed lasers are required in the 700-900 nm region. These require more energy than is presently available from dye lasers in this region with narrow (0.005 nm) linewidth and excellent stability for DIAL measurements. Special lasers are required in the UV region both for more energy output than is currently available and a requirement exists for a high brightness mode locked laser at 225.6 nm.
- Narrow Band ($\sim$ 0.01 nm) filters are required for use in the ultraviolet region.
- Fabry-Perot detector refinement of existing Fabry-Perot detector techniques are required in order to obtain a space flyable unit.

The only long lead item identified in the study is the mirror blank for the receiving telescope primary mirror.

11.0 CONCLUSIONS AND RECOMMENDATIONS

The Atmospheric Lidar Multi-User Instrument System Definition Study has accomplished the initially defined goal and objectives. The results define evolutionary systems that meet the scientific, technological, and programmatic requirements. The primary conclusions are summarized in Figure 11-1.

- SIGNIFICANT SCIENCE CAN BE ACCOMPLISHED
  - EVOLUTIONARY GROWTH FROM INITIAL FACILITY
- SHUTTLE/SPACELAB CAN ACCOMMODATE THE EVOLUTIONARY LIDAR INSTRUMENT
- INITIAL FACILITY CONCEPT TECHNOLOGICALLY READY
- OTHER EQUIPMENT CAN BE INCLUDED IN INITIAL FACILITY
  - CW CO_2
  - MULTIPLE Nd:YAG LASERS
- PROGRAMMATIC PLANNING ASSESSMENT
  - COST } HIGH CONFIDENCE
  - SCHEDULE } HIGH CONFIDENCE

Figure 11-1. Conclusions.

Of fundamental and primary importance the study concluded that significant science can be accomplished using an orbital evolutionary growth Lidar instrument aboard the Shuttle/Spacelab. The base Lidar MUIS and its envisioned evolutionary growth can be adequately accommodated with the partial payload "fair share" of the weight, power, volume, and payload specialist resources of the Shuttle/Spacelab. The equipment defined for the base Lidar MUIS is technologically ready and additionally, equipment such as the continuous wave (CW) CO_2 laser, is sufficiently developed to be included in the first procurement, if desired.

Science Accomodation - The science that can be accommodated with the defined Lidar Instrument MUIS includes all category 1 experiment classes, with the exception of experiment class 10, and portions of the category 2 and category 3 experiment classes. A widely diverse and significant portion of the experiments can therefore be accomplished with the base MUIS. Furthermore the system was defined in a manner that accommodates these experiment classes to provide the highest practical signal to noise ratio and accuracy. For example, the receiver field of view (FOV) variation from 0.1 milliradian to 6.0 milliradian provides capability for both day and night maximization of signal to noise ratio, and the seven module laser configuration provides for multiple wavelength capability to accommodate different experiment classes during the same mission.

Shuttle/Spacelab Compatability - The study results show that the "base" MUIS and its evolutionary growth can be accomodated by the Shuttle/Spacelab. The Spacelab pallet weight and volume capability far exceeds the Lidar Instrument requirements, providing margin not only for envisioned growth in CW and pulsed CO_2 lasers and their associated detectors but also for the potential equipment of Principal Investigators. The power requirements of the Lidar, although high, are within the Shuttle/Spacelab capability. Sequencing of laser operation, experiment flexibility in pulse repetition rate, and low non-operating or "standby" power are design features incorporated into the Lidar MUIS.

Technological Readiness - The Lidar MUIS was defined from equipment that is essentially state-of-the-art and technologically ready. The receiver is well within the available technology. The laser modules have been demonstrated separately and must be packaged and automated for Lidar Instrument usage. The lasers do represent the most technologically demanding subsystem of the Lidar. The detector modules require only "packaging" for space flight. The support subsystems for data power,

thermal control, and structural integrity are well within already demonstrated space hardware capability. Additionally, if it is desired, the CW CO_2 laser can be provided with the "base" Lidar MUIS and requires only redesign to the desired experiment class power level.

Program Plan - The schedule established for the Lidar program is a high confidence schedule. As such, the mean cost estimation is also a high confidence number with a low percentage value standard deviation. The programmatic planning assessment, therefore, is in accord with the study goal and objectives.

The high confidence in the established schedule and cost values is a result of the in-depth definition of the Lidar MUIS and its evolutionary growth equipment, and the implementation of a "bottoms-up" approach from the assembly level. These factors, combined with the use of Monte-Carlo computer techniques which provided the standard deviation from the mean schedule and cost values provide high credibility to total programmatic planning.

As a result of the above conclusions and the supporting efforts leading to these conclusions, it can be strongly recommended that the defined Lidar MUIS proceed to program implementation. The program has well defined and quantified science, a feasible system definition and concept, and requisite confidence level program planning.

1. Report No.	2. Government Accession No.	3. Recipient's Catalog No.
NASA CR-3303		

4. Title and Subtitle	5. Report Date
Atmospheric Lidar Multi-User Instrument System Definition Study	August 1980
	6. Performing Organization Code
7. Author(s)	8. Performing Organization Report No.
R. V. Greco, Editor	
9. Performing Organization Name and Address	10. Work Unit No.
General Electric Company Space Division Valley Forge, PA	146-20-01-08
	11. Contract or Grant No.
	NAS1-15476
12. Sponsoring Agency Name and Address	13. Type of Report and Period Covered
National Aeronautics and Space Administration Washington, DC 20546	Contractor Report
	14. Sponsoring Agency Code

15. Supplementary Notes

Langley technical monitor: Kenneth H. Crumbly

Final Report

16. Abstract

The Atmospheric Lidar Multi-User Instrument System Study (NAS1-15476) was performed to quantify and definitize a spaceborne lidar system for atmospheric studies. The primary inputs to this effort were the Science Objectives Experiment Description and Evolutionary Flow Document (SEED), generated by the Atmospheric Lidar Working Group and the Space Shuttle Payload Accommodation Handbook. The first task of the study was to perform an experiment evolutionary analysis of the SEED. The second task was the system definition effort of the instrument system. The third task was the generation of a program plan for the hardware phase. The fourth task was the supporting studies which included a Shuttle deficiency analysis, a preliminary safety hazard analysis, the identification of long lead items, and development studies required. As a result of the study an evolutionary Lidar Multi-User Instrument System (MUIS) was defined. The MUIS occupies a full Spacelab pallet and has a weight of 1300 kg. The Lidar MUIS will provide a 2 joule frequency doubled Nd:YAG laser that can also pump a tuneable dye laser with wide frequency range and bandwidth. The MUIS includes a 1.25-meter diameter aperture Cassegrain receiver, with a moveable secondary mirror to provide precise alignment with the laser. The receiver can transmit the return signal to three single and multiple PMT detectors by use of a rotating fold mirror. The study concluded that the Lidar MUIS proceed to program implementation.

17. Key Words (Suggested by Author(s))	18. Distribution Statement
Lidar, Shuttle Experiments Atmospheric, Laser Radar	Unclassified - unlimited Subject category 46

19. Security Classif. (of this report)	20. Security Classif. (of this page)	21. No. of Pages	22. Price
Unclassified	Unclassified	343	A15

For sale by the National Technical Information Service, Springfield, Virginia 22161

NASA-Langley, 1980